



University
of Glasgow

Burdett, Heidi L. (2013) *DMSP dynamics in marine coralline algal habitats*. PhD thesis.

<http://theses.gla.ac.uk/4108/>

Copyright and moral rights for this thesis are retained by the author

A copy can be downloaded for personal non-commercial research or study

This thesis cannot be reproduced or quoted extensively from without first obtaining permission in writing from the Author

The content must not be changed in any way or sold commercially in any format or medium without the formal permission of the Author

When referring to this work, full bibliographic details including the author, title, awarding institution and date of the thesis must be given

DMSP Dynamics in Marine Coralline Algal Habitats

Heidi L. Burdett
MSc BSc (Hons) University of Plymouth

Submitted in fulfilment of the requirements for the
Degree of Doctor of Philosophy

School of Geographical and Earth Sciences
College of Science and Engineering
University of Glasgow

March 2013

Dedication

In loving memory of my Grandads; you may not get to see this in person,
but I hope it makes you proud nonetheless.

John Hewitson Burdett

1917 - 2012

and

Denis McCarthy

1923 - 1998

Abstract

Dimethylsulphoniopropionate (DMSP) is a dimethylated sulphur compound that appears to be produced by most marine algae and is a major component of the marine sulphur cycle. The majority of research to date has focused on the production of DMSP and its major breakdown product, the climatically important gas dimethylsulphide (DMS) (collectively DMS/P), by phytoplankton in the open ocean. A number of functions for intracellular DMSP (DMSPi) in phytoplankton have been identified and the cycling of DMS/P appears to be critical for ecosystem function. However, mechanisms for the production and release of DMS/P in the coastal ocean are poorly understood, despite the region's economic and ecological importance. Coralline algal habitats (e.g. maerl beds, coral reefs, seagrass meadows, kelp forests) are distributed throughout the coastal oceans worldwide. Their three-dimensional structure supports high biodiversity and provides numerous services, generating considerable economic wealth. DMSPi in coralline algae is known to be high, thus coralline algal habitats may be critical components of the coastal sulphur cycle.

This research aimed to improve our understanding of the production of DMS/P by coralline algal habitats by investigating (1) natural spatiotemporal variation and (2) the influence of environmental pressures. This was achieved through a number of laboratory and field-based studies, utilising modern and well-established techniques.

The first objective of this research was to better understand the photosynthesis of red coralline algae (Chapter 3), as the algal precursor to DMSPi is methionine, a product of photosynthesis. The photosynthetic characteristics of coralline algae exhibited acclimation to changing light conditions (e.g. over a diurnal cycle or between natural and static lighting conditions). Further, for the species tested, coralline algae are often subjected to light-saturating natural conditions, therefore requiring efficient photo-protective mechanisms, which may include DMSPi regulation.

On a global scale, DMSPi in coralline algae may decline with latitude, reinforcing the role of DMSPi as an antioxidant (Chapter 4). At smaller spatial

scales, DMS/P production, release and recycling mechanisms were apparent in a number of habitat types (Chapter 4). A strong seasonal trend in DMS/P was also observed at a Scottish maerl bed, driven by water temperature and cloud cover (Chapter 5). Annually averaged DMS and DMSP concentrations were 230% and 700% respectively higher than the open ocean, highlighting the potential importance of the coastal ocean in the marine sulphur cycle (Chapter 5).

The influence of environmental pressures (decreased salinity, variable pH and grazing) on DMS/P production by coralline algal habitats was examined (Chapters 6 - 8). In agreement with the phytoplankton literature, a chronic, but not acute, reduction in salinity led to a significant decline in coralline algal DMSPi concentrations and a sinking of the surface epithelial cells but no apparent impact on photosynthesis (Chapter 6). In the naturally variable tropical reef environment, calcifying algae continually regulated DMSPi concentrations in response to the diurnal cycling of carbonate saturation state (Chapter 7), suggesting that DMSPi may be enhanced under low pH regimes to compensate for enhanced oxidant production. Under low pH conditions, cracks were observed between the surface epithelial cells of coralline algae, potentially allowing DMSPi to leak from the cells (Chapter 7). In the field, grazing by urchins appeared to facilitate the release of DMS/P from kelp in coralline algal habitats (Chapter 8). In the laboratory, DMSPi in coralline algae increased in response to chemical cues from grazers rather than direct grazing activity, as had been previously proposed.

Prior to this research, little information was available on DMS/P concentrations in coralline algal habitats. The marine sulphur cycle may impact climate regulation and ecosystem function on a global scale. This research provides a comprehensive source of information on the importance of coralline algal habitats in the marine sulphur cycle by examining natural variability and potential changes in response to environmental perturbations. This work will form a baseline for continued research in this field, investigating, for example, the impact of multiple stressors on DMS/P production, release and recycling in coastal marine habitats.

Table of contents

Dedication	ii	
Abstract	iii	
List of figures.....	xii	
List of tables.....	xv	
Publications arising from this research	xvi	
International conference presentations	xviii	
Acknowledgements.....	xix	
Author's declaration	xxi	
Definitions and abbreviations	xxii	
Chapter 1	Introduction.....	25
1.1	The oceanic sulphur cycle.....	25
1.1.1	Dimethylsulphide	26
1.1.1.1	The CLAW hypothesis	26
1.1.2	Dimethylsulphoniopropionate.....	28
1.1.2.1	The production of DMSP	29
1.1.2.2	The release of DMSP	30
1.1.2.3	The degradation of DMSP	31
1.1.3	Cycling of dimethylated compounds in the ocean	33
1.1.4	Dimethylated sulphur production in the coastal ocean	35
1.2	Non-geniculate red coralline algae	36
1.2.1	Distribution of coralline algal habitats	37
1.2.1.1	Maerl and rhodolith beds.....	37
1.2.1.2	Coralligène	39
1.2.1.3	Kelp forests	39
1.2.1.4	Coral Reefs	40
1.2.1.5	Seagrass meadows.....	40
1.2.2	Taxonomy.....	41
1.2.3	Growth	42
1.2.3.1	Morphology	42
1.2.3.2	Growth banding.....	43
1.2.4	Red algal photosynthesis	45
1.2.4.1	Red algal chloroplasts	47
1.2.4.2	Phycobiliprotein pigments	47
1.2.5	Importance of coralline algal habitats	52
1.2.5.1	Ecosystem service provision	52
1.2.5.2	Carbon sequestration and cycling.....	53
1.2.5.3	Palaeoclimatic proxies	53
1.2.6	Threats to coralline algal habitats	54
1.2.6.1	Fishing	54
1.2.6.2	Harvesting.....	54
1.2.6.3	Eutrophication	55
1.2.6.4	Climate change	55
1.3	Aims of this research.....	56

Chapter 2	Methods and techniques	59
2.1	DMSP and DMS analysis	59
2.1.1	Different methods of analysing DMSP and DMS.....	59
2.1.2	The Gas Chromatograph	60
2.1.2.1	The purge and cryotrap system	61
2.1.3	Standard calibrations	63
2.1.3.1	Headspace standards: high DMS concentrations	64
2.1.3.2	Liquid standards: low DMS concentrations	64
2.1.3.3	Precision, accuracy and detection limit	65
2.1.4	Sample preparation and analysis.....	65
2.1.4.1	Intracellular DMSP.....	65
2.1.4.2	Particulate and dissolved DMS/P in seawater	66
2.2	Pulse Amplitude Modulation fluorometry	66
2.2.1	Chlorophyll fluorescence	67
2.2.2	Modulation fluorometry	67
2.2.3	The Diving-PAM	68
2.2.4	Parameter notation	70
2.2.5	Quantum efficiency	72
2.2.6	Electron transport rate	72
2.2.7	Dark acclimation.....	73
2.2.7.1	Quasi-dark acclimation	73
2.2.8	Rapid Light Curves (RLCs)	74
2.2.9	Photosynthetic parameters	75
2.2.10	Quenching parameters.....	77
2.3	Scanning Electron Microscopy	78
2.3.1	Secondary Electron Imaging	79
2.3.2	Sample preparation	80
2.3.3	Imaging protocol.....	81
2.3.4	Environmental SEM	82
2.4	Optical spectroscopy.....	82
Chapter 3	The photosynthetic characteristics of red coralline algae .	85
3.1	Introduction	85
3.1.1	The relationship between DMSP and photosynthesis	85
3.1.2	Pulse Amplitude Modulation fluorometry	86
3.1.2.1	PAM and red coralline algae	87
3.1.3	The diurnal pattern of photosynthesis	88
3.2	Aims of this chapter.....	89
3.3	Methods: temperate alga <i>Lithothamnion glaciale</i>	90
3.3.1	Collection of algal material.....	90
3.3.2	Fluorescence measurements.....	90
3.3.2.1	Dark acclimation	91
3.3.3	Experimental design	93
3.3.3.1	<i>In situ</i> measurements.....	93
3.3.3.2	Laboratory measurements	93
3.3.4	Statistical analyses	93
3.4	Methods: tropical coralline algae (diurnal response)	94
3.4.1	Measurement of ambient PAR	94
3.4.2	Collection of algal material.....	94
3.4.3	Fluorescence measurements.....	95

3.4.4	Statistical analyses	96
3.5	Results: temperate coralline algae	96
3.5.1	<i>In situ</i> field measurements in May	97
3.5.2	Laboratory measurements in March and May	98
3.5.3	Laboratory and field measurements in May	101
3.6	Results: tropical coralline algae (diurnal response)	101
3.6.1	Ambient PAR	102
3.6.2	Optical reflectance	102
3.6.3	Intracellular DMSP	103
3.6.4	Minimum saturating intensity, E_k	104
3.6.5	Maximum quantum efficiency, $F_q'/F_{m'_{max}}$	105
3.6.6	E_k and $F_q'/F_{m'_{max}}$ regression with PAR	106
3.6.7	Quantum efficiency	107
3.6.8	Photochemical quenching	110
3.6.9	Relative electron transport rate	110
3.6.10	Non photochemical quenching, NPQ	111
3.6.11	Non photochemical quenching, qN	113
3.7	Discussion	113
3.7.1	Saturation intensity (E_k) is variable relative to light regime	114
3.7.2	Diurnal trends in photosynthesis	115
3.7.3	Intra-thallus heterogeneity	116
3.7.4	Which non-photochemical parameter to use?	117
3.8	Conclusions	118
Chapter 4	Spatial variation of DMSP in coralline algae	121
4.1	Spatial variation of DMS/P in the epipelagic zone	121
4.2	Spatial variation of DMS/P in benthic systems	123
4.3	Aims of this chapter	124
4.4	Methods: Global scale	127
4.4.1	Sampling locations	127
4.5	Methods: Regional scale	130
4.5.1	Trans-Atlantic comparison	130
4.5.2	West coast of Scotland	131
4.6	Methods: Local scale	133
4.6.1	Sinai Peninsula, Egypt	133
4.6.2	North-west Mediterranean	134
4.6.3	Western Antarctic Peninsula	136
4.7	Statistical and data analysis	138
4.8	Results: Global scale	139
4.9	Results: Regional scale	141
4.9.1	Trans-Atlantic comparison	141
4.9.2	West coast of Scotland	143
4.10	Results: Local scale	143
4.10.1	Sinai Peninsula, Egypt	143
4.10.2	North-west Mediterranean	144
4.10.3	Western Antarctic Peninsula	145
4.11	Discussion	147

4.11.1	Phylum-specific DMSPi concentrations	147
4.11.2	Latitudinal trends	148
4.11.3	Diurnal patterns	149
4.11.4	Sources and sinks of coastal DMS/P.....	149
4.11.5	Ecosystem function.....	150
4.12	Conclusions	151
Chapter 5	Temporal trends in DMSP dynamics	153
5.1	Seasonal DMS/P trends: Plankton	153
5.2	Seasonal DMS/P trends: Benthic primary producers.....	158
5.3	Aims of this chapter.....	158
5.4	Methods	159
5.4.1	Study site and sample collection.....	159
5.4.2	Abiotic variables.....	161
5.4.3	Statistical analyses	162
5.5	Results	163
5.5.1	Abiotic parameters.....	163
5.5.2	DMS/P measurements.....	165
5.5.3	GAM modelling.....	168
5.6	Discussion.....	169
5.6.1	Seasonal cycle of DMS/P concentrations.....	169
5.6.1.1	Decoupling of dimethyl sulphur species	170
5.6.1.2	Coralline algal DMSPi	170
5.6.2	The impact of the maerl bed on DMS/P pools.....	171
5.6.2.1	Summer phytoplankton blooms	171
5.6.2.2	Autumnal decay of seasonal macroalgae	172
5.6.2.3	Ecosystem function	172
5.6.3	Temperature and cloud cover are driving factors	172
5.6.4	Implications for the future.....	173
5.7	Wider significance.....	173
5.8	Conclusions	174
Chapter 6	Environmental pressures: Reduction in salinity	175
6.1	DMSP and osmotic regulation	175
6.2	Global precipitation patterns.....	177
6.2.1	Extreme events	178
6.2.2	Cloud formation	178
6.3	Ice melt	179
6.4	Regional focus: west coast of Scotland	180
6.5	Regional focus: Central Chilean coast.....	182
6.6	Aims of this chapter.....	183
6.7	Methods: Chronic salinity reduction, Scotland.....	184
6.7.1	Experimental set up.....	184
6.7.2	Sample measurements.....	186
6.7.3	Statistical analyses	186
6.8	Methods: Acute salinity reduction, Chile	187

6.8.1	Experimental set-up	187
6.8.2	Sample measurements	189
6.8.3	Statistical analysis	190
6.9	Results: Chronic salinity reduction, Scotland	190
6.9.1	Abiotic parameters	190
6.9.2	Visual observations	191
6.9.3	Intracellular DMSP	192
6.9.4	Photosynthetic parameters	193
6.9.5	Photoprotective characteristics	195
6.9.6	Pigment composition	196
6.9.7	Epithelial cell morphology	197
6.10	Results: Acute salinity reduction, Chile	199
6.10.1	Abiotic parameters	199
6.10.2	Intracellular DMSP	199
6.10.3	Maximum quantum efficiency, F_v/F_m	200
6.10.4	Diurnal variation in F_v/F_m	202
6.11	Discussion	203
6.11.1	DMSPi as a compatible solute in red coralline algae	203
6.11.2	The impact of reduced salinity on photosynthesis	204
6.11.3	Characterisation of red coralline algal pigments in <i>L. glaciale</i> ...	205
6.11.4	The effect of reduced salinity on cell morphology	205
6.11.5	Diurnal variation in quantum efficiency	206
6.11.6	Species-specific natural variability	206
6.12	Conclusions	207
Chapter 7	Environmental pressures: Ocean acidification	209
7.1	Ocean acidification	209
7.1.1	Natural variability in the coastal ocean	211
7.1.1.1	CO ₂ vents	212
7.1.1.2	Upwelling zones	212
7.1.1.3	Coral reefs	213
7.1.2	Carbon capture and storage	213
7.1.3	Ocean acidification and calcifying macroalgae	214
7.1.4	DMSP and ocean acidification	216
7.2	Aims of this chapter	216
7.3	Methods: Laboratory study, UK	217
7.3.1	Experimental set-up	217
7.3.2	Sampling protocol	219
7.3.3	Statistical analyses	220
7.4	Methods: <i>In situ</i> field study, Egyptian Red Sea	220
7.4.1	Field site	220
7.4.2	Sampling regime	221
7.4.3	Statistical analyses	223
7.5	Results: Laboratory study, UK	223
7.5.1	Water chemistry	223
7.5.2	Percentage biomass and DMS/P measurements	224
7.5.3	Outer epithelial cell morphology	226
7.6	Results: <i>In situ</i> field study, Egyptian Red Sea	227
7.6.1	Water chemistry	227

7.6.1.1	Physical parameters	227
7.6.1.2	Carbonate parameters.....	228
7.6.2	Percentage calcification.....	231
7.6.3	Macroalgal and water column DMS/P.....	231
7.7	Discussion.....	233
7.7.1	Regulation of intracellular DMSP	233
7.7.2	Species-specific response to ocean acidification	234
7.7.3	Biological control on carbonate chemistry	235
7.7.4	Structural sensitivity to ocean acidification.....	236
7.7.5	Laboratory and field experiments	237
7.7.6	Wider implications	237
7.8	Conclusions	238
Chapter 8	Environmental pressures: Grazing-hurricane interactions ..	241
8.1	DMS and DMSP as a grazing defence	241
8.2	DMSP as a grazer attractant	242
8.3	Regional focus: The eastern Canadian kelp forests	243
8.3.1	The role of kelp forests in biogeochemical cycles.....	245
8.4	Aims of this study	246
8.5	Methods: <i>In situ</i> field sampling.....	246
8.5.1	Sample collection	246
8.5.2	Hurricane Earl.....	247
8.5.3	Statistical analyses	248
8.6	Methods: Laboratory experiment	248
8.6.1	Sample collection	248
8.6.2	Mesocosm set-up	248
8.6.3	Statistical analyses	252
8.7	Results: <i>In situ</i> sampling	253
8.8	Results: Laboratory experiment.....	254
8.8.1	Dissolved DMS/P	254
8.8.2	Intracellular DMSP	255
8.9	Discussion.....	256
8.9.1	The grazing front as a source of DMS/Pd	256
8.9.2	Chemical signals	258
8.9.3	Impact of storm activity on DMS/Pd	258
8.9.4	North Atlantic hurricanes	259
8.9.4.1	Future hurricane projections.....	260
8.9.5	Impact of hurricanes on kelp forests	261
8.9.6	Impact of hurricanes on ocean circulation	262
8.9.7	Implications for the future.....	262
8.10	Conclusions	264
Chapter 9	Discussion and conclusion.....	265
9.1	The photosynthetic characteristics of coralline algae	266
9.1.1	Light saturation mechanisms	266
9.1.2	Diurnal trends.....	267
9.2	Natural variability of coralline algal habitats	268
9.2.1	Spatio-temporal variability	268

9.2.2	Phylum-specific trends	270
9.2.3	Latitudinal trends	270
9.2.4	Abiotic drivers	271
9.3	The effect of environmental and biological perturbations	271
9.3.1	Intracellular DMSP functions	272
9.3.2	Structural integrity	272
9.3.3	Ecosystem shifts	273
9.4	Future work and research direction	273
9.4.1	Intra-thallus heterogeneity	273
9.4.2	The role of the microbial community	274
9.4.3	Characterisation of associated compounds	274
9.4.4	Photosynthesis of red algae	275
9.5	Wider applications of this research	276
9.5.1	Habitat conservation and natural capital	276
9.5.2	Algal biofuels and bioproducts	276
9.5.3	Climate modelling	277
9.6	Conclusion	278
References		279
Appendix A.....		301

List of figures

Figure 1.1 The proposed DMS climatic feedback mechanism.	27
Figure 1.2 The three known DMSP production pathways.	30
Figure 1.3 The two major DMSP degradation pathways.	32
Figure 1.4 Important compounds in the biogenic marine sulphur cycle.....	34
Figure 1.5 The cycling of dimethylated sulphur compounds in the ocean.	34
Figure 1.6 Example of a free-living coralline algal thallus.	37
Figure 1.7 The global distribution of free-living red coralline algae.	38
Figure 1.8 The global distribution of major kelp forests.	39
Figure 1.9 The global distribution of coral reefs.	40
Figure 1.10 The global distribution and diversity of seagrass meadows.	41
Figure 1.11 The currently accepted taxonomy of red coralline algae.....	42
Figure 1.12 Growth bands of <i>Lithothamnion glaciale</i>	44
Figure 1.13 Growth and banding patterns of coralline algae.	45
Figure 1.14 The light and dark reactions of photosynthesis.	46
Figure 1.15 The probable organisation of the thylakoid membrane.	47
Figure 1.16 The phycobilisome structure.	49
Figure 1.17 Spectral reflectance of eight benthos types from the Bahamas.	51
Figure 1.18 Reflectance spectra of temperate macroalgae and seagrass.....	52
Figure 1.19 Thesis structure and the links between each chapter.....	57
Figure 2.1 The gas chromatograph set up for DMS analysis.	61
Figure 2.2 The purge-cryotrap system for pre-concentration of DMS.	62
Figure 2.3 Time taken to purge DMS from solution.....	63
Figure 2.4 Example DMS calibrations.	64
Figure 2.5 The fate of light energy when absorbed by chlorophyll (Chl).	67
Figure 2.6 Pulse Amplitude Modulation fluorescence measurements.....	69
Figure 2.7 The Walz Diving-PAM underwater fluorometer.	70
Figure 2.8 Fluorescence response notation.....	71
Figure 2.9 The Walz Diving-PAM surface holder attachment.	73
Figure 2.10 RLC fluorescence signal from the seagrass <i>Zostera marina</i>	75
Figure 2.11 Photosynthesis-irradiance curve.	76
Figure 2.12 Relationship between q_N and NPQ.	78
Figure 2.13 Schematic representation of an SEM.	79
Figure 2.14 Generation of secondary electrons in a sample.	80
Figure 2.15 Gold-coated coralline algae branches.	80
Figure 2.16 SE image of red coralline algal epithelial cells.	81
Figure 2.17 Method for recording the reflectance spectra of coralline algae....	83
Figure 3.1 Diurnal photosynthetic response of coral and microalgae.	88
Figure 3.2 Coralline algal thallus and PAM fibre optic probes.	91
Figure 3.3 Dark acclimation response of <i>L. glaciale</i>	92
Figure 3.4 Quantum sensor for PAR measurements.	94

Figure 3.5 Free-living coralline algal thallus from Suleman reef, Egypt.	95
Figure 3.6 Comparison of RLC data plotted against E and E/E_k	97
Figure 3.7 Photochemical response of <i>L. glaciale</i>	99
Figure 3.8 Photoprotective response of <i>L. glaicale</i>	100
Figure 3.9 Ambient PAR on Suleman reef, November 2011.	102
Figure 3.10 Coralline algal absorbance on Suleman reef, Egypt.	103
Figure 3.11 DMSP _i in free-living coralline algae from Suleman Reef, Egypt.	104
Figure 3.12 E_k over a diurnal period on Suleman Reef, Egypt.	105
Figure 3.13 Coralline algal $F_q'/F_{m'_{max}}$ over a diurnal period.	106
Figure 3.14 (a) E_k and (b) $F_q'/F_{m'_{max}}$ of coralline algae against PAR light levels.	107
Figure 3.15 Photochemical parameters over a diurnal cycle.	109
Figure 3.16 Non-photochemical parameters over a diurnal cycle.	112
Figure 4.1 Measured global DMS concentrations.	122
Figure 4.2 Spatial sampling regime and links between spatial scales.	126
Figure 4.3 Locations of the global coralline algae / DMSP sampling sites.	127
Figure 4.4 Red coralline algae from the six global sampling locations.	129
Figure 4.5 West coast of Scotland sampling site locations.	132
Figure 4.6 Suleman reef transect location and sampling points.	134
Figure 4.7 Transect routes for Mediterranean sampling.	135
Figure 4.8 Horizontal and vertical Mediterranean sampling.	136
Figure 4.9 Antarctic sampling locations.	137
Figure 4.10 Antarctic encrusting coralline algae.	138
Figure 4.11 Coralline algal DMSP _i at six locations worldwide.	140
Figure 4.12 Transatlantic comparison of DMSP _i in macroalgae.	142
Figure 4.13 DMSP _i in red coralline algae from the west coast of Scotland.	143
Figure 4.14 DMS/P (nmol L ⁻¹) on Suleman reef, Egypt.	144
Figure 4.15 DMS/Pd profiles from Banyuls-sur-Mer, France.	146
Figure 4.16 DMSP _i in red coralline algae from Western Antarctic Peninsula. ...	147
Figure 5.1 Seasonal variation in DMS/P in the Western English Channel.	155
Figure 5.2 Modelled global DMS, DMSP _p and DMSP _d across an annual cycle.	157
Figure 5.3 Sampling locations in Loch Sween, west coast of Scotland.	160
Figure 5.4 Abiotic variables in Loch Sween, March 2010 - March 2012.	165
Figure 5.5 DMS/P measurements in Loch Sween.	167
Figure 6.1 Global surface warming projections to year 2100.	177
Figure 6.2 Global trends of very wet days since 1951.	179
Figure 6.3 Location of low and variable salinity habitats in Scotland.	181
Figure 6.4 Surface salinity at Las Cruces, central Chile, during a storm.	183
Figure 6.5 Aquarium set-up for chronic salinity reduction experiment.	185
Figure 6.6 Encrusting coralline algae from central Chile.	187
Figure 6.7 Experimental set-up for acute salinity reduction.	188
Figure 6.8 Abiotic parameters of the 21 day salinity experiment.	191
Figure 6.9 Thalli at the end of the 21-day salinity experiment.	192
Figure 6.10 Intracellular DMSP concentrations in <i>L. glaciale</i>	192

Figure 6.11 Photosynthetic parameters of <i>L. glaciale</i>	194
Figure 6.12 Photochemical response of <i>L. glaciale</i>	195
Figure 6.13 Photoprotective response of <i>L. glaciale</i>	196
Figure 6.14 Pigment composition of <i>L. glaciale</i>	198
Figure 6.15 ESEM images of the epithelial cells of <i>L. glaciale</i>	199
Figure 6.16 Results from the 64 hour runoff simulation experiment.	201
Figure 6.17 Diurnal variation in F_v/F_m in coralline algae at Las Cruces, Chile.	202
Figure 7.1 The oceanic carbonate equilibrium.	210
Figure 7.2 Observed atmospheric and oceanic CO ₂ and oceanic pH.	211
Figure 7.3 Mesocosm set-up for laboratory OA experiment.	218
Figure 7.4 Cross-section of Suleman reef, Gulf of Aqaba, Egypt.	221
Figure 7.5 Examples of the macroalgae sampled at Suleman reef, Egypt.	223
Figure 7.6 DMS/P at the end of the laboratory OA experiment.	226
Figure 7.7 Surface epithelial cells of <i>L. glaciale</i>	227
Figure 7.8 Abiotic parameters from Suleman reef, Egypt.	229
Figure 7.9 Carbonate system parameters from Suleman reef, Egypt.	230
Figure 7.10 DMS/P on the reef flat and crest of Suleman Reef, Egypt.	232
Figure 8.1 Structure of the kelp forest ecosystem in Nova Scotia.	244
Figure 8.2 Hurricane Earl track, 25 th August - 4 th September 2010.	247
Figure 8.3 Mesocosm set-up for kelp DMS/Pd experiment.	249
Figure 8.4 Mesocosm set-up for coralline algae (CA) DMS/Pd experiment.	250
Figure 8.5 Examples of (a) kelp and (b) coralline algae mesocosms.	251
Figure 8.6. Experimental set-up for coralline algal DMSPi experiment.	252
Figure 8.7. Examples of experiment three set-up.	252
Figure 8.8 Dissolved DMS/P (nmol L ⁻¹) within the kelp bed ecosystem.	254
Figure 8.9. Dissolved DMS/P (nmol L ⁻¹) following two days incubation.	255
Figure 8.10. Coralline algal DMSPi (mg S g ⁻¹ biomass as DMS/P).	256
Figure 8.11 Hurricane tracks in the eastern Pacific and north Atlantic.	260
Figure 8.12 Proposed future kelp forest ecosystem.	263
Figure 9.1 Annually averaged DMS/P in Loch Sween, Scotland.	269

List of tables

Table 1.1 Major fluxes of the global atmospheric sulphur gases.	35
Table 1.2. Growth rates of five free-living coralline algae species.	43
Table 1.3 Absorbance wavelengths of photosynthetic pigments.	48
Table 1.4 Carotenoid composition of species within the Order Corallinales.	49
Table 2.1 Photosynthetic characteristics and definitions.	71
Table 3.1 Photosynthetic parameters calculated from RLCs of <i>L. glaciale</i>	97
Table 3.2 t-test comparisons of coralline algal E_k between 0700 and 1200.	104
Table 3.3 t-test comparisons of coralline algal $F_q'/F_{m'_{max}}$	105
Table 3.4 Linear relationships between E_k or $F_q'/F_{m'_{max}}$ and PAR.	106
Table 4.1 Details of the global scale sampling locations.	129
Table 4.2 Macroalgae sampled for the trans-Atlantic comparison.	131
Table 4.3 Details of the west coast of Scotland regional sampling locations.	132
Table 4.4 Species classification of Antarctic encrusting algae.	138
Table 4.5 Abiotic parameters associated with global-scale samples.	140
Table 4.6 Transatlantic comparison t-test results.	141
Table 5.1 DMS/P sampling regime in Loch Sween, Mar 2010 - Feb 2012.	161
Table 5.2 Most parsimonious GAM models from the mgcv package in R.	168
Table 6.1 Target salinities for the 21-day experiment.	185
Table 6.2 Acute salinity reduction sampling regime.	190
Table 7.1 Carbonate system parameters for the laboratory OA experiment.	224
Table 7.2 Nutrient concentrations at the end of the OA experiment.	224
Table 7.3 Percent calcification of macroalgae from Suleman Reef, Egypt.	231
Table 8.1 The Saffir-Simpson Hurricane Wind Scale.	259

Publications arising from this research

Published:

Chapter 3: BURDETT, H. L., HENNIGE, S., FRANCIS, F., T.-Y. & KAMENOS, N. A. 2012. The photosynthetic characteristics of red coralline algae, determined using pulse amplitude modulation (PAM) fluorometry. *Botanica Marina*, 55, 499-509.

Chapter 7: BURDETT, H. L., ALOISIO, E., CALOSI, P., FINDLAY, H. S., WIDDICOMBE, S., HATTON, A. D. & KAMENOS, N. A. 2012. The effect of chronic and acute low pH on the intracellular DMSP production and epithelial cell morphology of red coralline algae. *Marine Biology Research*, 8, 756-763.

Under review:

Chapter 4 and 7: BURDETT, H. L., DONOHUE, P. J. C., HATTON, A. D., ALWANY, M. A. & KAMENOS, N. A. in review. Spatiotemporal variability of dimethylsulphoniopropionate on a fringing coral reef: the role of reefal carbonate chemistry and environmental variability. PLoS ONE.

In preparation:

Chapter 3: BURDETT, H. L., KEDDIE, V., MACARTHUR, N., MCDOWALL, L., MCLEISH, J., SPIELVOGEL, E. & KAMENOS, N. A. Biochemical and photosynthetic properties of tropical red coralline algae in the Red Sea across a diurnal period. *Tropical ecology*.

Chapter 4: BURDETT, H. L., HATTON, A. D. & KAMENOS, N. A. Irradiance-mediated decrease in dimethylsulphoniopropionate (DMSP) in Antarctic red coralline algae. *Polar Biology*.

Chapter 5: BURDETT, H. L., HATTON, A. D. & KAMENOS, N. A. Seasonal variation in dimethylsulphoniopropionate and dimethylsulphide in a Scottish maerl bed. *Estuarine Coastal and Shelf Science*.

Chapter 6: BURDETT, H. L., HATTON, A. D. & KAMENOS, N. A. Effect of chronic salinity reduction on intracellular DMSP, photosynthetic characteristics and pigment composition in red coralline algae. *Estuarine Coastal and Shelf Science*.

Associated publications not directly contributing to this research:

BURDETT, H., KAMENOS, N. A. & LAW, A. 2011. Using coralline algae to understand historic marine cloud cover. *Palaeogeography, Palaeoclimatology, Palaeoecology*, 302, 65-70.

CARRUTHERS, M., BURDETT, H. L., DONOHUE, P. J. C., WICKS, L. C., HENNIGE, S. J., ROBERTS, J. M. & KAMENOS, N. A. In review. The effect of elevated temperature and CO₂ on intracellular DMSP in the cold-water coral *Lophelia pertusa*. *Deep Sea Research Part I: Oceanographic Research Papers*.

RIX, L. N., BURDETT, H. L. & KAMENOS, N. A. 2012. Irradiance-mediated dimethylsulphoniopropionate (DMSP) responses of red coralline algae. *Estuarine, Coastal and Shelf Science*, 96, 268-272.

International conference presentations

Chapter 3:

Two-tone rhodoliths: the photosynthetic and biochemical properties of free-living coralline algae in the Egyptian Red Sea (poster presentation). 4th International Rhodolith Workshop, Granada, Spain, September 2012.

Chapter 4:

The potential impact of coralline algal habitats on local climate (oral presentation). Assemble Marine, Olhão, Portugal, October 2012.

Chapter 5:

Seasonal cycling of DMSP in a Scottish maerl bed (oral presentation). 4th International Rhodolith Workshop, Granada, Spain, September 2012.

Chapter 7:

Biochemical and morphological effect of low pH on *Lithothamnion glaciale* (oral presentation). 4th International Rhodolith Workshop, Granada, Spain, September 2012.

High CO₂ induces a new pathway for the release of DMSP from coralline algae (oral presentation). ASLO Aquatic Sciences Meeting, San Juan, Puerto Rico, February 2011.

Coming apart at the seams (poster). 5th International Symposium on the Biological and Environmental Chemistry of DMS(P) and Related Compounds, Goa, October 2010.

Chapter 8:

Might climate change play a role in urchin-mediated export of DMSP in eastern Canada? **Outstanding Student Presentation Award**, Ocean Sciences meeting, Salt Lake City, February 2012.

Acknowledgements

Firstly, I thank NERC for awarding me a MSc studentship prior to this PhD and for providing the initial funding for this research. Additional financial research support was also gratefully received from The Geological Society, Assemble Marine and the College of Science and Engineering Mobility fund at the University of Glasgow.

I am indebted to my two supervisors, Nick Kamenos (Glasgow) and Angela Hatton (Scottish Association for Marine Science). Your unbounded knowledge and remarkable enthusiasm on all things algae and DMSP made my PhD journey exciting and diverse, if a little frantic! A special mention also goes to Seb Hennige at Heriot-Watt University for introducing me to the acronym-plagued world of photosynthesis. In addition, I could not have completed the work presented here without the help of many mildly insane academics, technicians and grad students (in no particular order): Bob Scheibling, Kira Krumhansl, Fiona Francis (Miss CA), John Lindley, Andy Mogg, Jean-Claude Roca, Bruno Hesse, the OOB boat crew, Peter Chung, Simon Morley, Jon James, Helen Findlay, Piero Calosi, Virginie Boutel, John Liddell and Randy Finke. I also thank the Biomin (now Biogeo) group meeting attendees for interesting and productive discussions about biominerals (which will be forever exquisite), biogeochemistry and climate change.

My sincerest gratitude extends to Dr Lemoine at the Clinique de l'Esperance, Cluses, France, for bolting my elbow back together mid-way through my PhD (oops...), and to my physios Iain and Shona for helping me to prove the fracture clinic wrong and get my arm back in excellent working order.

The past few years have no doubt been made easier by excellent office buddies past and present: Susan, Laura, Joanne (Dr Joe), Clare (Mrs Frew), Mahmood, Ram, Bohzi, Rachael, (psycho-) Heiko, Penny, Rebecca, Jill(do), Heather, Crystal, Callum, Mark and Eric. Special thanks also go to Joanne and all those at Dumbarton AAC - I can't understand most of you (particularly after a

few drinks) but you keep me smiling nonetheless! And of course to my girls - Ruth W, Ruth B and Lucy: thank you for the weekends away from work, for numerous bottles of wine and for spectacular dancing!

Last, but by no means least, an enormous thank-you goes to my family at Fairhaven - Mum, Dad, Grandma, Charlie and Poppy (and the rest of the menagerie, especially the late Tigger). Without your financial and moral encouragement for the past 20-something years, I would not have been able to achieve my potential. Without the isolation of rural North Devon as a retreat from city life, I would have most certainly gone (even more) insane. Without your undying love and support, my time as a PhD student would not have been as enjoyable or productive. Thank you.

“The nitrogen in our DNA, the calcium in our teeth, the iron in our blood and the carbon in our apple pies were made in the interiors of collapsing stars. We are made of starstuff.”

— Carl Sagan

Author's declaration

I declare that this thesis, except where acknowledged to others, represents my own work carried out in the School of Geographical and Earth Sciences, University of Glasgow, and the Scottish Association for Marine Science. The research presented here has not been submitted for any other degree at the University of Glasgow, nor at any other institution. Any published or unpublished work by other authors has been given full acknowledgement in the text.

Heidi Burdett

Definitions and abbreviations

AB	Above Bed
ABS	Above Bed Side
ADP	Adenosine diphosphate
AIS	Antarctic Ice Sheet
AL	Actinic light
AMO	Atlantic Meridonal Oscillation
ANOVA	Analysis of variance
APC	Allophycocyanin
ATP	Adenosine triphosphate
BATS	Bermuda Atlantic Time Series
BoA	Bridge over the Atlantic
BS	Bed Side
C	Control
Ca ²⁺	Calcium ion
CaCO ₃	Calcium carbonate
CC	Cloud cover
CCN	Cloud condensation nuclei
CCS	Carbon capture and storage
Chl- <i>a</i>	Chlorophyll- <i>a</i>
CLAW	Climate feedback hypothesis involving DMS
CO ₂	Carbon dioxide
CO ₃ ²⁻	Bicarbonate ion
COS	Carbonyl sulphide
CS ₂	Carbon disulphide
D	Dark
DIC	Dissolved Inorganic Carbon
DL	Daylength
DMS	Dimethylsulphide
DMS/P	DMS+DMSP
DMS/Pd	Dissolved DMS+DMSP
DMS/Pp	Particulate DMS+DMSP
DMSHB	4-dimethylsulphonio-2-hydroxybutyrate
DMSO	Dimethylsulphoxide
DMSP	Dimethylsulphoniopropionate
DMSPd	Dissolved DMSP
DMSPi	Intracellular DMSP
DMSPp	Particulate DMSP
DMSPt	DMSPd+DMSPp
DO	Dissolved oxygen
<i>E</i>	<i>See PAR</i>
<i>E_k</i>	Light saturation coefficient ($\mu\text{mol photons m}^{-2} \text{s}^{-1}$)
EN	Encrusting
ENSO	El Niño Southern Oscillation
ESEM	Environmental Scanning Electron Microscope
ETR	Electron Transport Rate ($\mu\text{mol electrons m}^{-2} \text{s}^{-1}$)

F'	Fluorescence under actinic light
FLT	Free-living topside
FLU	Free-living underside
F_m	Maximum fluorescence (dark acclimated)
F_m'	Maximum fluorescence (light acclimated)
F_o	Minimum fluorescence (dark acclimated)
F_o'	Minimum fluorescence (light acclimated)
FPD	Flame Photometric Detector
F_q'	Fluorescence quenched ($F_m - F'$)
F_q'/F_m'	Effective quantum efficiency of PSII under actinic light
$F_q'/F_{m'_{max}}$	Calculated maximum quantum efficiency of PSII
F_q'/F_v'	Photochemical quenching (qP) under actinic light
FR	Far-red illumination
F_v	Variable fluorescence (dark acclimated)
F_v'	Variable fluorescence under actinic light
F_v/F_m	Maximum quantum efficiency of PSII (dark acclimated)
F_v'/F_m'	Non photochemical quenching (qN) under actinic light
GAM	Generalised Additive Model
GC	Gas Chromatography
GCV	Generalised Cross Validation
H_2CO_3	Carbonic acid
H_2S	Hydrogen sulphide
HC	Hangar Cove
HCl	Hydrochloric acid
HCO_3^-	Hydrogen carbonate ion
$HgCl_2$	Mercuric chloride
IPCC	Intergovernmental Panel on Climate Change
IPO	Inter-decadal Pacific Oscillation
ISSAC	Imaging Spectroscopy and Analysis Centre
KB	Kentra Bay
L	Low salinity treatment group
LA	Loch Ailort
LED	Light Emitting Diode
LS	Loch Sween
LT	Loch Torridon
MB	Maerl bed site
MeSH	Methanethiol
Mg	Magnesium
MSA	Methane sulphonic acid
NADP	Nicotinamide adenine dinucleotide phosphate
NAO	North Atlantic Oscillation
NaOH	Sodium hydroxide
NC	Not cleaned
NOAA	National Oceanic and Atmospheric Administration
NPQ	Non-photochemical quenching ($[F_m - F_m']/F_m'$)
O_2	Oxygen
OA	Ocean acidification
PA	Plockton Airstrip

PAM	Pulse Amplitude Modulation
PAR	Photosynthetically Active Radiation ($\mu\text{mol photons m}^{-2} \text{ s}^{-1}$)
PC	Phycocyanin
$p\text{CO}_2$	Partial pressure of CO_2
PDO	Pacific Decadal Oscillation
PE	Phycoerythrin
PML	Plymouth Marine Laboratory
PS I	Photosystem I
PS II	Photosystem II
PTFE	Polytetrafluoroethylene
Q_A	First electron carrier
Q_B	Second electron carrier
QBO	Quasi-biennial oscillation
qN	Non photochemical quenching
qP	Photochemical quenching
$r\text{ETR}$	Relative electron transport rate ($\mu\text{mol electrons m}^{-2} \text{ s}^{-1}$)
$r\text{ETR}_{\text{max}}$	Maximum relative electron transport rate ($\mu\text{mol electrons m}^{-2} \text{ s}^{-1}$)
RG	Rose Garden
RLC	Rapid Light Curve
SC	South Cove
SCUBA	Self-Contained Underwater Breathing Apparatus
SE	Secondary electron
SEM	Scanning Electron Microscope
SLE	St Lawrence Estuary
SO_2	Sulphur dioxide
SO_4	Sulphate
SP	Saturating pulse
SST	Sea Surface Temperature
T	<i>In situ</i> water temperature
TA	Total alkalinity
TPRS	Thin plate regression spline
UV	Ultraviolet
VL	Very low salinity treatment group
WAP	Western Antarctic Peninsula
WEC	Western English Channel
α	Initial slope of the light dependent part of a Rapid Light Curve
ΔpH	Proton gradient across photosynthetic membrane
Ω_{Ar}	Aragonite saturation state
Ω_{Ca}	Calcite saturation state

1

Introduction

Research into the marine biogenic sulphur cycle has historically focussed on the role of plankton in the open ocean. Some studies have eluded to the potential importance of the coastal ocean in the marine sulphur cycle (e.g. Lana et al., 2011), but this suggestion is bounded by large uncertainties. Coralline algal habitats are fundamental ecological and structural components of the global coastal zone and thus may be important in the coastal biogeochemical cycling of macronutrients such as sulphur.

1.1 The oceanic sulphur cycle

The global sulphur cycle involves the atmosphere, the lithosphere, the hydrosphere and the biosphere. The oceans are a particularly important component, acting as a source for, and sink of, sulphur compounds. Sulphur is transported to the oceans via rivers, where it is derived from the weathering of sulphides and the dissolution of calcium sulphates (Hurtgen, 2012). Such processes have led to sulphate becoming the fourth most abundant ion in seawater (Halevy et al., 2012). The microbial reduction of sulphur compounds can affect the biogeochemical cycling of sulphur in the oceans and the oxidation state of the atmosphere (Halevy et al., 2012); it has been suggested that the oceanic sulphur cycle is critical in determining atmospheric oxygen levels over geological timescales (Hurtgen, 2012; Canfield, 2005). Moreover, sulphate aerosols derived from the oceans may instigate an atmospheric cooling effect, in part driving global climate cooling (Wortmann and Paytan, 2012).

1.1.1 Dimethylsulphide

The oceanic biosphere regulates the reduction and oxidation of sulphur compounds, thus affecting the balance of the global sulphur cycle. Dimethylsulphide (DMS) is a significant natural source of atmospheric reduced sulphur and is primarily derived from biological activity in the oceans (Brimblecombe et al., 1989). DMS ($\text{CH}_3\text{-S-CH}_3$) was first reported by Haas (1935) in the red macroalga *Polysiphonia* (now *Vertebrata*) *lanosa*, which also contains high concentrations of the major precursor to DMS, dimethylsulphoniopropionate (DMSP). DMS is considered one of the most important compounds within the marine sulphur cycle; it is estimated that more than 90% of the total oceanic biogenic sulphur emissions are derived from DMS, equating to 50% of the world's total biogenic sulphur budget (Wiesemeier and Pohnert, 2007).

1.1.1.1 The CLAW hypothesis

The emission of DMS from the oceans has been linked to a climate feedback mechanism known as the CLAW hypothesis (Figure 1.1) (after the authors of the associated paper, Charlson et al., 1987). Shaw (1983) was the first to propose a biothermostasis mechanism involving the sulphur cycle rather than the previously favoured carbon cycle. He described how oxidation of the sulphur gases cycling within the ocean-atmosphere cycle could form sulphate (SO_4) aerosols, altering planetary albedo. However, this remained a purely hypothetical proposition as no empirical evidence was available. Instead, it was suggested that this process might only be important if atmospheric carbon dioxide levels were low enough to cause metabolic stress.

Charlson et al. (1987) developed Shaw's idea and showed how a SO_4 aerosol feedback mechanism may buffer atmospheric temperature (Figure 1.1): marine algal productivity is intensified following an enhanced greenhouse effect from a rise in atmospheric CO_2 , increasing the production of DMS. This increases the net flux of DMS from the ocean to the atmosphere, promoting the formation of acidic aerosols including methanesulphonic acid (MSA), sulphur dioxide (SO_2) and SO_4 (Yoch, 2002), generating more cloud condensation nuclei (CCN), increasing cloud albedo and counter-acting the warming effect of increased atmospheric CO_2 (Charlson et al., 1987).

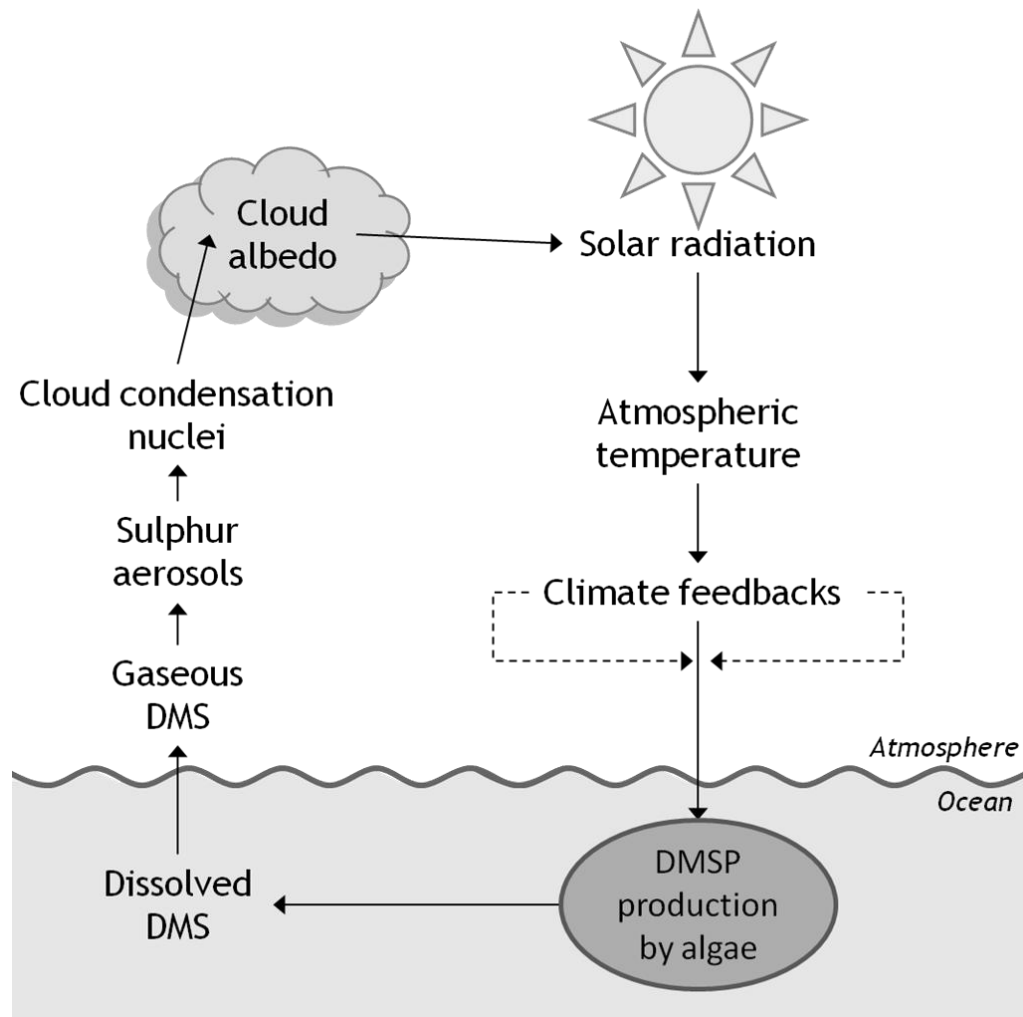


Figure 1.1 The proposed DMS climatic feedback mechanism. Termed the CLAW hypothesis after Charlson et al. (1987). Adapted from: Andrews et al. (2004).

Charlson et al. (1987) could not quantitatively describe the relationship between DMS emissions and CCN formation. It was estimated that to counteract the warming effect of a doubling in atmospheric CO_2 , double the number of CCN would be required (Charlson et al., 1987). Modelling studies have since estimated that 27% of the globally averaged atmospheric SO_2+SO_4 concentrations are derived from DMS emitted from the open ocean (>300 m deep, Kloster et al., 2006). The contribution of the coastal ocean to atmospheric SO_2+SO_4 (representing ~10% of the ocean surface, but with higher DMS concentrations than the open ocean; Lana et al., 2011) has not yet been quantified.

The CLAW hypothesis relies on a number of somewhat large assumptions. Firstly, that sulphate aerosols derived from oceanic DMS create new clouds rather than adding to existing ones (which have a lower albedo, Wingenter et al., 2007a). This process is dependent on many factors such as atmospheric

temperature and oxidant concentration (Wingenter et al., 2007a). Secondly, the impact of increased / decreased temperature on the production of DMSP by algae is unclear. For example, the community composition and absolute numbers of phytoplankton in the surface ocean will significantly influence the amount of DMSP produced and subsequent potential for DMS emission (e.g. Archer et al., 2009). As such, uncertainty still lies around the global applicability of the CLAW hypothesis (e.g. Vogt et al., 2008 and Environmental Chemistry, 2007, vol. 4). It has been proposed that the CLAW hypothesis may not significantly regulate climate at a global scale, but may still be important on local scales (Ayers and Cainey, 2007). Despite this, geoengineering projects (such as iron fertilisation) have been proposed to increase CO₂ sequestration and to increase oceanic DMS emissions and subsequent CCN formation (e.g. Wingenter et al., 2007a).

Another assumption associated with the CLAW hypothesis is the direct link between algal DMSP, dissolved DMS and the flux of DMS from the ocean. A number of alternative reaction pathways may limit the amount of algal DMSP that reaches the atmosphere via DMS emissions. DMS dissolved in the water column may be oxidised to form dimethylsulphoxide (DMSO) or methanethiol (MeSH) and formaldehyde, through photo-oxidation or bacterial action (Del Valle et al., 2009). Faecal pellets may be important sinks for DMS and DMSP, which can be subsequently oxidised to DMSO (Hatton, 2002), acting as a sulphur removal mechanism out of the photic zone into deeper waters and / or benthic sediments (Hatton et al., 2004; Hatton, 2002). Bacterial utilisation may also reduce DMSO to DMS, acting as a source of dissolved DMS to the water column (Spiese et al., 2009; Vila-Costa et al., 2006). Dimethylated sulphur compounds (including DMS, DMSP and DMSO) are important bacterial carbon and sulphur sources (Green et al., 2011; Schäfer et al., 2010; Vila-Costa et al., 2006), and their utilisation may be driven by the availability of other carbon substrates (Hatton et al., 2012a). Thus, the cycling of dimethylated sulphur compounds may have significant implications for overall ecosystem function.

1.1.2 Dimethylsulphoniopropionate

DMSP (C₅H₁₁O₂S) was first discovered by Challenger and Simpson (1948) in the red macroalga *Polysiphonia fastigiata* (now *Vertebrata lanosa*). Since then, it has been established that DMSP is produced by most marine algae and has

numerous cellular functions, including as a compatible solute (Kirst, 1996; Kirst et al., 1991; Kirst, 1989), an antioxidant (Sunda et al., 2005; Sunda et al., 2002), a cryoprotectant (Karsten et al., 1996; Kirst et al., 1991), a grazing deterrant (Van Alstyne et al., 2001; Wolfe et al., 1997; Wolfe and Steinke, 1996) and as a grazing attractant (Seymour et al., 2010). Chapters 3 - 8 provide more detailed discussions on the intracellular functions of DMSP.

1.1.2.1 The production of DMSP

Algal DMSP production is highly species-specific. In phytoplankton, prymnesiophytes and dinoflagellates typically have high intracellular DMSP (DMSPi) concentrations compared to diatoms, which are considered low DMSPi-producers. In macroalgae, Chlorophyta generally contain more DMSPi than Ochrophyta (formerly Phaeophyta) and Rhodophyta (Van Alstyne and Puglisi, 2007, and see Chapter 4). The intracellular precursor to DMSPi is the amino acid methionine ($C_5H_{11}NO_2S$) (Greene, 1962), an indirect product of photosynthesis and an essential component of the proteins involved in photosynthesis (Wirtz and Droux, 2005). There appears to be at least three production pathways for DMSPi, identified from different primary producers (Figure 1.2) (Stefels, 2000). This, combined with the high inter-species variation in DMSPi, has led to the suggestion that the ability to produce DMSP has evolved several times (Van Alstyne and Puglisi, 2007).

The most well-known pathway is that from the Indo-Pacific strand plant, *Wollastonia biflorai* (Hanson et al., 1994). This pathway utilises the Ado-Met protein for the methylation of methionine to form S-methylmethionine and continues to DMSP via DMSP-aldehyde (Figure 1.2). The pathway identified in the salt-marsh grass *Spartina alterniflora* is similar, but with an additional intermediate of 3-dimethylsulphoniopropylamine (Figure 1.2) (Kocsis et al., 1998). The marine algal DMSP production pathway was first identified in *Ulva* (previously *Enteromorpha*) *intestinalis* and appears to be completely different (Figure 1.2) (Summers et al., 1998; Gage et al., 1997). Firstly, a reversible transamination step forms 4-methylthio-2-oxobutyrate. The second reduction step, mediated by reduced nicotinamide adenine dinucleotide phosphate (NADPH), forms 4-methylthio-2-hydroxybutyrate. This is followed by an Ado-Met driven methylation to form 4-dimethylsulphoio-2-hydroxybutyrate (DMSHB), and

subsequent decarboxylation to DMSP (Figure 1.2). The presence of the DMSHB intermediate in other marine phytoplankton (*Emilania huxleyi*, *Melosira nummuloides* and *Tetraselmis* sp.) has led to the belief that this is the primary route for DMSP production in marine algae (Gage et al., 1997).

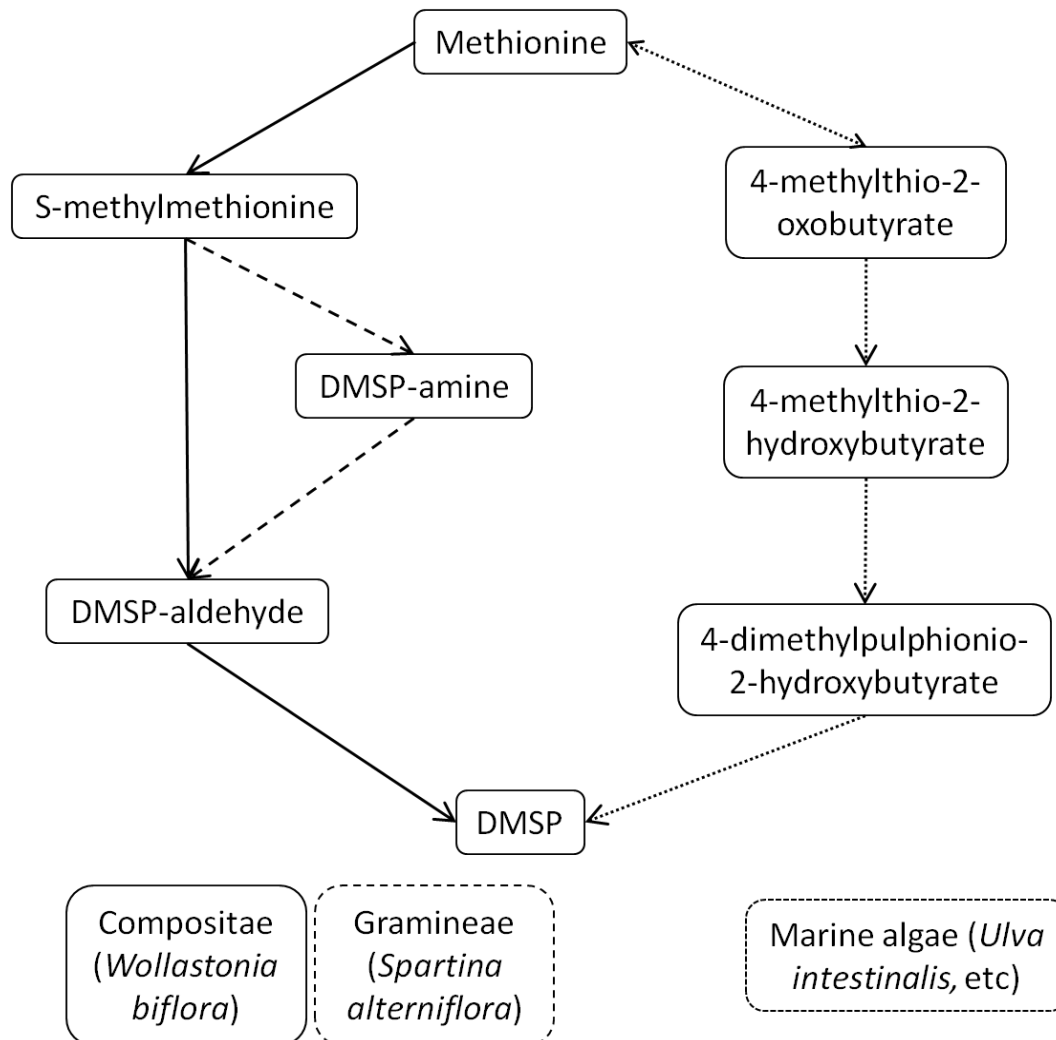


Figure 1.2 The three known DMSP production pathways. Source: Stefels (2000).

1.1.2.2 The release of DMSP

It was originally speculated that DMSP was released from algal cells by enzymatic action (Challenger and Simpson, 1948). However, more recent studies have shown that DMSP is primarily lost from cells due to grazing damage (Wolfe et al., 2002; Wolfe et al., 1994), viral (Bratbak et al., 1995) and microbial lysis (van Boekel et al., 1992) or senescence (Yoch, 2002). DMSP may also be actively exported out of the cell during periods of nitrogen limitation, acting as an overflow mechanism (Stefels, 2000). More detailed discussions on the processes involved in the release of DMSP from algae can be found in Chapters 6 - 8.

1.1.2.3 The degradation of DMSP

When DMSP is released from algal cells, it becomes available to bacterioplankton for subsequent degradation and utilisation (Kiene et al., 2000). Two DMSP degradation pathways have been identified (Figure 1.3) (Moran et al., 2012):

1. Cleavage to form DMS, which may then flux to the atmosphere, and acrylate or 3-OH propionate.
2. Demethylation to form MeSH, which may then be readily oxidised by biological and chemical processes.

The genes required for DMSP cleavage are relatively widespread, particularly in the α -*Proteobacteria* (Zubkov et al., 2002; Gonzalez et al., 2000; Gonzalez et al., 1999), and may be subject to horizontal gene transfer between bacterial species and from bacteria to fungi (Todd et al., 2009). Acrylate, which may be produced from the cleavage pathway (Figure 1.3), is utilised by a range of bacteria as a carbon source (Noordkamp et al., 2000), although it can inhibit bacterial growth at high concentrations (Noordkamp et al., 2000).

Photobacterium, *Halomonas*, *Shewanella*, *Proteobacteria* and *Vibrio* spp. all appear to positively respond to acrylate enrichment (Raina et al., 2009; Johnston et al., 2008; Ansele et al., 2001; Sjoblad and Mitchell, 1979). Given that *Vibrio* spp. are associated with coral disease (Thomas et al., 2010; Sussman et al., 2008; Reshef et al., 2006), it has been proposed that DMSP cleavage and subsequent acrylate metabolism may play a role in coral health (Raina et al., 2009).

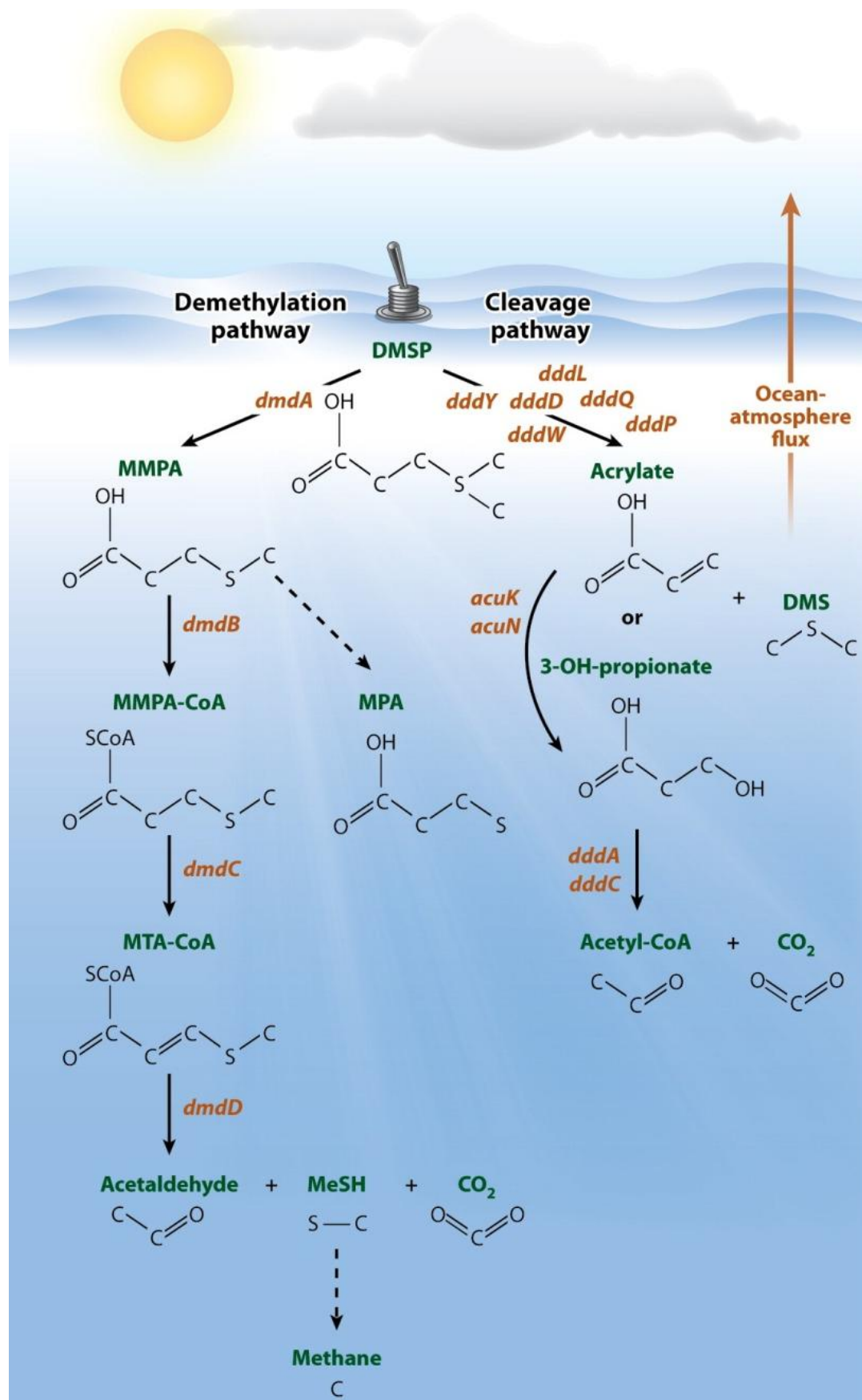


Figure 1.3 The two major DMSP degradation pathways.

Orange italic text indicates the genes required for each step. Green bold text indicates the reaction products at each step. Abbreviations: CoA, coenzyme A; MeSH, methanethiol; MMPA, 3-methylpropionate; MPA, 3-mercaptopropionate; MTA, methylthioacrylyl. Source: Moran et al. (2012).

The demethylation pathway yields compounds that may be utilised by the demethylating organism, thus may be more ecologically advantageous than the cleavage pathway (Simo et al., 2002; Kiene et al., 2000; Kiene et al., 1999). The enzymes required for demethylation appear to be ubiquitous in marine bacteria (Reisch et al., 2011), which may explain why up to 90% of dissolved DMSP may be degraded by demethylation rather than cleavage (Kiene and Linn, 2000; Kiene et al., 2000). The demethylation pathway may also have significant atmospheric implications (Damm et al., 2010) by:

1. Directly competing with the cleavage pathway that yields DMS.
2. Producing MeSH, which may ultimately lead to methane, an important greenhouse gas.

The chemical hydrolysis of DMSP to DMS, although in principle a valid pathway, is unlikely to be a major factor in the breakdown of DMSP to DMS in the oceans due to the slow reaction time; the half life of DMSP in 10 °C seawater is ~ 8 years (Dacey and Blough, 1987).

1.1.3 Cycling of dimethylated compounds in the ocean

The oceanic sulphur cycle involves a number of biogenically produced compounds (Figure 1.4) and a complex series of production, release, degradation and utilisation mechanisms (Figure 1.5). The majority of dimethylated sulphur research has taken place in the open ocean because of its apparently high natural sulphur emissions (Table 1.1) (Brimblecombe et al., 1989), and focussed on phytoplankton because of their potential importance in DMS-mediated climate regulation (Charlson et al., 1987). However, pelagic phytoplankton blooms are temporally and spatially unstable and their species composition has a significant effect on DMSP production and DMS emissions (e.g. Archer et al., 2009). A recent update to oceanic DMS flux estimates suggests that global DMS emissions are 28.1 Tg S yr⁻¹ (Lana et al., 2011). However, the large uncertainties surrounding flux estimates (such as transfer velocity parameters) lead to an error at least as large as this estimate (Lana et al., 2011).

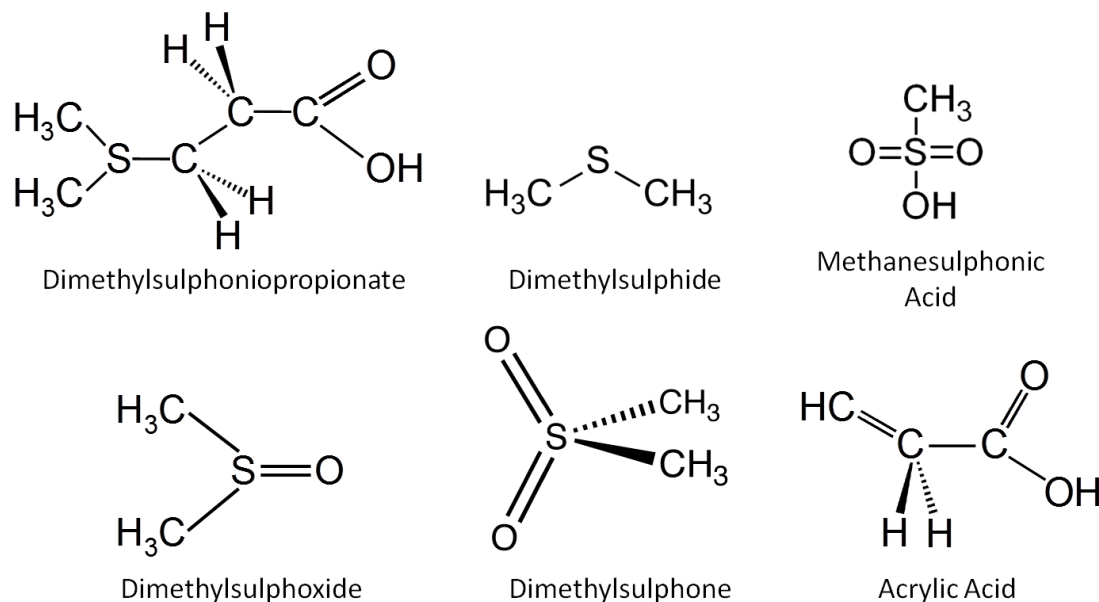


Figure 1.4 Important compounds in the biogenic marine sulphur cycle.

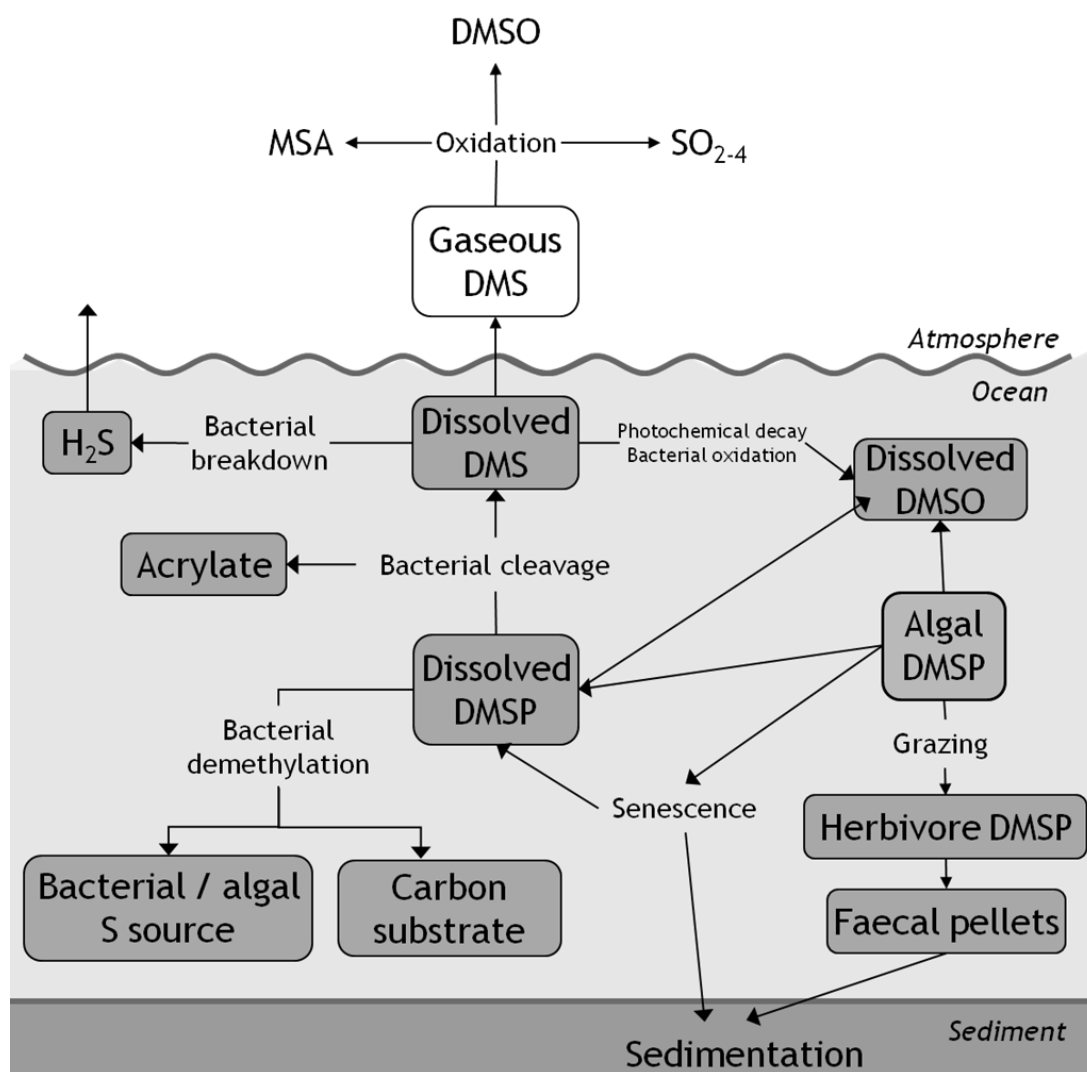


Figure 1.5 The cycling of dimethylated sulphur compounds in the ocean. Adapted from Yoch (2002) and Bigg (1996). DMS: dimethylsulphide, DMSP: dimethylsulphoniopropionate, DMSO: dimethylsulphoxide, MSA: methane sulphonic acid, SO_{2-4} : sulphur dioxide and sulphate, H_2S : hydrogen sulphide, S: sulphur

Table 1.1 Major fluxes of the global atmospheric sulphur gases. Fluxes given as Tg (S) year⁻¹. Parentheses indicate the possible range in flux. COS: carbonyl sulphide, CS₂: carbon disulphide, H₂S: hydrogen sulphide. Source: Brimblecombe et al. (1989).

Flux	SCOPE-19 (Ivanov and Freney, 1983)	Brimblecombe et al. (1989)
Anthropogenic emission SO ₂ , SO ₄ ²⁻	113 (94-132)	93 (79-107)
Volcanic activity, SO ₂ ^a	28 (14-42)	20 (10-30)
Aeolian emission, SO ₄ ²⁻	20 (10-30)	20 (10-30)
COS and CS ₂ emission	5 (3.5-6.5)	5 (3.5-6.5) ^b
Natural terrestrial emissions, DMS, etc	16 (4-30)	20 (5-35)
Natural emissions in coastal oceanic waters, H ₂ S, DMS, etc	5 (0-10)	5 (1-9)
Natural emissions from open ocean, H ₂ S, DMS, etc	15 (0-30)	35 (20-50)
Sea salt emissions, SO ₄ ²⁻	140 (77-203)	144 (77-203)
Precipitation removal over the continents	51 (37.5-64.5)	51 (38-64)
Dry deposition over the continents, SO ₄ ²⁻	16 (5-47)	16 (5-47)
Absorption by the continental surface, SO ₂	17 (7-27)	17 (7-27)
Precipitation removal over the oceans	230 (160-300)	230 (160-300)
Dry deposition over the oceans, SO ₄ ²⁻	17 (3-48)	17 (3-48)
Absorption by the ocean surface, SO ₂	11 (5-17)	11 (5-17)
Transport from the oceanic to the continental atmosphere	20	20
Transport from the continental to the oceanic atmosphere	100.5	81

^a Half of volcanic emission contributes to the oceanic atmosphere

^b 1.5 Tg (S) year⁻¹ contributes to the continental atmosphere

1.1.4 Dimethylated sulphur production in the coastal ocean

A recent estimate suggests that the coastal ocean, which represents 10% of the ocean surface by area, is the source of 11% of the global atmospheric DMS budget (Lana et al., 2011), suggesting that, by area, the coastal ocean (10% of the total ocean surface area) is at least as important as the open ocean in terms of DMS emissions (Table 1.1). Further, anthropogenic sulphate aerosol emissions from ships may be the source of up to half the total atmospheric sulphate load over the open ocean (Capaldo et al., 1999), complicating our understanding of natural oceanic DMS emissions. DMS oxidation and the subsequent potential for CCN formation is enhanced in the coastal zone due to higher atmospheric nitrate

radical (NO_3) concentrations (Brown and Stutz, 2012; Stark et al., 2007; Yvon et al., 1996), highlighting the importance of understanding the coastal marine sulphur cycle.

The ecosystem function of dimethylated sulphur compounds (e.g. Kiene et al., 2000; Kiene and Bates, 1990) may be more important in the coastal ocean relative to the open ocean due to the high biodiversity of coastal habitats at numerous trophic levels. The utilisation of dimethylated sulphur compounds by microbes as a carbon and sulphur source (section 1.1.2.3) and accumulation by macroinvertebrates (Van Alstyne and Puglisi, 2007) may significantly impact sulphur cycling in coastal habitats. The sulphur cycle may also be more complex in the coastal ocean due to enhanced primary productivity and continental influences (Brimblecombe et al., 1989). The sulphur load in coastal waters may be affected by terrestrial processes such as land runoff from sulphur enriched mine and agricultural drainage (which also increases nutrients, further increasing primary productivity), river damming (reducing land runoff) and coastal development (increasing sulphur-enriched land runoff).

In recent years, the production of DMSP by benthic coastal macroalgae has been more thoroughly investigated. Macroalgal systems may be more spatially and / or temporally stable than phytoplankton blooms and some macroalgae produce large quantities of DMSP (see Chapter 4). Thus, coastal macroalgal systems (such as coralline algal systems) may be important contributors to the biogenic marine sulphur cycle. In addition, anthropogenic pressures on the coastal zone may influence the sulphur cycle by disrupting the sources, sinks and turnover of sulphur compounds, demanding a requirement to better understand sulphur dynamics in the coastal ocean.



1.2 Non-geniculate red coralline algae

Non-geniculate red coralline algae (i.e. those that do not possess uncalcified joints) and their associated habitats were the primary focus of this research; geniculate red coralline algae (i.e. those that do possess uncalcified joints, e.g. *Corallina* spp.) will not be considered further. Non-geniculate red

coralline algae (termed coralline algae herein) may encrust rocks or grow as free-living thalli - commonly known as maerl or rhodoliths (Figure 1.6) (Foster, 2001). Coralline algae grow in a wide range of environments within the photic zone and can be major ecological and structural components of coastal habitats such as maerl beds, kelp forests, seagrass meadows, coral reefs and Mediterranean coralligène formations (banks of encrusting coralline algae). The ecological characteristics of coralline algae are directed towards *K*-selection (Pianka, 1970), where population densities are high, population size is stable and individuals exhibit high competitive ability and long life-spans (> 100 years; Parry, 1981; Pianka, 1970).

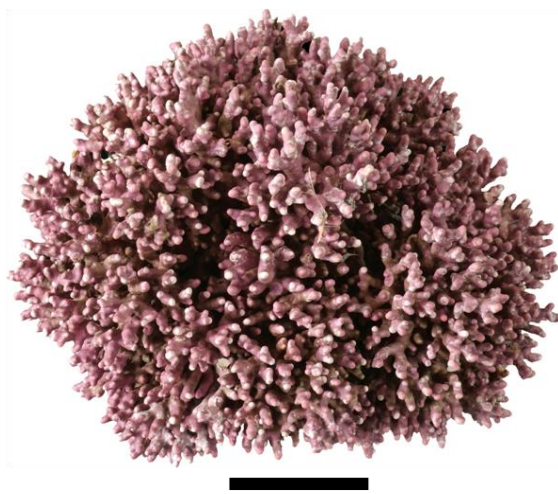


Figure 1.6 Example of a free-living coralline algal thallus. Spherical *Lithothamnion glaciale* thallus collected from the west coast of Scotland, UK, from a depth of 6 m. Scale bar = 20 mm. Photo: L. Hill.

1.2.1 Distribution of coralline algal habitats

The ubiquity of coralline algae has led to their appearance in many coastal habitats from the poles to the equator. Indeed, coralline algae (encrusting and free-living) are key components of a range of economically and ecologically important coastal habitats worldwide, including maerl beds, coralligène formations, kelp forests, coral reefs and seagrass meadows.

1.2.1.1 Maerl and rhodolith beds

When environmental conditions are suitable (light availability, current flow), free-living coralline algae can form dense aggregations on the sea bed, known as maerl or rhodolith beds. Maerl beds are globally distributed, perhaps most notably along the coast of Brazil, the Gulf of California and in the North

Atlantic (Figure 1.7) (Foster, 2001). However, this may simply reflect the areas where scientific studies have taken place, with the true distribution far more widespread (Foster, pers. comm., 2009). Free-living coralline algae have the largest depth range of any aquatic photosynthetic organism and may be found from the intertidal zone (thus forming a maerl beach) to >250 m depth (Peña and Bárbara, 2008; BIOMAERL et al., 2003; Littler et al., 1991). The depth of maerl growth is constrained by the availability of light and a suitable current speed - sufficient water movement is required to prevent sedimentation and algal overgrowth, but not so much as to cause mechanical damage or transport (Foster, 2001).



Figure 1.7 The global distribution of free-living red coralline algae. Black dots indicate recorded locations. Adapted and updated from: Foster (2001).

Individual species distribution appears to be primarily driven by temperature (Foster, 2001; Lüning, 1990; Adey and Adey, 1973). For example, there are three major species in Europe, each with distinct shallow-water distributions: *Phymatolithon calcareum* is the most abundant and ranges from Norway to the Mediterranean, *Lithothamnion coralloides* is found from England and Ireland to the Mediterranean and *Lithothamnion glaciale* occurs from Scotland to the Arctic (JNCC, 2012; Teichert et al., 2012). Interestingly, *L. glaciale* has also been recorded in deeper waters (50 - 250 m) off the coast of

Brazil - where light availability and temperature are comparable to shallower waters at higher latitudes (Foster et al., In press).

1.2.1.2 Coralligène

Encrusting coralline algae may be found along almost every coastline worldwide. However, in the Mediterranean and southeast Brazil (Bassi, pers. comm), encrusting coralline algae forms a unique habitat known as coralligène, where layers of coralline algae overgrow each other, creating large formations which are similar in morphology to tropical coral reefs (Ballesteros, 2006). Coralligène deposits may be >4 m thick and more than 8000 years old (Sartoretto et al., 1996). A comprehensive review of the current knowledge on coralligène has been published by Ballesteros (2006).

1.2.1.3 Kelp forests

Kelp forests 'dominate the shallow rocky coasts of the world's cold-water marine habitats' (Figure 1.8), despite their low taxonomic diversity (Steneck et al., 2002). Kelp forests are located in coastal regions where water temperatures do not exceed 20°C, thus are generally restricted to >30° latitude. Encrusting and free-living coralline algae are a major algal component of kelp forests, often found growing on the rocky substrate within the forest and below the kelp's depth limit. More information on coralline algal-associated kelp forests is provided in Chapter 8, particularly focussing on kelp forests in eastern Canada.

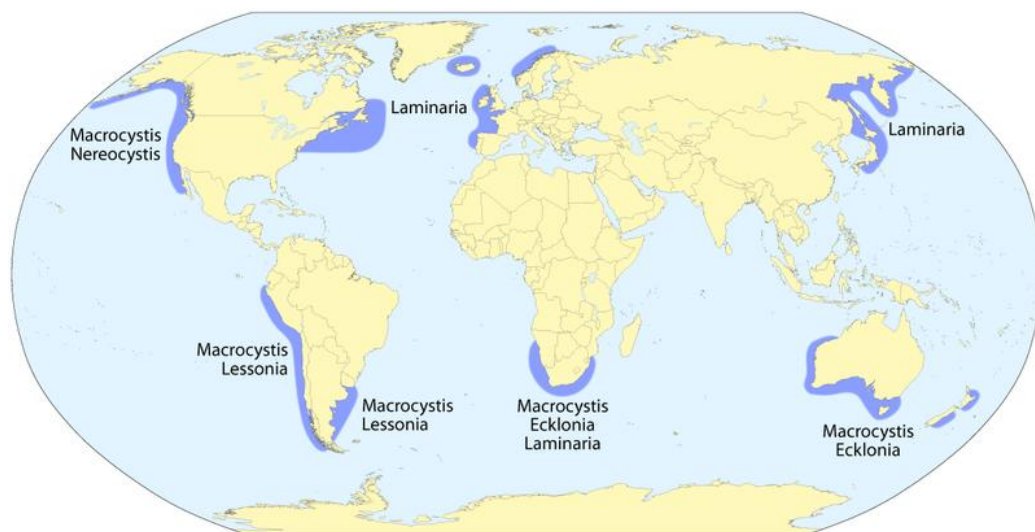


Figure 1.8 The global distribution of major kelp forests. The major genera for each area are listed. Source: Steneck et al. (2002).

1.2.1.4 Coral Reefs

Coral reefs are only found in areas where water temperatures are between 20 - 38°C for the majority of the year (Nybakken and Bertness, 2005). Thus, in contrast to kelp forests, coral reefs are restricted to the low latitude oceans (<30°, Figure 1.9). Coralline algae are critical components of coral reef structures, acting as biogenic cement, stabilising coral-derived carbonate deposits (Tierney and Johnson, 2012; Wilkinson, 2008).

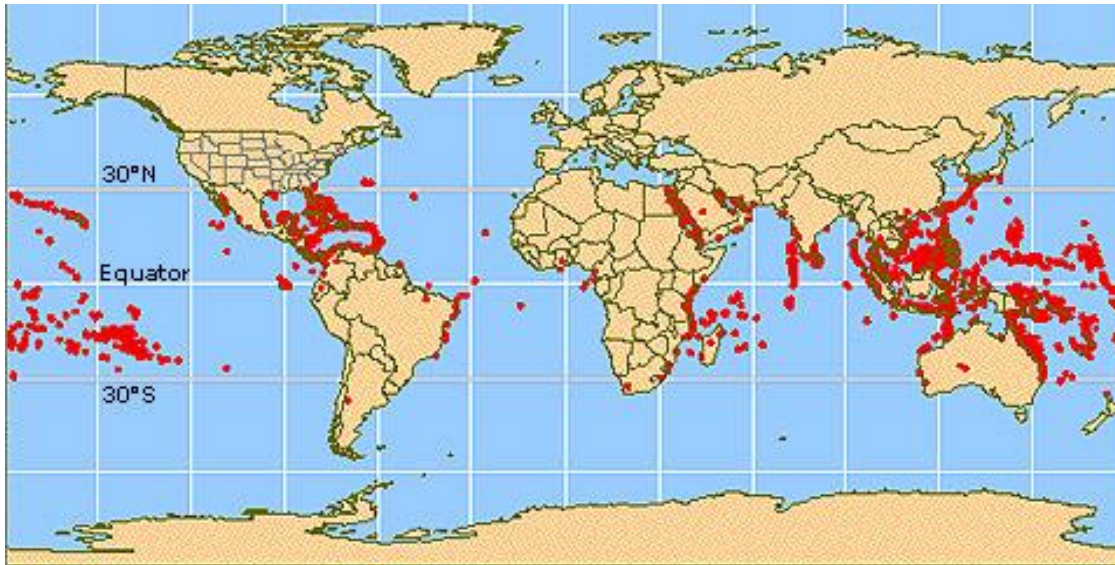


Figure 1.9 The global distribution of coral reefs.
Source: NOAA (2012d).

1.2.1.5 Seagrass meadows

Seagrasses are the only marine angiosperms and, despite their low taxonomic diversity (only ~60 species), form dense meadows in shallow coastal waters worldwide (Figure 1.10) (Green and Short, 2003). The highest diversity in seagrass species may be found in the Indo-Pacific region (Figure 1.10); free-living coralline algae are another important primary producer in seagrass meadows (Burdett, per.obs.). Seagrass meadows may be reliant on sediment supplies from maerl beds, as observed in the north west Mediterranean (Martin et al., 2008).

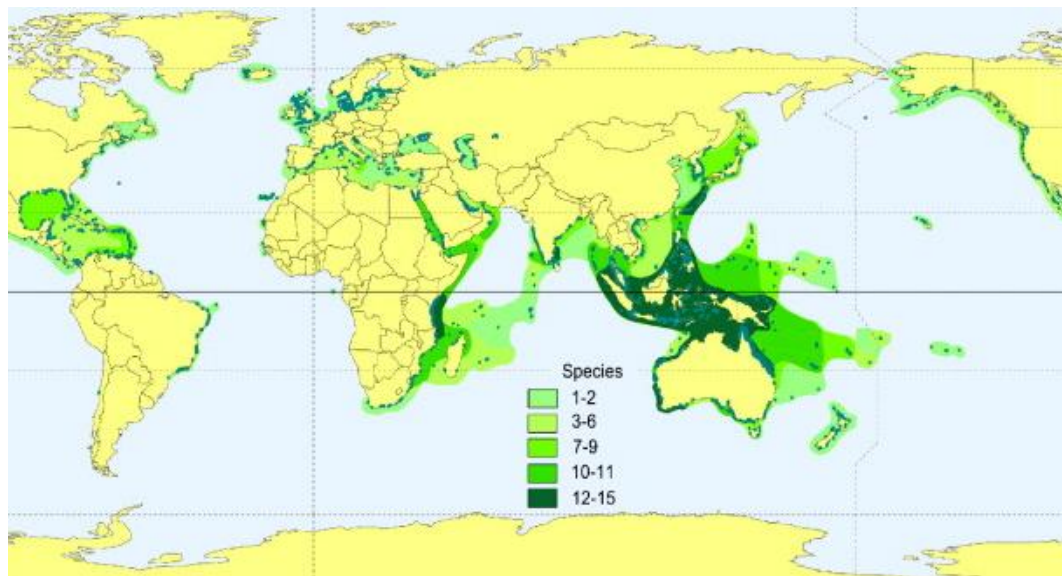


Figure 1.10 The global distribution and diversity of seagrass meadows. Green shading indicates the number of species reported, blue dots indicate documented reports of seagrass occurrence. Source: Short et al. (2007).

1.2.2 Taxonomy

Most non-geniculate coralline algal genera are found within the order Corallinales (Figure 1.11). Only one family (Sporolithaceae) is found in the Order Sporolithales, and is solely non-geniculate (Figure 1.11). The Corallinaceae family contains four sub-families of non-geniculate genera, whilst the Hapalidiaceae family is solely non-geniculate (Figure 1.11).

The taxonomy of coralline algae has been historically based on morphological features, but has recently been backed up by state-of-the-art molecular techniques. A summary of the main diagnostic features associated with each non-geniculate subfamily is given in Harvey et al. (2003). The growth morphology of coralline algae (e.g. the absence / presence of protuberances or colour) may vary within species depending on the specific environmental conditions and is generally not suitable for reliable taxonomic identification. Thus, more detailed examinations of the internal cell structures, particularly focusing on reproductive bodies such as conceptacles, are used in morphological taxonomy. This approach is problematic when considering asexual specimens; asexual reproduction of coralline algae (e.g. by fragmentation) may be just as important as sexual reproduction (Foster, 2001). The molecular identification of coralline algae through DNA sequencing began to develop in the early 2000s; an ever-growing DNA database is available for reference (Harvey et al., 2003).

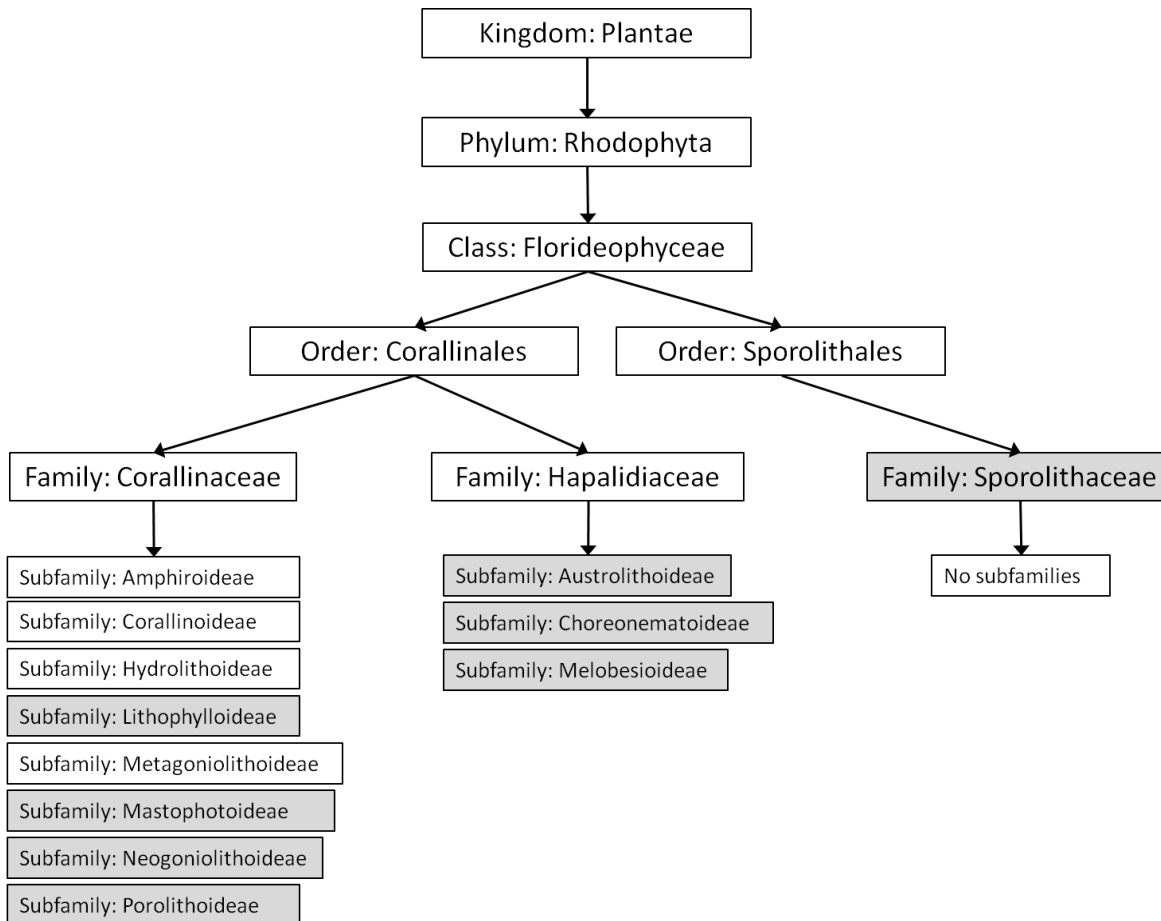


Figure 1.11 The currently accepted taxonomy of red coralline algae. Grey shading indicates (sub)families containing non-geniculate coralline algal genera. Source: Guiry (2013)

1.2.3 Growth

The growth of coralline algae is extremely slow - generally $<1\text{mm yr}^{-1}$ (Table 1.2). Encrusting algae can overgrow each other to form banks of coralline algae with a structure similar to coral reefs, known as coralligène (Ballesteros, 2006). Smaller banks of coralligène have also recently been documented off the coast of Brazil (Basso, pers. comm., 2012). Free-living coralline algal thalli can be formed from one (or more) coralline algae species or have a core composed of a different material (which may itself be fossil coralline algae, Goldberg, 2006), providing evidence for both fragmental growth and spore settlement on hard substrates (Foster, 2001).

1.2.3.1 Morphology

Free-living thalli can possess protuberances from an encrusting base or have well-developed interlocking branches (Figure 1.6). Thallus shape and branch density may be determined by, amongst other factors, water conditions

and depth (Peña and Bárbara, 2008). Highly branched thalli may form in slower moving (Peña and Bárbara, 2008) or shallower waters (Steller et al., 2003). Discoidal (i.e. flat) forms may be more abundant in deep waters where downward growth is unfavourable, while spherical and ellipsoidal forms may occur in shallower water (Peña and Bárbara, 2008).

Table 1.2. Growth rates of five free-living coralline algae species.

Species	Location	Depth (m)	Growth Rate (mm yr ⁻¹)	Reference
<i>Lithothamnion coralloides</i>	Spain	5.5	0.105	Bosence (1983)
	Ireland	-	1.0	Fazakerly and Guiry (1998)
	Ireland	*	0.561 (lab)	Blake and Maggs (2003)
<i>L. crassiusculum</i>	Gulf of California	3	0.6	Frantz et al. (2000)
	Gulf of California	3	0.25-0.45	Halfar et al. (2000)
<i>L. glaciale</i>	Norway	7	1.0	Freiwald and Henrich (1994)
	Norway	18	0.6	Freiwald and Henrich (1994)
	Scotland	7	0.158 (modern)	Kamenos et al. (2008a)
	Scotland	*	0.090 (subfossil)	Kamenos et al. (2008a)
	Newfoundland	-	0.25 – 0.45	Halfar et al. (2000)
<i>L. muelleri</i>	Gulf of California	-	0.60 (field)	Rivera et al. (2004)
	Gulf of California	*	0.87 (lab)	Rivera et al. (2004)
<i>Phymatolithon calcareum</i>	Spain	5.5	0.486	Bosence (1983)
	Ireland	5	0.606	Blake and Maggs (2003)
	Ireland	10	0.900	Blake and Maggs (2003)
	Ireland	*	0.545 (lab)	Blake and Maggs (2003)
	Scotland	7	0.152	Kamenos et al. (2008a)

- depth not specified

* depth not applicable

1.2.3.2 Growth banding

The branches of free-living thalli generally have a radial core, where the cells divide simultaneously to form bands of cells in longitudinal sections which may be visible without a microscope. As the algae grow, a high-magnesium (high-Mg) calcite skeleton is deposited around each cell. Growth is generally faster in the summer, leading to larger, less calcified cells, whilst winter growth is slow, with smaller, more highly-calcified cells (Figure 1.12) (Kamenos and Law, 2010). This creates internal growth bands that may form on an annual basis (Figure 1.12), in a manner similar to tree rings. Such growth patterns have led to the emergence of ‘densitometric algeochronology’, where the calcite density of coralline algae is used to reconstruct past climate (Burdett et al., 2011; Kamenos and Law, 2010). More information on the use of coralline algae in palaeoenvironmental reconstructions is given in section 1.2.5.3.

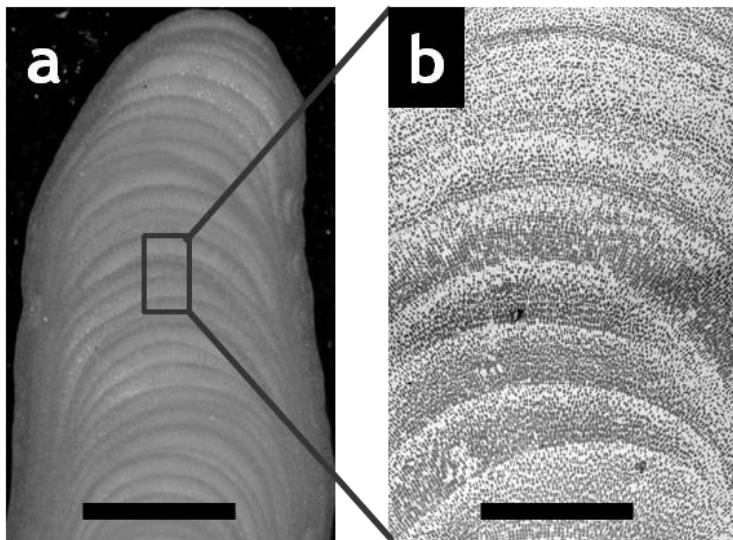


Figure 1.12 Growth bands of *Lithothamnion glaciale*.

(a) Longitudinal cross-section of a branch, scale bar = 1 mm, (b) individual cell growth, with darker areas (less calcified) representing summer growth and lighter areas (more calcified) representing winter growth, scale bar = 500 μ m. Images: N. Kamenos.

However, banding periodicity is not consistent across all genera - *L. glaciale* (Kamenos et al., 2008a) and *Clathromorphum compactum* (Halfar et al., 2008) exhibit annual banding, while other species such as *P. calcareum* have sub-annual banding (Blake and Maggs, 2003). Growth band formation may be dictated primarily by temperature and light availability (Burdett et al., 2011; Kamenos et al., 2008a; Halfar et al., 2000), affected by burial, lunar and seasonal growth patterns and temperature-induced changes caused by the El Niño Southern Oscillation (Kamenos et al., 2008a).

Four orders of coralline algal banding have been proposed (Figure 1.13) (Foster, 2001; Freiwald and Henrich, 1994; Bosence, 1976):

- 1st order bands: single row of cells.
- 2nd order bands: rows of cells separated by sutures - organically enriched 'joins', present in *L. glaciale*.
- 3rd order bands: numerous rows of 1st level bands formed in summer (larger cells) or winter (smaller cells).
- 4th order bands: full band growth (may be formed annually).

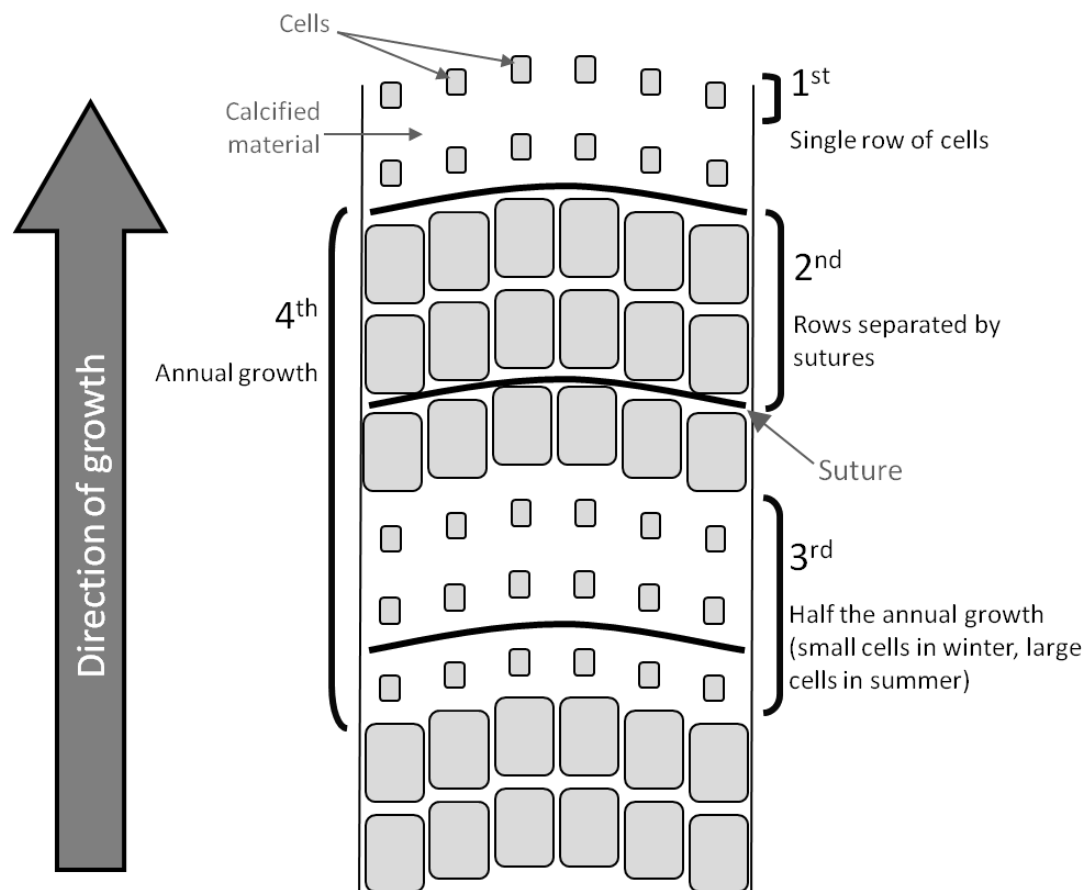
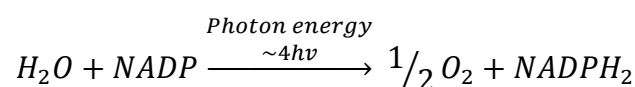


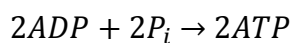
Figure 1.13 Growth and banding patterns of coralline algae. Banding patterns in a coralline algal branch, from 1st order (one row of cells) to 4th order (annual growth) bands. Adapted from Foster (2001).

1.2.4 Red algal photosynthesis

The oldest taxonomically identified eukaryote is *Bangiomorpha pubescens*, a red alga that lived ca. 1200 million years ago and is almost indistinguishable from its modern Bangiophyceae relatives (Butterfield, 2000; Butterfield et al., 1990). Since their evolution, red algae have maintained relatively primitive chloroplasts, with a system similar to cyanobacteria (Kirk, 2011; Falkowski and Raven, 2007). The photosynthetic process can be split into light and dark reactions (Figure 1.14). The light reactions, which take place in the thylakoid membranes in photosystems II (PS II) and I (PS I) (Figure 1.14 and Figure 1.15), require light energy to proceed. Energy absorbed by photosynthetic pigments (e.g. Chlorophyll-*a*, Chl-*a*) splits water molecules to yield oxygen and reduce nicotinamide adenine dinucleotide phosphate (NADP) to NADPH₂ (Figure 1.14):



The subsequent electron transport system that is set-up yields adenosine triphosphate (ATP) from adenosine diphosphate (ADP) and inorganic phosphate (P_i) (Figure 1.14):



When light is absorbed by PSII, electrons are transferred to the first electron carrier (Q_A) then onto the second (Q_B). However, Q_A can only accept one electron at a time, so the reaction centres are closed and unavailable until electrons are transferred from Q_A and Q_B (Maxwell and Johnson, 2000). Thus, the electron transport system limits the rate of photosynthesis and ultimate carbohydrate formation.

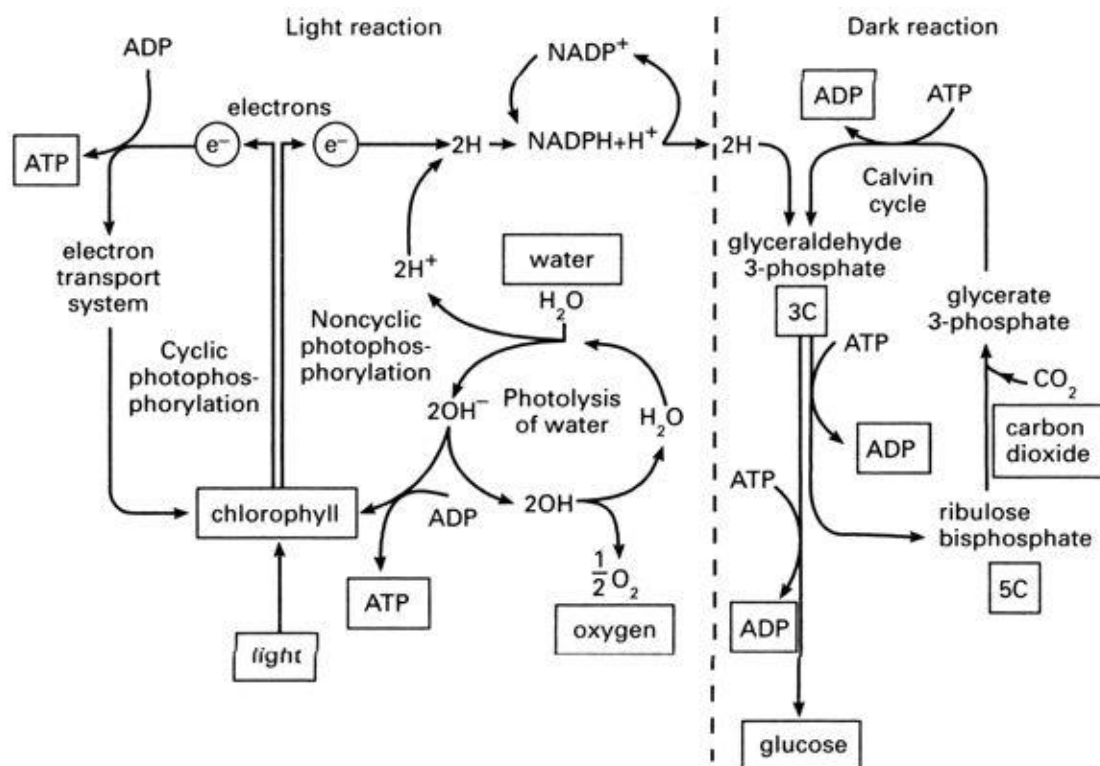


Figure 1.14 The light and dark reactions of photosynthesis.
 Source: Oxford Dictionary of Chemistry (2004).

The dark reactions, which take place in the stroma, use $NADPH_2$ from the light reactions to reduce CO_2 to a carbohydrate (the Calvin cycle) (Figure 1.14):



Energy for this reaction is gained from the breakdown of ATP back to ADP, thus can proceed in the dark (Figure 1.14):



1.2.4.1 Red algal chloroplasts

The Florideophycidae, of which all coralline algae are members (Figure 1.11), typically have many small, lens-shaped chloroplasts around the periphery of the cells (Kirk, 2011). This is in contrast to the Bangiophycidae which have only one, stellate (star-shaped), axial chloroplast (Kirk, 2011). The chloroplasts consist of a bilayer membrane bounding a granular matrix known as the stroma. Within the stroma, individual flattened membrane-bound sacs ~20 nm thick are present - the thylakoid (Figure 1.15) (Kirk, 2011). In other algae and higher plants, the thylakoids are grouped in stacks of three or more (Kirk, 2011). Attached to the outside of the thylakoid membranes are particles 30 - 40 nm in diameter known as phycobilisomes (Figure 1.15), which are unique to the red algae and cyanobacteria.

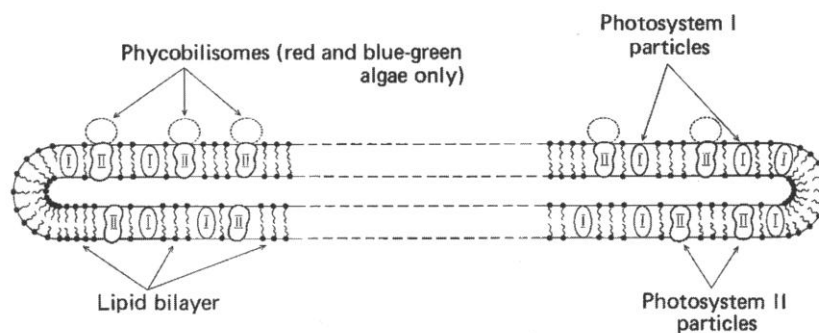


Figure 1.15 The probable organisation of the thylakoid membrane. Source: Kirk (2011).

1.2.4.2 Phycobiliprotein pigments

Phycobilisomes consist primarily of biliproteins - the light harvesting pigments. In red algae, the three biliprotein pigments are phycoerythrin (PE), phycocyanin (PC) and allophycocyanin (APC) (Table 1.3), which can also be found in Cryptophyta (unicellular, flagellated algae) and Cyanophyta (blue-green algae) but not the Chlorophyta (green algae) or Ochrophyta (brown algae) (Hedley and Mumby, 2002). PE is generally the dominant biliprotein, with APC often the minor constituent.

Table 1.3 Absorbance wavelengths of photosynthetic pigments.

Pigments found in the Chlorophyta (Chloro., green algae), Ochrophyta (Ochro., brown algae), Rhodophyta (Rhodo., red algae) and Pyrrhophyta (Pyrrho., zooxanthellae). Black dot indicates at least one record from the division. Adapted and updated from: Hedley and Mumby (2002) and Schubert et al. (2006).

Pigments	Absorbance peaks (nm)			Chloro. (green)	Ochro. (brown)	Rhodo. (red)	Pyrrho. (zoox.)
Chlorophylls							
chl- <i>a</i>	435	670 - 680		•	•	•	•
chl- <i>b</i>	480	650		•			
chl- <i>c</i>		645			•		•
Carotenoids							
α	423	444	473 ^a			•	
β	427	449	475	•	•	•	•
peridinin		475					•
Xanthophylls							
antheraxanthin	470	487	520	•		•	
zeaxanthin	428	450	478	•		•	
neoxanthin	415	438	467	•	•		
lutein	422	445	474	•		•	
violaxanthin	417	440	469	•	•	•	•
fucoxanthin	426	449	465 ^b		•		•
diatoxanthin	425	449	475		•		•
diadinoxanthin	424	445	474		•		•
dinoxanthin	418	442	470				•
siphonxanthin		540		•			
Phycobilins							
phycocyanin		618				•	
phycoerythrin	490	546	576			•	
allophycocyanin		654				•	

^a peak may shift to 500 nm *in vivo*

^b absorption extends to 580 nm *in vivo*

In vivo, phycobiliproteins aggregate to form the phycobilisome particles observed on the surface of the thylakoids (Figure 1.15). The phycobilisomes have an ordered structure consisting of all three phycobiliprotein pigments (Figure 1.16) - PE on the outside surrounding PC, with APC at the base. APC subsequently transfers the harvested light energy to Chl-*a* within the PSII complex. Chl-*a* constitutes ~15% of the photosynthetic pigments associated with PSII in red algae (Figuerola et al., 2003; Goldstein et al., 1992).

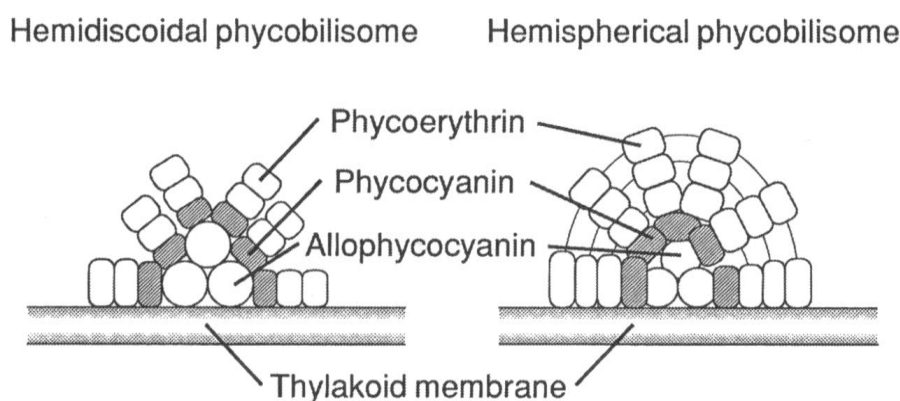


Figure 1.16 The phycobilisome structure.
Source: Kirk (2011).

A number of other light harvesting pigments, the carotenoids, may also be found in red macroalgae (Table 1.3): α -carotene, β -carotene, lutein (often predominant), zeaxanthin, antheraxanthin, violaxanthin and β -cryptoxanthin (Schubert and García-Mendoza, 2008; Schubert et al., 2006). Within the Rhodophyta, carotenoid profiles generally vary according to Order, except for the Orders Corallinales (to which most red coralline algae belong, Figure 1.11 and Table 1.4) and Ceramiales, where within-Order variations are observed (Schubert et al., 2006).

Table 1.4 Carotenoid composition of species within the Order Corallinales.
Carotenoids identified: violaxanthin (Vio.), antheraxanthin (Ant.), lutein (Lut.), zeaxanthin (Zea.), β -cryptoxanthin (β -cryp.), α -carotene (α -car.) and β -carotene (β -car.). Source: Schubert et al. (2006).

Family & Subfamily	Species	Carotenoid pigment composition (% of total)						
		Vio.	Ant.	Lut.	Zea.	β -cryp.	α -car.	β -car.
Corallinaceae								
Corallinoideae	<i>Bossiella californica</i>	5.1	69.5		19.3			6.2
	<i>B. orbignyana</i>	1.8	61.2		8.5	5.2	2.2	21.2
	<i>Calliarthron tuberculosum</i>	0.7	78.0		4.8	7.7		8.8
	<i>Corallina officinalis</i>	3.1	56.7		32.3	4.6	0.3	2.9
	<i>C. vancouverensis</i>	1.0	67.1		13.9	10.5		7.5
	<i>Jania tenella</i>	3.5	69.2		12.4	5.2		9.7
Lithophylloideae	<i>Lithophyllum margaritae</i>			47.3	2.8		5.8	44.0
	<i>Lithothrix aspergillum</i>			48.2	5.2	5.2	9.8	31.7
	<i>Amphiroa zonata</i>			67.4	8.6	6.7	3.9	13.5
Hapalidiaceae								
Melobesiodeae	<i>Melobesia mediocris</i>			77.5	8.7		3.3	10.5

As well as light harvesting, carotenoids have an important photoprotective role with algal cells (Schubert and García-Mendoza, 2008; Wilson et al., 2006) by:

1. Controlling the amount of light reaching PSII (by screening or heat production).
2. Quenching triplet chlorophyll to minimise the formation of singlet oxygen.
3. Quenching singlet oxygen.

Thus, it has been proposed that the pigment composition of algae will affect its photoprotective abilities, although this has yet to be shown experimentally (Schubert and García-Mendoza, 2008). Each photosynthetic pigment has a specific absorbance wavelength (Table 1.3) and the proportion of each pigment within the algal cells determines the algae's colour and its light reflective properties (Kutser et al., 2006). In the shallow coastal ocean, light may be reflected, absorbed or re-emitted as fluorescence within the water column and at the sea bed, depending on the benthic habitat. This has a direct effect on the spectral composition of the light field (Ackleson, 2003), thus may affect the primary production of important benthic habitats such as maerl beds, coralligène, kelp forests, seagrass meadows and coral reefs.

Given the impact benthic composition can have on the ambient light field, spectral techniques (both direct and remotely sensed) have been used in the monitoring and conservation of coastal benthic habitats in response to short-term (e.g. pollution and storm events) and long-term (e.g. climate change) perturbations (Diersson et al., 2003; Hochberg and Atkinson, 2000). Tropical seagrass beds and coral reefs have been most well studied, with more limited research on temperate macroalgae. Coral and algae sampled from Hawaii exhibited similar reflectance magnitudes (8.0% and 6.6% respectively), while sand was highly reflective (36.7%) (Hochberg and Atkinson, 2000). All bottom types were characterised by peaks at 600 and 650 nm, while corals had a third peak at 570 nm (Hochberg and Atkinson, 2000). In contrast, significant species-specific differences were observed between algal and coral species in the

Bahamas (Lubin et al., 2001), with the highest reflectance from sand and coralline algae (Figure 1.17) (Lubin et al., 2001).

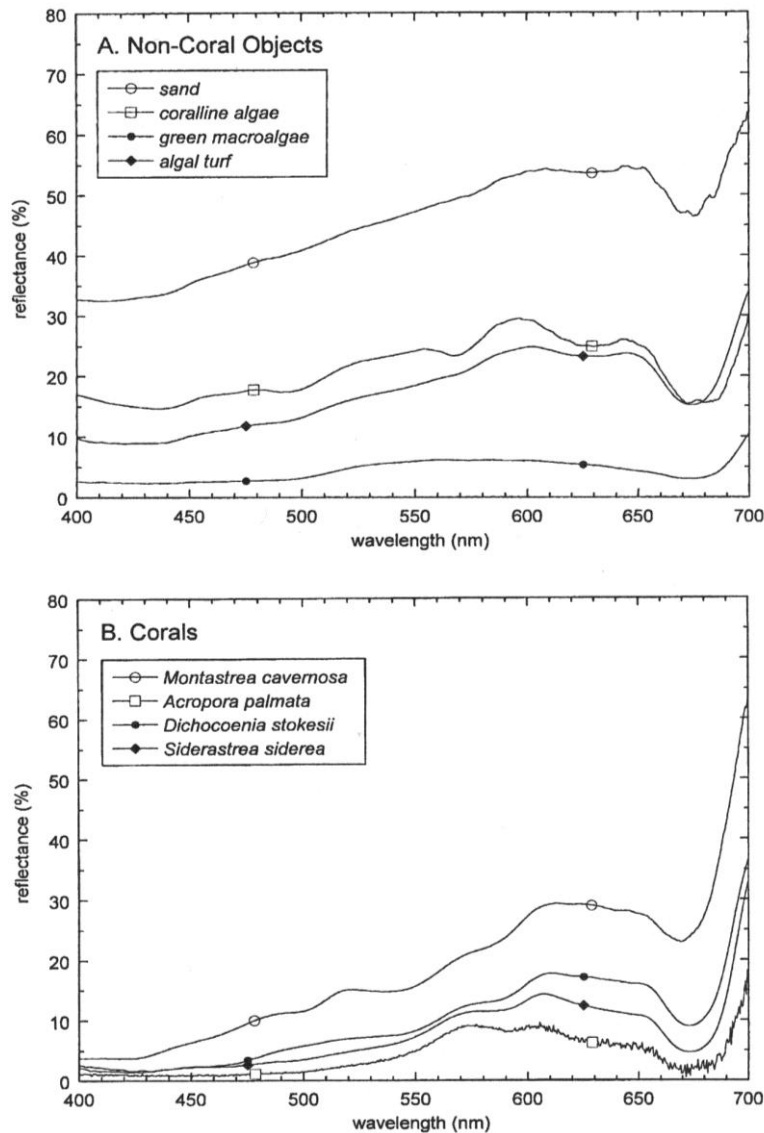


Figure 1.17 Spectral reflectance of eight benthos types from the Bahamas. (A) Non-coral objects and (B) four coral species. Source: Lubin et al. (2001).

In temperate regions, the often turbid waters can hinder the use of remote sensing to map bottom types using reflectance data (Kutser et al., 2006). In the Baltic Sea, broken shells and limestone pebbles exhibited the highest reflectance (40% and 22% respectively), whilst algal reflectance was less than 20%. The brown alga *Fucus vesiculosus* was characterised by three peaks at 580, 600 and 650 nm (Figure 1.18) (Kutser et al., 2006), similar to zooxanthellae-containing corals (Hochberg and Atkinson, 2000). The red alga *Furcellaria lumbricalis* exhibited two peaks at 600 and 650 nm (Figure 1.18), while green algae (*Chara* sp., *Enteromorpha* sp. and *Cladophora glomerata*) and the seagrass

Zostera marina were characterised by peaks at 545, 600 and 640 nm (Figure 1.18) (Kutser et al., 2006).

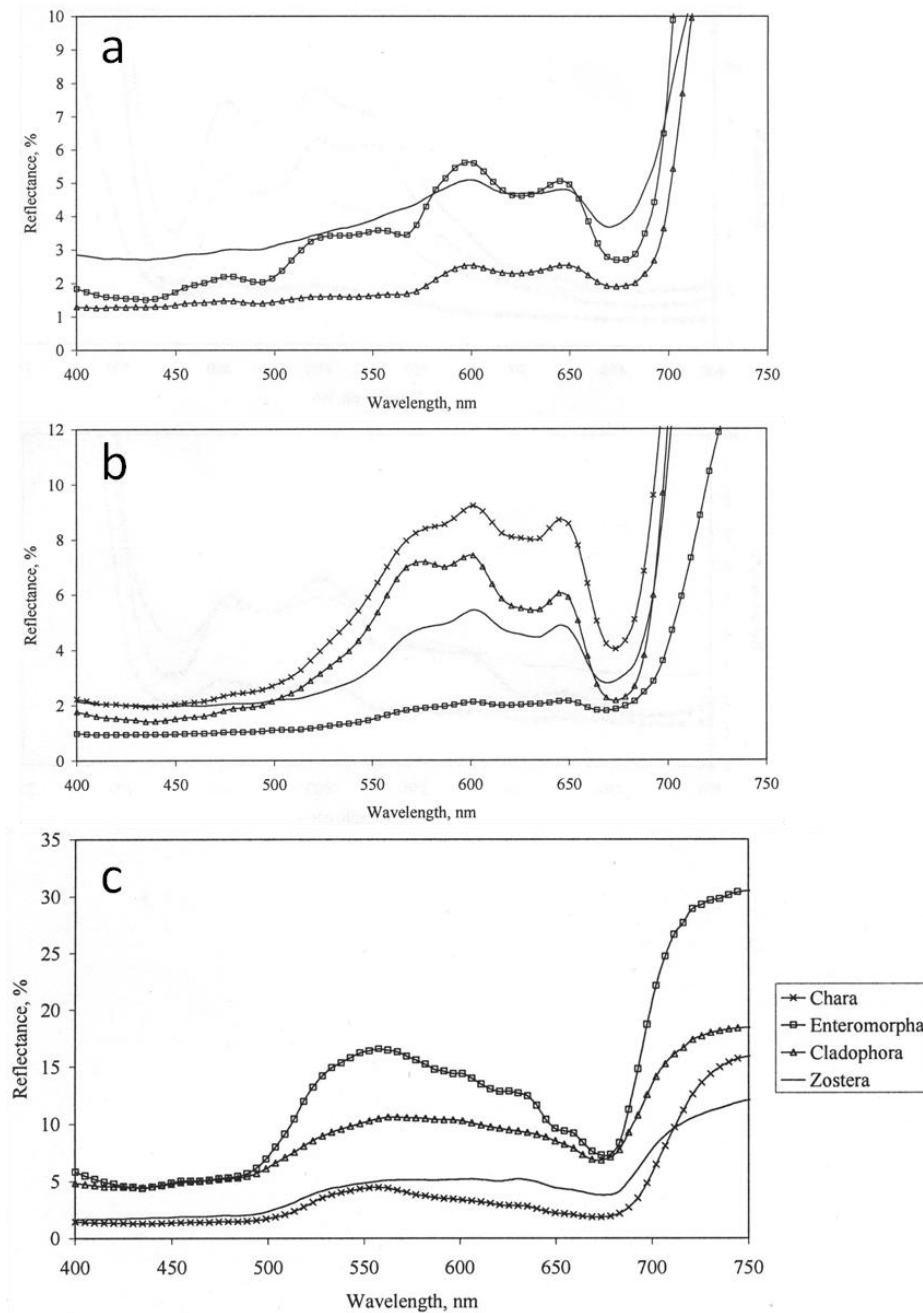


Figure 1.18 Reflectance spectra of temperate macroalgae and seagrass. (a) Three specimens of the red alga *Furcellaria lumbricalis*, (b) four specimens of the brown alga *Fucus vesiculosus* and (c) three green algae: *Chara* sp., *Enteromorpha* sp., *Cladophora glomerata* and the seagrass *Zostera marina*. Source: Kutser et al. (2006).

1.2.5 Importance of coralline algal habitats

1.2.5.1 Ecosystem service provision

The major coralline algal habitats (maerl beds, coralligène, kelp forests, coral reefs and seagrass meadows) are ‘hot spots’ for marine biodiversity at

various trophic levels (Ballesteros, 2006; Orth et al., 2006; Foster, 2001). The benthic primary producers which constitute these ecosystems form a three-dimensional structure that provides an ideal habitat for vast array of flora and fauna (e.g. Ballesteros, 2006; BIOMAERL et al., 2003; Steneck et al., 2002; De Grave et al., 2000), often supporting globally threatened or charismatic species such as sirenians (dugongs and manatees), sea turtles and sea horses (Short et al., 2007). In addition, coralline algae can act as settlement cues for various invertebrates (Steller and Cáceres-Martinez, 2009; Steinberg and De Nys, 2002). Thus, coralline algal habitats often act as nursery areas for many commercially important fish and shellfish species such as scallops (Peña and Bárbara, 2008; Ballesteros, 2006; Kamenos et al., 2004a; Kamenos et al., 2004b; Kamenos et al., 2004c; Heck Jr. et al., 2003; Steneck et al., 2002).

1.2.5.2 Carbon sequestration and cycling

Given their widespread distribution, coralline algae may significantly contribute to the carbon cycle in coastal systems (BIOMAERL et al., 2003), and the high primary productivity of coralline algal habitats such as seagrass meadows may act as a significant sink of atmospheric carbon dioxide over geological timescales (Bensoussan and Gattuso, 2007; Short et al., 2007). Maerl beds provide the most carbonate of all coastal habitats in Europe (BIOMAERL et al., 2003) and are major calcifiers in coral reefs (Tierney and Johnson, 2012), providing stability and supplementing calcium carbonate reserves (Kuffner et al., 2008; Koop et al., 2001). Kelp forests can dampen waves, promoting the sedimentation of carbon-laden organic matter (Eckman et al., 1989). Seagrass roots can stabilise soft sediments, and their high productivity can oxygenate the overlying water column and facilitate the cycling of nutrients in coastal waters (Constanza et al., 1997). The high productivity of coralline algal habitats provides a direct carbon source to herbivores, detritivores and microbes, which in turn may circulate the carbon to suspension feeders and plankton (Krumhansl and Scheibling, 2012; Krumhansl and Scheibling, 2011; Eckman et al., 1989).

1.2.5.3 Palaeoclimatic proxies

The global distribution of coralline algae may provide us with more information compared to other biogenic climatic proxies such as corals, which

have a limited geographic distribution (Figure 1.9) (Bosscher, 1992). The presence of fossil coralline algae in geological facies suggests that the deposit was formed in the oceanic photic zone and thallus morphology may provide information on water depth and conditions (Barattolo et al., 2007; Bassi, 2005; Copper, 1994). Chave (1954) first proposed that the Mg content of coralline algae skeletons may be related to water temperature. Since then, the calcification, Mg content and ^{18}O and ^{14}C isotopic ratios of *L. glaciale*, *L. crassiculum* and *C. compactum* skeletons have been used to reconstruct recent Holocene temperature (Kamenos and Law, 2010; Hetzinger et al., 2009; Halfar et al., 2008; Kamenos et al., 2008a; Frantz et al., 2000; Halfar et al., 2000), cloud cover (Burdett et al., 2011) and relative salinity changes (Kamenos et al., 2012), with up to fortnightly resolution (Kamenos et al., 2008a). This has been further applied to understand fluctuations in copepod abundance in the North Atlantic (Kamenos, 2010) and salmon stocks in the Bering Sea (Halfar et al., 2011).

1.2.6 Threats to coralline algal habitats

1.2.6.1 Fishing

As discussed above (section 1.2.5.1), coralline algal habitats are often important nursery areas to numerous commercially important species. As such, maerl beds are often targeted for scallops in the northeast Atlantic and demersal fish and cephalopods in the Mediterranean (Hall-Spencer et al., 2003). The trawling or dredge techniques commonly employed can damage maerl beds after just one campaign (Kamenos et al., 2003; Hall-Spencer and Moore, 2000).

1.2.6.2 Harvesting

The slow growth rate of non-geniculate coralline algae makes it vulnerable to harvesting pressures and are thus considered a non-renewable resource (Foster, 2001). Coralline algae are harvested for use in a variety of industries including agriculture, water purification, mineralisation, medicine and cosmetic production (Aslam et al., 2009; Frestedt et al., 2009; Frestedt et al., 2008; Foster, 2001). France once had the largest maerl extraction program in the world (Grall and Hall-Spencer, 2003); Breton maerl has been harvested for centuries, peaking in the 1970s at $600\,000\text{ t yr}^{-1}$, leading to the total loss of

maerl cover in some areas. Conservation efforts have recently led to a total ban on all Breton maerl harvesting in an effort to preserve the habitats (Grall, pers. comm., 2012).

The suitability of kelp as a human food source and biofuel is becoming realised, increasing pressure on kelp forests through deforestation. Such activities remove the canopy layer, exposing benthic organisms such as coralline algae to a higher irradiance. Coralline algae are generally considered to be low light adapted (e.g. Burdett et al., 2012b, and see Chapter 3), thus may be particularly susceptible to high light-induced stress (Rix et al., 2012; Payri et al., 2001).

1.2.6.3 Eutrophication

Anthropogenic factors that contribute to eutrophication such as turbidity, sedimentation and nutrient loading (e.g. aquaculture) are detrimental to coralline algae (Peña and Bárbara, 2008; Hily et al., 1992). Phosphate may be an inhibitor to the calcification of coralline algae (Koop et al., 2001), although this is met with some debate: the ENCORE experiment found no effect of nitrogen or phosphate enrichment on the growth, primary production or calcification of *Lithophyllum kotschyannum* (Koop et al., 2001).

1.2.6.4 Climate change

Climate projections for the next century suggest that atmospheric and oceanic temperatures will increase and oceanic pH will decrease at an unprecedented rate (IPCC, 2007). Such changes will directly affect oceanographic and atmospheric processes such as storm intensity and frequency, ocean circulation and carbonate saturation states (IPCC, 2007). The coastal zone may be more affected by these climatic changes than the open ocean due to its shallow depth and continental proximity (Scavia et al., 2002). Carbonates with a Mg content of more than 8 - 12 molar% are the most soluble polymorph of calcium carbonate (Kuffner et al., 2008). Red coralline algae are composed of high Mg-calcite, with a Mg content of 8 - 29 molar % (Kamenos et al., 2009; Kamenos et al., 2008a; Chave, 1954), thus may be more susceptible to low carbonate saturation states compared to other marine calcifiers (Martin et al., 2008) such as corals (aragonite) or mussels (low-Mg calcite and aragonite). See

Chapter 7 for more information on the effects of carbonate chemistry on coralline algae.

1.3 Aims of this research

There is a significant knowledge gap with regards to DMSP and DMS concentrations in the coastal ocean, despite the area's potential importance in the global marine sulphur cycle (Lana et al., 2011). Coralline algal habitats are globally ubiquitous and coralline algae are known to contain high quantities of DMSP (Rix et al., 2012; Kamenos et al., 2008b), thus may significantly contribute to the coastal sulphur cycle. Despite this, the majority of macroalgal DMSP research to date has focussed on species from the Phylum Chlorophyta (e.g. Lyons et al., 2010; Van Alstyne, 2008; Lyons et al., 2007; Van Alstyne et al., 2007; Van Alstyne and Puglisi, 2007). Thus, this research aimed to improve our understanding of the production and release of DMSP by coralline algae, and the subsequent DMSP and DMS concentrations associated with coralline algal habitats. This was achieved through a number of separate, yet interlinked, foci that are presented in Chapters 3 - 8 (Figure 1.19). The methods and techniques adopted to achieve this aim are described in Chapter 2. Specifically, this research aimed to provide:

1. A detailed analysis of the photosynthetic characteristics of red coralline algae (Chapter 3), as the algal precursor to DMSP (methionine) is a product of photosynthesis.
2. A spatial (Chapter 4) and temporal (Chapter 5) evaluation of DMSP production by coralline algae to better understand the natural variability associated with coralline algal habitats.
3. An assessment of the effect of environmental and biological perturbations on DMSP production and release by coralline algae and their habitats, including reduced salinity (Chapter 6), reduced and variable pH (Chapter 7) and herbivorous grazing (Chapter 8).

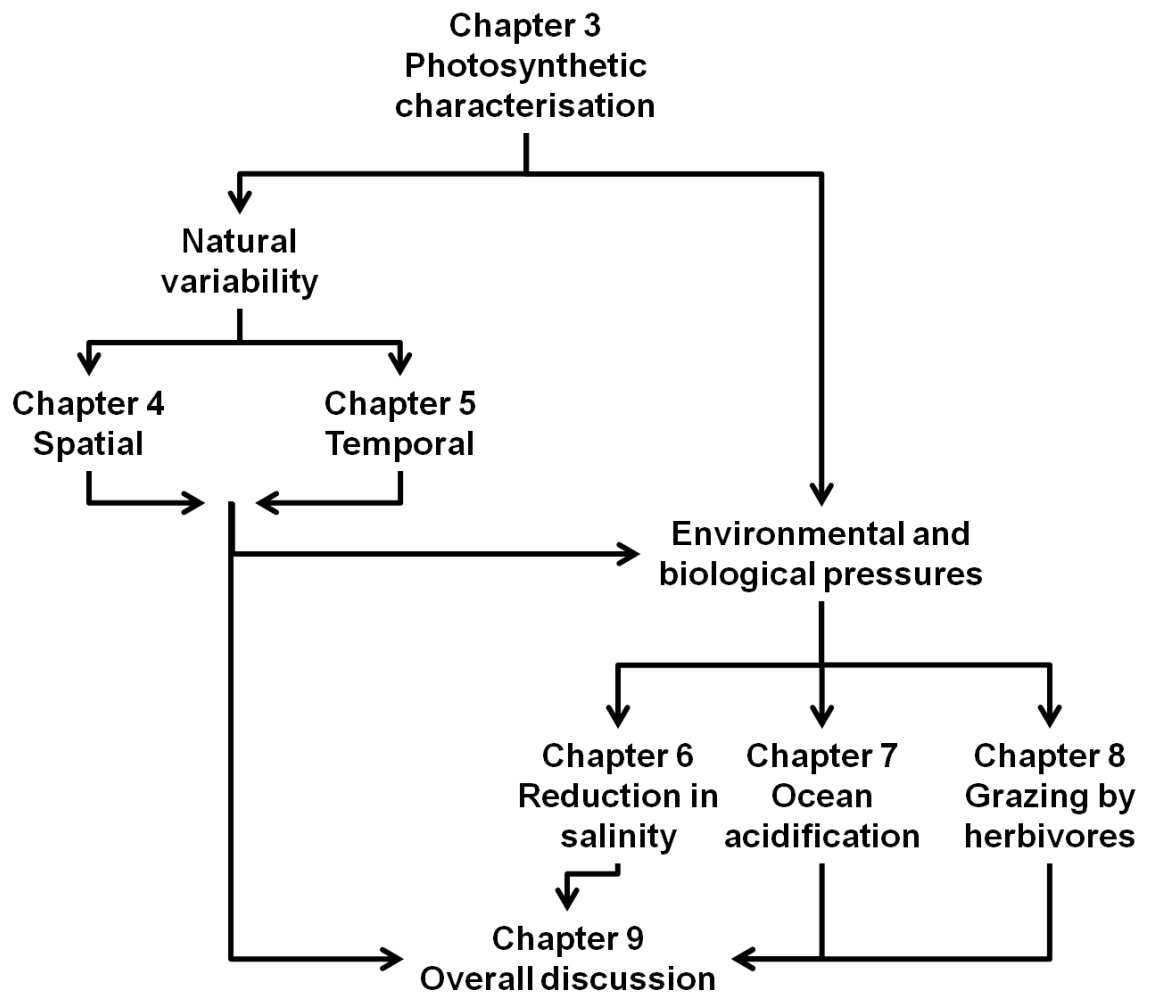


Figure 1.19 Thesis structure and the links between each chapter.

2

Methods and techniques

This research established the natural variability and potential effect of environmental perturbations on biogenic sulphur in coralline algal habitats using intra- and extracellular dimethylsulphoniopropionate (DMSP) and dimethylsulphide (DMS) quantification, Pulse Amplitude Modulation (PAM) fluorometry, scanning electron microscopy (SEM) and reflectance spectrometry. This chapter discusses these techniques and the methodologies employed. Details of sample collections and Chapter-specific methods are described in relevant chapters.

2.1 DMSP and DMS analysis

2.1.1 Different methods of analysing DMSP and DMS

DMS and DMSP (collectively DMS/P) have been characterised and quantified from marine algae and seawater using a variety of methods since their discovery by Haas (1935) and Challenger and Simpson (1948). Mercuric chloride, sodium hydroxide and potassium chloroplatinite with acidified bromine were used to first determine the structure of the sulphonium compounds produced by marine algae (Challenger and Simpson, 1948; Haas, 1935). Subsequent quantification of DMSP and DMS has utilised various techniques such as:

- Thin layer chromatography (Greene, 1962) with mass spectrometry (Hanson et al., 1994).

- High performance liquid chromatography (Colmer et al., 2000; Gorham, 1986) with UV detection (Wiesemeier and Pohnert, 2007).
- Ultra performance liquid chromatography with mass spectrometry (Wiesemeier and Pohnert, 2007).
- Gas chromatography with flame photometric detection (FPD) and a cryotrap (Turner et al., 1990) or flow injection system (Howard et al., 1998).
- Gas chromatography with mass spectrometry (Zhou et al., 2009).
- Capillary electrophoresis (Zhang et al., 2005).
- Stable and radio-isotope labelling (Hanson et al., 1994; Greene, 1962) with proton-transfer-reaction mass spectrometry (Stefels et al., 2009) or dry crushing (Stefels et al., 2012).
- Nuclear magnetic resonance (Ansedè et al., 2001).

The gas chromatography / cryotrap method for analysing DMS first proposed by Turner et al. (1990) is the most widely used technique and has a proven record in the literature. Thus, this technique was adopted throughout this research for quantification of DMS in algal and water samples.

2.1.2 The Gas Chromatograph

A Shimadzu GC-2014 gas chromatograph (GC) was used at the University of Glasgow for DMS quantification (DMSP was quantified by hydrolysis to DMS). The GC was fitted with a 25 m Restek Rtx®-5MS fused silica, chemically bonded capillary column and a sulphur-specific FPD detector (fitted with a 394 nm interference filter). The operational settings for the GC (Figure 2.1) were: air pressure: 105 kPa (15.2 psi), hydrogen air pressure: 35 kPa (5.1 psi), injection port and oven temperature: 45 °C, FPD detector temperature: 200 °C (Figure 2.1). The square-root of peak area was linearly related to DMS concentration, permitting DMS quantification.

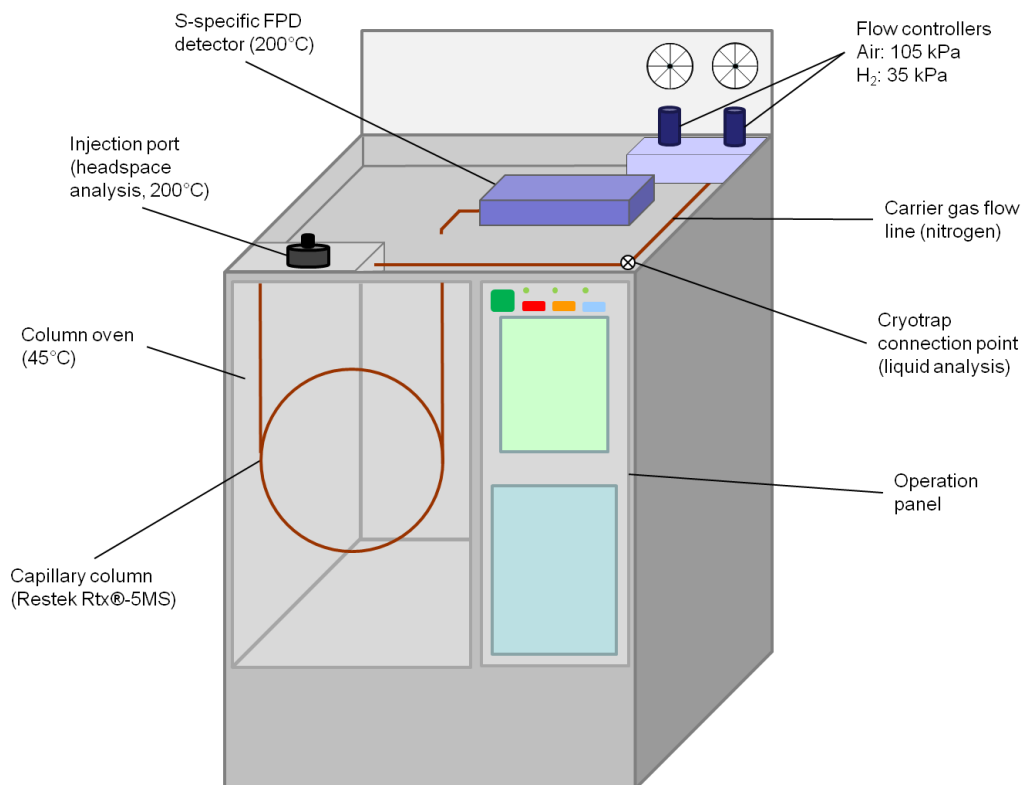


Figure 2.1 The gas chromatograph set up for DMS analysis. The Shimadzu GC-2014 gas chromatograph set up for liquid and headspace analysis of DMS and operational settings. Note the cryotrap connection point – see section 2.1.2.1 for further cryotrap information.

2.1.2.1 The purge and cryotrap system

DMS and DMS concentrations in the ocean are often extremely low (<2.8 nM, Kiene and Slezak, 2006). Thus, it is necessary to pre-concentrate the sample's DMS in order to allow quantification by the GC-FPD method. This is achieved using a purge and cryotrap system (Figure 2.2), described by Turner et al. (1990).

Samples were purged with nitrogen gas (60 ml min^{-1}) through a fritted glass base. Purged DMS was subsequently transported through two drying stages (glass wool and 4\AA molecular sieve) before being directed into the cryotrap - a loop of PTFE tubing maintained at -155°C using liquid nitrogen, trapping DMS in the tubing. Prior to any sample analyses, the time required to purge all DMS from solution was determined; for samples up to 20 ml, 15 minutes purge time was probably sufficient to purge all DMS (Figure 2.3). However, a 25 minute purge time was used throughout to ensure all DMS had been purged from the sample as natural samples may purge slower (e.g. due to the presence of surfactants).

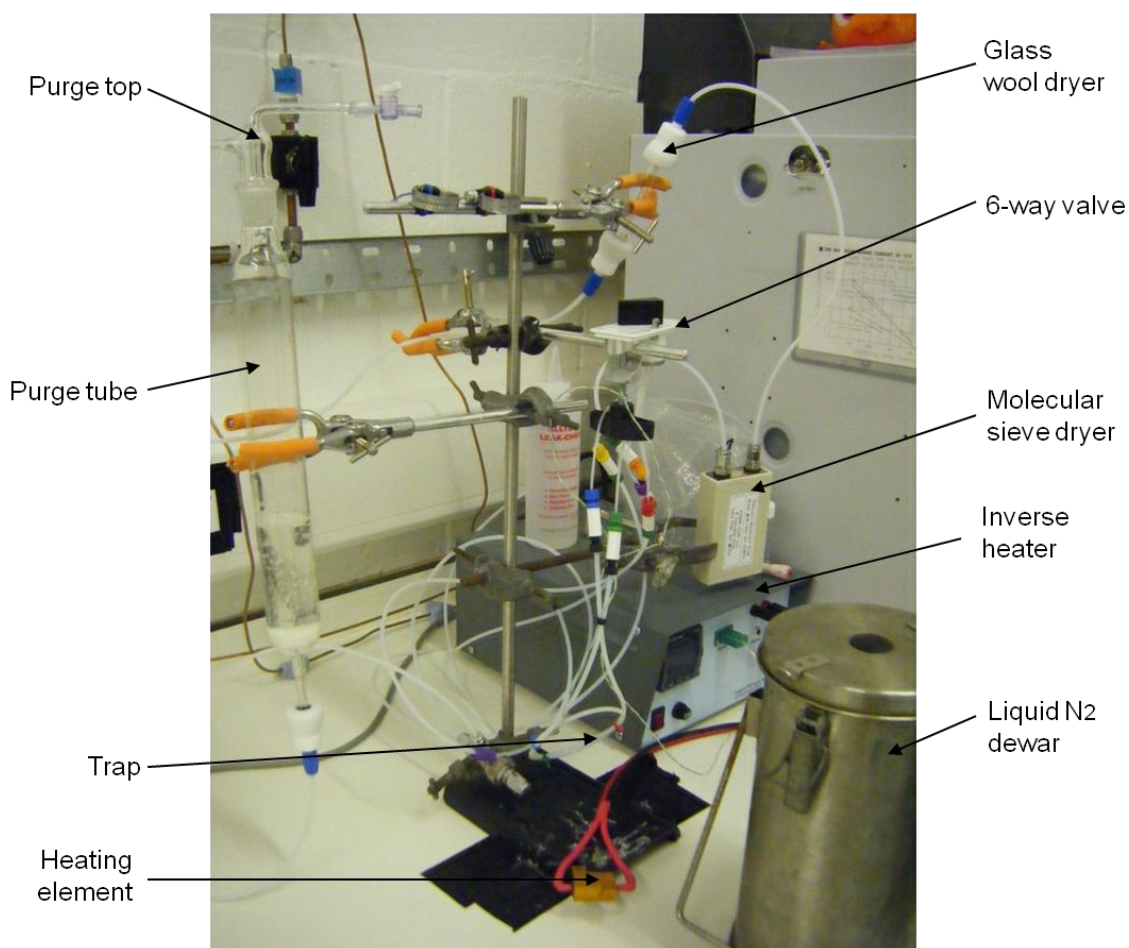
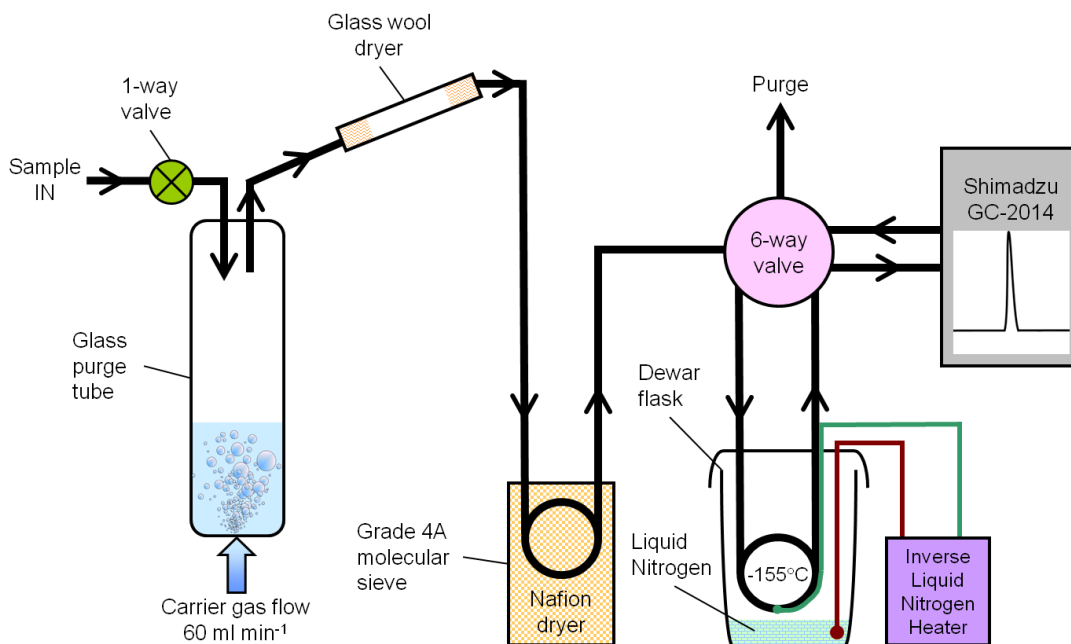


Figure 2.2 The purge-cryotrap system for pre-concentration of DMS. Diagrammatic representation of the cryotrap (top) and a photo of the cryotrap at the University of Glasgow (bottom).

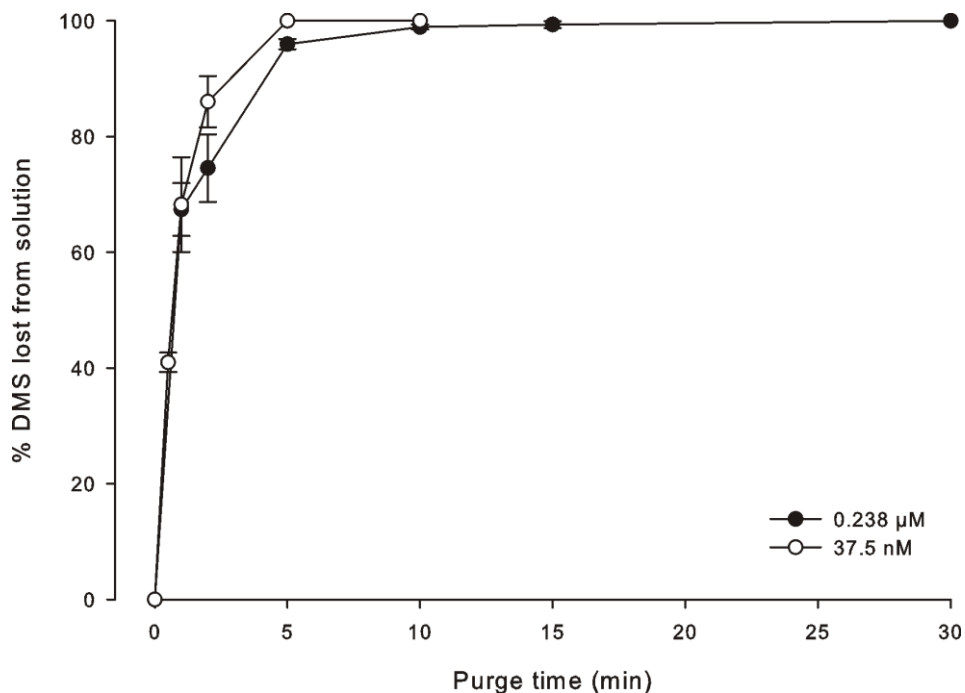


Figure 2.3 Time taken to purge DMS from solution. High (0.238 μM , black circle) and low (37.5 nM, open circle) concentration DMS solutions purged with nitrogen gas using the cryotrap system at 60 ml min^{-1} nitrogen flow.

The 6-way valve (Figure 2.2) maintains two distinct circuits in the system in ‘Load’ or ‘Inject’ modes: (1) ‘Load’ - purge tube and trap are linked; (2) ‘Inject’ - trap and GC are linked. Following purging, the 6-way valve was turned to divert the flow from trap into the GC. The trap temperature was rapidly increased to $+80^\circ\text{C}$ by transferring the cryotrap into boiling water for 10 seconds, stripping all DMS from the trap and transporting the sample to the GC for detection by the FPD detector.

2.1.3 Standard calibrations

DMS concentrations in samples were quantified through the construction of standard calibration curves. DMSP crystals were supplied by Research Plus Inc. The crystals were dissolved in autoclaved Milli-Q water using a sterile preparation technique to yield a DMSP standard solution of known concentration. Aliquots of the standard were stored in 1 ml volumes at -20°C until required. Standards from the same batch of DMSP crystals were used throughout this research.

2.1.3.1 Headspace standards: high DMS concentrations

Intracellular DMSP (DMSPi) concentrations in macroalgae were high enough to quantify DMS by direct injection of equilibrated headspace rather than using the cryotrap. Headspace standards were prepared using 10 ml Wheaton™400 crimp top serum vials. Total vial volume was 14ml. DMSP stock solution was diluted with autoclaved Milli-Q water (total volume 1100 µl) to achieve a range of headspace standards. This was added to vials with 900 µl 10M sodium hydroxide (NaOH) to give a final volume of 2000 µl (equal to the sample preparation, see section 2.1.4.1) and quickly crimped shut with Pharma-fix septa (Discovery Sciences). Standards were left in the dark for two days to ensure DMSP was fully hydrolysed to DMS and DMS had equilibrated between the NaOH solution and vial headspace. 100 µl of headspace from each standard was injected directly into the GC using a gas tight syringe fitted with a 24 gauge needle to achieve a standard calibration curve similar to Figure 2.4a.

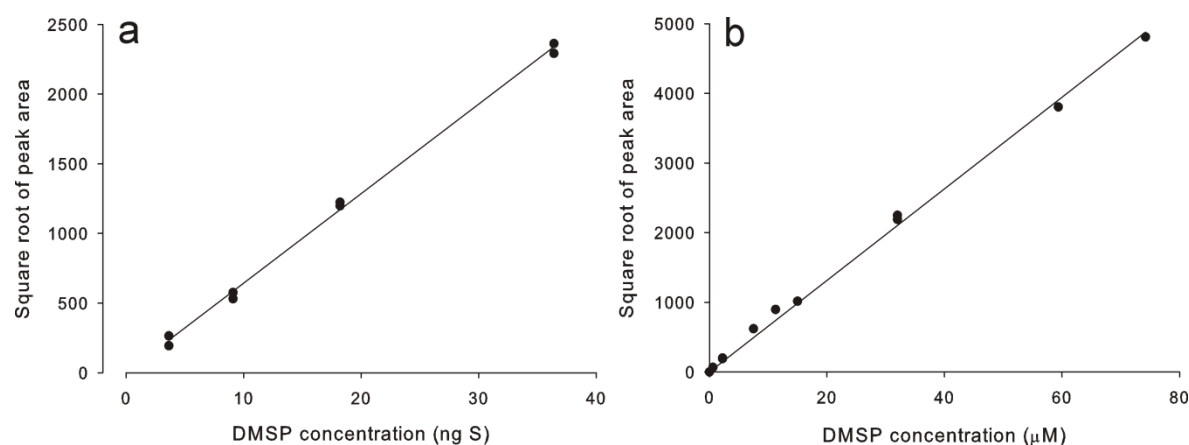


Figure 2.4 Example DMS calibrations.

(a) Headspace calibration. Regression equation: $(\text{Peak area})^{0.5} = 65.72 [\text{DMSP}]$, $R^2 = 0.997$, Std error of residuals = 15.6, $n = 11$. (b) Liquid calibration. Regression equation: $(\text{Peak area})^{0.5} = 64.28 [\text{DMSP}]$, $R^2 = 0.998$, Std error of residuals = 5.7, $n = 8$. Units on the y-axes are arbitrary.

2.1.3.2 Liquid standards: low DMS concentrations

Liquid standard stock was prepared by diluting DMSP standard stock in 250 ml Milli-Q water. This DMSP solution was kept up to one week in the dark at 4 °C. Varying volumes of standard were analysed using the purge-cryotrap system by adding 4 ml 10M NaOH to the purge tube with the standard to achieve a standard calibration curve similar to Figure 2.4b.

2.1.3.3 Precision, accuracy and detection limit

To determine precision, multiple (3-5) standards of the same concentration were run during the same calibration session. To determine accuracy, freshly prepared standards were compared to the previous batch of standards (the first batch of standards was compared to standards from SAMS, c/o Prof. Angela Hatton). Precision and accuracy errors throughout were 1 - 2%.

The GC detection limit was determined by calculating the 'peak areas' of the detector baseline with no injection of DMS. Detection limits for this research were 960 ng S per injection volume (headspace) and 0.64 ng S per injection volume (liquid).

2.1.4 Sample preparation and analysis

Due to the remote location of field locations and the collection of samples from small, open boats, it was not practical to analyse samples for DMS/P *in situ*. Thus, all samples were fixed for DMS/P using NaOH in the field and returned to the laboratory for analysis. All samples were kept in the dark to prevent photo-oxidation of DMS to DMSO.

2.1.4.1 Intracellular DMSP

Macroalgae samples (typically 0.2 - 0.5 g) were patted dry and their mass recorded. Samples were placed in 10 ml Wheaton[®] 400 glass serum vials (total volume 14 ml) with 2 ml of 10M NaOH and quickly crimp-sealed with Pharma-Fix septa (Discovery Sciences). This methodology does not distinguish between intracellular DMSP (DMSP_i) and intracellular DMS, therefore represents total intracellular DMSP+DMS. However, this was not considered an important factor as it is generally accepted that DMS concentrations within algal cells are negligible compared to the concentration of DMSP (Hatton, pers. comm). All macroalgae samples were analysed by direct headspace injection, typically injecting 100 µl of sample headspace. DMSP_i was quantified by comparison to the headspace calibration curve and normalised for sample mass and presented as mg S g⁻¹ algae as DMSP.

2.1.4.2 Particulate and dissolved DMS/P in seawater

A known volume of water sample (typically 50 ml) was filtered through a GF/F 0.7 μm depth filter (Millepore) into a Wheaton[®] 400 50 ml glass serum vial (total vial volume: 60 ml). A pore size of 0.7 μm has been recommended due to the plasticity of ultraplankton (Keller et al., 1989). 2 ml of 10 M NaOH was added to the vial and filled to the brim with Milli-Q water to give a final vial concentration of 0.33 M NaOH. Vials were crimped shut with Pharma-Fix septa. These samples represented total dissolved DMSP+DMS (DMS/Pd). Without allowing the filter to dry out (as suggested by Kiene and Slezak, 2006), the filter was placed in another vial filled with 0.33 M NaOH and crimp-sealed with a Pharma-Fix septum. These samples represented the total water column particulate DMSP+DMS (DMS/Pp) fraction.

Another volume of sample water (typically 50 ml) was filtered into a HDPE container and purged with nitrogen gas for at least ten minutes at a pressure of 0.4 bar. The purged sample was transferred to a Wheaton[®] 400 50 ml vial and prepared as for the DMS/Pd samples. These purged samples represented dissolved DMSP only (DMSPd). Thus, the concentration difference between DMS/Pd and DMSPd samples represents dissolved DMS (DMSd).

Water samples were pre-concentrated using the purge and cryotrap technique as outlined in section 2.1.2.1, typically purging 20 ml of sample. Sample DMS was quantified by comparison to the calibration curve and presented as nmol L^{-1} .



2.2 Pulse Amplitude Modulation fluorometry

Photosynthesis can be directly measured through a variety of techniques, such as radiocarbon fixation or oxygen evolution (Kirk, 2011). An alternative method to establish quantum efficiency and to characterise the photosynthetic characteristics of a plant is to measure chlorophyll fluorescence (Kirk, 2011). For this research, fluorescence was preferable to other techniques as it is non-destructive and may be conducted *in situ*. Chlorophyll fluorescence measurements are presented in Chapters 3 and 6.

2.2.1 Chlorophyll fluorescence

When light is absorbed by a chlorophyll molecule in photosynthesising organisms, the energy is distributed through three, competing pathways (Maxwell and Johnson, 2000) (Figure 2.5):

1. Emission of red light-chlorophyll fluorescence.
2. Heat dissipation.
3. Transfer to photosystems II and I to drive photochemical reactions.

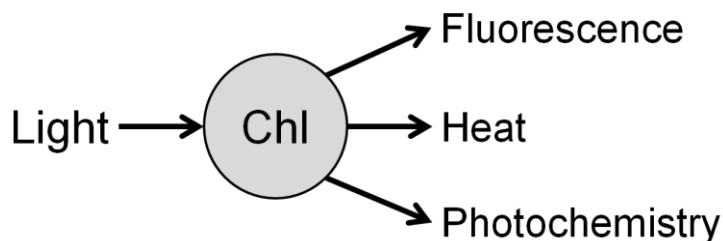


Figure 2.5 The fate of light energy when absorbed by chlorophyll (Chl). **Fluorescence:** the re-emission of red-light, **Heat:** dissipation of heat as a photoprotective mechanism, **Photochemistry:** transfer of energy to photosystems II and I to drive photosynthesis.

Thus, by measuring chlorophyll fluorescence one can gain information on quantum efficiency and heat dissipation (Maxwell and Johnson, 2000). The amount of energy re-emitted as fluorescence is low (1 - 2% of total light absorbed), but is sufficient for accurate measurements (Maxwell and Johnson, 2000).

2.2.2 Modulation fluorometry

By measuring total fluorescence emitted during light exposure, the photosynthetic characteristics of an organism cannot be manipulated under different light regimes to assess its acclimatory responses. Thus, in a conventional fluorometer, the fluorescence signal is simply proportional to the light intensity (Figure 2.6 A,B). The development of pulse amplitude modulation (PAM) fluorometry has overcome this problem. PAM fluorometer detectors only measure the variable fluorescence signal created by a modulated light, rather than the continuous light source (e.g. ambient sunlight, Figure 2.6 C), enabling

the effect of continuous light regimes on chlorophyll fluorescence to be calculated.

2.2.3 The Diving-PAM

A Walz Diving-PAM was used for all fluorescence measurements in this research, obtained from the NERC Field Spectroscopy facility. The Diving-PAM has been specifically designed to operate underwater, enclosed within a watertight Perspex casing, with infrared buttons to allow measurements to be taken underwater *in situ*.

Fluorescence is excited by a pulse modulated red light from a light emitting diode (LED, 655 nm, 3 μ s pulse width). The LED light travels through a cut-off filter (Balzers DT Cyan, special), producing an excitation band that peaks at 650 nm with a negligible tail beyond 700 nm. Fluorescence is detected by a PIN photodiode (type BPY 12, Siemens) at wavelengths >700 nm, as defined by a long-pass filter (type RG 9, Schott). A miniature 8 V/20 W halogen lamp (type Bellaphot, Osram) is used as the saturating light source. The light is filtered by a heat-reflecting filter (Balzers, DT Cyan, special) and a short-pass filter (Balzers, DT Cyan, special) to obtain a white light with little signature at wavelengths >700 nm.

To achieve the best signal to noise ratio, standard operational settings were determined for red coralline algae and applied to all PAM measurements: measuring intensity = 12, pulse frequency = 0.6 kHz, saturation intensity = 3, saturation width = 0.8 μ m, actinic intensity = 5, actinic width = 30 seconds, actinic light factor = 1, gain = 9, damping = 2, light offset = 0, light gain = 1. Those settings specific to an individual study (e.g. Rapid Light Curve irradiances, see section 2.2.8) are detailed in the relevant methods sections of Chapters 3 - 6.

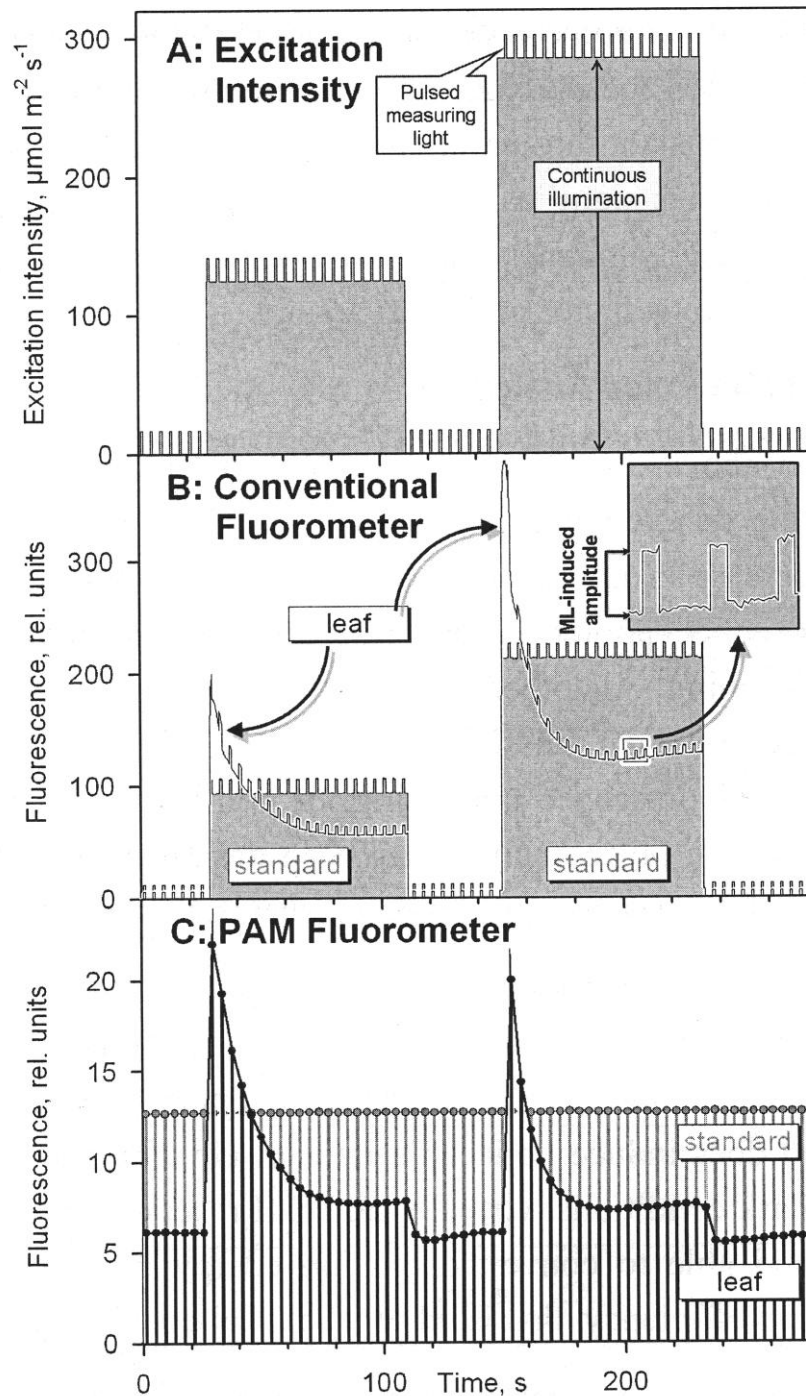


Figure 2.6 Pulse Amplitude Modulation fluorescence measurements.

A: Two separate 80 second intervals of actinic illumination of two intensities with the addition of a pulsed light source with constant, low intensity; **B:** Fluorescence response from standards (grey shading) and leaves (curved black line) to the 80 s illumination periods; **C:** height of fluorescence peaks from the pulsed measuring light (see panel B insert) in response to the 80 s illumination periods for both standards (grey symbols) and leaves (black symbols). Source: Walz (2007).

To minimise the effect of light scattering and to improve measurement precision and accuracy, the water column background signal was removed using the 'Autozero' function of the Diving-PAM before taking measurements in every new water body (e.g. different laboratory aquaria or different state of the tide), thus subtracting the background signal from all measurements.



Figure 2.7 The Walz Diving-PAM underwater fluorometer.
Source: Walz (2012).

2.2.4 Parameter notation

Saturating pulses of actinic light strong enough to close all reaction centres were used to characterise numerous photosynthetic parameters (Figure 2.8). When a saturating pulse is administered in the dark, fluorescence yield reaches a maximum (F_m) and returns to its original level (F_o ; indicating that all reaction centres are open) once in the dark again. When a saturating pulse is applied after exposure to actinic (i.e. photosynthetically active) light, the maximum fluorescence yield is lower (F_m') and returns to a new baseline (F') due to the creation of a high proton gradient across the photosynthetic membrane (ΔpH) (Figure 2.8).

Fluorescence notation in the literature is varied, despite efforts by some to normalise the language used (e.g. Kromkamp and Forster, 2003). Notation in this research remains consistent with that described in Figure 2.8 and Table 2.1.

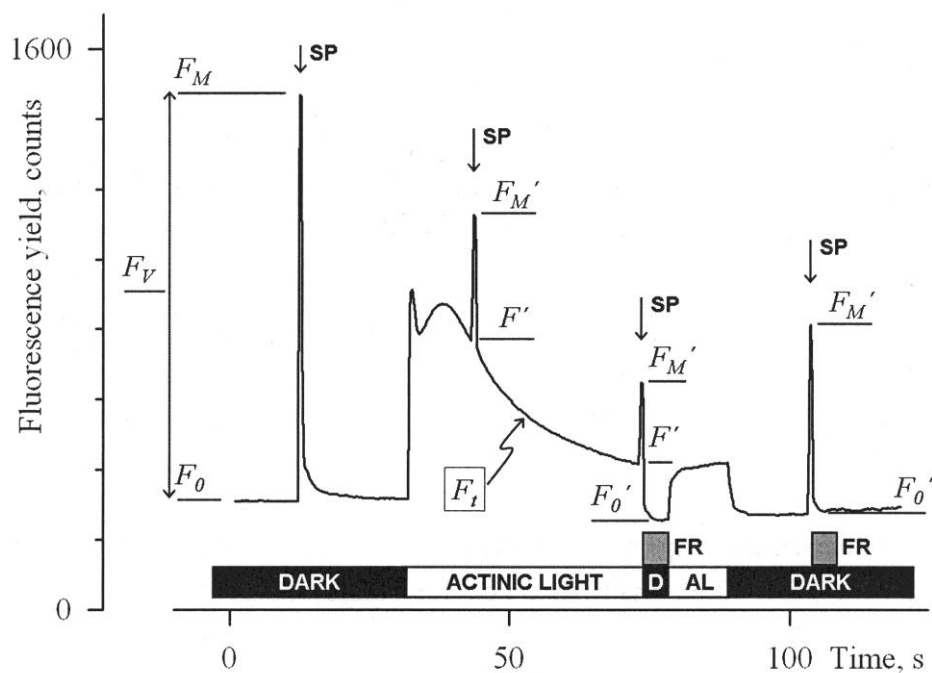


Figure 2.8 Fluorescence response notation.

AL: actinic light, D: dark, SP: saturating pulse, FR: far-red illumination. Source: Heniz Walz (2007).

Table 2.1 Photosynthetic characteristics and definitions.

Fluorescence notation is consistent with this table throughout this research. Fluorescence yields have instrument specific units, ratios are dimensionless.

Parameter	Definition
F_0	Minimum fluorescence (dark acclimated)
F_0'	Minimum fluorescence (light acclimated)
F_m	Maximum fluorescence (dark acclimated)
F	Fluorescence under actinic light
F_v	Variable fluorescence (dark acclimated); $(F_m - F_0)$
F_v'	Variable fluorescence yield under actinic light; $(F_m' - F_0')$
F_q'	Fluorescence quenched; $(F_m - F)$
F_v/F_m	Maximum quantum efficiency of PSII (dark acclimated)
F_q'/F_m'	Effective quantum efficiency of PSII under actinic light; $(F_m - F)/F_m'$
$F_q'/F_{m' \max}$	Calculated maximum quantum efficiency of PSII
F_v'/F_m'	Non photochemical quenching, qN, under actinic light
F_q'/F_v'	Photochemical quenching, qP, under actinic light
NPQ	Non-photochemical quenching; $(F_m - F_m')/F_m'$
α	Initial slope of the light dependent part of a Rapid Light Curve
$rETR_{\max}$	Maximum relative electron transport rate ($\mu\text{mol electrons m}^{-2} \text{s}^{-1}$)
E_k	Light saturation coefficient ($\mu\text{mol photons m}^{-2} \text{s}^{-1}$)

2.2.5 Quantum efficiency

Quantum efficiency (F_v/F_m) was calculated from the difference between fluorescence before and after a saturating pulse. F_v/F_m describes the maximum quantum efficiency of energy transfer to the PSII reaction centre. F_v/F_m , ranging from zero to one, is defined as:

$$F_v/F_m = \frac{F_m - F_o}{F_m}$$

Thus, F_v/F_m was calculated from fluorescence recordings before and after a saturating pulse in the dark. Under actinic light, the effective quantum efficiency, F_q'/F_m' , was calculated by:

$$F_q'/F_m' = \frac{F_m' - F'}{F_m'}$$

2.2.6 Electron transport rate

The electron transport rate (ETR, $\mu\text{mol electrons m}^{-2} \text{s}^{-1}$), a measure of the flow of electrons through the photosystem apparatus, is defined in red algae as (Burdett et al., 2012b; Figueroa et al., 2003; Grzymiski et al., 1997):

$$ETR = Yield \times PAR \times 0.15 \times A$$

Where yield is the maximum or effective quantum efficiency (F_v/F_m or F_q'/F_m'), PAR is photosynthetically active radiation ($\mu\text{mol photons m}^{-2} \text{s}^{-1}$), 0.15 represents the total amount of chlorophyll associated with PSII in red algae (15%), and A is the absorbance cross section ($\text{m}^2 \text{mg chl a}^{-1}$) of the algae. However, the logistics of accurately measuring an algal absorbance value for every sample, particularly *in situ*, led to the use of relative ETR (rETR), a parameter commonly quoted in fluorescence literature:

$$rETR = Yield \times PAR \times 0.15$$

2.2.7 Dark acclimation

In the dark, the complete opening of reaction centres allows for a measurement of maximum, rather than effective, quantum efficiency (F_v/F_m). The time required to fully relax PSII, open all reaction centres and achieve F_v/F_m is termed the dark acclimation time and is an essential baseline measurement from which other measurements were based. Dark acclimation time is species-specific and was determined specifically for coralline algae in Chapter 3.

2.2.7.1 Quasi-dark acclimation

It was often logistically impractical to perform a full dark acclimation prior to conducting fluorescence measurements *in situ*. Thus, 'quasi-dark acclimation was used as a substitute (Burdett et al., 2012b; Hennige et al., 2008), where the photosynthetic tissue was briefly shaded for 10 s prior to fluorescence measurements. Despite the small timeframe, such shading has been shown to cause quantum efficiency to rise to >95% of the maximum achieved after full dark acclimation (Burdett et al., 2012b; Hennige et al., 2008, also see Chapter 3). Quasi-dark acclimation was achieved for coralline algae using the Walz surface holder attachment (Diving-SH) to shade the sample for 10 s prior to measurements (Figure 2.9). The fibre optic probe was always 10 mm from the algal surface for all measurements.

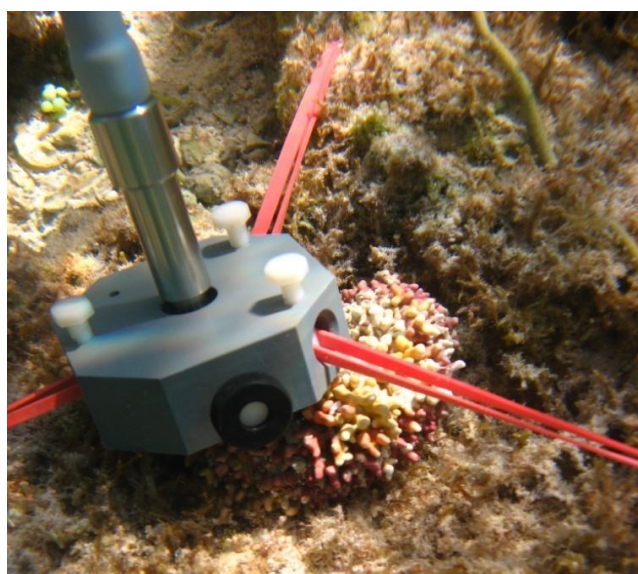


Figure 2.9 The Walz Diving-PAM surface holder attachment. Surface holder is 65 mm wide and attached to a free living red coralline algal thallus. Photo: N. Kamenos.

2.2.8 Rapid Light Curves (RLCs)

Traditional light curves have been used to determine the optimal photosynthetic capacity of plants for many decades (Falkowski and Raven, 2007). Plants are exposed to increasing levels of irradiance for several minutes to achieve steady state acclimation (F') to the light regime. Using O_2 or CO_2 evolution gas measurements, the optimal photosynthetic capacity of the plants can be determined (Ralph and Gademann, 2005). As measurements are made only after a steady state has been achieved, traditional light curve data is independent of previous light history effects (Ralph and Gademann, 2005).

Rapid Light Curves (RLCs) have become well established in fluorescence research due to their short run time and the acquisition of a large amount of information regarding an organism's photosynthetic characteristics (Ralph and Gademann, 2005; White and Critchley, 1999). In RLCs, saturating light pulses are interspersed with (typically) eight short periods of gradually increasing irradiance (Figure 2.10), providing photosynthetic information during light-limiting, optimal and light-saturating conditions.

Irradiance periods were rapid (10 s in length), thus, unlike traditional light curves, the algae did not achieve steady state conditions at each light step, (Ralph and Gademann, 2005). As such, information regarding the actual, rather than optimal, photosynthetic state are gained (Ralph and Gademann, 2005). RLC data highlight the photosynthetic plasticity of algae but, as the algae do not reach a steady state, results are affected by previous light history (e.g. high / low light acclimation) (Ralph and Gademann, 2005).

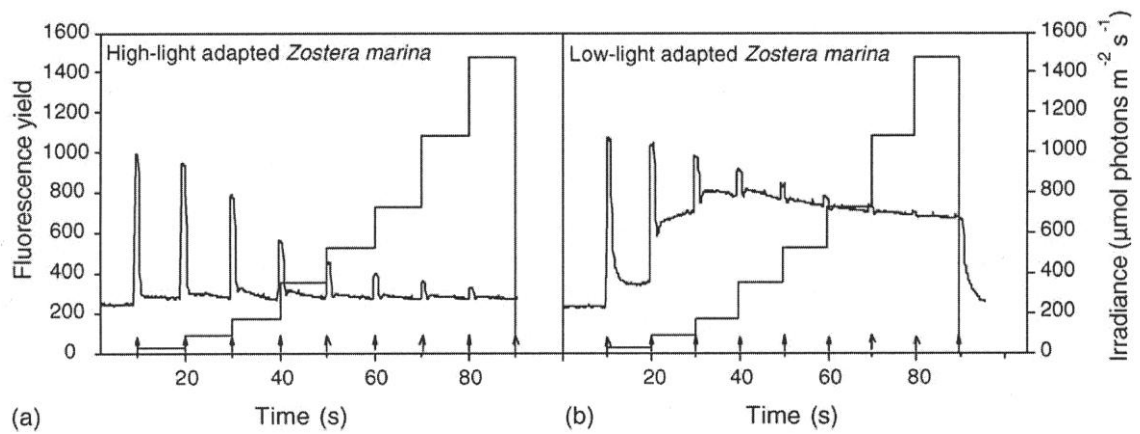


Figure 2.10 RLC fluorescence signal from the seagrass *Zostera marina*. RLCs of 10 s periods of increasing irradiance (stepped curve) conducted on (a) high-light adapted *Zostera marina* leaves and (b) low-light adapted *Z. marina* leaves. Fluorescence trace shows maximum fluorescence peaks (F_m') following each saturating pulse (arrows). Source: Ralph and Gademann (2005).

2.2.9 Photosynthetic parameters

RLC data were used to construct photosynthesis-irradiance curves similar to those from traditional light curves (known as *P-E* curves). However, as a steady state is not achieved during RLCs, the results could not be interpreted the same as *P-E* curves. Nonetheless, both light curves have three regions (Figure 2.11):

1. Light limitation.
2. Light saturation.
3. Photo-inhibition.

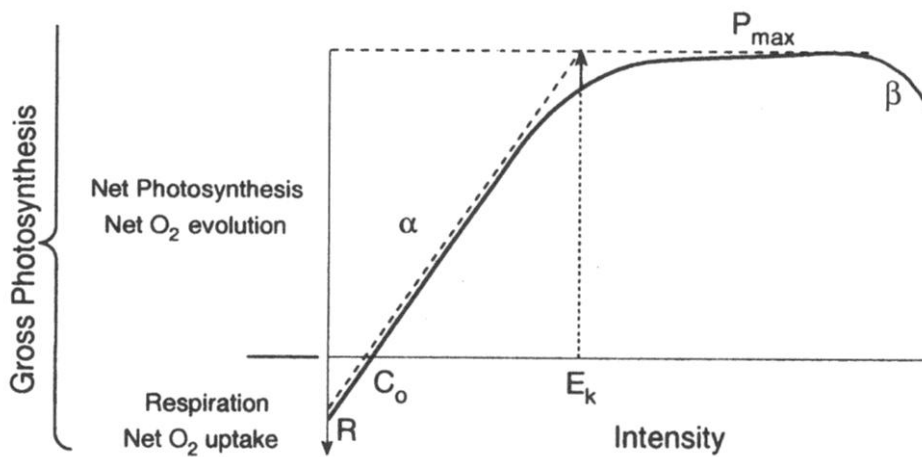


Figure 2.11 Photosynthesis-irradiance curve.

Dark respiration, R , is constant in the light, α : linear relationship between photosynthesis and irradiance at low light levels, P_{\max} : maximum photosynthesis, E_k : intercept between α and P_{\max} , β : decline in photosynthesis at high irradiance. Source: Falkowski and Raven (2007).

These curves provide a lot of information in addition to the quantum efficiency and quenching obtained from an individual saturating pulse. The linear rise of the light limited region (α , dimensionless, Figure 2.11) is proportional to the ‘efficiency of light capture’, i.e. the effective quantum efficiency under actinic light, thus providing information on an organism’s light acclimation level. Using least squares non-linear regression, α and the theoretical maximum of $rETR$ under saturating actinic light ($rETR_{\max}$, $\mu\text{mol electrons m}^{-2} \text{s}^{-1}$) were calculated from $rETR$ at each RLC step (Hennige et al., 2008; Jassby and Platt, 1976):

Where $E = \text{PAR}$ ($\mu\text{mol photons m}^{-2} \text{s}^{-1}$).

The light saturation coefficient (E_k), defined as the intercept between α and maximum quantum efficiency (Figure 2.11), represents the optimum light level for maximum quantum efficiency (Hill et al., 2004). PAR levels below E_k are light limiting; light levels above E_k are light saturating. E_k and the theoretical maximum effective quantum efficiency ($F_q'/F_{m' \max}$) were calculated from $F_q'/F_{m'}$ at each RLC step using least squares non-linear regression (Hennige et al., 2008; Suggett et al., 2007; Moore et al., 2005):

Where $E = \text{PAR}$ ($\mu\text{mol photons m}^{-2} \text{ s}^{-1}$). For the first RLC data point, F_v/F_m was used as the first RLC measurement was taken from (quasi)dark acclimated thalli.

2.2.10 Quenching parameters

Photochemical quenching (qP) and non-photochemical quenching (qN) are both derived from F_q'/F_m' and have a range from zero to one:

$$qP = \frac{F_v' - F_o'}{F_m' - F_o'}$$

$$qN = \frac{F_m' - F_v'}{F_m' - F_o'}$$

qP and qN describe the decrease in fluorescence due to photochemical (enzymatic carbon metabolism) and non-photochemical (heat production efficiency) quenching respectively. Thus, decreasing values of qN represent increased non-photochemical quenching. However, to aid interpretation, qN results were plotted as $1 - qN$, thus a graphical increase represents an increase in non-photochemical quenching. qP and qN rely on the assumption that only the variable fluorescence (F_v), and not F_o , is affected by fluorescence quenching. However, at high levels of qN, this assumption does not hold. F_o' , used in the determination of qP and qN was derived according to Suggett et al. (2003) as F_o' is difficult to measure directly due to residual 'glow' from actinic lamps after they are turned off (Kromkamp and Forster, 2003). Thus, another expression of non-photochemical quenching, Stern-Volmer non-photochemical quenching (NPQ), that does not rely on measurements of F_o' , was also used:

$$NPQ = \frac{F_m' - F_v'}{F_v'}$$

NPQ best describes the heat dissipation of energy (which occurs at high qN) (Hanelt and Nultsch, 1995). However, at low qN values (<0.4), where thylakoid membrane excitation is typically predominant, NPQ is relatively insensitive (Figure 2.12) (Hanelt and Nultsch, 1995).

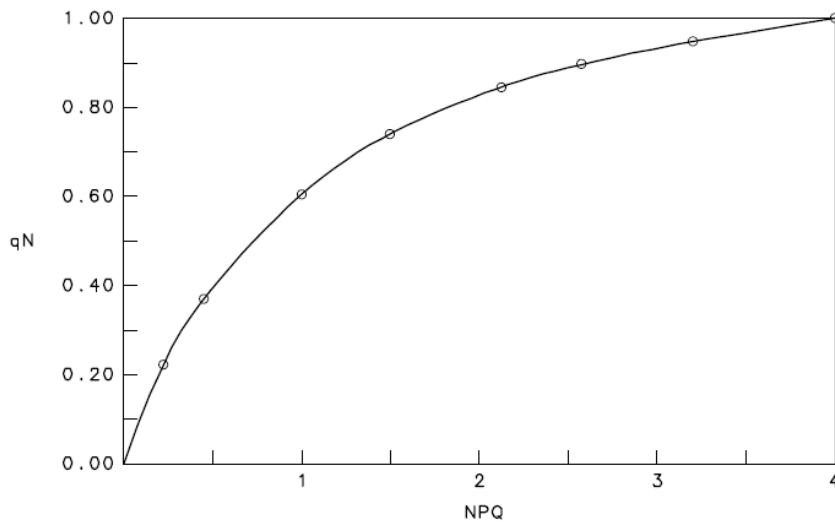


Figure 2.12 Relationship between qN and NPQ.
Source: Walz (1999).



2.3 Scanning Electron Microscopy

Scanning electron microscopy (SEM) imaging was used to image the morphology of the outer epithelial layer of red coralline algae following periods of environmental stress caused by reduced salinity and variable pH conditions (Chapter 6 and 7). All samples were imaged at the University of Glasgow Imaging Spectroscopy and Analysis Centre (ISSAC). A schematic of the SEM chamber, electron beam and detectors is given in Figure 2.13. Electron-sample interactions allow numerous analyses to be undertaken within an SEM, revealing, for example, the morphology, composition and crystallography of a sample (Goldstein et al., 1992). Electron-sample interactions can be divided into two groups (Goldstein et al., 1992):

1. Elastic scattering: electron path is altered but the kinetic energy remains near constant. Yields electron backscattering information required for some imaging techniques.
2. Inelastic scattering: little electron path deviation but a transfer of energy from the beam electrons to the sample atoms occurs. Results in secondary electron (SE) generation as well as x-rays, cathodoluminescence and heat.

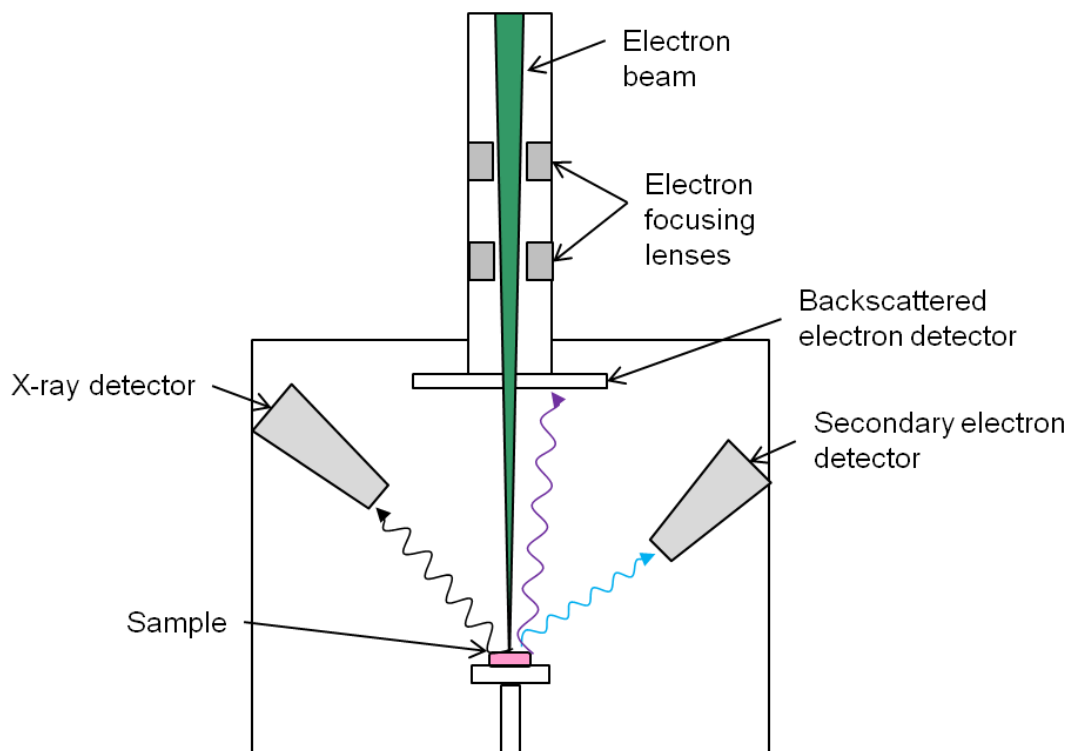


Figure 2.13 Schematic representation of an SEM.
Note the three types of emissions from elastic and inelastic electron scattering.

2.3.1 Secondary Electron Imaging

SEs are produced throughout the interaction volume of the sample (Figure 2.14), but due to their low energy, only those produced close to the sample surface can be used for imaging (Goldstein et al., 1992). SEs produced as the beam electrons pass through the sample (SE_1) yield a high resolution signal, whilst those derived from the backscattered electrons (SE_2) are typically low-resolution (Goldstein et al., 1992).

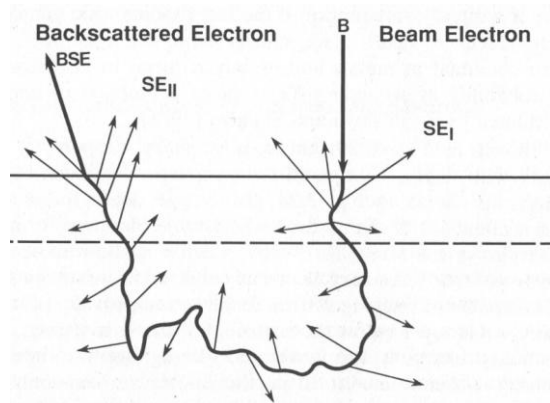


Figure 2.14 Generation of secondary electrons in a sample. Beam electrons (B) generate SE₁ electrons upon entering the sample. Backscattered electrons (BSE) generate SE₂ electrons whilst leaving the sample. Dashed line represents the depth limit of electron escape from the sample for subsequent detection. Image from Goldstein et al. (1992).

2.3.2 Sample preparation

Coralline algal branches (ca. 10 mm in length) were air-dried at least overnight and fixed onto glass slides using Blu-tack® prior to applying a 40 nm gold coating to minimise charging effects caused by the high resistivity of coralline algae. Silver-dag paint was applied to provide a constant connection between the algal branches and the SEM stage, ‘earthing’ the sample and further minimising charging effects (Figure 2.15).

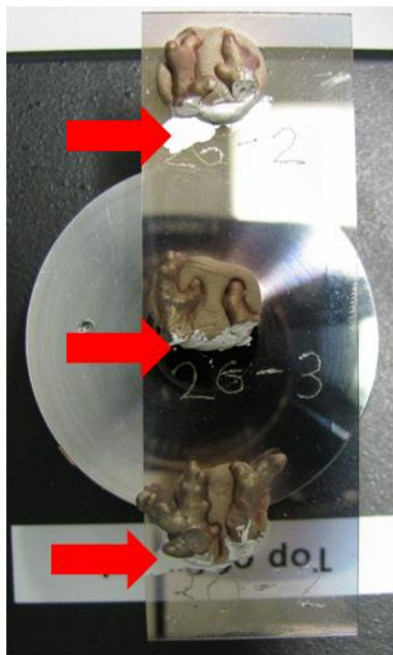


Figure 2.15 Gold-coated coralline algae branches. 40 nm thick gold coating in preparation for SEM imaging. Red arrows indicate the silver-dag paint to reduce charging effects.

2.3.3 Imaging protocol

The Zeiss Sigma field emission SEM was used for SE imaging of red coralline algal branches in Chapter 7 (ocean acidification, laboratory study). Coralline algal epithelial cells are sensitive to structural degradation under high vacuum (Kamenos, pers. obs.), thus a low vacuum setting was employed. However, under low vacuum, gas remains in the SEM chamber, increasing the spread of the electron beam, which can lead to reduced image quality. The application of a gold coat and silver-dag minimises these deleterious effects and high quality images may be resolved. Additional operational settings were: accelerating voltage 15.0 kV, working distance of 10 mm.

Even in low vacuum mode, the pressures within a standard SEM chamber are low enough to evaporate water from biological samples, thus samples must be completely dry before being placed in the SEM chamber. This, however, often creates desiccation artefacts (Goldstein et al., 1992). In coralline algae, such preparation artefacts are seen as cracks between the cell membrane and the calcite cell wall, as observed in the laboratory-based ocean acidification experiment described in Chapter 7 (Figure 2.16).

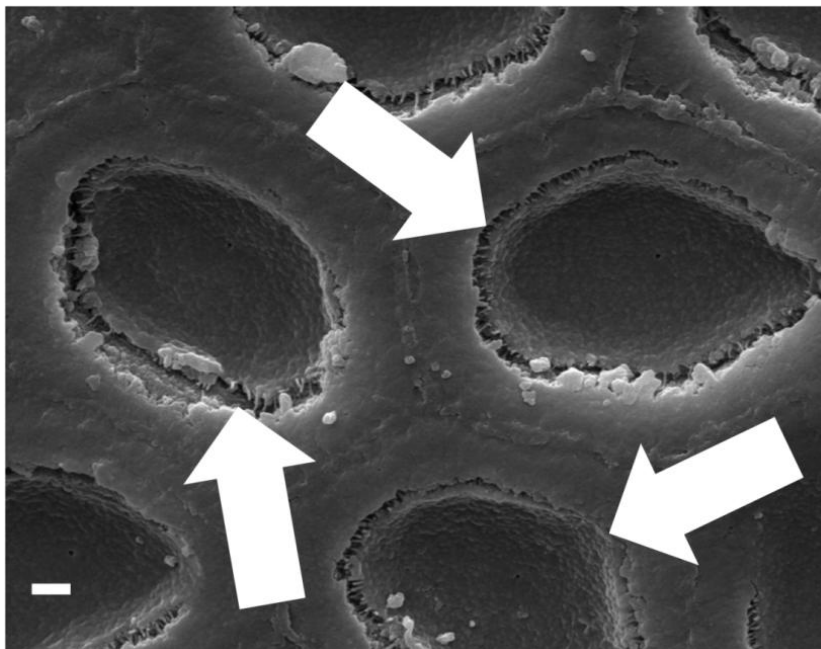


Figure 2.16 SE image of red coralline algal epithelial cells. Arrows indicate desiccation damage because of air-drying the sample prior to imaging. Magnification: 12000X, scale bar = 1 μ m. Source: Chapter 7 and Burdett et al. (2012a).

2.3.4 Environmental SEM

To prevent desiccation artefacts, samples may be imaged at high pressure and humidity (environmental SEM, ESEM). A FEI Quanta 200F environmental SEM was used for ESEM imaging of coralline algal branches in Chapter 6 (chronic salinity reduction). In ESEM mode, the samples were maintained in the SEM chamber at 100% humidity, at a starting pressure of 860 Pa. No sample preparation was required prior to imaging: excess water was removed from the algal branches (ca. 10 mm in length) and they were placed directly onto the ESEM stage (cooled to 3°C). Droplets of Milli-Q ultrapure 18Ω water were used to create a humid environment surrounding the sample. Chamber pressure was gradually reduced to evaporate water from the surface of the algae to allow imaging of the surface epithelial layer. Care was required to ensure the chamber humidity did not drop too far; below 100%, water evaporation and subsequent cell desiccation was rapid.

The inevitable elastic electron scattering by gas molecules within the high pressure environment of an ESEM chamber leads to a significant spreading of the electron beam. To maintain a high image resolution, the working distance was low (6 mm), minimising electron scattering effects. Additional ESEM operational settings were: accelerating voltage of 10.0 kV, spot size of 3.0 (no units).



2.4 Optical spectroscopy

By measuring reflectance spectra from algae, their pigment composition may be inferred based on the pigment absorbance peaks outlined in Chapter 1 (Table 1.3). The optical reflectance of free-living red coralline algae was recorded on two occasions:

1. To quantitatively assess differences in pigmentation between the top and underside of free-living coralline algal thalli under naturally high irradiance (Chapter 3).
2. To record changes in free-living coralline algal pigmentation because of freshwater runoff (Chapter 6).

Reflectance spectra were recorded using a USB 2000+ Ocean Optics spectrometer. The spectral range of the instrument was 200 - 1100 nm. Spectra were sampled at 0.4 nm intervals and the resolution of the spectrometer was 0.35 nm.

Coralline algal branches were patted dry and light was shone onto the algal branch using a 5 mm multi-fibre optic probe (Walz Inc.). Reflected light was transmitted to the spectrometer using a 400 μm single-fibre optic (Ocean Optics) probe (Figure 2.17). The specific light source used to determine reflectance is detailed in the relevant results sections of Chapters 3 and 6. Due to the small diameter and non-linearity of coralline algal branches, it was logistically difficult to maintain a fixed angle between the two fibre optics. Thus, for each sample, the cables were positioned to achieve maximum reflectance output based on the real-time trace from the spectrometer. Percentage reflectance was calculated based on the difference between sample reflectance and the reflectance of white paper (100% reflectance). Black paper was used as a negative control (zero reflectance).

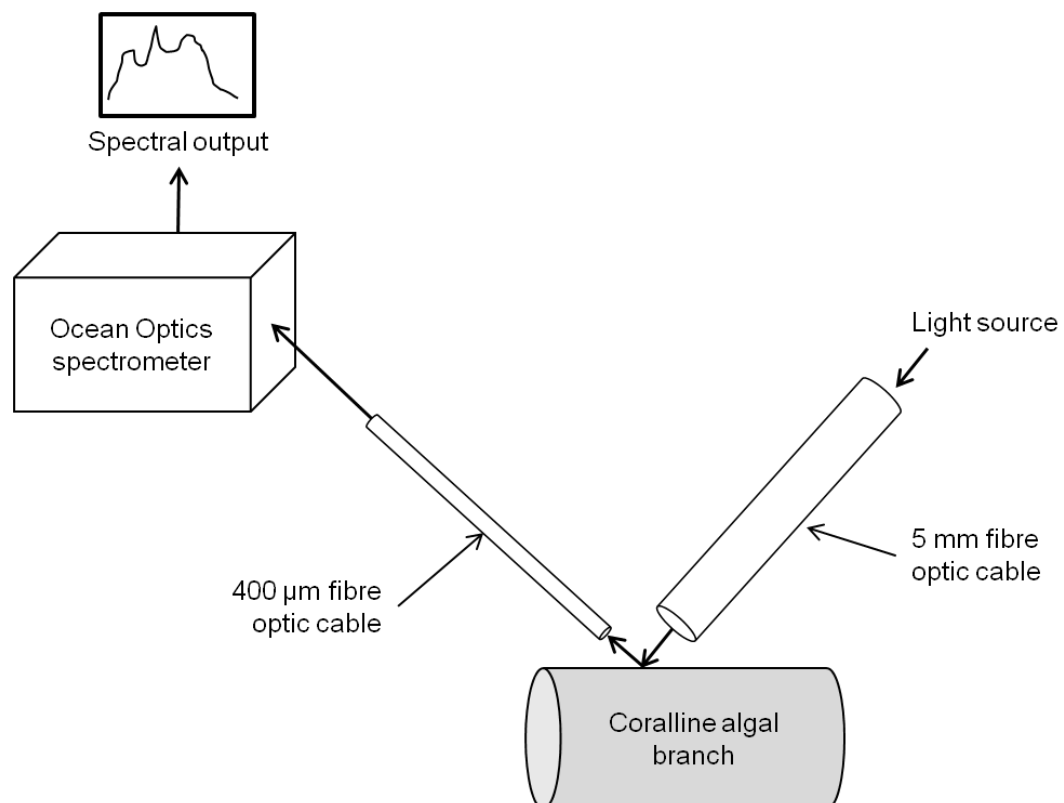


Figure 2.17 Method for recording the reflectance spectra of coralline algae.

3

The photosynthetic characteristics of red coralline algae

The growth and cellular function of coralline algae, as with any photosynthetic organism, are dependent on photosynthesis. Thus, a knowledge and appreciation of the photosynthetic characteristics of coralline algae is crucial for more detailed research into the ecosystem function, biogeochemistry, palaeoenvironmental reconstruction and climate change effects on coralline algal habitats.

3.1 Introduction

3.1.1 The relationship between DMSP and photosynthesis

The cellular precursor to dimethylsulphoniopropionate (DMSP) in photosynthetic organisms is methionine (Stefels, 2000), although the synthesis pathways appear to vary between higher plants and algae (Figure 1.2) (Stefels, 2000). Methionine is a sulphur-containing amino acid that is an indirect product of photosynthesis - the activity of methionine synthase is dependent on ATP (energy), carbohydrates and reduction agents derived from the photosynthetic electron transport chain (Wirtz and Droux, 2005). Methionine is also an essential component of a number of photosynthetic proteins such as RuBisCO and the D1-protein (Wirtz and Droux, 2005). Thus, an alteration in intracellular methionine concentrations, perhaps due to the up-regulation of DMSP production in response to environmental stress, may impact photosynthesis. Similarly, the availability of

intracellular methionine may ultimately affect an alga's ability to produce DMSP; an increase in intracellular DMSP (DMSPi) was observed in the microalga *Tetraselmis subcordiformis* following culture in seawater dosed with methionine (Gröne and Kirst, 1992). Currently, the photosynthetic characteristics of coralline algae are poorly understood. However, this information may enhance our understanding of the processes and drivers involved in regulating DMSPi production.

3.1.2 Pulse Amplitude Modulation fluorometry

As described in Chapter 2, Pulse Amplitude Modulation (PAM) fluorometry provides a simple but effective means of gathering detailed information on the photosynthetic characteristics of photosynthetic organisms and their response to the natural environment. PAM fluorometry has been used to study the photosynthetic characteristics of various marine photosynthetic organisms such as seagrass, corals, micro- and macro-algae.

PAM fluorometry has identified eco-physiological differences between tropical and temperate seagrass species such as the lack of photorespiration in *Cymodocea nodosum* (Beer et al., 1998). More recently, PAM fluorometry has been used in seagrass meadow conservation and monitoring by translating organism responses to a landscape scale (Durako, 2012; Belshe et al., 2008; Belshe et al., 2007; Durako and Kunzleman, 2002).

In corals, heterogeneity in photosynthetic characteristics has been observed when specimens were exposed to different environmental conditions, including flow rate (Carpenter and Patterson, 2007), turbidity (Hennige et al., 2008) and depth (Hennige et al., 2008). Significant variations in photoacclimation and photorepair rates of *Symbiodinium* spp. (coral zooxanthellae) have also been observed (Hennige et al., 2011; Hennige et al., 2009), with implications for bleaching susceptibility and coral survival.

For algae, the use of PAM fluorometry historically focused on microalgae (Enríquez and Borowitzka, 2010). However, enhanced cell movement through stirring to maintain a homogenous sample can affect fluorescence results due to the exposure of previously shaded cells directly into the light path (Cosgrove and

Borowitzka, 2006). When utilising PAM fluorometry on macroalgae, it is important to take this information into account by considering the absorbance and thickness of the thalli (Nielsen and Nielsen, 2008). These factors can result in distinct seasonal and species-specific differences (Saroussi and Beer, 2007). Photoinhibition appears to be more pronounced in macroalgae from deeper waters, with weak or no potential for recovery (Häder et al., 1998). The effect of metal toxicity on quantum efficiency is also highly species-specific (Baumann et al., 2009). At high irradiance ($1700 \mu\text{mol photons m}^{-2} \text{s}^{-1}$), macroalgal oxygen evolution (i.e. photosynthetic rate) is less closely related to PAM-derived electron transport rate (ETR) compared to low irradiances ($200 \mu\text{mol photons m}^{-2} \text{s}^{-1}$) (Beer and Axelsson, 2004).

3.1.2.1 PAM and red coralline algae

The use of non-invasive chlorophyll-*a* techniques such as PAM fluorometry on red coralline algae is limited and studies thus far have not attempted to fully describe the photosynthetic characteristics of these organisms. Quantum efficiency (F_v/F_m) has been used as an indicator of coralline algal stress response to various environmental perturbations such as temperature, salinity, light, heavy metals, burial fragmentation and desiccation (Wilson et al., 2004). In kelp forest ecosystems, a reduction in ETR per unit of PAR was observed in coralline algae following kelp canopy removal and a subsequent increase in ambient light levels (Irving et al., 2004). Some more detailed studies (using PAM fluorometry and oxygen production measurements) suggest that coralline algae are often low-light adapted relative to ambient light, although the extent of low-light adaptation is species and site-specific (Schwarz et al., 2005; Chisholm, 2003; Roberts et al., 2002; Payri et al., 2001).

The response of red algae to PAM fluorometry techniques is different to other algae due to the presence of phycobilisomes in the photosynthetic apparatus (see section 1.2.4.1). Thus, the photosynthetic response of red algae is more similar to cyanobacteria (Enríquez and Borowitzka, 2010). Baseline fluorescence measurements (F_o and F_o') from a red-modulated PAM originate from phycobiliproteins as well as PSII, thus introducing a small, but noteworthy, potential error in the calculation of qN (Campbell et al., 1998). It has been suggested that the use of a blue-light PAM overcomes this issue by recording

signals from chlorophyll only (Campbell et al., 1998), but can also stimulate pigment and protein production, affecting photosynthetic capacity (Figuerola et al., 1995). Unfortunately, a blue-light PAM fluorometer was not available during this research for comparison, thus all measurements were made with a red-light Diving-PAM.

3.1.3 The diurnal pattern of photosynthesis

The rate of photosynthesis is not directly proportional to irradiance (Kirk, 2011), as other factors can play a more limiting role. This includes, but is not restricted to, the number of PSII reaction centres, whether the primary electron acceptor (Q_A) is open and the time required for Q_A to re-open post-reaction (Kirk, 2011). The number of available PSII reaction centres is reduced as irradiance increases, resulting in increased fluorescence emissions, increased photoprotection (NPQ) and non-photochemical quenching (qN) (White and Critchley, 1999) and a reduction in quantum efficiency (F_v/F_m) (Ralph and Gademann, 2005) (Figure 3.1).

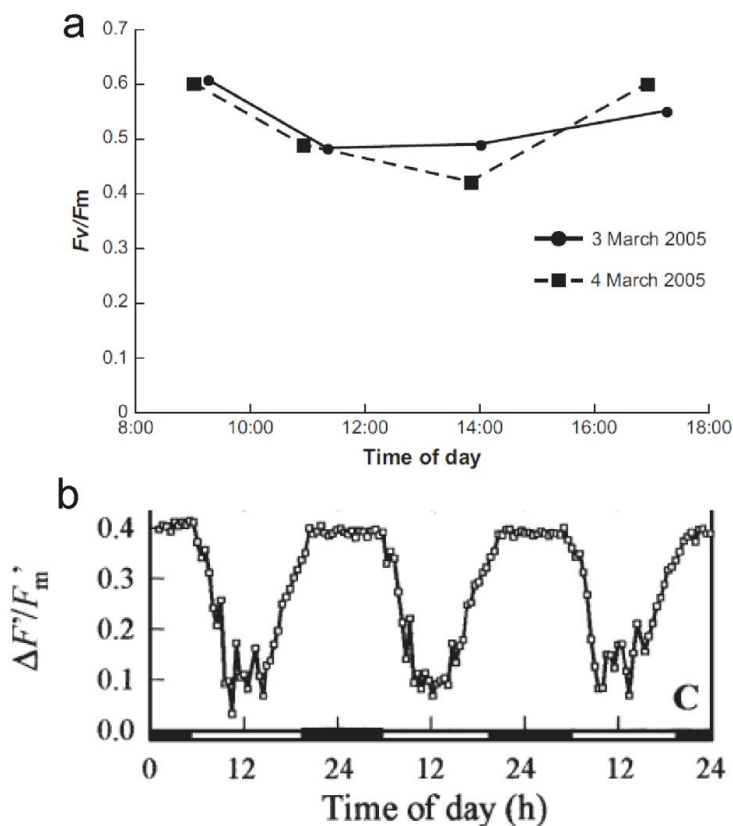


Figure 3.1 Diurnal photosynthetic response of coral and microalgae. Quantum efficiency over a diurnal cycle in (a) the coral *Montastrea faveolata* (Levy et al., 2004) and (b) an ice algal community (Aikawa et al., 2009).

Continued photoacclimation throughout the day results in diurnal photocharacteristic patterns (Figure 3.1). Such trends have been observed in numerous aquatic organisms including seagrass (Belshe et al., 2008; Belshe et al., 2007; Durako and Kunzelman, 2002), corals (Piniak and Storlazzi, 2008; Levy et al., 2004; Winters et al., 2003), microalgae (Aikawa et al., 2009; Yoshikawa and Furuya, 2006) and macroalgae (Edwards and Kim, 2010; Figueroa et al., 2009; Häder et al., 1998). However, certain organisms do not exhibit clear diurnal trends in quantum efficiency (e.g. giant kelp, Edwards and Kim, 2010). Thus, the photosynthetic characteristics of red coralline algae cannot be assumed.

3.2 Aims of this chapter

The primary aim of this chapter was to determine PAM fluorescence techniques suitable for coralline algae and to provide baseline photosynthetic data, from which more complex ecological and photosynthetic studies could be based (both within this research and in a wider context). Little is known about the photosynthetic characteristics of temperate free-living coralline algae, despite their potential to be significantly affected by climate change (e.g. ocean acidification, see Chapter 7). Thus a comprehensive understanding of the basic photosynthetic response of temperate coralline algae is crucial if we are to make predictions for the future. Tropical coralline algae experience a much larger range in daily irradiance than those in temperate regions, therefore are more likely to have well developed mechanisms for diurnal photoacclimation.

Specifically this research aimed to:

1. Identify suitable PAM fluorescence methodologies and techniques to study the photosynthesis of free-living coralline algae using the temperate alga *Lithothamnion glaciale*.
2. Compare the fluorescence response of *L. glaciale* in the laboratory and *in situ*.
3. Characterise the diurnal photosynthetic response of the tropical coralline algae *Porolithon* sp. and *Lithophyllum kotschyianum* due

to the algae's exposure to a naturally high diurnal variability compared to temperate regions (maximum c.a. 2500 $\mu\text{mol photons m}^{-2} \text{ s}^{-1}$ in the summer, c.a. 900 $\mu\text{mol photons m}^{-2} \text{ s}^{-1}$ in the winter).

It was hypothesised that (1) PAM fluorometry would be a useful tool in determining the photosynthetic characteristics of red coralline algae, (2) laboratory and *in situ* responses of *L. glaciale* would differ due to the inherently unnatural conditions in laboratory culture and (3) tropical coralline algae would continually photoacclimate throughout the day in response to the changing light regime.

3.3 Methods: temperate alga *Lithothamnion glaciale*

3.3.1 Collection of algal material

Free-living thalli of *L. glaciale* were collected from Loch Sween, Scotland (56°01.99'N, 05°36.13'W) at a depth of 6 m using SCUBA in March and May 2011. Algae were either measured *in situ* or transported to the University of Glasgow in seawater (ambient temperature, in the dark) for laboratory experimentation in 120 litre re-circulating seawater tanks at ambient conditions.

3.3.2 Fluorescence measurements

Fluorescence measurements were made using the Diving-PAM fluorometer and WinControl software (Walz GmbH, Germany) as described in Chapter 2. Photocharacteristic parameters were calculated as described in Chapter 2 using F_o and F_m outputs from the Diving-PAM. Five and 2 mm fibre optic probes were used in this research to assess the benefits and drawbacks of different sized probes. The diameter of the probes relative to a typical *L. glaciale* thallus is shown in Figure 3.2.

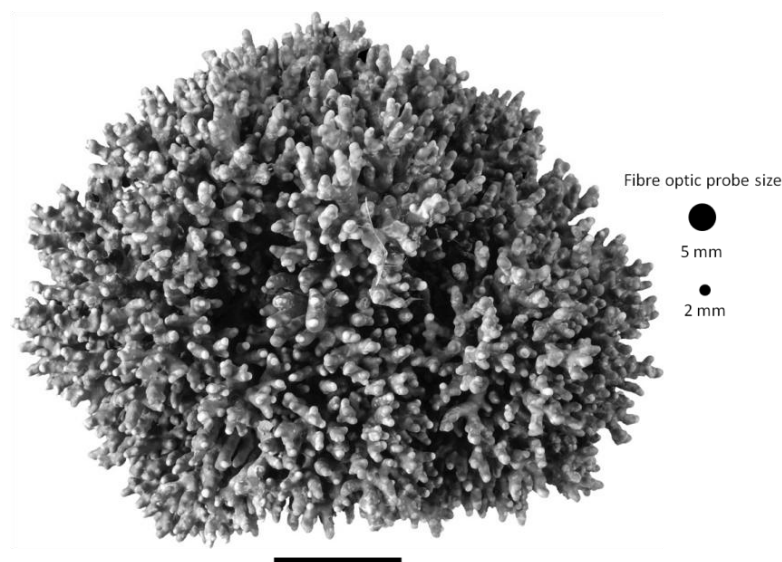


Figure 3.2 Coralline algal thallus and PAM fibre optic probes.
Free-living *L. glaciale* thallus and the relative size of two fibre optic probes: 5 mm and 2 mm.
Scale bar = 20 mm.

3.3.2.1 Dark acclimation

To assess the time required for full dark-acclimation of *L. glaciale*, dark acclimation experiments were conducted in re-circulating seawater tanks (800 x 400 x 350 mm) at the University of Glasgow. Discrete fluorescence measurements were conducted on thalli ($n = 5$ per timepoint) maintained in the laboratory under actinic light ($90 \mu\text{mol photons m}^{-2} \text{s}^{-1}$). Thalli were subjected to saturating light pulses at 5 min intervals ($t = 0, 5, 10$ mins) whilst illuminated by the aquarium lights. Aquarium lights were switched off after 14 mins 50 s and a further eight saturation measurements were taken at $t +15, 20, 25, 30, 35, 40, 60$ and 100 mins. Measurements were made at thallus branch tips using the 5 mm and 2 mm probes and the branch base using the 2 mm probe only (the 5 mm probe would not fit between the algal branches). Measurements were taken from the same area of thallus throughout the dark acclimation experiment; probes were maintained at a distance of 10 mm - this was sufficient to achieve a F_o / F_o' value of between 300 - 800 counts for all samples.

The dark acclimation experiments suggested that a five minute dark period was sufficient to fully relax PSII (as indicated by increased quantum efficiency, F_v/F_m , Figure 3.3), and that 10 s of 'quasi' dark acclimation was sufficient when sample collections were time constrained (e.g. *in situ*). Quantum efficiency increased by an average of 12.5% (SE $\pm 1.7\%$) after 10 s of darkness, further increasing to a maximum after five mins in the dark for the 5

mm and 2 mm branch tip measurements. 10 s dark-acclimation quantum efficiency values represented ca. 95 - 98% of the maximum quantum efficiency achieved after five mins of dark acclimation, and was thus deemed suitable for *in situ* dark-acclimation.

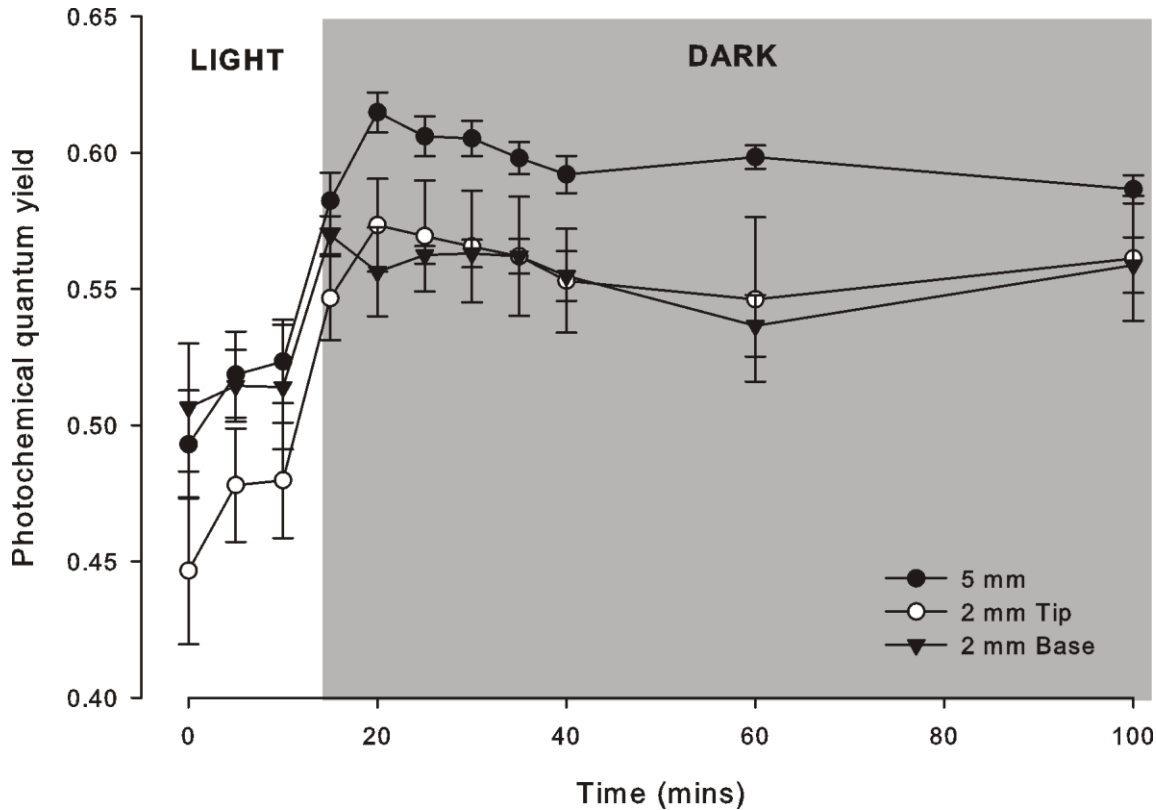


Figure 3.3 Dark acclimation response of *L. glaciale*.

Quantum efficiency measurements (yield) of *L. glaciale* thalli in the light (0 – 10 mins) and dark (15 – 100 mins). Lights were turned off after 14 mins 50 s. Measurements were taken from thalli branch tips using 5 mm (black circle) and 2 mm (open circles) fibre optic probes and from the branch bases using a 2 mm probe (black triangles). Data presented as mean±SE.

Rapid light curves (RLCs)

RLCs were conducted on *L. glaciale* thalli from Loch Sween both in the laboratory and *in situ*. RLC step intensities ranged from 2 to 997 $\mu\text{mol photons m}^{-2} \text{s}^{-1}$ PAR. RLCs were conducted at the tips of branches using 5 mm and 2 mm fibre optic probes, and at the base of branches using only the 2 mm probe. For information on experimental design see section 3.3.3, for RLC conduct see Chapter 2.

3.3.3 Experimental design

3.3.3.1 *In situ* measurements

RLCs were conducted *in situ* at Loch Sween in May 2011 on undisturbed thalli at 6 m depth, following quasi-dark acclimation where the thalli were shaded for 10 s prior to running the light curve. 95 - 98% of the maximum quantum efficiency is achieved after 10s in the dark (see dark acclimation results in section 3.3.2). Measurements were conducted on thalli tips (n = 5) using both 5 mm and 2 mm probes at a distance of 10 mm from the algal surface. In the field, it was not possible to see the locality of the fibre optic end to obtain reliable 2 mm probe base measurements. Thus, no base measurements were conducted *in situ*.

3.3.3.2 Laboratory measurements

Thalli were collected in March and May 2011 for laboratory measurements. In the laboratory, thalli were maintained under ambient conditions for that time of year in 120 litre re-circulating seawater aquaria (800 x 350 x 400 mm):

March: $7\pm 1^\circ\text{C}$, 32 salinity and 10:14h light:dark cycle.

May: $12\pm 1^\circ\text{C}$, 32 salinity and 17:7h light:dark cycle.

Irradiance was maintained at $90\ \mu\text{mol photons m}^{-2}\ \text{s}^{-1}$ during daylight hours, corresponding to average light intensities in Loch Sween (Rix et al., 2012). RLCs were conducted after five mins dark acclimation as follows:

1. 5 mm fibre optic: thalli tips only (n = 5).
2. 2 mm fibre optic: thalli tips and bases (n = 5).

3.3.4 Statistical analyses

All analyses were performed using Minitab v15. Normality and homogeneity of variance assumptions for parametric testing were met without

the need for data transformation. For data comparisons, general linear models were used throughout, $n = 5$ for all data sets.

3.4 Methods: tropical coralline algae (diurnal response)

3.4.1 Measurement of ambient PAR

This research was conducted on the Suleman fringing reef, Sinai peninsula, Egypt ($28^{\circ}28.8''N$ $34^{\circ}30.8'E$). Chapter 7 (ocean acidification) describes in more detail the reef structure at this site. To enable photokinetic parameters to be compared to ambient light levels, *in situ* PAR ($\mu\text{mol photons m}^{-2} \text{s}^{-1}$) on the reef flat was measured using an Apogee QSO-E underwater quantum sensor (calibrated to electric light) and a Gemini voltage data logger (Figure 3.4) over a full diel cycle.

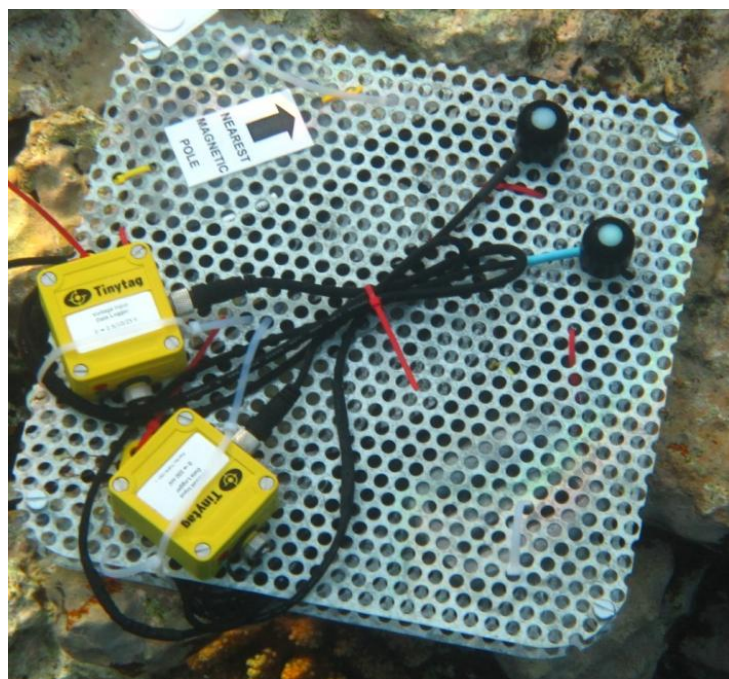


Figure 3.4 Quantum sensor for PAR measurements. Measurements were taken on Suleman Reef, Egypt. To minimise azimuth error, probes were positioned in a north-south alignment. Quantum sensor's field of view is 80° . Baseplate width is 270 mm.

3.4.2 Collection of algal material

Encrusting coralline algae (*Porolithon* sp.) were located on the wave-exposed reef crest, ~120 m from the shore. Free-living coralline algae (*Lithophyllum kotschyannum*) were located on the more sheltered reef flat, ~80 m from the shore (see Chapter 7 for a diagram of the reef structure and algal

distribution). *L. kotschyanum* thalli were characterised by a bleached topside and a pigmented underside, dark pink in colour (Figure 3.5).

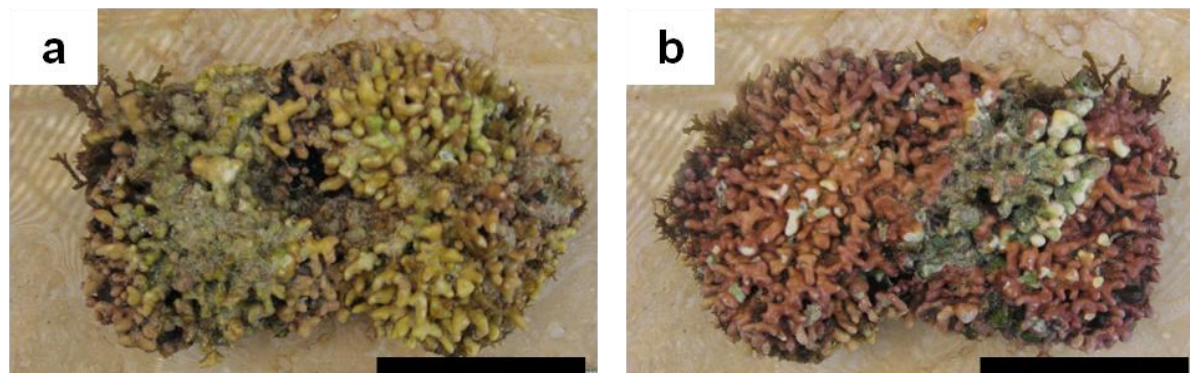


Figure 3.5 Free-living coralline algal thallus from Suleman reef, Egypt. (a) Bleached topside and (b) pigmented underside of the thallus. Scale bar = 50 mm.

Such distinct differences in pigment between the topside and undersides of these thalli prompted additional parameters to be assessed - pigment composition and intracellular DMSP (DMSP_i). DMSP_i may be part of an antioxidant cascade to protect algae against oxidative damage (Sunda et al., 2002). To quantify the observed differences in colour and identify cell pigments, the absorbance of the topside and underside of free-living thalli (n = 7) was measured with an Ocean Optics spectrophotometer using the methodology described in Chapter 2. DMSP_i was measured by breaking branches from the topside and underside of thalli (n = 7) and analysing for DMSP_i using the algal headspace method described in Chapter 2.

3.4.3 Fluorescence measurements

Fluorescence measurements were taken *in situ* using a Diving-PAM (Walz) equipped with the standard 5 mm fibre optic probe at a distance of 10 mm from the algal surface. RLCs (n = 5) were conducted throughout the diurnal cycle at 0700, 0930, 1200, 1430 and 1600 hours on (1) the topside (FLT) and (2) the underside (FLU) of free-living coralline algal thalli and (3) encrusting (EN) coralline algae. In addition, RLCs (n = 5) were conducted on free-living thalli (topside and underside) at 1830 hours. Logistical constraints prevented *in situ* sampling at this time. Instead, thalli were collected and stored in seawater on shore at ambient temperature (25°C) in the dark whilst running the light curves. All RLCs were run following 10 s of quasi-dark acclimation. FLT and FLU light

curve intensities ranged from 2 - 2540 $\mu\text{mol photons m}^{-2} \text{s}^{-1}$, whilst EN intensities ranged from 2 - 6561 $\mu\text{mol photons m}^{-2} \text{s}^{-1}$.

Using F_o and F_m values from the PAM output, photokinetic parameters were computed, as detailed in section 2.2. The least squares regression model used to calculate $r\text{ETR}_{\text{max}}$ and α did not yield a significant fit due to the poor signal to noise ratio, thus $r\text{ETR}_{\text{max}}$ and α are not presented in the results.

3.4.4 Statistical analyses

2-sample t-tests were conducted on individual comparisons (equal variance not assumed) between 0700 (early morning) and 1200 (midday) on FLT, FLU and EN samples (no repeat sampling of thalli was conducted). A Dunn-Sidak adjusted p-value was used to test for significance (95% confidence at $p = 0.0057$) to allow for multiple pairwise tests.

3.5 Results: temperate coralline algae

Often, RLC fluorescence data are frequently expressed relative to the applied PAR light (E). However, calculated minimum saturation intensities (E_k) of samples *in situ* and in the laboratory had a large range (from 4.45 - 54.61 $\mu\text{mol m}^{-2} \text{s}^{-1}$, Table 3.1). To compare these differing datasets, RLC fluorescence measurements were normalised against E/E_k rather than E to assess relative sample response to limiting ($E/E_k < 1$), optimal ($E/E_k = 1$) and saturating ($E/E_k > 1$) irradiance (compared in Figure 3.6). E/E_k can also partially account for differences in light absorption and the light history of the sample (Hennige et al., 2011; Hennige et al., 2008), making it useful for comparisons between the laboratory and *in situ* experiments of this research.

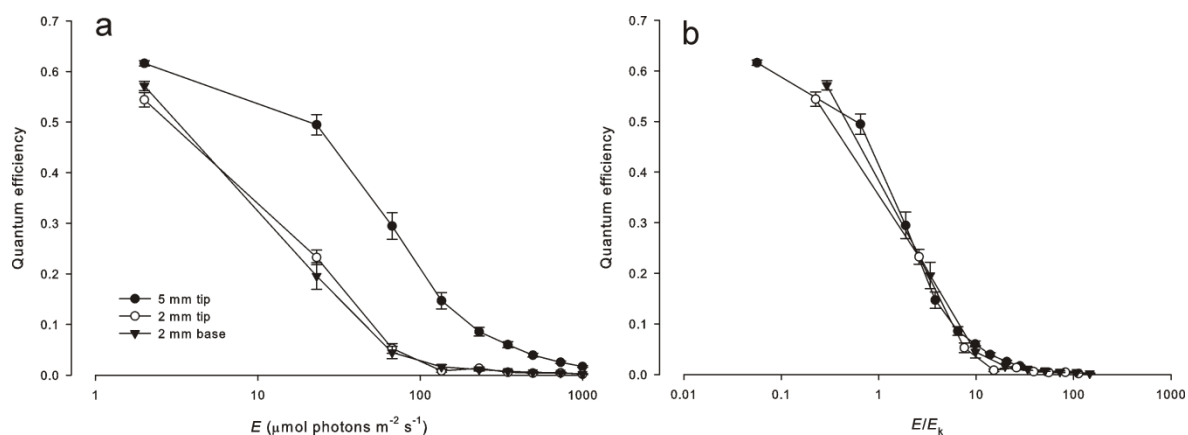


Figure 3.6 Comparison of RLC data plotted against E and E/E_k . Comparison of quantum efficiency in *L. glaciale* in March under laboratory conditions plotted against (a) E (= PAR) and (b) E/E_k of each step of the RLC, determined using a 5 mm probe at the branch tip (black circles) and a 2 mm probe at the branch tip (open circles) and bases (black triangles). Data presented as mean \pm SE.

3.5.1 *In situ* field measurements in May

- Measurements: 5 mm and 2 mm probe on thallus tips.

Photochemical parameters

Maximum effective quantum efficiency ($F_q'/F_{m'_{max}}$) of branch tips measured with both probes showed no relevant differences from each other and had the lowest $F_q'/F_{m'_{max}}$ values of this study (relative to laboratory specimens) (Table 3.1). E_k of branch tips measured in the field were the highest recorded in both laboratory and field studies (Table 3.1); the 5 mm probe had a larger E_k relative to the 2 mm probe. Signal to noise ratios using the 2 mm probe were not high enough to calculate maximum relative electron transport rate ($rETR_{max}$) and the initial slope of the light dependent part of the RLC (α).

Table 3.1 Photosynthetic parameters calculated from RLCs of *L. glaciale*. Five or two mm fibre optic probes were used throughout. Measurements were taken in March and May 2011, *in situ* (field) or in the laboratory (lab) and at thallus branch tips or bases. Data are presented as mean \pm SE.

Sample		E_k ($\mu\text{mol photons m}^{-2} \text{s}^{-1}$)	$F_q'/F_{m'_{max}}$	$rETR_{max}$ ($\mu\text{mol electrons m}^{-2} \text{s}^{-1}$)	α
March sampling					
5 mm probe	Lab tip	35.46 \pm 3.00	0.65 \pm 0.02	9.73 \pm 0.42	0.44 \pm 0.17
2 mm probe	Lab tip	8.88 \pm 1.15	0.62 \pm 0.03	-	-
	Lab base	6.81 \pm 0.75	0.70 \pm 0.03	-	-
May sampling					
5 mm probe	Lab tip	15.77 \pm 1.47	0.63 \pm 0.02	5.59 \pm 0.31	0.24 \pm 0.10
	Field tip	54.61 \pm 5.29	0.53 \pm 0.02	12.90 \pm 0.55	0.32 \pm 0.07
2 mm probe	Lab tip	5.45 \pm 0.87	0.61 \pm 0.04	-	-
	Field tip	19.15 \pm 2.68	0.51 \pm 0.02	-	-
	Lab base	4.45 \pm 0.49	0.75 \pm 0.04	-	-

When $E/E_k \leq 1$, photochemical quenching (qP) and effective quantum efficiency (F_q'/F_m') values did not decrease with the 5 mm probe. However, a decrease was observed with the 2 mm probe (Figure 3.7). When $E/E_k \geq 1$, qP and F_q'/F_m' values were comparable between both probe sizes (Figure 3.7). At supersaturating irradiances ($E/E_k \sim 10$), qP decreased to 0.1 and F_q'/F_m' decreased to 0.05 with both probes.

Non-photochemical parameters

Calculated non-photochemical quenching (NPQ and qN) between the two probe sizes exhibited some differences. Using the 5 mm probe, the first two light steps showed no increase in NPQ or decrease in qN (Figure 3.8). As E/E_k approached 1, non-photochemical quenching increased using both calculations (NPQ and $1-qN$). With the 2 mm probe, initial increases were slower than with the 5 mm probe, but variability between replicates was larger with the 2 mm probe. A plateau in NPQ and qN was not observed at the higher PAR irradiances, despite supersaturating irradiance levels (Figure 3.8).

3.5.2 Laboratory measurements in March and May

- Measurements: 5 mm tip, 2 mm tip, 2 mm base.

Photochemical parameters

Using the 2 mm probe, E_k was not significantly different between the branch tip and base in March ($F_1 = 1.56$, $p = 0.227$) or May ($F_1 = 0.35$, $p = 0.568$) (Table 3.1). In contrast, $F_q'/F_{m'_{max}}$ was highest at the branch bases and lowest at the tips in both March and May ($F_1 = 11.03$, $p = 0.003$).

5 mm tip $F_q'/F_{m'_{max}}$ values were intermediate in both months (Table 3.1). E_k and $F_q'/F_{m'_{max}}$ values were significantly higher in March than May (E_k : 2.3 times higher, $F_1 = 13.20$, $p = 0.003$; $F_q'/F_{m'_{max}}$: 0.02 units higher, $F_1 = 4.98$, $p = 0.044$, Table 3.1).

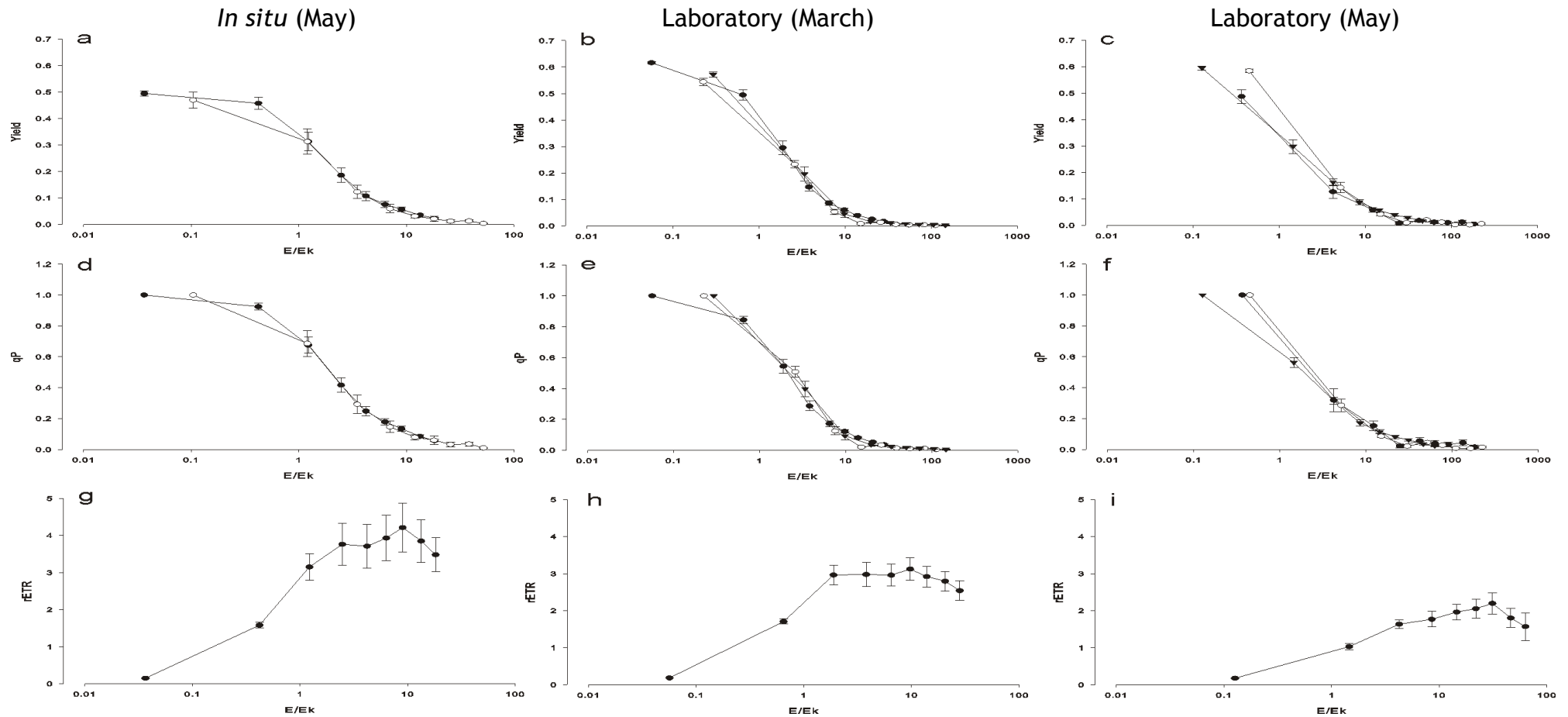


Figure 3.7 Photochemical response of *L. glaciale*.

5 mm probe on branch tips (black circle), 2 mm probe on branch tips (open circle) and 2 mm probe on branch bases (black triangle) *in situ* in May (1st column) and in the laboratory in March (2nd column) and May (3rd column); (a, b, c) Quantum efficiency (yield), (d,e,f) qP and (g, h, i) rETR. Data normalised to E/E_k and presented as mean \pm SE.

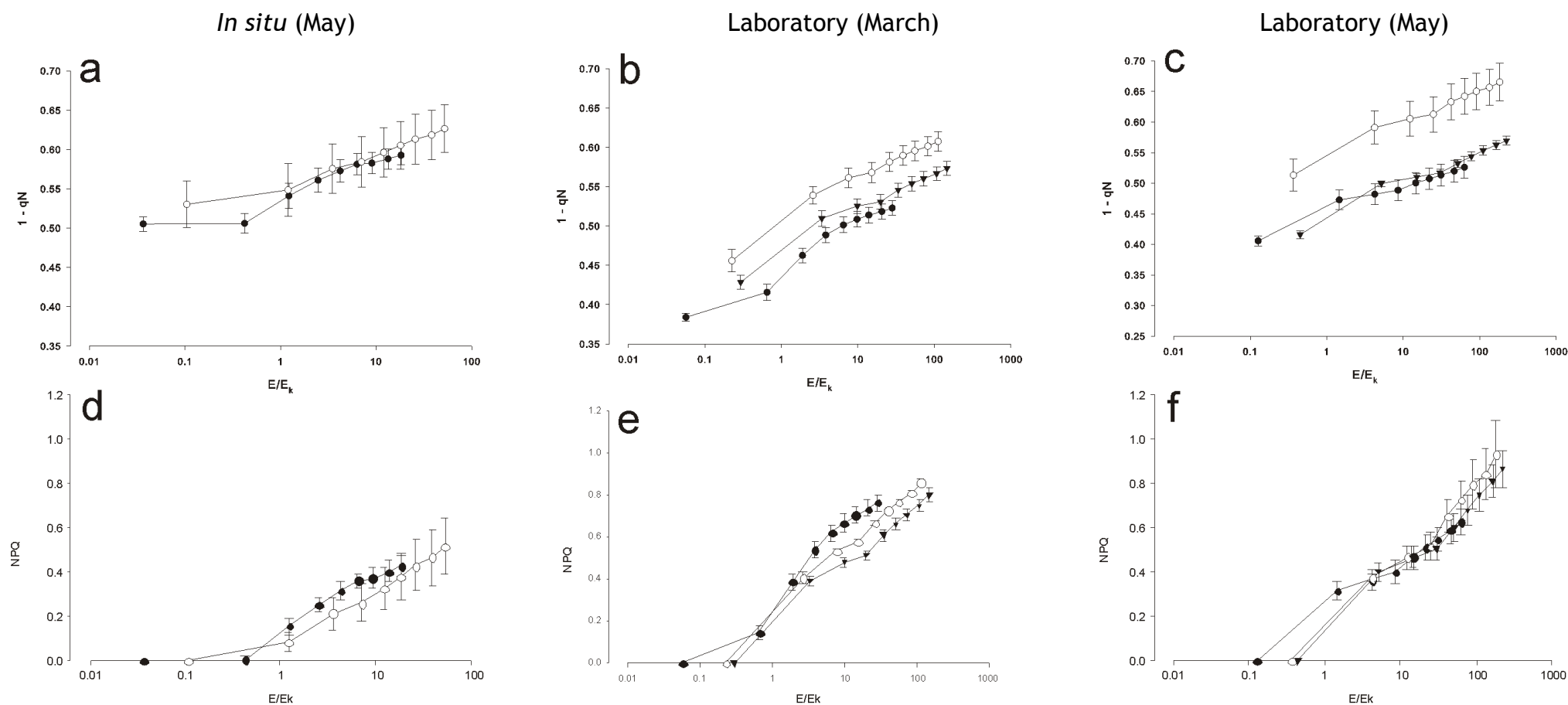


Figure 3.8 Photoprotective response of *L. glaucale*.

5 mm probe on branch tips (black circle) and a 2 mm probe on branch tips (open circle) and branch bases (black triangle) *in situ* in May (1st column) and in the laboratory in March (2nd column) and May (3rd column); (a, b, c) $1 - qN$, (d,e,f) NPQ. Data normalised to E/E_k and presented as mean \pm SE.

E_k calculated from the 5 mm probe was significantly higher than that calculated from the 2 mm probe, with a larger difference observed in March than May. No difference in $rETR_{max}$ ($F_1 = 2.97$, $p = 0.109$) or α ($F_1 = 1.03$, $p = 0.328$) was observed between March and May using the 5 mm probe (Table 3.1). Additionally, initial declines in qP and quantum efficiency were more rapid in May compared to March (Figure 3.7).

Non-photochemical parameters

NPQ and qN differed between tips and bases in March but not in May (Figure 3.8). For both months, the 5 mm probe NPQ rose slowly to $E/E_k \sim 1$, before rising to a maximum of ~ 0.8 (Figure 3.8). Tip and base NPQ from the 2 mm probe increased linearly relative to E/E_k (Figure 3.8), although NPQ and $1-qN$ in the tip were consistently higher than those from the base in March. The difference in non-photochemical quenching between tip and base was more pronounced in qN data. $1-qN$ recorded with the 5mm probe was lower than 2 mm $1-qN$ data from the branch tip (Figure 3.8). As with the field data, NPQ and qN did not plateau throughout the RLCs despite supersaturating irradiances.

3.5.3 Laboratory and field measurements in May

Initial qP values were 0.1 units higher in the laboratory compared to the field (Figure 3.7). E_k ($F_1 = 23.30$, $p = 0.001$) and $rETR_{max}$ ($F_1 = 6.65$, $p = 0.033$) were significantly higher in the field than in the laboratory (Table 3.1), while $F_q'/F_{m_{max}}'$ was significantly higher in the laboratory ($F_1 = 31.93$, $p < 0.001$). No significant difference in α between field and laboratory thalli was observed ($F_1 = 0.77$, $p = 0.405$).

When $E/E_k < 1$, $rETR$ values in the field and in the laboratory were similar (Figure 3.7). Maximum $rETR$ was achieved at $E/E_k \sim 10$, however growth in $rETR$ was highest in the field (although associated with a larger variation) and lowest in the laboratory (Figure 3.7).

3.6 Results: tropical coralline algae (diurnal response)

As previously described in section 3.4, RLC data are usually expressed relative to E . E_k values from free-living topside (FLT), free-living underside (FLU)

and encrusting (EN) samples ranged from 71 - 723 $\mu\text{mol photons m}^{-2} \text{s}^{-1}$ throughout the diurnal cycle. Thus, RLC fluorescence measurements were expressed against E/E_k , to assess sample response relative limiting ($E/E_k < 1$), optimal ($E/E_k = 1$) and saturating ($E/E_k > 1$) irradiance for photosynthesis when $E/E_k < 1$, = 1 or > 1 respectively. Importantly for this study, E/E_k can also account for differences in light absorption and light history (Hennige et al., 2011; Hennige et al., 2008) as E_k is partly determined by light history. The three algal morphotypes exhibited different ranges of E/E_k across the light curves: FLT: 0 - 12.2, FLU: 0 - 34.8 and EN: 0 - 27.4

3.6.1 Ambient PAR

PAR was zero between 1700 and 0600 (Figure 3.9). Maximum PAR was between 1000 and 1200 at $\sim 800 - 900 \mu\text{mol photons m}^{-2} \text{s}^{-1}$. RLC sampling timepoints were distributed throughout the PAR cycle, as indicated by the arrows on Figure 3.9.

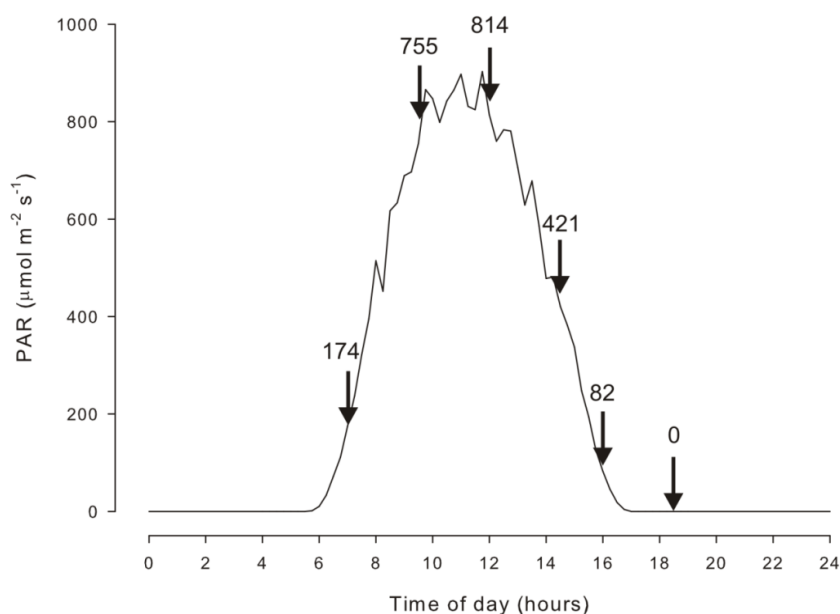


Figure 3.9 Ambient PAR on Suleman reef, November 2011. Arrows indicate ambient PAR levels ($\mu\text{mol photons m}^{-2} \text{s}^{-1}$) at RLC sampling timepoints for encrusting and free-living coralline algae at 0700, 0930, 1200, 1430, 1600 and 1830. RLCs were not measured for encrusting algae at 1830.

3.6.2 Optical reflectance

There was a clear difference in absorbance between thalli topsides and undersides between 400 and 750 nm (Figure 3.10). Absorbance by cellular

pigments is observed as troughs in reflectance. Both FLT and FLU exhibited a large trough at 435 - 445 nm, representing Chl-*a* and α -carotenoids (Figure 3.10). Additional α -carotenoid absorbance was detected at 500 nm in FLU. Distinct troughs present in the FLU spectrum relate to the phycobilin pigments unique to Rhodophyta and cyanobacteria: phycoerythrin (576 nm), phycocyanin (618 nm) and allophycocyanin (654 nm)(Figure 3.10). The spectrum of FLT was much flatter, with no detectable peaks in Rhodophyte-pigment absorbance (Figure 3.10).

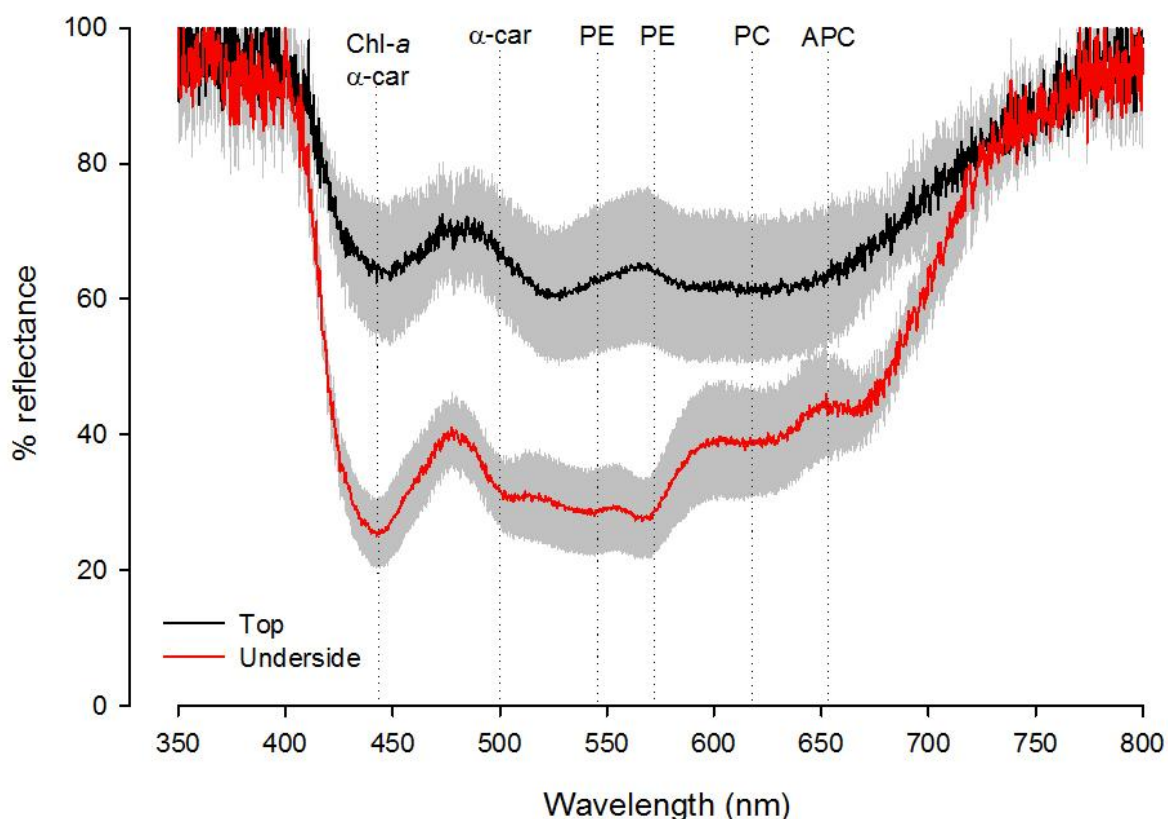


Figure 3.10 Coralline algal absorbance on Suleman reef, Egypt. Mean % absorbance of the topside (black line) and underside (red line) of free-living coralline algae. Error bars (grey) represent SE.

3.6.3 Intracellular DMSP

DMSP_i was higher in FLT than FLU, although this was not significant due to the high variability associated with FLT ($F_1 = 4.18$, $p = 0.064$).

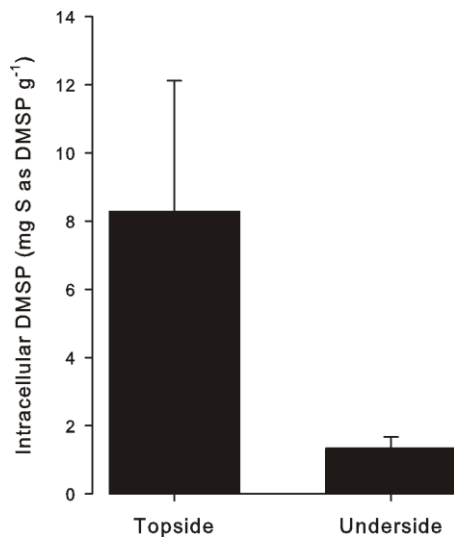


Figure 3.11 DMSP_i in free-living coralline algae from Suleman Reef, Egypt. DMSP_i determined from the bleached topside and pigmented underside of the free-living coralline alga *Lithophyllum kotschyannum*. Data presented as mean±SE.

3.6.4 Minimum saturating intensity, E_k

There was no significant difference between E_k from FLT, FLU and EN at 0700 (Table 3.2 and Figure 3.12). FLT was characterised by a (non-significant) rise in E_k from 0700 ($329 \pm 38 \mu\text{mol photons m}^{-2} \text{s}^{-1}$) to 0930 ($428 \pm 33 \mu\text{mol photons m}^{-2} \text{s}^{-1}$), a plateau from 0930 to 1430 and a fall from 1430 to a minimum value at 1830 ($206 \pm 20 \mu\text{mol photons m}^{-2} \text{s}^{-1}$, Figure 3.12, Table 3.2). FLU exhibited no significant change in E_k throughout the diurnal cycle ($\sim 100 \mu\text{mol photons m}^{-2} \text{s}^{-1}$ throughout the day), although FLU E_k was significantly lower than FLT at 1200 (Table 3.2). EN E_k significantly rose from a minimum at 0700 ($221 \pm 34 \mu\text{mol photons m}^{-2} \text{s}^{-1}$) to a maximum at 1200 ($724 \pm 35 \mu\text{mol photons m}^{-2} \text{s}^{-1}$) and recovered throughout the afternoon (Figure 3.12, Table 3.2). At 1200, EN was significantly higher than both FLT and FLU (Table 3.2).

Table 3.2 t-test comparisons of coralline algal E_k between 0700 and 1200. Comparisons between free-living topsides (FLT) and underside (FLU) and encrusting (EN) coralline algae at 0700 and 1200. t-statistic given in upper right, p-value in lower left. Bold text indicates Dunn-Sidak adjusted significance at the 95% confidence level.

	FLT 0700	FLU 0700	EN 0700	FLT 1200	FLU 1200	EN 1200
FLT 0700		5.86	2.15	-1.98	*	*
FLU 0700	0.002		-3.50	*	-1.43	*
EN 0700	0.069	0.017		*	*	-10.40
FLT 1200	0.088	*	*		7.25	-6.18
FLU 1200	*	0.203	*	<0.001		-13.97
EN 1200	*	*	<0.001	<0.001	<0.001	

* Comparisons were not relevant thus not calculated

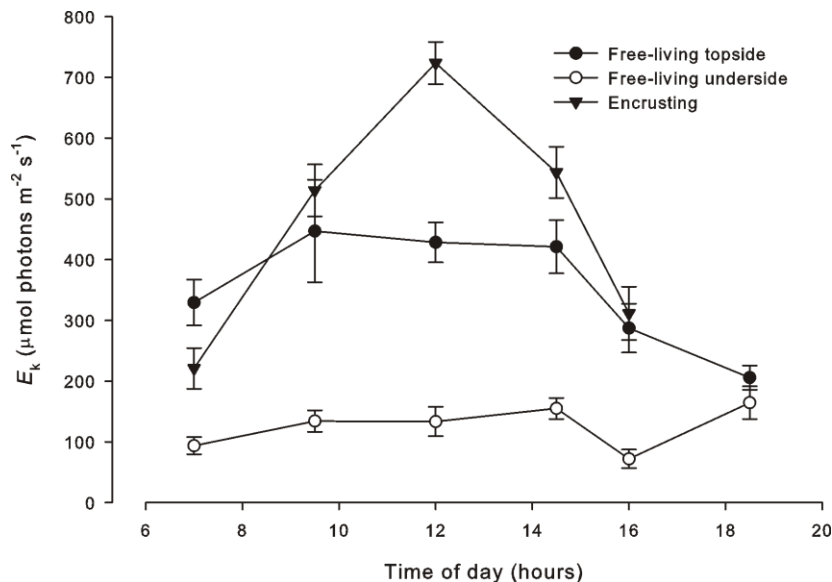


Figure 3.12 E_k over a diurnal period on Suleman Reef, Egypt.

Three morphotypes of coralline algae were considered: free-living topside (black circle) and underside (open circle) and encrusting algae (black triangle). Data presented as mean \pm SE.

3.6.5 Maximum quantum efficiency, $F_q'/F_{m' \max}$

There was no significant difference in $F_q'/F_{m' \max}$ between algal morphotypes at 0700 or 1200 (Figure 3.13). FLT $F_q'/F_{m' \max}$ fell from 0700 (0.53 ± 0.05) to a plateau at 0930 (0.36 ± 0.06), rising between 1430 and 1600 to a maximum of 0.60 ± 0.02 (Figure 3.13). Mean FLT $F_q'/F_{m' \max}$ at 1830 (0.51 ± 0.08) was lower than at 1600, but was characterised by high variation. FLU $F_q'/F_{m' \max}$ fell slightly from 0700 (0.41 ± 0.06) to 0930 (0.35 ± 0.07), but then rose to a maximum at 1830 (0.56 ± 0.04 , Figure 3.13). EN $F_q'/F_{m' \max}$ fell from a maximum at 0700 (0.55 ± 0.01) to a minimum at 1200 (0.32 ± 0.03 , Figure 3.13), followed by a recovery by 1600 (0.52 ± 0.02 , Figure 3.13).

Table 3.3 t-test comparisons of coralline algal $F_q'/F_{m' \max}$.

Comparisons between free-living top sides (FLT) and underside (FLU) and encrusting (EN) coralline algae at 0700 and 1200 from Suleman Reef, Egypt. t-statistic given in upper right, p-value in lower left. Bold text indicates Dunn-Sidak adjusted significance at the 95% confidence level.

	FLT 0700	FLU 0700	EN 0700	FLT 1200	FLU 1200	EN 1200
FLT 0700		1.52	-0.4	2.31	*	*
FLU 0700	0.173		-2.38	*	-0.48	*
EN 0700	0.711	0.076		*	*	8.11
FLT 1200	0.054	*	*		-1.25	1.25
FLU 1200	*	0.649	*	0.252		2.87
EN 1200	*	*	0.001	0.251	0.024	

* Comparisons were not relevant thus not calculated

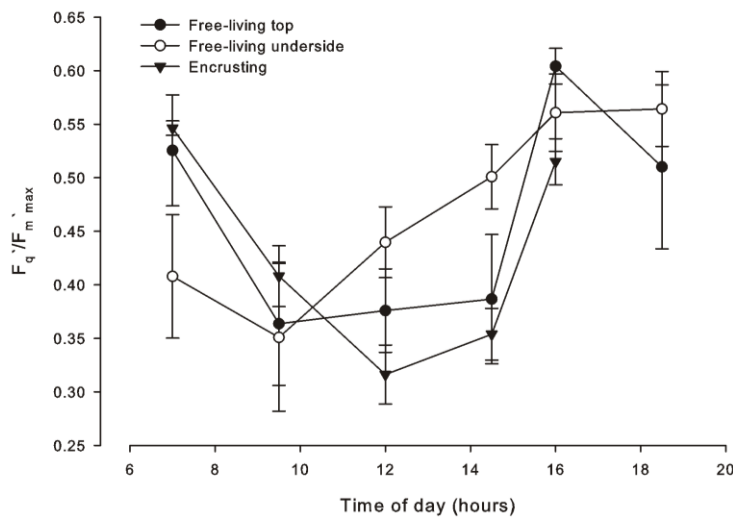


Figure 3.13 Coralline algal $F_q'/F_{m' \max}$ over a diurnal period. Three morphotypes from the Suleman Reef, Egypt, were considered: free-living topside (black circle) and underside (open circle) and encrusting algae (black triangle). Data presented as mean \pm SE.

3.6.6 E_k and $F_q'/F_{m' \max}$ regression with PAR

FLT and EN E_k values were well described by a positive linear regression of PAR (Figure 3.14, Table 3.4). Minimum modelled E_k values were similar for both FLT and EN (258 and 226 $\mu\text{mol photons m}^{-2} \text{s}^{-1}$ respectively). The gradient of increase was highest in EN and less steep for FLT (Figure 3.14). For FLT, an increase of 4 $\mu\text{mol photons m}^{-2} \text{s}^{-1}$ PAR induced a 1 $\mu\text{mol photons m}^{-2} \text{s}^{-1}$ increase in E_k whilst EN E_k increased by 2.12 $\mu\text{mol photons m}^{-2} \text{s}^{-1}$ (Figure 3.14, Table 3.4). FLU E_k was not well described with a linear regression (Figure 3.14, Table 3.4), perhaps because of the slight increases in E_k at 0 and 421 $\mu\text{mol photons m}^{-2} \text{s}^{-1}$ PAR (Figure 3.14). The minimum E_k for FLU was lower at 115 $\mu\text{mol photons m}^{-2} \text{s}^{-1}$. $F_q'/F_{m' \max}$ was best described through linear regressions with no gradient associated with PAR values due to the high variability associated with this data (Figure 3.14). $F_q'/F_{m' \max}$ regressions were very similar for all algal morphotypes (Figure 3.14, Table 3.4).

Table 3.4 Linear relationships between E_k or $F_q'/F_{m' \max}$ and PAR. Regression statistics R^2 , p-value, standard error of residuals (SER) and n are shown for free-living topside and underside thalli and encrusting coralline algae.

Algal morphotype	Relationship	R^2	p	SER	n
Free-living topside	$E_k = 258 + 0.25 * \text{PAR}$	0.40	<0.001	11.3	28
	$F_q'/F_{m' \max} = 0.55 + \text{PAR}$	0.30	0.002	<0.1	29
Free-living underside	$E_k = 115 + 0.03 * \text{PAR}$	0.03	0.405	6.0	28
	$F_q'/F_{m' \max} = 0.53 + \text{PAR}$	0.21	0.013	<0.1	29
Encrusting	$E_k = 226 + 0.53 * \text{PAR}$	0.64	<0.001	12.5	25
	$F_q'/F_{m' \max} = 0.54 + \text{PAR}$	0.54	<0.001	<0.1	25

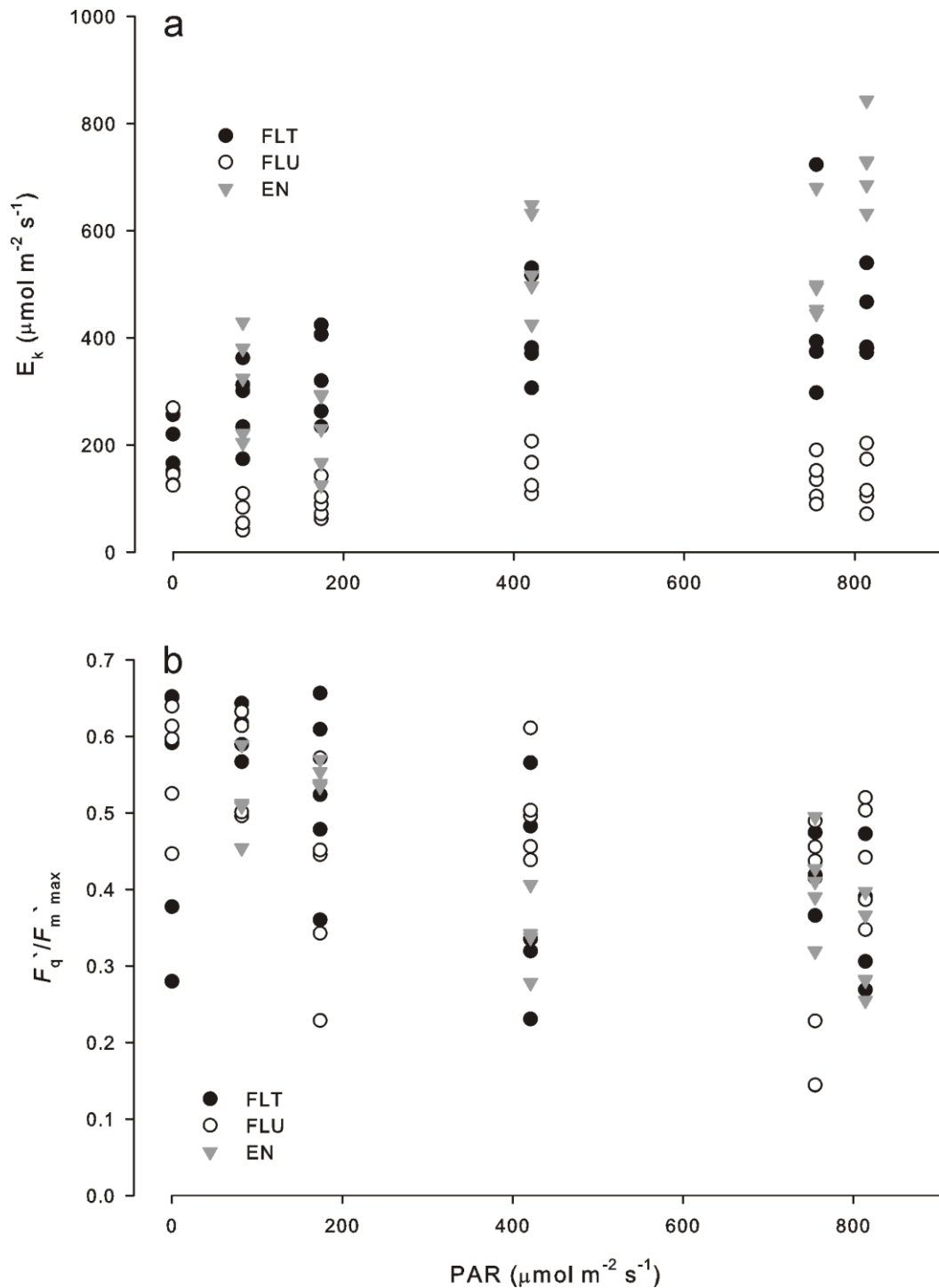


Figure 3.14 (a) E_k and (b) $F_q'/F_{m' \max}$ of coralline algae against PAR light levels. Three morphotypes were tested: free-living topside (FLT, black circle) and underside (FLU, open circle) and encrusting algae (EN, grey triangle). Data presented as mean \pm SE. Linear regressions for FLT, FLU and EN against PAR are presented in Table 3.4.

3.6.7 Quantum efficiency

When $E/E_k = 1$ (i.e. when available PAR = minimum saturation intensity), all algal morphotypes had a quantum efficiency value of ~ 0.3 (Figure 3.15). As EN, FLT and FLU had significantly different E_k values, the x-axes of the graphs in

Figure 3.15 have different scales to enable the diurnal differences within each algal type to be seen.

Topside of free-living thalli (Figure 3.15a)

Initial quantum efficiency values (quasi dark-adapted = F_v/F_m) ranged from ~ 0.6 at 1600 to ~ 0.35 at 1200. There was a gradual decline in F_v/F_m from early morning / late afternoon to midday. The steepest decline in quantum efficiency was when $E/E_k < 1$. When $E/E_k > 1$ quantum efficiency measurements split into two groups - 0700, 1600 and 1830 had higher quantum efficiency values (and higher E/E_k values for the RLC steps) than 0930, 1200 and 1430.

Underside of free-living thalli (Figure 3.15b)

Initial quantum efficiency values (F_v/F_m) had a slightly smaller range than FLT (~ 0.55 - 0.35) and there was no time pattern. As with FLT, the steepest decline in quantum efficiency was when $E/E_k < 1$. Samples exhibited similar quantum efficiency responses throughout the diurnal cycle, reaching a minimum at $E/E_k \sim 16$.

Encrusting algae (Figure 3.15c)

Initial quantum efficiency values (F_v/F_m) had a similar range to FLT, but with lower absolute values by ~ 0.5 units. At $E/E_k > 1$, three groups appeared: the highest quantum efficiency values were at 0700 and 1600 (minimum reached at $E/E_k = 12$), intermediate values at 0930 and 1430 (minimum reached at $E/E_k = 7$) and lowest values at 1200 (minimum reached at $E/E_k = 5$).

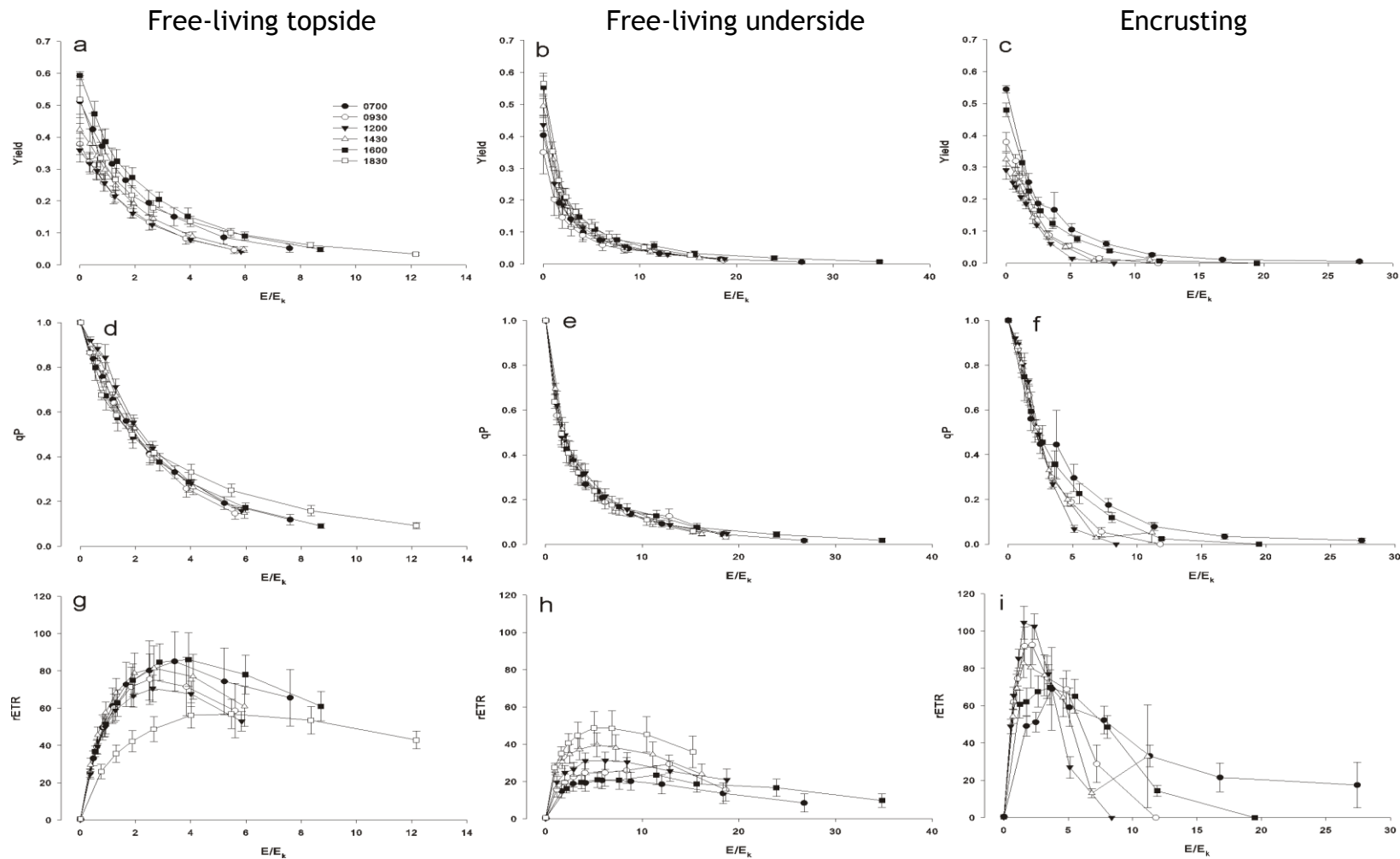


Figure 3.15 Photochemical parameters over a diurnal cycle.

Topside (a, d, g) and underside (b, e, h) of free-living thalli and encrusting (c, f, i) coralline algae. Characteristics presented: quantum efficiency (= yield, a,b,c), qp (d,e,f) and $rETR$ (g,h,i), Data normalised to E/E_k and presented as mean \pm SE. Note different x-axis scales due to differing E_k values between morphotypes.

3.6.8 Photochemical quenching

Top and underside of free-living thalli (Figure 3.15d,e)

All timepoints exhibited a similar trend in qP decline with increasing E/E_k , except FLT 1830, which had a less steep decline in qP than the others at $E/E_k > 3$. Minimum FLT qP values were ~ 0.1 , higher than FLU (but FLU minimum qP corresponded to higher E/E_k values).

Encrusting algae (Figure 3.15f)

A decline of 0.5 units was observed at all timepoints up to $E/E_k \sim 3$. A divergence of the timepoints occurred at $E/E_k > 3$; decline was rapid at 1200, intermediate at 0930 and 1430 and slowest at 0700 and 1600. At all timepoints, qP had declined to essentially zero by the end of the RLC.

3.6.9 Relative electron transport rate

Top of free-living thalli (Figure 3.15g)

$rETR$ increased similarly in the low E/E_k range for all timepoints except 1830, followed by a decline as PAR continued to increase. Maximum $rETR$ at 0700, 1600 and 1830 was achieved when $E/E_k = 4$. Maximum $rETR$ at 0930, 1200 and 1430 was achieved when $E/E_k = 2$. Maximum $rETR$ declined towards midday, except 1830 which had the lowest maximum $rETR$ of $57 \mu\text{mol electrons m}^{-2} \text{s}^{-1}$.

Underside of free-living thalli (Figure 3.15h)

$rETR$ values were generally lower than FLT. $rETR$ at 1830 (dark acclimated) was similar to FLT 1830, with a maximum of $49 \mu\text{mol electrons m}^{-2} \text{s}^{-1}$ at $E/E_k = 5$. There was no clear diurnal trend in $rETR$, with maximum values at all timepoints attained between $E/E_k = 4 - 5$ across a range of $20 - 60 \mu\text{mol electrons m}^{-2} \text{s}^{-1}$.

Encrusting algae (Figure 3.15i)

EN *rETR* was characterised by a rapid increase, followed by a rapid decrease at all timepoints. Maximum *rETR* values were observed at 1200 (104 $\mu\text{mol electrons m}^{-2} \text{s}^{-1}$), 0930 (93 $\mu\text{mol electrons m}^{-2} \text{s}^{-1}$) and 1430 (83 $\mu\text{mol electrons m}^{-2} \text{s}^{-1}$) when $E/E_k = 2$. Maximum *rETR* at 0700 (69 $\mu\text{mol electrons m}^{-2} \text{s}^{-1}$) and 1600 (70 $\mu\text{mol electrons m}^{-2} \text{s}^{-1}$) were achieved at $E/E_k = 4$. 1200, 0930 and 1600 declined to zero by the end of the RLC, 0700 to 18 $\mu\text{mol electrons m}^{-2} \text{s}^{-1}$ and 1430 to 33 $\mu\text{mol electrons m}^{-2} \text{s}^{-1}$ (although this was characterised by a large variance).

3.6.10 Non photochemical quenching, NPQ*Top and underside of free-living thalli (Figure 3.16a,b)*

NPQ rose from zero to a plateau of between 0.2 - 0.5 by $E/E_k = 6$ in both FLT and FLU. No diurnal trend was apparent in terms of NPQ for FLT nor FLU.

Encrusting algae (Figure 3.16c)

As with FLT and FLU, a plateau in NPQ was attained when $E/E_k = 6$. In contrast to FLT / FLU, a diurnal trend was observed: 0930, 1200 and 1430 were similar to FLT / FLU, with a maximum of ~ 0.5 units. Maximum NPQ at 1600 was 0.9 units, while 0700 rose to 1.5 units, although this was characterised by a large variance at $E/E_k > 5$.

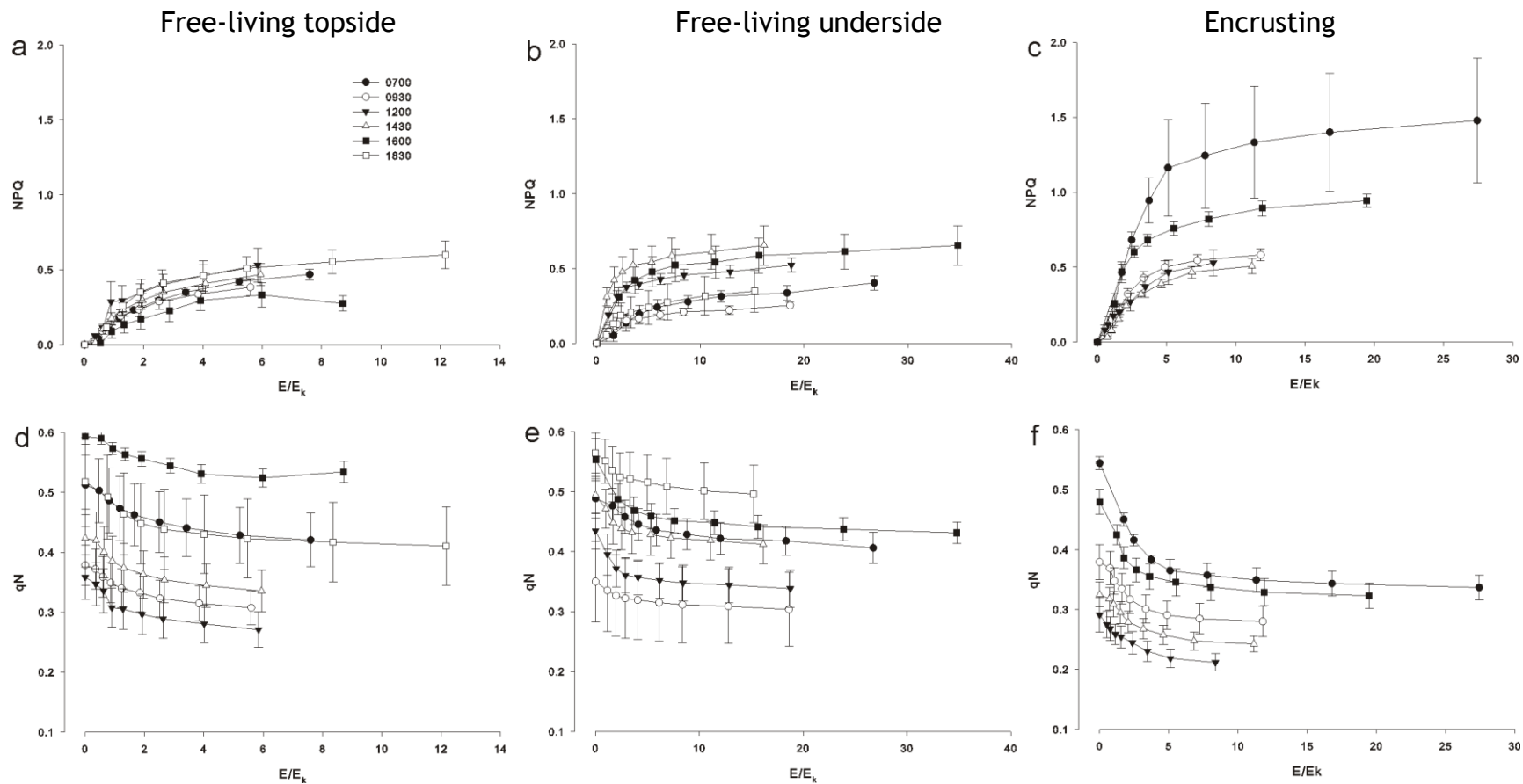


Figure 3.16 Non-photochemical parameters over a diurnal cycle. Topside (a, dg) and underside (b, eh) of free-living thalli and encrusting (c, f) coralline algae. Charactersitics presented: NPQ (a,b,c) and q_N (d,e,f), Data normalised to E/E_k and presented as mean \pm SE. Note different x-axis scales due to differing E_k values between morphotypes.

3.6.11 Non photochemical quenching, qN

Top of free-living thalli (Figure 3.16d)

Initial 1-qN values were highest at 0700, 1600 and 1830 (0.4 - 0.5 units), intermediate at 0930 and 1430 (~0.6 units) and lowest at 1200 (0.65 units); these groupings remained throughout the RLC. 0700, 1600 and 1830 appeared to reach a plateau, whilst the trend at 0930, 1200 and 1430 did not appear to plateau.

Underside of free-living thalli (Figure 3.16e)

FLU had a similar range in qN, with a similar diurnal pattern of increased qN capacity towards midday. One exception was 1430 which was more similar to 0700 and 1600 than 0930 and 1200.

Encrusting algae (Figure 3.16f)

Initial qN values were ~ 0.5 units lower than FLT / FLU. At $E/E_k > 3$, qN at all timepoints was < 0.4, lower than FLT / FLU where qN was maintained above 0.4 for the entire RLC in the FLT / FLU 0700 / 1600 / 1830 qN group. As with FLT and FLU, three groupings were apparent throughout the RLC : 0700 and 1600 (high qN), 0930 and 1430 (intermediate) and 1200 (low qN).

3.7 Discussion

Red coralline algae are important for coastal ecosystem function from tropical to polar waters. Fluorescence studies so far have demonstrated that the light adaptation potential of coralline algae can be species specific (Schwarz et al., 2005). Thus, it is important to understand the basic photosynthetic characteristics of different algal species from different environmental regimes if we are to make projections under future global change scenarios. PAM fluorometry proved to be an excellent tool for assessing the photosynthetic characteristics of coralline algae, allowing baseline data to be collected from temperate (*L. glaciale*) and tropical (*Porolithon* sp. and *Lithophyllum kotschyannum*) specimens.

3.7.1 Saturation intensity (E_k) is variable relative to light regime

Overall, E_k values from the temperate coralline algae ranged from 4.45 to 54.61 $\mu\text{mol photons m}^{-2} \text{s}^{-1}$. Although these values may be considered low, relative to the maximum irradiance level of ca. 90 $\mu\text{mol photons m}^{-2} \text{s}^{-1}$ *in situ* and in the laboratory, the upper values of measured E_k are relatively high. Results from this study, which suggest that *L. glaciale* is low light adapted (relative to ambient conditions), complement previous photosynthetic work on red coralline algae which purported general low light adaptation of coralline algae (e.g. Irving et al., 2005; Irving et al., 2004; Wilson et al., 2004; Johansen, 1981). This low light adaptation could, along with temperature (Foster, 2001), play a key role in defining and restricting the distribution of this species to high latitudes, turbid regions or to non-shallow depths. Higher values of E_k and lower effective quantum efficiency observed in field samples relative to the laboratory indicate that field samples were higher light acclimated relative to laboratory-kept samples, despite laboratory light levels being similar to *in situ* maximum PAR. An organisms' previous light history is an important consideration for RLC analysis (Ralph and Gademann, 2005) and may be the cause of the *in situ* / laboratory differences observed in this study. Transfer from *in situ* diurnal light variability to static laboratory light conditions can affect photoacclimation, although this can result in an intermediate level (Lavaud et al., 2002). Differences in the light spectra between the laboratory and *in situ* may also have contributed to the observed differences in light acclimation between the laboratory and *in situ* samples.

However, it appears that tropical species may be high or low light adapted depending on species or exposure. The plateau in FLT E_k values between 0930 and 1430 suggests that the upper limit of this alga's saturation irradiance is ca. 450 $\mu\text{mol photons m}^{-2} \text{s}^{-1}$, half the ambient PAR in November and a quarter of summer PAR levels (see Chapter 7). Such an apparent weakness in photoacclimation may be offset by the lack of pigmentation; excess incoming solar radiation may be reflected off the algae before photosynthetic saturation and cellular damage can occur. The high DMSP_i content of FLT compared to FLU may also help to protect against oxidative damage through an antioxidant cascade (Sunda et al., 2002), although it is energetically costly to maintain high levels of DMSP_i (Stefels, 2000). In contrast, EN E_k peaked at 1200 at 723 μmol

photons $\text{m}^{-2} \text{s}^{-1}$, following the trend in ambient PAR. Thus, EN appears to be higher light adapted than FLT, enabling EN to better acclimatise throughout the day in response to changing light levels. Results from this research are higher than previous work on tropical red coralline algae (*Hydrolithon onkodes*, E_k of $110 \mu\text{mol photons m}^{-2} \text{s}^{-1}$) (Payri et al., 2001), but are similar to corals (E_k range of $300 - 800 \mu\text{mol photons m}^{-2} \text{s}^{-1}$) (Hennige et al., 2008).

Possible reasons for the differences in E_k between EN and FLT may be four-fold: (1) EN may be subject to periodically higher amounts of PAR relative to FLT due to wave attenuation of irradiance at the reef crest (Payri et al., 2001), (2) the reef crest can be exposed to the air during spring tides (Burdett pers. obs.), (3) free-living thalli may be turned over by water motion and / or bioturbation, periodically exposing the topside to considerably lower light levels and (4) the differing morphology of FLT and EN. The complex three-dimensional structure of free-living coralline algae can lead to branch heterogeneity, with branch bases more low-light adapted than branch tips (see section 3.7.3). The larger 5 mm probe used in this research will have recorded signals from branch tips and the shaded branch bases, creating an intermediate signal for interpretation. Thus, if this research was repeated with a smaller fibre optic probe, the branch tips of FLT may be more similar to EN, whilst the branch bases of FLT may be more similar to FLU (see below). In contrast, the homogenous morphology of EN will likely limit any within-thallus differences.

3.7.2 Diurnal trends in photosynthesis

As has been observed in other macroalgae (e.g. Edwards and Kim, 2010; Figueroa et al., 2009; Häder et al., 1998), FLT and EN exhibited clear diurnal photosynthetic trends across most parameters (the exceptions being FLT qP and NPQ): photosynthetic quantum efficiency and $rETR$ were suppressed whilst non-photochemical quenching was enhanced during periods of high ambient PAR. This suggests that FLT and EN are able to continually acclimate to the ambient PAR conditions in order to maintain efficient photosynthesis and to limit photodamage. A reduction in quantum efficiency at high irradiance does not, however, imply a reduction in net photosynthesis (e.g. in the freshwater aquatic plant, *Lagarosiphon major*, Hussner et al., 2011). This could be investigated by additionally measuring oxygen evolution throughout the diurnal cycle.

A diel assessment of the photosynthetic characteristics of *L. glaciale* would provide an interesting temperate comparison to the tropical data presented here. It may be expected that *L. glaciale* would have only a small diurnal response, given initial measurements where the maximum E_k was about half the maximum irradiance expected at Loch Sween on a sunny day ($\sim 120 \mu\text{mol photons m}^{-2} \text{s}^{-1}$, Burdett, pers. obs.).

3.7.3 Intra-thallus heterogeneity

Differences in photosynthetic characteristics within individual thalli were identified in both temperate and tropical systems. Fluorescence measurements on *L. glaciale* indicated that algal branch tips were consistently higher-light adapted than branch bases, despite a typical branch length of no more than ca. 20 mm. Due to the complex morphology of *L. glaciale*, intra-thallus patterns were determined using only the custom 2 mm fibre optic probe and not the 5 mm probe. The low signal to noise ratio from the 2 mm probe did, however, prevent comparisons of $rETR_{\text{max}}$ and α between branch tips and bases. The values of $F_q'/F_{m \text{ max}}'$ taken at thallus tips using the 5 mm probe were intermediate between 2 mm tip and base measurements, demonstrating that the 5 mm probe was not suitable for intra-thallus heterogeneity determination of free-living coralline algal thalli. This may complicate interpretation of the data obtained from the 5 mm probe when taken at branch tips. However, the increased signal available through the 5 mm probe relative to the 2 mm probe due to the 'sample size' area may make the 5 mm fibre optic a more favourable tool where thallus heterogeneity information is not required. Such heterogeneity indicates that the cells at branch tips and bases are likely to have different pigment compositions and / or chloroplast numbers (Kirk, 2011).

The top side of *Lithophyllum kotschyannum* (FLT) in Egypt appears to have adapted to tolerate high variations in ambient PAR levels by (1) continual photoacclimation throughout the day, (2) reduced pigmentation (bleaching) to increase reflectance of excess photons and (3) increased DMSPi concentrations. In contrast, the shaded underside (FLU) was able to maintain pigmentation and low DMSPi concentrations and (in general) did not exhibit a diurnal response. E_k remained low throughout the day, suggesting a low-light adaptation for FLU. Methionine, a product of, and compound for, photosynthesis, and the cellular

precursor to DMSP, may be reduced in cells with low photosynthetic activity (such as FLU), thus it may be expected that DMSPi would also be consequently lower. The underside of free-living thalli, whilst not exposed to full ambient PAR levels, may receive some light through seabed reflectance, thus experiencing some modest diurnal change in irradiance. The carbonate sand of the Suleman reef is likely to be highly reflective given its coral source - coral skeletons (even when powdered) reflect ultraviolet radiation as yellow light to maximise photosynthesis within coral tissues (Reef et al., 2009). Additionally, FLU may periodically receive ambient PAR through thallus rolling. The rate of thallus turnover in this region is not known, but is likely to be low, given the stark differences in pigmentation. Additionally, the rate of pigment loss / recovery in high / low light conditions is unknown but would further affect the thalli's ability to tolerate the ambient conditions. Further studies investigating the plasticity of free-living coralline algae to changing light regimes (as a result of storm induced turnover or bioturbation by sea urchins, for example), would provide information on the adaptability of these key reefal organisms.

3.7.4 Which non-photochemical parameter to use?

While Stern-Volmer NPQ ($[F_m - F_m'] / F_m'$), and qN (F_v' / F_m') both describe non-photochemical quenching, NPQ is usually used due to difficulties in determining light acclimated minimum fluorescence (F_o'). However, qN describes non-photochemical quenching due to changes in F_o' and F_m' , rather than just changes in F_m' , as Stern-Volmer quenching does. Both methods describe the photoprotective capacity of an alga to dissipate excess absorbed excitation energy as heat, and changes in F_m' often correspond in part to xanthophyll cycling (Lavaud et al. 2002), an important photoprotection process in many algae. However, many rhodophytes do not appear to possess an active xanthophyll cycle (Enríquez and Borowitzka, 2010; Ursi et al., 2003). The three xanthophyll carotenoids (violaxanthin, antheraxanthin and zeaxanthin) have been identified in the red alga *Gracilaria birdiae*, although the molecules' photoprotective effect are yet to be observed (Ursi et al., 2003). Consequently, it is also important to consider other photoprotective mechanisms that may be observed through changes in F_o' relative to F_o , which is a phenomenon prevalent in algae (Kromkamp and Forster, 2003; Lavaud et al., 2002). For this work, qN was informative in conjunction with NPQ, as it identified that the increased

photoprotection in thalli tips relative to thalli bases was contributed to by decreases in F_o' and F_m' . This increase in photoprotection in thallus tips corresponded to observations that branch tips were higher light acclimated relative to branch bases, despite the small physical distances between them. The acclimation of bases to lower light irradiances was therefore likely to be due to self shading. Both bases and tips examined here were still low light acclimated compared to the tropical specimens, as expected due to the low light regime in which they were assessed (in the laboratory and *in situ*). The lack of difference between tip and base qN and NPQ in the May measurements may be due to an increase in day-length in the field and the angle and location of the PAM measurements.

3.8 Conclusions

This chapter provides baseline studies from which more complex photosynthetic studies can build upon. Despite some concerns over the use of PAM fluorometry on red algae, this technique has been successfully used to assess the photosynthetic characteristics of temperate and tropical red coralline algae and a number of methodological considerations for PAM fluorometry on red coralline algae have been provided:

1. To identify intrathallus heterogeneity of branching thalli, use small diameter (ca. 2 mm) fibre optic probes, although a reduction in signal to noise ratio occurs.
2. For measurements designed to provide an 'average' across the thallus branch, use a wider fibre optic probe (ca. 5 mm). A larger probe is easier to handle underwater and provides an improved signal to noise ratio.
3. For all measurements, maintain the probe 10 mm from the algal surface - this has been found to be adequate for achieving a F_o and F_o' starting value of between 300 - 800 units (within the range recommended by Walz).

4. In time-restricted situations (e.g. in the field), 10 s of 'quasi-dark acclimation' is sufficient to achieve 95 - 98 % of the full dark-acclimation fluorescence state.
5. Static laboratory conditions may reduce the algae's light acclimation state, resulting in differences between laboratory and *in situ* measurements.
6. Photoprotection in red coralline algae is contributed to by decreases in F_o' and F_m' , thus both qN and NPQ parameters provide useful information on photoprotective characteristics.

Significant differences were observed between *in situ* and laboratory measurements, highlighting the need for field and laboratory controls in photosynthesis experiments. In high-light environments, algae fully exposed to ambient irradiance exhibit clear diurnal patterns. Intrathallus heterogeneity was also evident in both temperate and tropical thalli, presenting logistical complications when acquiring and interpreting fluorescence measurements. It may be concluded that, relative to the ambient light regime, coralline algae are low-light adapted but exhibit photoacclimation plasticity over short (diurnal) and longer (seasonal) timescales and the response may be species-specific.

4

Spatial variation of DMSP in coralline algae

Numerous functions have been proposed for dimethylsulphiopropionate (DMSP) in algal cells, including as an osmolyte (Karsten et al., 1992), an antioxidant (Sunda et al., 2002), a cryoprotectant (Karsten et al., 1996) and a grazing deterrent (Wolfe and Steinke, 1996) or attractant (Seymour et al., 2010). Physical, chemical and biological mechanisms regulate water column DMSP and its breakdown product dimethylsulphide (DMS, collectively DMS/P). Thus, environmental conditions may also determine macroalgal intracellular DMSP (DMSPi) production and water column DMSP+DMS (DMS/P) concentrations, creating spatial patterns in DMS/P that may highlight important areas for sulphur cycling.

4.1 Spatial variation of DMS/P in the epipelagic zone

A number of studies have investigated the spatial variations in DMS/P concentrations within the epipelagic zone - the surface layer of the open ocean that still receives sunlight (0 - 200 m) allowing photosynthesis to occur. There are a wide range in DMS concentrations within the oceans, with the majority of the open ocean having concentrations of <3 nM, whilst shelf sea and coastal areas can be much higher (Figure 4.1). Recent assessments of the Global Surface Seawater DMS database (Kettle et al., 1999) suggest a general trend of increased DMS concentrations at mid and high latitudes, particularly during the hemispheric summer and driven by solar radiation dose (Lana et al., 2012; Lana et al., 2011).

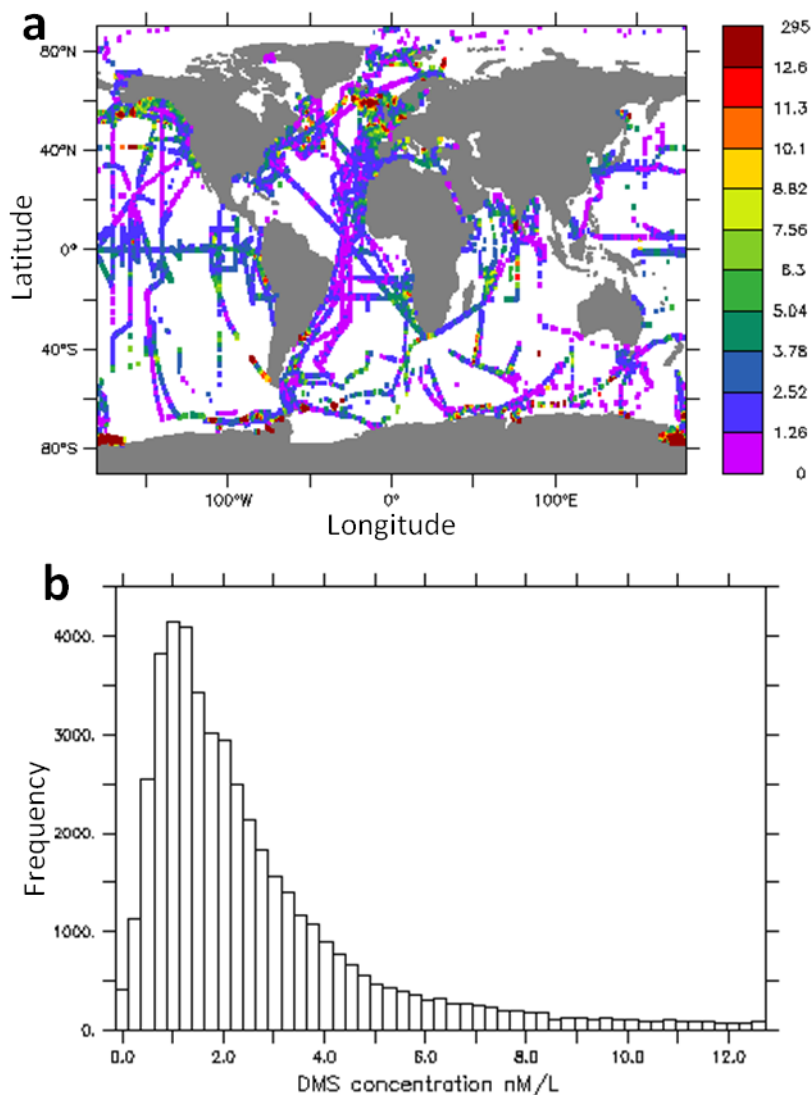


Figure 4.1 Measured global DMS concentrations. (a) Spatial distribution of global DMS concentrations (nM) and (b) frequency distribution of the DMS concentrations. Data from 245 data sets (cruise tracks or seasonal coastal studies, 48141 records) from 1972 – 2010, submitted to the DMS database (<http://saga.pmel.noaa.gov/dms>, Kettle et al., 1999). Average global DMS concentrations: mean = 4.18 nM L^{-1} , median = 2.00 nM L^{-1} , mode = 1.00 nM L^{-1} .

The availability of nutrients, and therefore potential for phytoplankton growth, can lead to significant differences in dimethyl sulphur concentrations over small spatial scales. In the French north-west Mediterranean, particulate DMSP (DMSPp) concentrations ranged from 2 - 59 nM in Little Bay (high nutrients) throughout the year, whilst Niel Bay (low nutrients) had significantly less DMSPp (0.5 - 24 nM) (Jean et al., 2006). In the Gulf of Oman, a decrease in DMS, DMSP and DMSO concentrations were observed from the eutrophic coastal waters of Oman to the oligotrophic Arabian Sea following the passage of a monsoon and a bloom of prymnesiophytes (high DMSP producers) (Hatton et al., 1999). In the Gulf of Mexico, DMSPp and DMSPd concentrations more than doubled in mesotrophic shelf waters compared to the oligotrophic oceanic waters (Kiene

and Linn, 2000). DMSPd turnover was 10 times higher in the shelf waters compared to the oceanic sites (39 nM d⁻¹ compared to 3.8 nM d⁻¹).

In the north-west Mediterranean, spatial variations in DMS concentrations are driven by the influence of continental runoff providing elevated nutrients and organic matter (Simo et al., 1997; Simo et al., 1995). This is particularly evident in the nearshore waters close to the Ebro and Rhone river deltas and Barcelona harbour (Simo et al., 1997; Simo et al., 1995). The dominant dimethyl sulphur species in surface waters was dimethylsulphoxide (DMSO), whilst dissolved DMSP (DMSPd) was low. An average ratio of 1:1:6 for DMS:DMSPd:DMSO (2.9:3.0:16.6 nM) has been reported in the area (Simo et al., 1997). A decrease in dimethyl sulphur species was observed away from the coast; the open ocean contained 2.7 times less DMS, 1.9 times less DMSPd and 1.7 times less DMSO (Simo et al., 1997).

4.2 Spatial variation of DMS/P in benthic systems

Epipelagic studies suggest that coastal systems, which will be affected by continentally-derived nutrients and organic matter may have an inherently higher DMS/P budget than oceanic systems. However, the benthos, particularly the benthic primary producers such as macroalgae and seagrass, may influence the observed DMS/P budget within these highly productive ecosystems.

Knowledge of spatial variations in DMSPi production by macroalgae is limited, primarily focussing on Chlorophyta species. DMSPi in *Codium fragile* from Nova Scotia, Canada, has been shown to slightly reduce with increasing depth, with bleached specimens from tide pools having less DMSPi than non-bleached individuals (Lyons et al., 2010). DMSPi in *Ulva* spp. appears to increase with increasing latitude in the northern hemisphere, from tropical to polar species (Van Alstyne and Puglisi, 2007). A significant trend in DMSPi concentrations in *Ulva lactuca* was observed across only a 0.6° latitudinal range in the eastern North Pacific (Van Alstyne et al., 2007), again with less DMSPi at the southernmost sites. Significant within-individual variations were also observed in *U. lactuca*, with DMSPi concentrations higher at the base (which is more accessible to benthic grazing) compared to the tip (Van Alstyne et al., 2007).

A general reduction in macroalgal DMSPi at lower latitudes has been suggested in the northern hemisphere; no latitudinal pattern was identified in the southern hemisphere (Van Alstyne and Puglisi, 2007). However, this hypothesis was based primarily on Chlorophyta species, due to the lack of information regarding Ochrophyta (formerly Phaeophyta) and particularly Rhodophyta species. Additionally, the abundance of Chlorophyta species increases with increasing latitude, perhaps further skewing the observed trends. Ochrophyta and Rhodophyta species generally had uniformly low DMSPi concentrations, except for the *Polysiphonia* (and *Vertebrata*) and *Halopithys* genera (Rhodophyta) (Van Alstyne and Puglisi, 2007).

Patterns in other macroalgal secondary metabolites such as phlorotannin have also been recorded across small (e.g. within the intertidal zone or along estuarine salinity gradients) and large (inter-continental) spatial scales (Dethier et al., 2001). Grazing pressures in tropical coastal habitats are thought to be higher than in temperate systems, resulting in an increase in anti-grazing compounds in tropical, compared to temperate, macroalgae (Dethier et al., 2001) - opposite to the apparent trend in DMSPi. When attributing causes of spatial patterns in macroalgal secondary metabolite production, it is important to consider evolutionary aspects (Dethier et al., 2001):

1. Historic selective pressures that may drive evolutionary change causing large-scale differences in populations.
2. Genetic drift between neighbouring populations due to the often limited dispersal capacity of algal propagules.

Genetic drift may be especially important in establishing spatial patterns of DMSPi in coralline algae due to their highly-specific environmental requirements and because asexual reproduction may be the dominant reproduction strategy for some populations.

4.3 Aims of this chapter

This chapter aims to extend our currently limited knowledge of DMS/P concentrations in coralline algal-dominated coastal benthic habitats by assessing

DMS/P within macroalgae and in the surrounding water column over various spatial scales. This will improve our understanding of the role DMS/P may play within coastal ecosystems and its importance as a secondary metabolite in macroalgae. Intracellular DMSP in coralline algae and the concentration of dissolved and particulate DMS/P associated with coralline algal habitats was assessed at a number of spatial scales (Figure 4.2):

1. **Global scale:** DMSPi in red coralline algae from polar, temperate and tropical regions.
2. **Regional scale:** A trans-Atlantic macroalgal comparison and an 1.5° latitudinal comparison of DMSPi in red coralline algae along the west coast of Scotland.
3. **Local scale:** water column dissolved and particulate DMS/P concentrations from Egyptian coral reefs, Mediterranean seagrass beds and Mediterranean coralligenous banks, and DMSPi in encrusting Antarctic coralline algae.

It was hypothesised that DMSPi production would increase with increasing latitude (and decreasing water temperature), in line with previous studies (Van Alstyne and Puglisi, 2007), and that DMS/P production by benthic primary producers would act as a source of DMS/P to the surrounding water column and atmosphere.

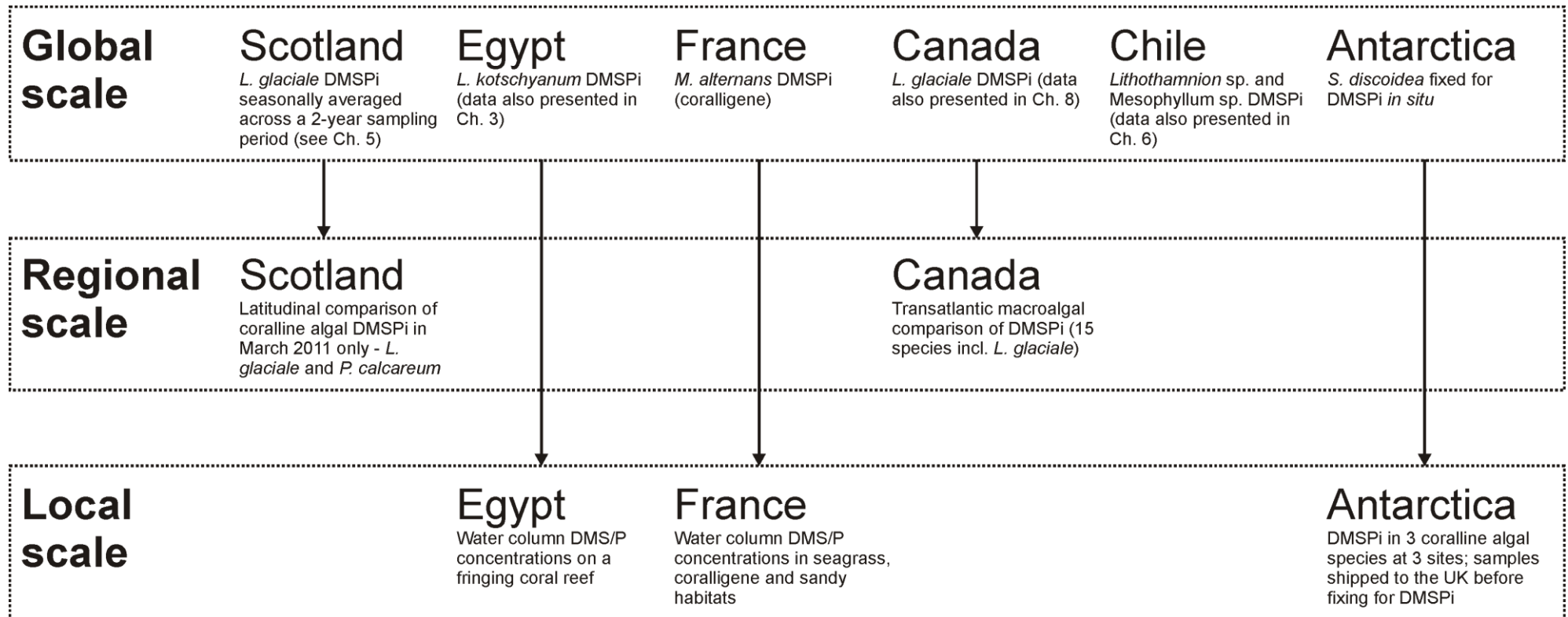


Figure 4.2 Spatial sampling regime and links between spatial scales.

4.4 Methods: Global scale

4.4.1 Sampling locations

Coralline algal samples were analysed for DMSPi from six locations worldwide: (1) west coast of Scotland, (2) Sinai Peninsula, Egypt, (3) south-west France, (4) Nova Scotia, Canada, (5) central Chile and (6) Western Antarctic Peninsula (Figure 4.3).

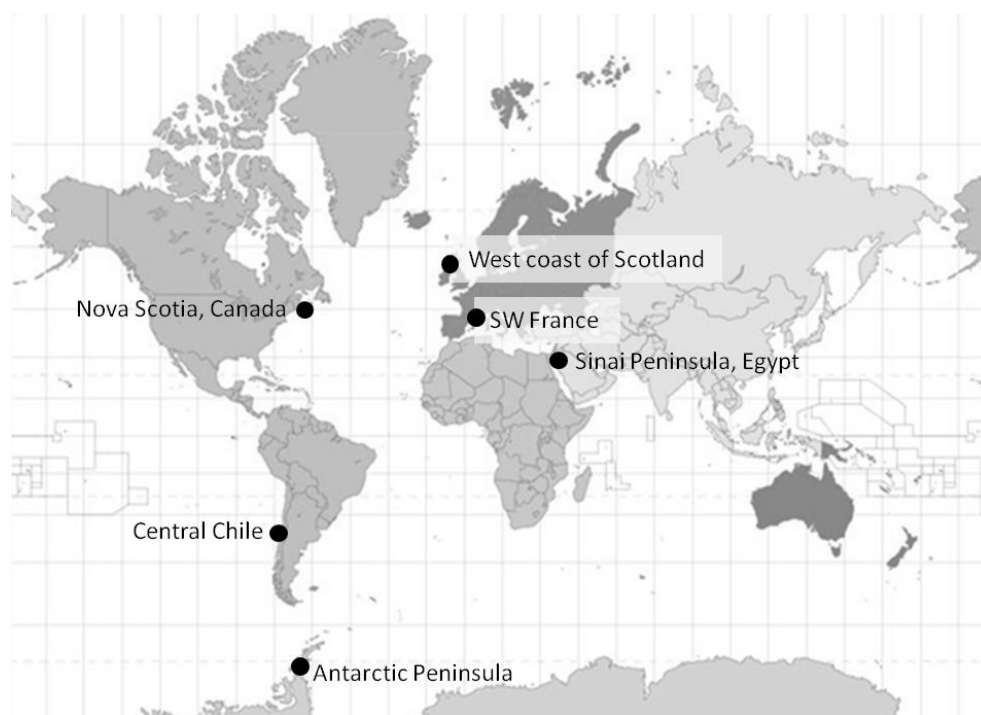


Figure 4.3 Locations of the global coralline algae / DMSP sampling sites.

Excess debris was removed from the samples prior to fixing for DMSPi and samples were fixed within two hours of collection using the algal headspace protocol described in Chapter 2. Samples (Figure 4.4) were collected by hand using SCUBA or snorkelling, and were generally taken in the summer months (Table 4.1):

1. **Loch Sween, Scotland:** Free-living *Lithothamnion glaciale* were collected using SCUBA from 6 m depth on 11 occasions from March 2010 - February 2012 (see Chapter 5 for more details). For this study, data were grouped according to season of collection - spring: March - May (n = 80), summer: June - August (n = 40), autumn: September - November (n = 58), winter: December - February (n = 58).

2. **Dahab, Sinai Peninsula, Egypt:** Free-living *Lithophyllum kotschyannum* (n = 7) were collected by snorkelling at 1 m depth in July 2011. Thalli were characterised by a bleached topside and a pigmented underside (see Chapter 3 for more details) - DMSPi samples were taken from both sides.
3. **Banyuls-sur-Mer, south-west France:** Encrusting *Mesophyllum alternans* (n = 10) samples were collected using SCUBA from 17 m depth from the upper surface of a coralligène bank (see section 4.6.2) in April 2012.
4. **Nova Scotia, Canada:** Free-living samples of *L. glaciale* (n = 24) were collected using SCUBA from 4 m depth in August 2010. See Chapter 8 for more details.
5. **Las Cruces, central Chile:** Encrusting samples of *Lithothamnion* sp. were collected by hand from 0.2 m depth (n = 14, intertidal) and *Mesophyllum* sp. at 15 m depth (n = 15, subtidal) using SCUBA in January 2012 (southern hemisphere summer). See Chapter 6 for more details.
6. **Western Antarctic Peninsula, Antarctica:** Encrusting samples of *Spongites discoidea* (n = 15, see section 4.6.3) were collected on cobbles using SCUBA from 9 m depth in February 2011 (southern hemisphere summer).

Table 4.1 Details of the global scale sampling locations. See Figure 4.4 for examples of the morphology of the algae at each site. WAP: Western Antarctic Peninsula.

Sampling site	Location	Depth (m)	Date collected	Species	Morphology
Loch Sween, Scotland	56° 01.99'N 05° 36.13'W	6	2010-12 ^{*^†‡}	<i>Lithothamnion glaciale</i>	Free-living thalli
Dahab, Sinai Peninsula	28° 28.79'N 34° 30.83'E	1	July 2011 [^]	<i>Lithophyllum kotschyannum</i>	Free-living thalli
Banyuls-sur-Mer, SW France	42° 30.03'N 03° 08.28'E	17	April 2012 [*]	<i>Mesophyllum alternans</i>	Bank forming coralligène
Nova Scotia, Canada	44° 04.11'N 64° 36.71'W	4	August 2010 [^]	<i>L. glaciale</i>	Free-living thalli
Las Cruces, Chile	33° 30.01'S 71° 37.93'W	0.2 / 15	January 2012 [^]	<i>Lithothamnion</i> sp. and <i>Mesophyllum</i> sp.	Encrusting on bedrock and cobbles
WAP, Antarctica	67° 36.71'S 68° 12.57'W	9	February 2011 [^]	<i>Spongites discoidea</i>	Encrusting on cobbles

* spring, ^ summer, † autumn, ‡ winter.

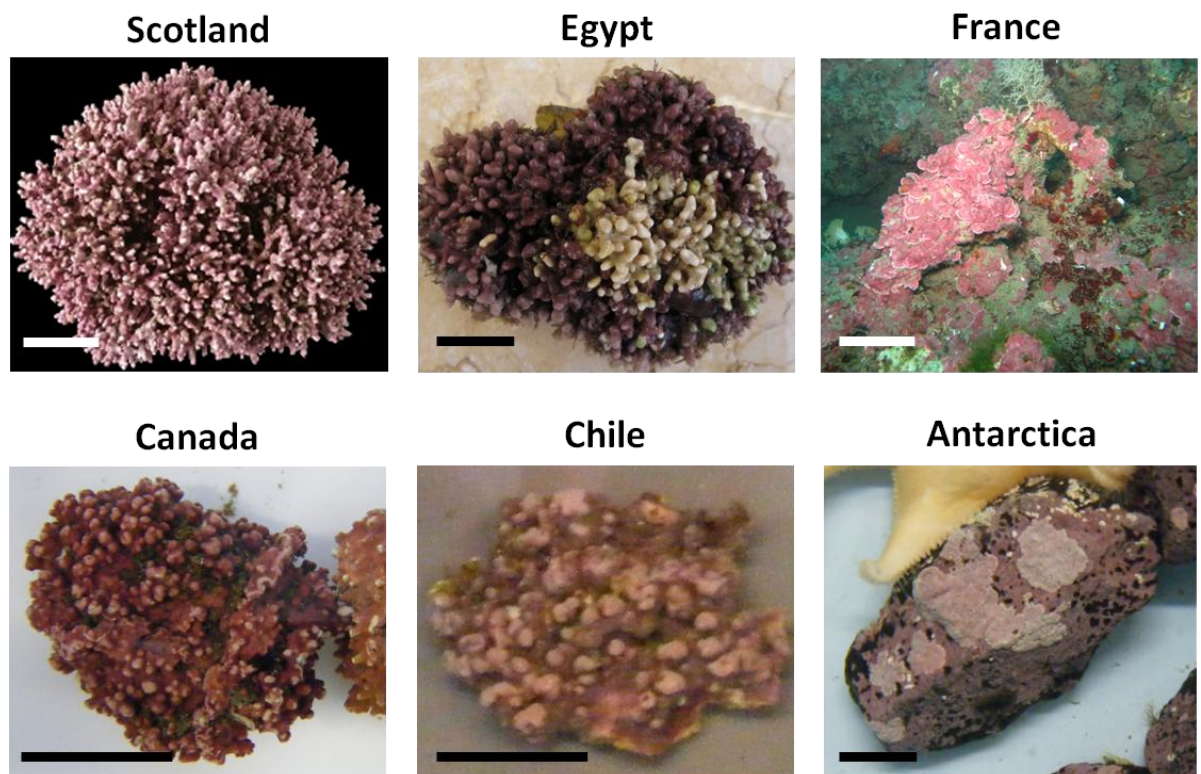


Figure 4.4 Red coralline algae from the six global sampling locations. Examples of the algae sampled for DMSPi. Scale bar = 20 mm throughout, except for France where the scale bar = 100 mm. Photos: Scotland: L. Hill, France: N. Kamenos, Egypt, Canada, Chile and Antarctica: H. Burdett.

4.5 Methods: Regional scale

Two studies were conducted to assess regional scale variability in coralline algal DMSPi production in shallow coastal systems:

1. **Trans-Atlantic macroalgae comparison:** DMSPi from a number of macroalgal genera in eastern Canada and western Scotland.
2. **West coast of Scotland:** coralline algal DMSPi from five sites along the west coast of Scotland over a 1.5° range in latitude.

4.5.1 Trans-Atlantic comparison

To assess DMSPi across the three algal Phyla, macroalgal samples in addition to those described used in the global-scale analysis (section 4.4) were analysed for DMSPi concentration. Samples of different macroalgae (fleshy and coralline) were collected by hand using SCUBA from St Margaret's Bay, Nova Scotia, Canada (44°34.83'N, 63°59.37'W) from a depth of 4 m and from Loch Sween, Scotland (56°01.99'N, 05°36.13'W) from a depth of 6 m. Samples from both locations were collected within one week of each other in September 2010. Where possible, the same algae (at least to genus level) were collected to allow direct comparisons (Table 4.2). All algae were prepared and analysed according to the headspace methodology described in Chapter 2.

Table 4.2 Macroalgae sampled for the trans-Atlantic comparison. Samples collected from St Margaret's Bay, Nova Scotia, Canada, and Loch Sween, west coast of Scotland. Macroalgae are arranged by Phylum and Family taxonomic classifications.

Taxonomic classification	Canada	Scotland
Chlorophyta		
Codiaceae	<i>Codium fragile</i>	<i>Codium fragile</i>
Ochrophyta (formerly Phaeophyta)		
Chordaceae	<i>Chorda filum</i>	<i>Chorda filum</i>
Desmarestiaceae	<i>Desmarestia aculeate</i>	
Fucaceae	<i>Ascophyllum nodosm</i>	<i>Fucus serratus</i>
Laminariaceae	<i>Agarum cribrosum</i> <i>Laminaria digitata</i> <i>Saccharina latissima</i>	<i>Laminaria digitata</i> <i>Saccharina latissima</i>
Sargassaceae		<i>Halidris siliquosa</i>
Rhodophyta		
Bonnemaisoniaceae	<i>Bonnemaisonia hamifera</i>	
Corallinaceae	<i>Corallina officinalis</i>	
Gigartinaceae	<i>Chondrus crispus</i>	
Hapalidiaceae	<i>Lithothamnion glaciale</i>	<i>Lithothamnion glaciale</i>
Palmariaceae		<i>Palmaria palmata</i>
Rhodomelaceae	<i>Vertebrata lanosa</i>	

4.5.2 West coast of Scotland

To assess latitudinal effects at a regional level for coralline algae, samples were taken from six sites along the west coast of Scotland, including one sampling point at Loch Sween (included in the global scale analysis and presented in Chapter 5). Free-living coralline algal samples were collected by hand using SCUBA (Figure 4.5 and Table 4.3) in March 2011 spanning a 1.5° latitudinal range. Two species were sampled - *L. glaciale* and *Phymatolithon calcareum* (Table 4.3), providing species and latitudinal information on DMSPi production. Water temperature was the same at all sites during the sampling period (6 - 7°C). All samples were fixed for DMSPi on-site and analysed according to the methodology provided in Chapter 2 for headspace analyses.

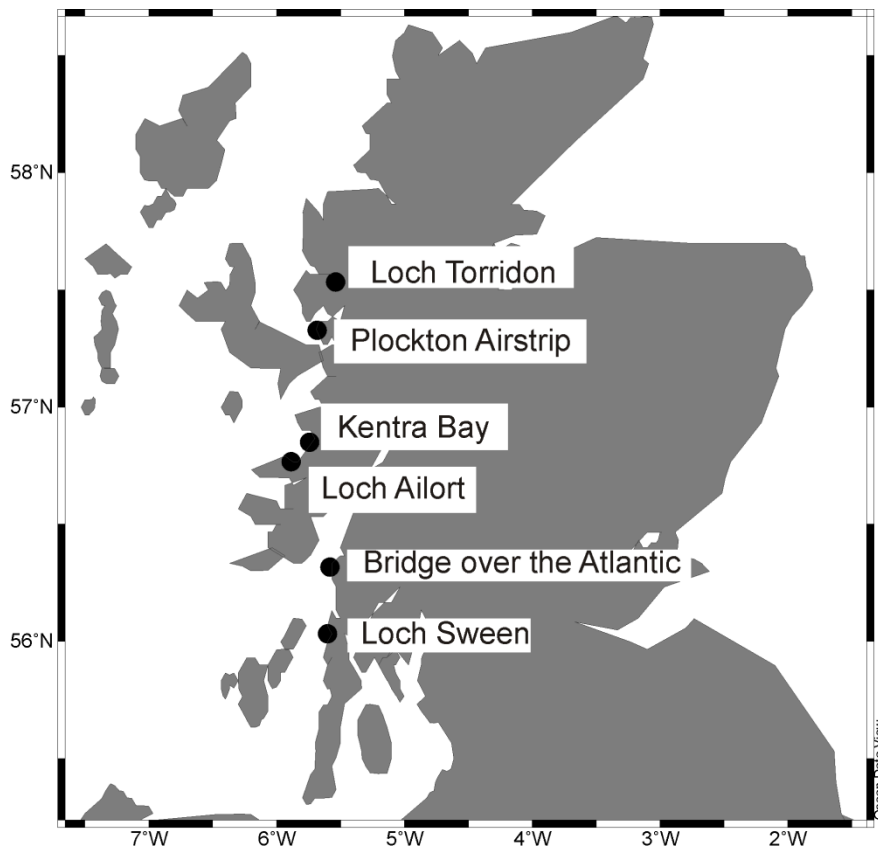


Figure 4.5 West coast of Scotland sampling site locations.
Map source: Ocean Data View.

Table 4.3 Details of the west coast of Scotland regional sampling locations.
RP: rock pool, BE: beach, Ø: diameter.

Site name	Location	Depth (m)	Date	Species	Morphology
Loch Sween (LS)	56° 01.99'N 05° 36.13'W	5	09/03/11	<i>L. glaciale</i>	Large free-living thalli (Ø: 40 - 100 mm)
Bridge over the Atlantic (BA)	56° 19.11'N 05° 35.00'W	1	10/03/11	Mixed - not identified	Encrusted onto small cobbles with protuberances (Ø: 40 - 60 mm)
Loch Ailort (LA)	56° 50.98'N 05° 44.58'W	3	11/03/11	<i>P. calcareum</i>	Small free-living fragments (Ø: 10 - 30 mm)
Kentra Bay (KB)	56° 46.09'N 05° 53.03'W	0.1 (RP)	11/03/11	<i>P. calcareum</i>	Small free-living fragments (Ø: 10 - 30 mm)
Plockton airstrip (PA)	57° 19.78'N 05° 40.89'W	0.05 (BE)	12/03/11	<i>P. calcareum</i>	Small free-living fragments (Ø: 10 - 30 mm)
Loch Torridon (LT)	57° 32.09'N 05° 32.34'W	7	14/03/11	<i>L. glaciale</i>	Large free-living thalli (Ø: 30 - 80 mm)

4.6 Methods: Local scale

Three studies were conducted to assess local scale variability in DMS/P production in coralline algal habitats:

1. **Coral reef:** Water column dissolved and particulate DMS/P (DMS/Pd and DMS/Pp) across a fringing coral reef transect, covering seagrass, algal and coral-dominated benthos communities.
2. **Mediterranean coralligène and seagrass:** Water column DMS/P from three transects (seagrass, coralligène and sandy benthos) in the north-western Mediterranean.
3. **Western Antarctic Peninsula:** Coralline algal DMSPi from encrusted cobbles.

4.6.1 Sinai Peninsula, Egypt

Water samples were collected by snorkelling from the Suleman fringing reef, Sinai Peninsula, Egypt (28° 28.79'N, 34° 30.83'E) in August 2011. Samples were prepared and analysed for DMS/Pd and DMS/Pp according to the liquid methodology described in Chapter 2. Samples (n = 3) were taken at the seabed along a transect 90° to the shore from the five distinct zones within the fringing reef (Figure 4.6):

1. **Seagrass beds:** 1.5 m depth, 10 m from the beach.
2. **Reef flat:** 0.7 m depth, 60m from the beach. Dominated by fleshy and coralline macroalgae.
3. **Reef crest:** 0.5 m depth, 120 m from the beach. Dominated by encrusting coralline algae and branching corals.
4. **Reef slope:** 5m depth, 120 - 130m from the beach. Dominated by massive corals.

5. **Offshore:** 10 m depth, 270 m from the beach. Sandy bottom with little discernible macro-primary production (e.g. from corals or macroalgae)

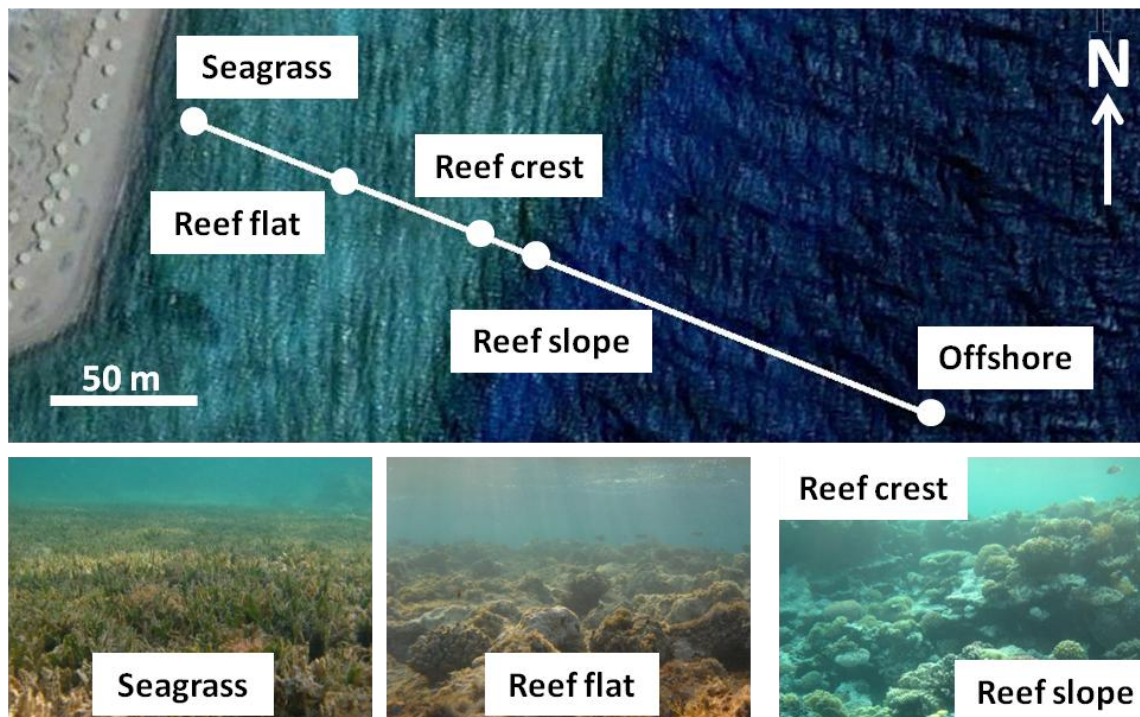


Figure 4.6 Suleman reef transect location and sampling points.

Water samples taken from five habitat zones along the transect: seagrass bed, reef flat, reef crest, reef slope and offshore. Distance from reef slope to shore is ~120 m. See Chapter 7 for more information on the habitat zones on Suleman Reef. Aerial image: Google Earth, photos: N. Kamenos.

Water samples were collected at 16:00. Water temperature at this time decreased away from the shore, from 30°C at the seagrass beds, to 27°C offshore. For more information on the species at each zone on the reef, see Figure 7.4 in Chapter 7.

4.6.2 North-west Mediterranean

Water samples were taken along easterly transects through three distinct habitats. Samples were collected by deploying a Niskin bottle from R/V Nereis and Ruffi II based at Observatoire Océanologique de Banyuls-sur-Mer, south-west France, across a depth gradient along three transect routes from the shore to 65 m depth (Figure 4.7):

1. **Sand:** bare sand throughout with no discernible macro primary productivity. Shallowest sampling point: 42° 29.27'N, 03° 07.69'E, transect length = 4.3 km.

2. **Coralligène:** A coralligenous habitat unique to the Mediterranean composed of a bank of encrusting coralline algae up to 4 m thick (coralligène ranges from 15 - 35 m as sampling could not be carried out in shallower waters). Shallowest sampling point: 42° 30.03'N, 03° 08.28'E, transect length = 3.0 km.
3. **Seagrass beds:** Shallow bed of *Posidonia oceanica* (beds range from 3 - 9 m). Shallowest sampling point: 42° 28.91'N, 03° 08.18'E, transect length = 3.8 km.

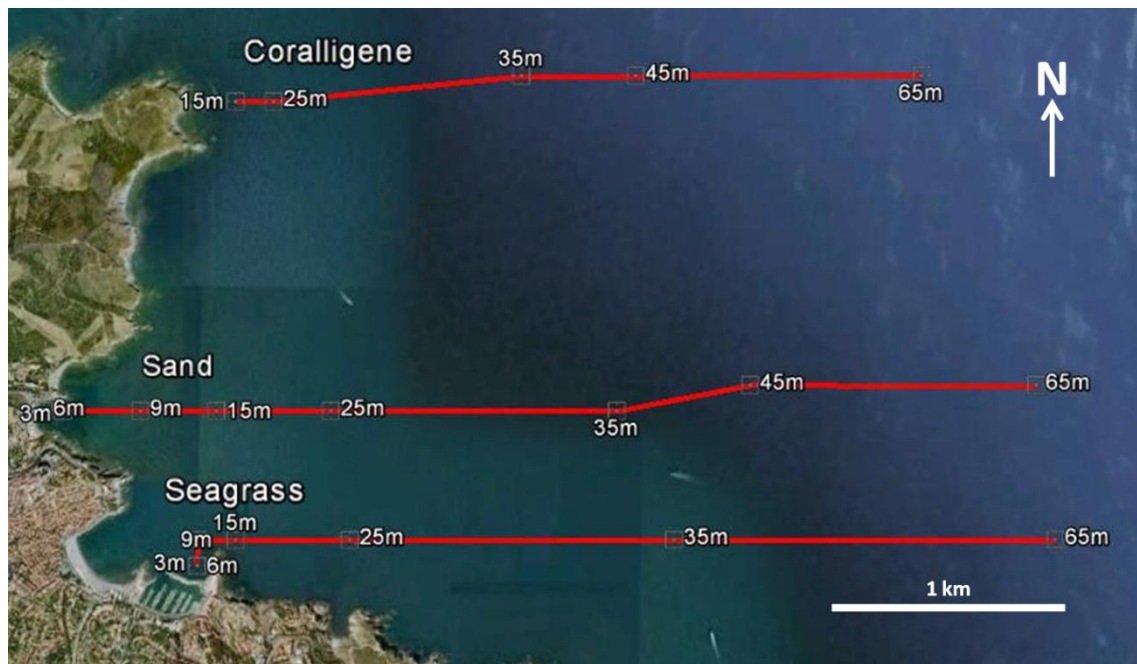


Figure 4.7 Transect routes for Mediterranean sampling. Three transects across three habitat types near to Banyul-sur-Mer, France. Transects crossed coralligène, sand and seagrass habitats. Sampling locations in each transect are indicated by their water depth. Image constructed in Google Earth.

Water samples ($n = 5$) were analysed for DMS/Pd according to the methodology described in Chapter 2. Samples were taken horizontally along a depth gradient, ranging from 3 m to 65 m depth, and at three points at each depth: at the seabed, at 3 m depth and mid-way between the two (Figure 4.8).

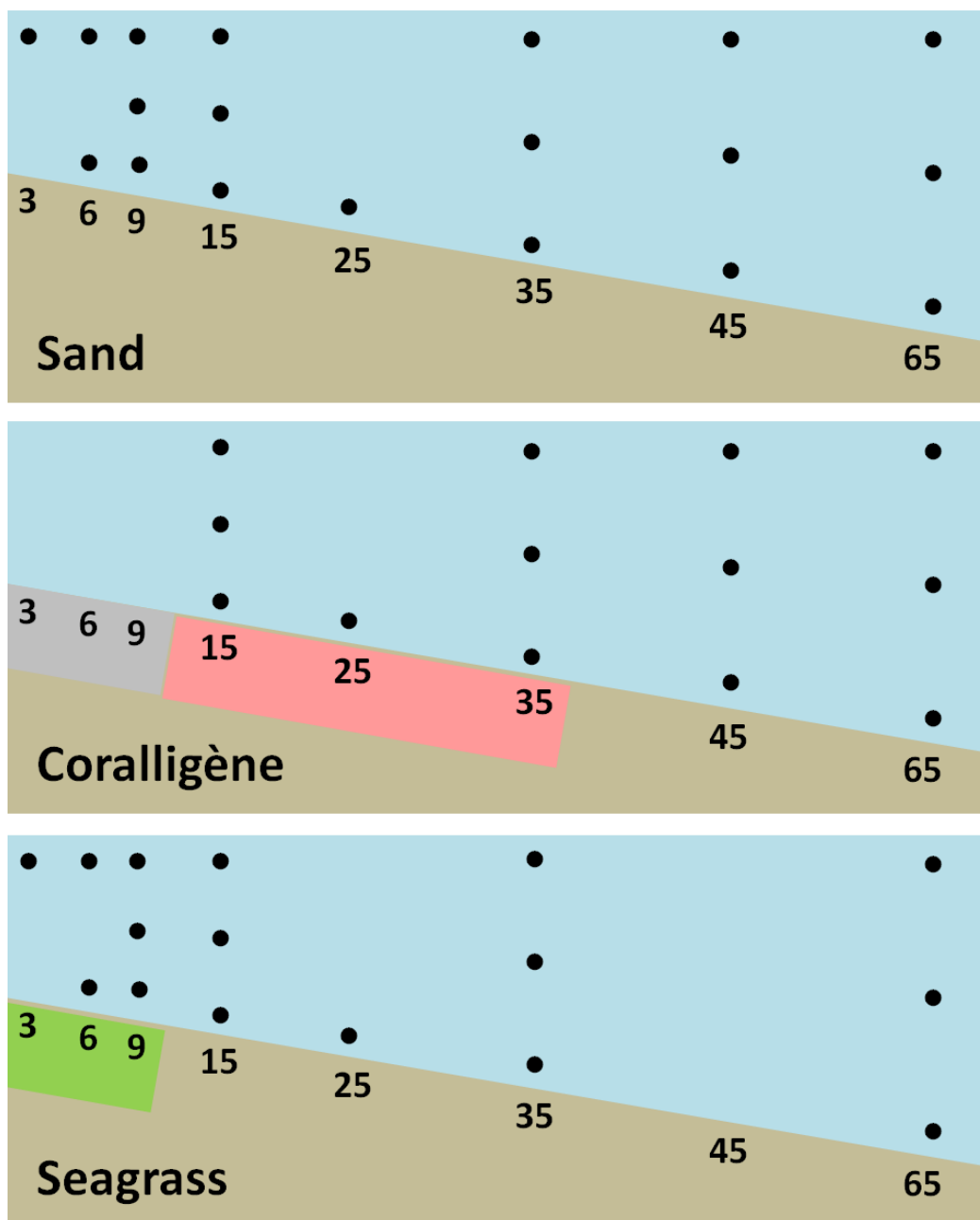


Figure 4.8 Horizontal and vertical Mediterranean sampling.

Numbers indicate water depth. Water column samples taken at 3 m depth, at the sea bed and midway between the two along the three transect routes. Sampling points are indicated by the black circles. Coloured shading indicates seabed bottom type: brown = sand, grey = rock, pink = coralligène, green = seagrass. Note: not to scale, diagrammatic representation only.

4.6.3 Western Antarctic Peninsula

To assess local-level variability on the WAP, coralline algal samples in addition to those presented in the global-scale analysis were analysed for DMSPi. Cobbles encrusted with coralline algae were collected from three sites around Adelaide Island, on the western Antarctic Peninsula, near to the British Antarctic Survey (BAS) Rothera research station. Cobbles were collected by hand using SCUBA in February 2010 and February 2011.

In February 2010, cobbles were collected from three sites (n = 10 per site) (Figure 4.9):

1. **Rose Garden:** 9 m depth, 67°36.713'S, 68°12.569'W.
2. **South Cove:** 4 m, 9 m and 16 m depth; 67°34.010'S, 68°07.398'W.
3. **Hangar Cove:** 9 m; 67°33.848'S, 68°07.488'W.

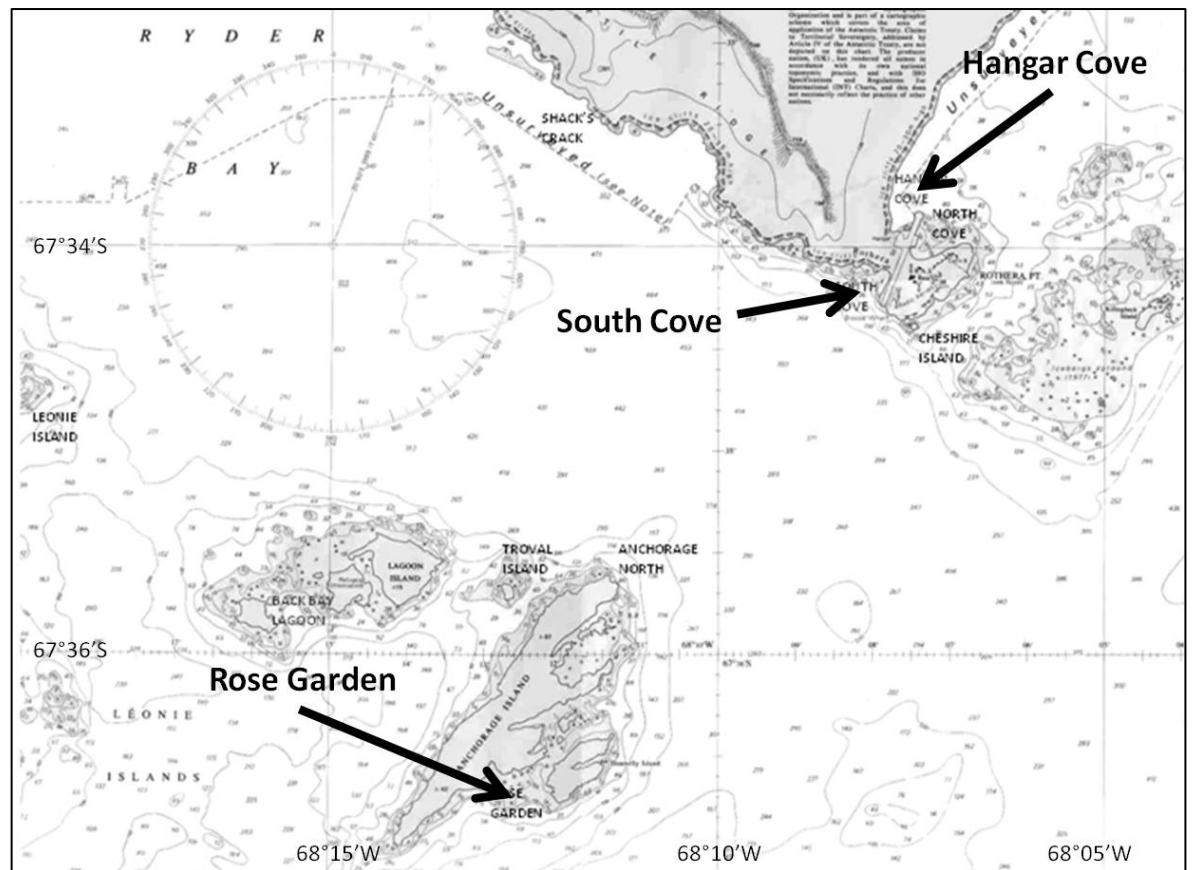


Figure 4.9 Antarctic sampling locations.

Cobbles collected in February 2010 were transported to Cambridge (UK) in flow-through seawater tanks maintained at ambient conditions (water temperature: -1 °C, 12h:12h light:dark regime). Encrusting coralline algae were sampled for DMSPi at midday (in the light) and following three hours of darkness in May 2010. Three algal species were identified during the first sampling campaign based on their morphology and colour (Figure 4.9, Table 4.4). Taxonomic identification was based on morphology and depth descriptions in Foslie (1907), with the classifications updated according to www.algaebase.org.

Further work (based on cell morphology or molecular approaches) is required to confidently identify the three species.

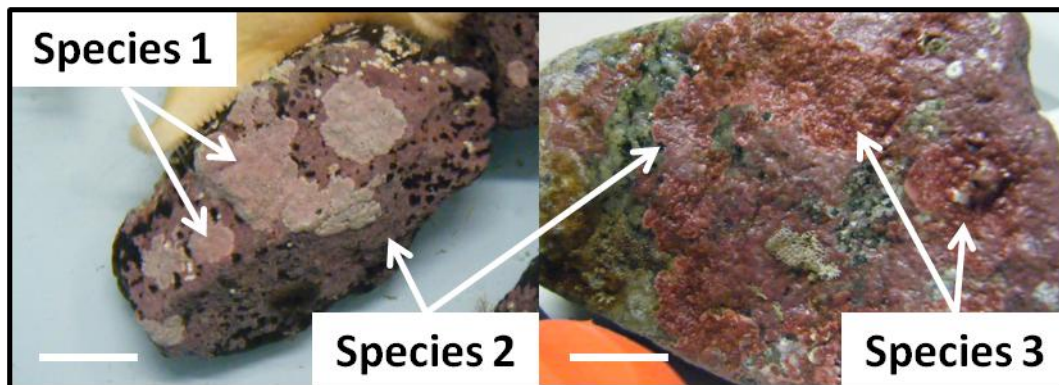


Figure 4.10 Antarctic encrusting coralline algae. Three species were identified based on their morphological characteristics, given in Table 4.4. Scale bars = 30 mm. Photos: H. Burdett.

Table 4.4 Species classification of Antarctic encrusting algae. Classification based on morphology, according to Foslie (1907). Location sites are Rose Garden (RG), South Cove (SC) and Hangar Cove (HC).

Species number	Probable species	Morphology	Location
1	<i>Spongites discoidea</i>	Pale pink, circular growth, smooth edges, thick crust, dimples in the centre	RG
2	<i>Clathromorphum obtectulum</i>	Mid pink, thin crust, thicker on the sides of rocks	RG, SC, HC
3	<i>Lithothamnion fuegianum</i>	Dark pink, plate form, lighter at the edges	HC

In February 2011, cobbles encrusted with *Spongites discoidea* (species 1, n = 15) were collected from the Rose Garden site only. The coralline algae were fixed for DMSPi within two hours of collection in Antarctica, to compare transportation effects which may have been incurred in 2010.

All samples were prepared and analysed for DMSPi using the headspace methodology described in Chapter 2.

4.7 Statistical and data analysis

Spatial differences were statistically assessed using ANOVA general linear models and Tukey pairwise comparisons for all data sets except the global scale

data set, where the test assumptions (normal distribution and homogeneity of variance) for ANOVA could not be met. Instead, a non-parametric multi-comparison Kruskal-Wallis test was used. For all other data sets, a \log_{10} transformation was used to achieve normality and homogeneity of variance prior to ANOVA testing. For correlation analyses of the global scale data set, the non-parametric Spearman's rank correlation coefficient was calculated. All statistical analyses were conducted in Minitab V14 or V15.

Two-dimensional concentration profiles were constructed for the North-west Mediterranean data using Ocean Data View 4 (Schlitzer, 2011). Interpolation was conducted using VG gridding. This interpolation technique utilises a variable resolution rectangular grid where grid-spacing along the x and y axes vary according to data density, resulting in higher resolution mapping in areas of higher data coverage. A neighbourhood weighted-averaging scheme is applied to interpolate between the data points, with decreasing computational weight applied as distance from the grid point increases (Schlitzer, 2011).

4.8 Results: Global scale

A significant difference in coralline algal DMSPi between global sites was observed (Figure 4.11, $H_{10} = 159.72$, $p < 0.001$). The highest concentrations were observed in Canada and Egypt, which were significantly higher than Scotland, Antarctica and the subtidal algae from Chile (Figure 4.11). Spearman's rank correlation suggested that absolute latitude (i.e. without differentiating between northern and southern hemisphere, Table 4.5) was most highly correlated to DMSPi concentration (Spearman's ρ : -0.40). Depth, temperature and PAR (Table 4.5) were not well correlated to DMSPi concentration (Spearman's ρ : -0.12, 0.18 and 0.12 respectively).

Table 4.5 Abiotic parameters associated with global-scale samples.

WAP: Western Antarctic Peninsula, Max. PAR: Maximum daily photosynthetically active radiation.

Site	Species	Latitude	Depth (m)	Temp (°C)	Max. PAR ($\mu\text{mol photons m}^{-2} \text{s}^{-1}$)
Scotland	<i>Lithothamnion glaciale</i>	56.0°N	6	4 - 17	10 - 120*
Egypt	<i>Lithophyllum kotschyianum</i>	28.5°N	1	28	1600
France	<i>Mesophyllum alternans</i>	42.5°N	17	14	10
Canada	<i>L. glaciale</i>	44.0°N	4	14	8
Chile	<i>Lithothamnion</i> sp. and <i>Mesophyllum</i> sp.	33.5°S	0.2 / 15	18	25
WAP	<i>Spongites discoidea</i>	67.5°S	9	-1	2 - 65†

* Estimated from subsequent measurements at Loch Sween.

† Estimated from previous macroalgal studies in Antarctica (Runcie and Riddle, 2006; Schwarz et al., 2005; Karsten et al., 1990).

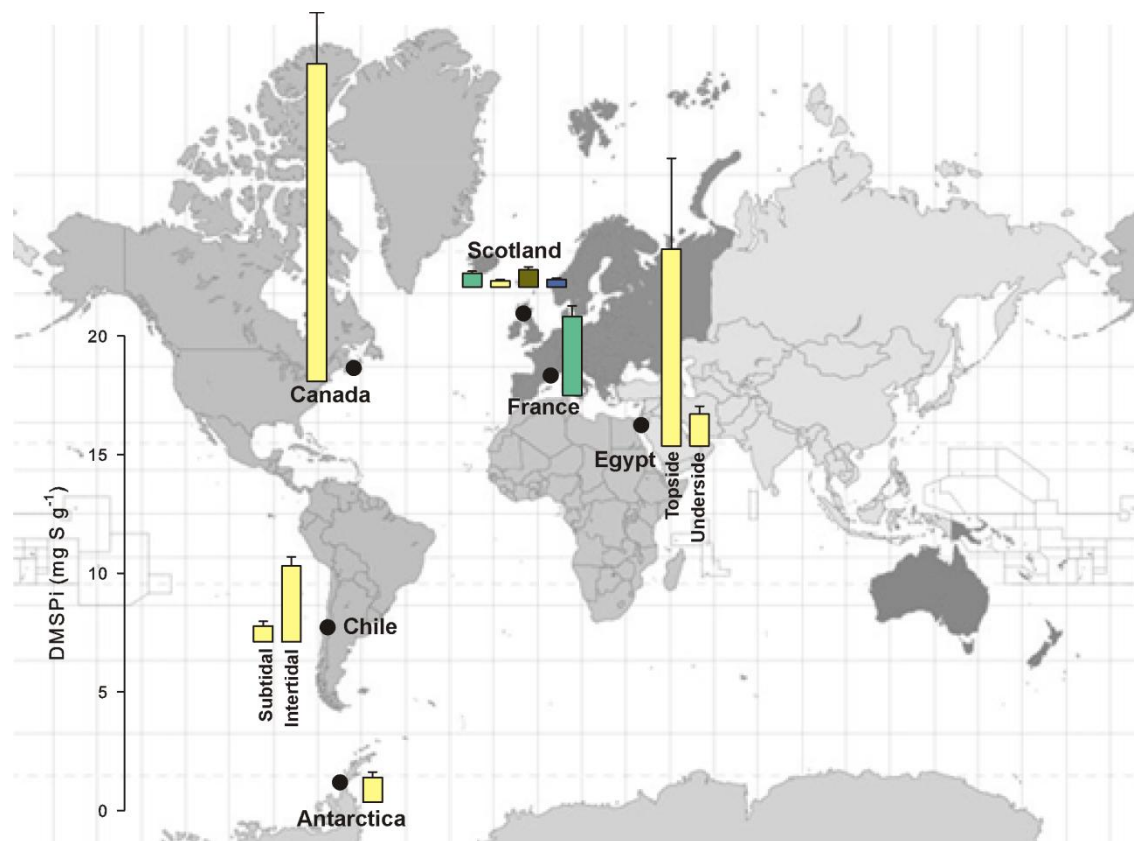


Figure 4.11 Coralline algal DMSPi at six locations worldwide.

DMSPi (mg S g^{-1} as DMS) determined in coralline algal samples collected in the spring (green bars), summer (yellow bars) autumn (brown bars) and winter (blue bars). Scale bar is on the left of the figure. In Egypt, samples were taken from the bleached topside and the pigmented underside of free-living thalli. In Chile samples were taken from subtidal and intertidal encrusting coralline algae. Data presented as mean \pm SE.

4.9 Results: Regional scale

4.9.1 Trans-Atlantic comparison

DMSPi was detected in all species analysed (Figure 4.12). There was considerable variation in DMSPi between algal species (Figure 4.12), ranging from $0.03 \pm 0.009 \text{ mg S g}^{-1}$ (*Bonnemaisonia hamifera*, mean \pm SE) to $56.35 \pm 8.13 \text{ mg S g}^{-1}$ (*Codium fragile*). There was a significant difference between algal Phyla ($F_2 = 24.91$, $p < 0.001$), with Chlorophyta > Ochrophyta > Rhodophyta. No significant difference between location (Canada / Scotland) was observed when all three algal Phyla were considered together ($F_1 = 2.26$, $p = 0.135$). However, when algal phyla were considered independently, DMSPi in Canadian macroalgae was lower than Scotland for Chlorophyta ($F_1 = 13.20$, $p = 0.002$) and Rhodophyta ($F_1 = 6.99$, $p = 0.011$), despite coralline algal DMSPi being higher in Canada compared to Scotland (Figure 4.11 and Figure 4.12). No significant difference between Canada and Scotland was observed for Ochrophyta ($F_1 = 1.05$, $p = 0.309$).

Where family-level comparisons could be made, there was a general trend towards higher DMSPi in Scotland (Figure 4.12), although this was only significant for two of the comparisons (Codiaceae and Fucaceae, Table 4.6). In contrast, the red coralline alga *Lithothamnion glaciale* (Haplidiaceae family) was significantly higher in Canada compared to Scotland (Table 4.6).

Table 4.6 Transatlantic comparison t-test results.

Where two species are given, the first was from Canada, the second from Scotland. Bold text indicates significant differences at the 95% confidence level. df = degrees of freedom.

Family	Species	T-value	p-value	df	Difference
Codiaceae	<i>Codium fragile</i>	-4.45	0.002	9	Canada < Scotland
Chordaceae	<i>Chorda filum</i>	-0.39	0.736	2	None
Fucaceae	<i>Ascophyllum nodosm</i> / <i>Fucus serratus</i>	-5.97	0.027	2	Canada < Scotland
Laminariaceae	<i>Laminaria digitata</i>	-2.39	0.062	5	None
Laminariaceae	<i>Saccharina latissima</i>	0.75	0.464	16	None
Haplidiaceae	<i>Lithothamnion glaciale</i>	6.26	0.001	6	Canada > Scotland

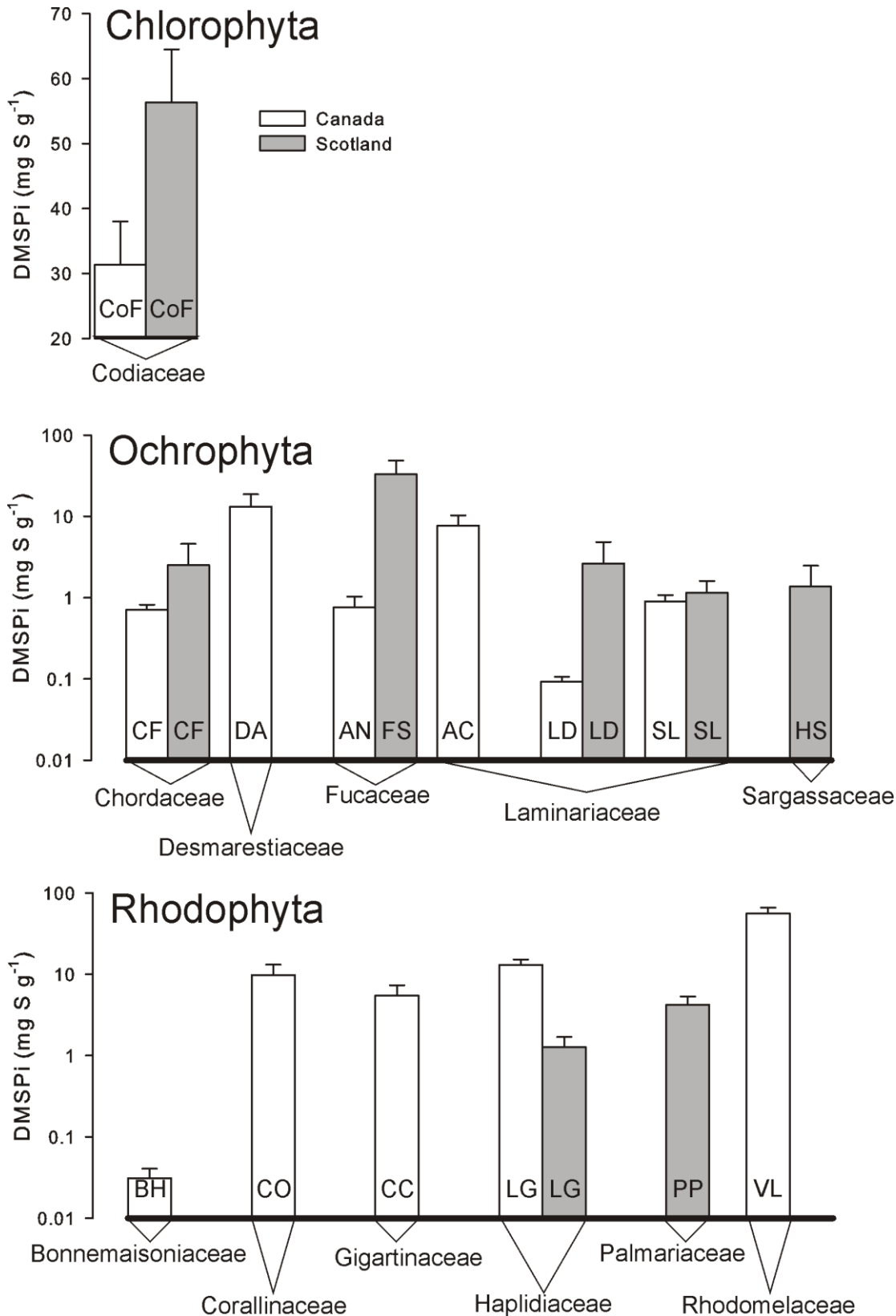


Figure 4.12 Transatlantic comparison of DMSPI in macroalgae. Samples taken from Nova Scotia, Canada and Loch Sween, Scotland in September 2010. Macroalgae arranged by Phylum and sub-divided by family: *Codium fragile* (CoF), *Chorda filum* (CF), *Desmarestia aculeate* (DA), *Ascophyllum nodosm* (AN), *Fucus serratus* (FS), *Agarum cribrosum* (AC), *Laminaria digitata* (LD), *Saccharina latissima* (SL), *Halidris siliquosa* (HS), *Bonnemaisonia hamifera* (BH), *Corallina officinalis* (CO), *Chondrus crispus* (CC), *Lithothamnion glaciale* (LG), *Palmaria palmata* (PP), *Vertebrata lanosa* (PL). Note log scales for Ochrophyta and Rhodophyta. Data presented as mean±SE.

4.9.2 West coast of Scotland

A significant difference between DMSPi in red coralline algae along the west coast of Scotland was observed ($F_5 = 8.05$, $p < 0.001$, Figure 4.13), although this was driven by the very low concentrations in algae from Kentra Bay ($0.02 \pm 0.01 \text{ mg S g}^{-1}$, mean \pm SE). No significant difference was observed between the other five sites.

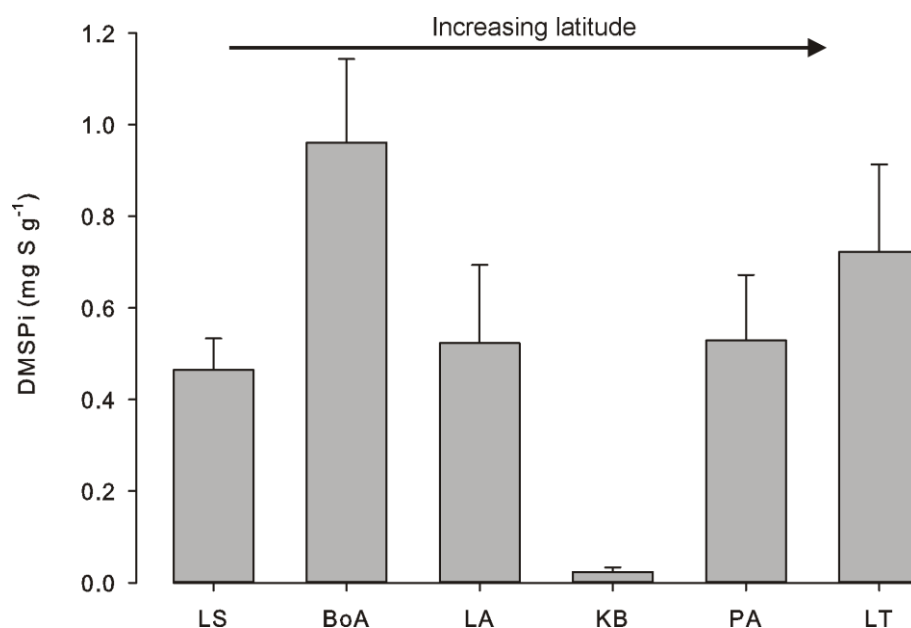


Figure 4.13 DMSPi in red coralline algae from the west coast of Scotland. Sample sites: Loch Sween (LS), Bridge over the Atlantic (BoA), Loch Ailort (LA), Kentra Bay (KB), Plockton Airstrip (PA) and Loch Torridon (LT). Species sampled at each site indicated in the bars: *L. glaciale* (LG), *Phymatolithon calcareum* (PC) or unknown (UN). See Table 4.3 for sampling details. Data presented as a mean \pm SE.

4.10 Results: Local scale

4.10.1 Sinai Peninsula, Egypt

A significant difference between sites on Suleman reef was observed for both DMS/Pd ($F_4 = 13.10$, $p = 0.001$) and DMS/Pp ($F_4 = 28.87$, $p < 0.001$), although they were characterised by reverse trends (Figure 4.14). DMS/Pd significantly decreased from the seagrass ($18.18 \pm 1.74 \text{ nmol L}^{-1}$) to the reef crest ($7.60 \pm 0.93 \text{ nmol L}^{-1}$, mean \pm SE), with a slight increase at the offshore site ($9.94 \pm 1.13 \text{ nmol L}^{-1}$). DMS/Pp was relatively stable from the seagrass to the reef crest ($\sim 4 \text{ nmol L}^{-1}$), increasing at the slope ($7.08 \pm 0.52 \text{ nmol L}^{-1}$) and offshore ($13.95 \pm 2.36 \text{ nmol L}^{-1}$).

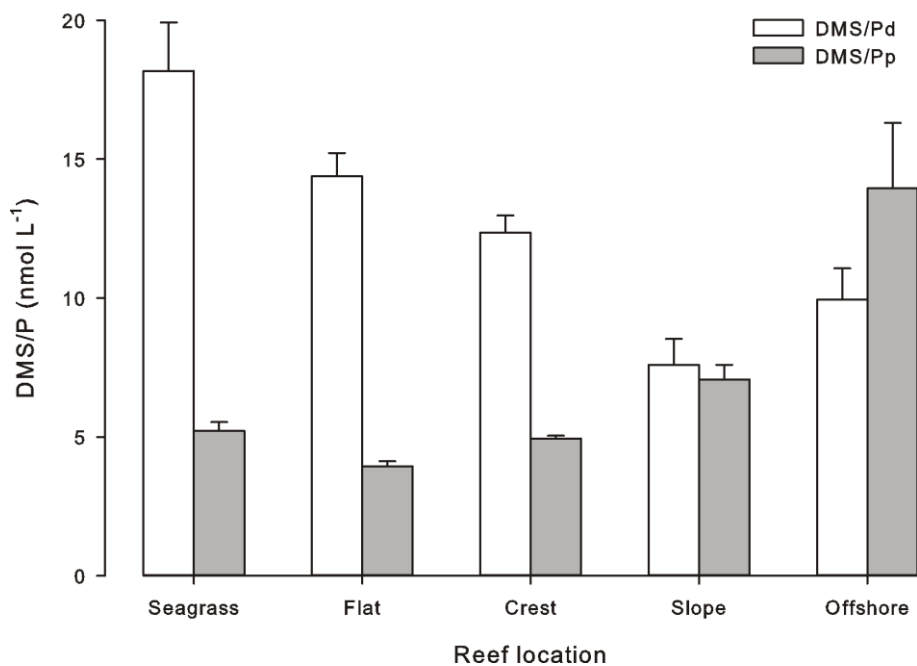


Figure 4.14 DMS/P (nmol L⁻¹) on Suleman reef, Egypt. Dissolved DMS/P (white bars) and particulate DMS/P (grey bars) from the five zones of Suleman reef: seagrass beds nearest the shore, the reef flat, reef crest, reef slope and 270 m offshore. Data presented as mean±SE.

4.10.2 North-west Mediterranean

Along the sand transect, water column DMS/Pd concentrations were highly stratified, with a steady decrease in DMS/Pd concentration with depth (Figure 4.15): >22 nmol L⁻¹ to 17 m depth, decreasing to 15 nmol L⁻¹ at 38 m depth and <5 nmol L⁻¹ at 60+ m depth. There was a slight elevation of DMS/Pd isolines further from the shore, with a peak in DMS/Pd at the surface in 65 m of water (4.3 km offshore).

Along the coralligène transect, there was a steady decline in DMS/Pd concentrations with depth, but the 17.5 nmol L⁻¹ contour shoaled further inshore compared to the sand transect, to ~18 m depth (Figure 4.15). Maximum concentrations were observed at the surface of the 15 m deep station (25 nmol L⁻¹). DMS/Pd isolines remained horizontal throughout the water column (Figure 4.15).

Along the seagrass transect, the water column was more homogenous than the sand or coralligène transects (Figure 4.15), ranging from 11 nmol L⁻¹ at 60+ m to 22 nmol L⁻¹ in the surface waters. Within the seagrass bed (<10 m depth), DMS/Pd concentrations were much lower compared to the sand transect

(<18 nmol L⁻¹ compared to >25 nmol L⁻¹) (Figure 4.15). A 10 m wide tongue of lower concentration water (<18 nmol L⁻¹) protruded offshore at ~15 m depth until total water depth was ~45 m (Figure 4.15), although this interpolation pattern was driven by the mid-depth sampling point at 35 m. DMS/Pd remained ~18 nmol L⁻¹ to ~27 m depth, where an increase to ~21 nmol L⁻¹ was observed. Concentrations at 60+ m depth were higher than the sand and coralligène transects, ~11 nmol L⁻¹ (Figure 4.15).

4.10.3 Western Antarctic Peninsula

There was a significant difference in DMSPi between the three Antarctic species identified ($F_2 = 33.51$, $p < 0.001$), with *Spongites discoidea* (species 1) having significantly less DMSPi than *Clathromorphum obteculum* (species 2) or *Lithothamnion fuegianum* (species 3; average of 2.4, 18.2 and 17.1 mg S g⁻¹ respectively, Figure 4.16). A significant increase in DMSPi was observed following three hours of darkness ($F_2 = 3.51$, $p = 0.035$) in all but one site at South Cove (mid-depth, *C. obteculum*). No significant difference in DMSPi between algae fixed for DMSP *in situ* in Antarctica and algae transported back to the UK was observed (Tukey's pairwise comparison, $p = 1.00$).

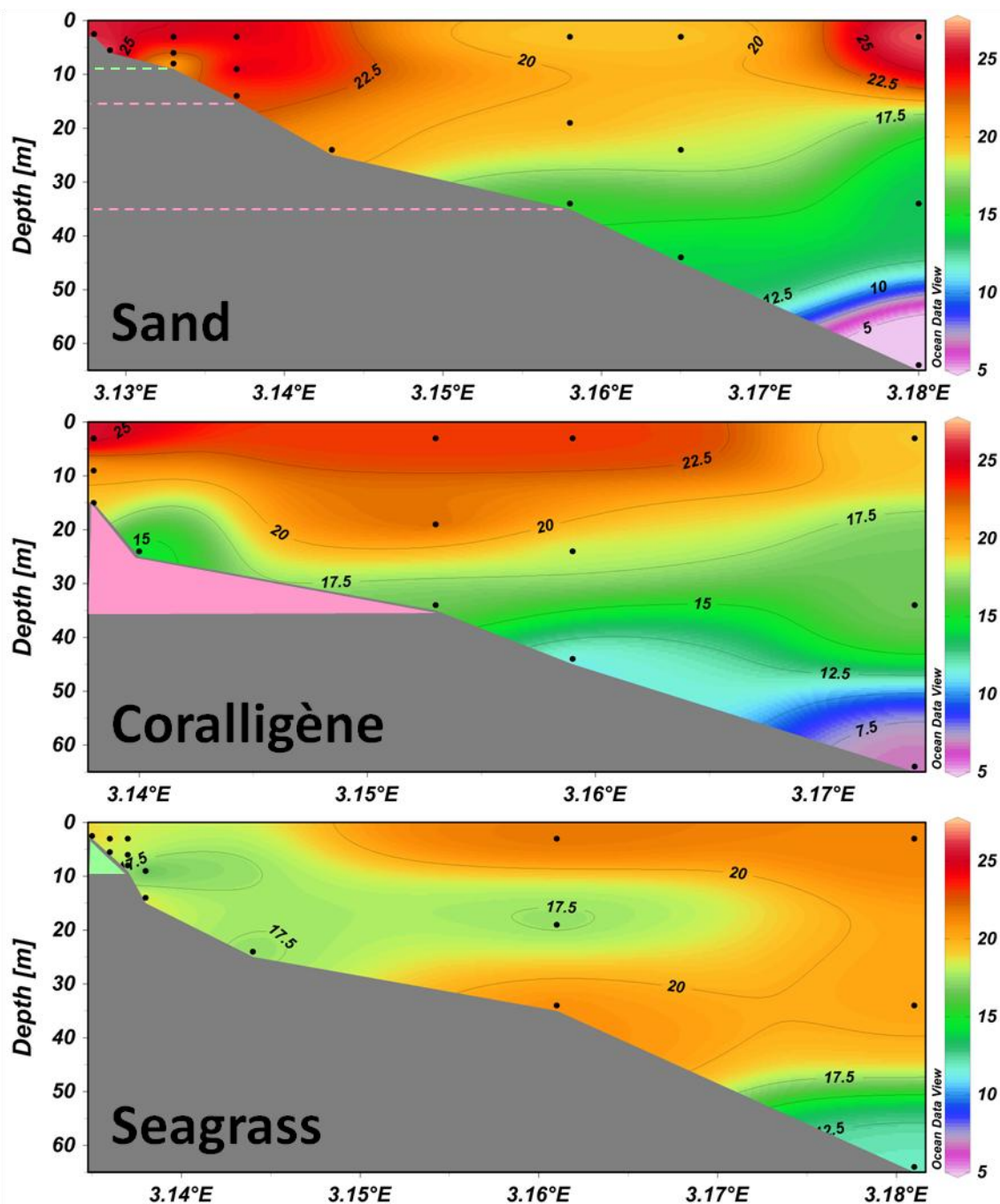


Figure 4.15 DMS/Pd profiles from Banyuls-sur-Mer, France.

Samples taken along three transects: bare sand, coralligène (15 – 35 m, followed by bare sand) and seagrass (0 – 9 m, followed by bare sand). Pink and green substrate shading indicates the extent of coralligène and seagrass respectively. Black dots indicate sampling locations, interpolation was created using VG gridding in Ocean Data View 4, an interpolation technique that utilises a variable resolution rectangular grid and weighted-averaging scheme (Schlitzer, 2011). Pink and green dashed lines on the sand transect are for reference only and correspond to the range of seagrass and coralligène habitat in the other two transects.

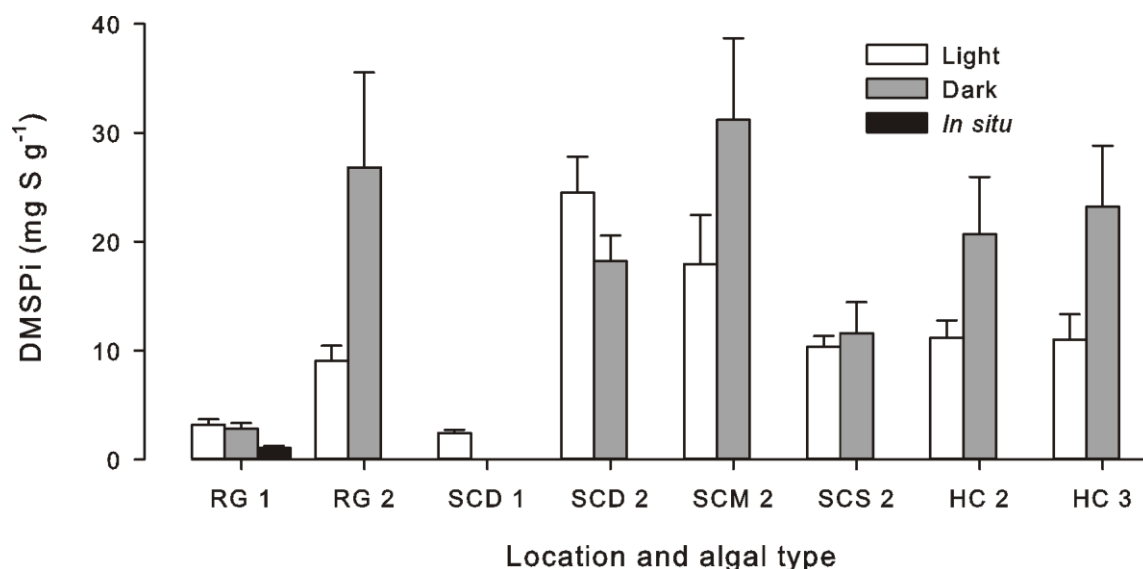


Figure 4.16 DMSPi in red coralline algae from Western Antarctic Peninsula. Samples taken in the light (white bars, after three hours in the dark (grey bars) having been transported back to the UK and *in situ* in Antarctica (black bar). Five sampling sites: Rose Garden (RG), South Cove Deep (SCD), Mid (SCM) and Shallow (SCS) and Hangar Cover (HC). Numbers indicate species: 1 = *Spongites discoidea*, 2 = *Clathromorphum obteculum*, 3 = *Lithothamnion fuegianum*. See Table 4.4 for algal details. Data presented as mean±SE.

4.11 Discussion

The research presented in this chapter compiles a number of algal and water measurements of DMS/P on global, regional and local scales, primarily based around coralline algae and their associated habitats. This is the first detailed spatial analysis of coralline algal DMS/P and provides new information regarding the potential ecosystem function of DMS/P in coralline algal habitats.

4.11.1 Phylum-specific DMSPi concentrations

Based on the transatlantic sampling, it may be suggested that there is a general pattern in DMSPi between the three algal Phyla, whereby Chlorophyta > Ochrophyta (Phaeophyta) > Rhodophyta. This has been previously suggested by Van Alstyne and Puglisi (2007), although their conclusions were based on only a small number of Ochrophyta and Rhodophyta samples. Importantly, large variations in DMSPi was observed within all three Phyla from all sampling locations, a factor which was not reported by Van Alstyne and Puglisi (2007). Unlike previous studies, all species analysed for DMSPi in this research yielded results above the detection limit. This research adds to previous knowledge by including a number of Rhodophyta and Ochrophyta samples for comparison to Chlorophyta. Only one Chlorophyta species (*Codium fragile*) was analysed for

DMSPi in this research, but it is well known that Chlorophyta generally have high DMSPi concentrations (Lyons et al., 2010; Van Alstyne, 2008; Van Alstyne et al., 2007; Van Alstyne and Puglisi, 2007).

4.11.2 Latitudinal trends

Within the transatlantic data set, macroalgal DMSPi was generally the same or higher in Scotland compared to Canada. The Scotland site is north of the Canadian site by 11.5°, supporting the suggestion that DMSPi increases with increasing latitude (Van Alstyne and Puglisi, 2007), although one must also consider the possibility of west / east coast continental and oceanographic influences and the variation in samples at the species level. If DMSP was used as a grazing deterrent by macroalgae (as has been previously suggested, e.g. Van Alstyne and Houser, 2003), it may be expected that DMSPi would be higher in Canada instead of Scotland as grazing pressure at the sampling sites was higher in Canada (and is the subject of investigation in Chapter 8). Environmental seasonality is more pronounced in Canada, with ice cover during the winter, thus it may be expected that Canadian macroalgae would upregulate DMSPi during the winter to allow metabolism to continue even during freezing conditions, as DMSP is known to act as a cryoprotectant (Karsten et al., 1996), perhaps reversing the trend observed during the summer.

When only coralline algae (*L. glaciale*) are considered, DMSPi was higher in Canada compared to Scotland. This followed a general trend that may be observed in the global coralline algal DMSPi data set, although accompanied by higher inter- and intracellular species variability. Only six locations were sampled so caution must be exercised, but DMSPi appears to increase in mid - low latitudes, particularly in the northern hemisphere, backed-up by the correlation trends for temperature and PAR (both were positive correlations). This is the opposite to what has been observed in Chlorophyta (Van Alstyne and Puglisi, 2007). The antioxidant potential of DMSP (Sunda et al., 2002) may be adopted by red coralline algae in low latitudes as these macroalgae may be regularly exposed to light-saturating conditions (see Chapter 3, Burdett et al., 2012b), thus may be more sensitive to light-induced damage compared to other macroalgae. Analysis of coralline algal DMSPi from more locations across a wider range of latitudes would further test this hypothesis.

However, it appears that DMSPi in coralline algae is not differentially regulated across small spatial scales such as the west coast of Scotland or on the WAP. This is in contrast to *Ulva latuca* which may up-regulate DMSPi with increasing latitude over just a 0.6° range (Van Alstyne et al., 2007). The opportunistic nature of *Ulva* spp., and its ability to survive in the intertidal, may necessitate an ability to produce high concentrations of secondary metabolites that may give the algae a competitive advantage over other species.

4.11.3 Diurnal patterns

The species-specific differences in DMSPi in the Antarctic samples suggests that latitude is not the only factor governing DMSPi concentrations in coralline algae, a feature that is to be expected given the large number of proposed cellular functions for DMSP in algae. The observed up-regulation of DMSPi at night in the Antarctic samples may be a circadian rhythm related to reduced water temperature at night and the cryoprotective properties of DMSP in ice algae (Karsten et al., 1996). The presence of a circadian rhythm is backed up by the constant storage conditions (the only parameter to change diurnally was light) and the lack of shipping and storage effects. The speed of DMSPi regulation by the Antarctic coralline algae was relatively fast compared to other regulation studies (see review by Stefels, 2000). This is perhaps because water temperature is always close to freezing so a fast regulatory response is required to maintain metabolism. In contrast, species-specific differences were not observed between *L. glaciale* and *P. calcareum* in Scotland, despite both species being at their respective southerly and northerly distributional limits.

4.11.4 Sources and sinks of coastal DMS/P

This research suggests that benthic biological fronts, such as the distinct substrate changes observed in Egypt and France, may be important in determining local-scale spatial variation in DMS/P concentrations. In Egypt, DMS/Pd at the seabed was elevated in areas dominated by seagrass and macroalgae rather than corals. Tropical corals have been described as one of the primary benthic sources of DMS/P in the coastal zone (Jones et al., 2007; Broadbent and Jones, 2006; Broadbent and Jones, 2004; Broadbent et al., 2002), but this has been based on the Great Barrier Reef, a barrier reef system that is

morphologically and hydrographically different to the fringing Suleman reef studied in this research. On the Suleman reef, seagrass beds and reef flat macroalgae were a more important source of DMS/Pd than corals. The shallow water depth on the reef flat might allow the seagrass and macroalgae to act as significant sources of atmospheric DMS (although this was not measured in the present research).

In contrast to Egypt, coralligène and seagrass beds in France appeared to act as a sink for DMS/Pd, with lower concentrations than corresponding depths on the sand transect. However, transects were conducted following a period of high winds, which may have affected the DMS/Pd concentrations, particularly in shallow waters. Further investigations, perhaps across a seasonal cycle, would elucidate the impact seagrass and coralligène have on DMS/P concentrations in the Mediterranean.

4.11.5 Ecosystem function

There is a growing body of evidence that suggests dimethyl sulphur species are perhaps more important for ecosystem function rather than as a source of atmospheric DMS (Lewis et al., 2011). This is particularly relevant in developed regions where levels of anthropogenically-derived sulphur aerosols may be considerably higher than oceanic DMS emissions (Grübler, 2002; Bates et al., 1992; Brimblecombe et al., 1989). Surface DMS/Pd concentrations remained high in all France transects, despite reduced concentrations at the seabed within the coralligène and seagrass habitats. This suggests that (1) these benthic habitats are not significant sources of atmospheric DMS (but perhaps surface phytoplankton are) and (2) DMS/P is re-circulated within the habitats, perhaps through microbial utilisation of DMS/P as a carbon and / or sulphur source (Pinhassi et al., 2005; Kiene et al., 2000). In areas of low macro-primary productivity (i.e. sand) the DMS/P isolines were horizontal, suggesting that DMS/P was not utilised by organisms within the benthos to the same extent as the biologically diverse coralligène or seagrass habitats.

4.12 Conclusions

Variations in DMS/P concentrations were investigated at global, regional and local spatial scales from a number of different coralline algal habitats including maerl beds, kelp forests, seagrass meadows, coralligène formations, coral reefs and rocky shores. This research built upon previous knowledge of macroalgal DMSPi, confirming that Chlorophyta generally contain more DMSPi than Ochrophyta and Rhodophyta. However, in contrast to other macroalgae, DMSPi in coralline algae may be higher in samples from mid- and low latitudes, although more research is required to confirm this. Species-specific DMSPi concentrations were observed in Antarctica but not in specimens from the west coast of Scotland, perhaps due to the freezing water temperatures experienced in Antarctica and the cryoprotective capacity of DMSP. Transect studies across benthic biological fronts in Egypt and France highlighted how water column DMS/P concentrations may be elevated or reduced in areas dominated by coralline algal habitats, suggesting an important ecosystem role for dimethyl sulphur compounds. Further research might suggest the specific processes involved in regulating intracellular and water column DMS/P in coralline algal habitats and improve our understanding of these complex shallow-water marine ecosystems.

5

Temporal trends in DMSP dynamics

Knowledge of the natural variability in dimethylated sulphur compounds within a habitat is crucial for understanding the factors (abiotic or biotic) that control the production and release of dimethylsulphoniopropionate (DMSP) and dimethylsulphide (DMS), and potential DMS emissions. Acquisition of such knowledge with respect to coralline algal habitats will allow us to (1) make conclusions regarding the importance of these habitats in the marine sulphur cycle and (2) predict the impact of climate change (e.g. global warming) on the biogeochemical cycling of sulphur within this ecosystem.

5.1 Seasonal DMS/P trends: Plankton

Whilst the majority of pelagic-based DMSP and DMS (collectively DMS/P) research has taken place within and during specific phytoplankton blooms, some information regarding longer-term, seasonal changes has been documented.

Strong seasonal cycles in DMSP and DMS have been recorded in the Western English Channel (WEC) (Figure 5.1) (Archer et al., 2009). Here, total dissolved DMSP and particulate DMSP (DMSP_d+DMSP_p, DMSP_t) patterns were characterised by a winter minimum ($\sim 3 \text{ nmol L}^{-1}$), a gradual increase from March, to a maximum in August (127 nmol L^{-1}). A rapid decline in concentrations was observed in September as water column stratification broke down. In contrast, DMS concentrations were characterised by two distinct peaks in April and June (up to 23 nmol L^{-1}). Thus, in the WEC, a decoupling between DMSP and DMS occurs (Figure 5.1), attributed to the 'taxonomic succession of eukaryotic

phytoplankton', with dinoflagellates playing a significant role in DMSP production during the summer months (Archer et al., 2009). DMSP/DMS decoupling has also been observed in the oligotrophic Sargasso Sea at the Bermuda Atlantic Time Series (BATS) station (Dacey et al. 1998, Lefèvre et al. 2002). At the BATS site (31° 40'N, 64° 10'W), the availability of photosynthetically active radiation (PAR) appears to be more important for driving DMS/P dynamics than in the WEC - water temperature is critical in the WEC (Toole & Siegel 2004, Vallina & Simó 2007).

In areas where seasonal water column stratification does not occur (e.g. due to tidal mixing), a strong relationship between DMSP and DMS may be found, such as the St Lawrence Estuary (SLE), eastern Canada (Michaud et al., 2007). Summer concentrations of DMSPt and DMS in SLE were 365 nmol L⁻¹ and 14 nmol L⁻¹ respectively, attained when water temperatures were greater than 10°C (Michaud et al., 2007). Average concentrations from May to October were 72 nmol L⁻¹ (DMSPt) and 3.2 nmol L⁻¹ (DMS) (Michaud et al., 2007). These concentrations are similar to other coastal regions including the Baltic Sea (Leck et al., 1990) and around the British Isles (Turner et al., 1988). In the southern North Sea, peak DMS concentrations were recorded in May (25 nM) (Turner et al.). This, however, was not coincident with the peak DMS air-sea flux which was observed in June (16.4 μM m⁻² day⁻¹) when wind speeds were higher (5.9 m s⁻¹ in June compared to 3.7 m s⁻¹ in May)(Turner et al., 1996).

In the northwest Mediterranean Sea, where the annual range in water temperature is >20°C, a strong seasonal cycle in DMS/P has been observed (Vila-Costa et al., 2008), although concentrations appear to be lower than in temperate seas. Summer peaks in DMSd ranged from 10 - 20 nmol L⁻¹, whilst peaks in DMSPt (up to 80 nmol L⁻¹) occurred a few weeks after peaks in chlorophyll-*a* (February and December 2003 and March 2004) (Vila-Costa et al., 2008). Minimum DMSPt concentrations (<10 nmol L⁻¹) occurred in autumn (Vila-Costa et al., 2008).

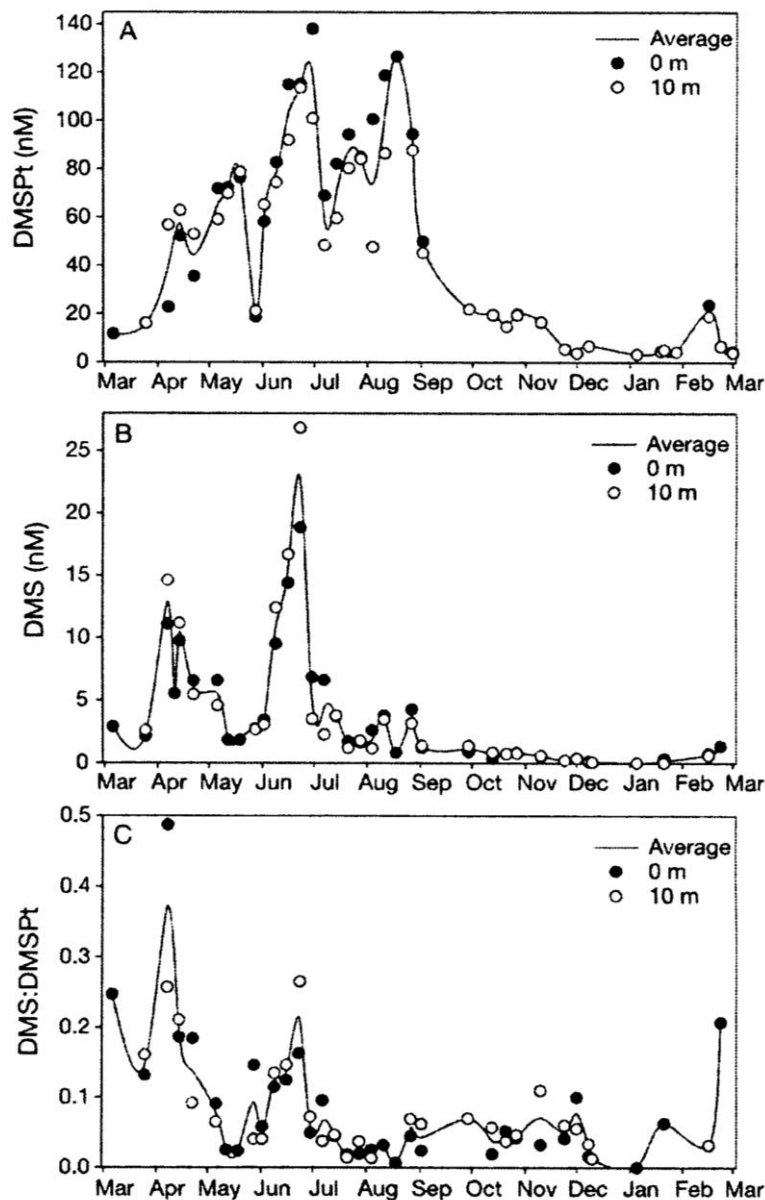


Figure 5.1 Seasonal variation in DMS/P in the Western English Channel.

(A) Total dissolved+particulate DMS (DMSPt), (B) dissolved DMS in the upper 10 m of the water column and (C) the DMS/DMSPt ratio. Measurements were taken at 10 m depth and the surface, the line is the average of these measurements. Source: Archer et al. (2009).

In India, where the climate is differentiated by wet and dry seasons only, peak DMS/P production is observed during the monsoon season (June - September) (Kumar et al., 2009). DMS/P concentrations are low pre-monsoon, increase during the monsoon season and remain high throughout the post-monsoon season (October - December) (Kumar et al., 2009). Peak surface DMS concentration during monsoon season were 12.8 nmol L^{-1} in July 2000, although DMS flux did not exhibit a seasonal pattern (Shenoy and Patil, 2003). Peak DMSPt was $419.5 \text{ nmol L}^{-1}$ in July, coinciding with a mixed dinoflagellate / diatom bloom (Shenoy and Patil, 2003).

On a global scale, attempts have been made to model observed open ocean DMS/P concentrations and DMS emission fluxes (e.g. Lana et al.; Vogt et al., 2010; Korhonen et al., 2008; Kloster et al., 2006). In high latitudes ($>40^\circ$), a single peak in DMS/P concentrations is observed in the summer, coinciding with a peak in chlorophyll (Figure 5.2). However, at lower latitudes, where chlorophyll remains constant (but low) throughout the year, a double peak in DMS/P is evident (Figure 5.2)(Vogt et al., 2010). This is known as the ‘DMS summer paradox’ and highlights the two DMS/P production regimes present in the open ocean - the bloom-forced high latitudes and the stress-forced (primarily as a result of high irradiance and DMS exudation) low latitudes (Vogt et al., 2010; Toole and Siegel, 2004). In the biologically productive upwelling regions, DMS/P production may be relatively high throughout the year (Kloster et al., 2006). In the Southern Ocean, high DMS production and air-sea flux in the summer causes the amount of cloud condensation nuclei in the atmosphere to increase two or three times compared to the winter (Korhonen et al., 2008).

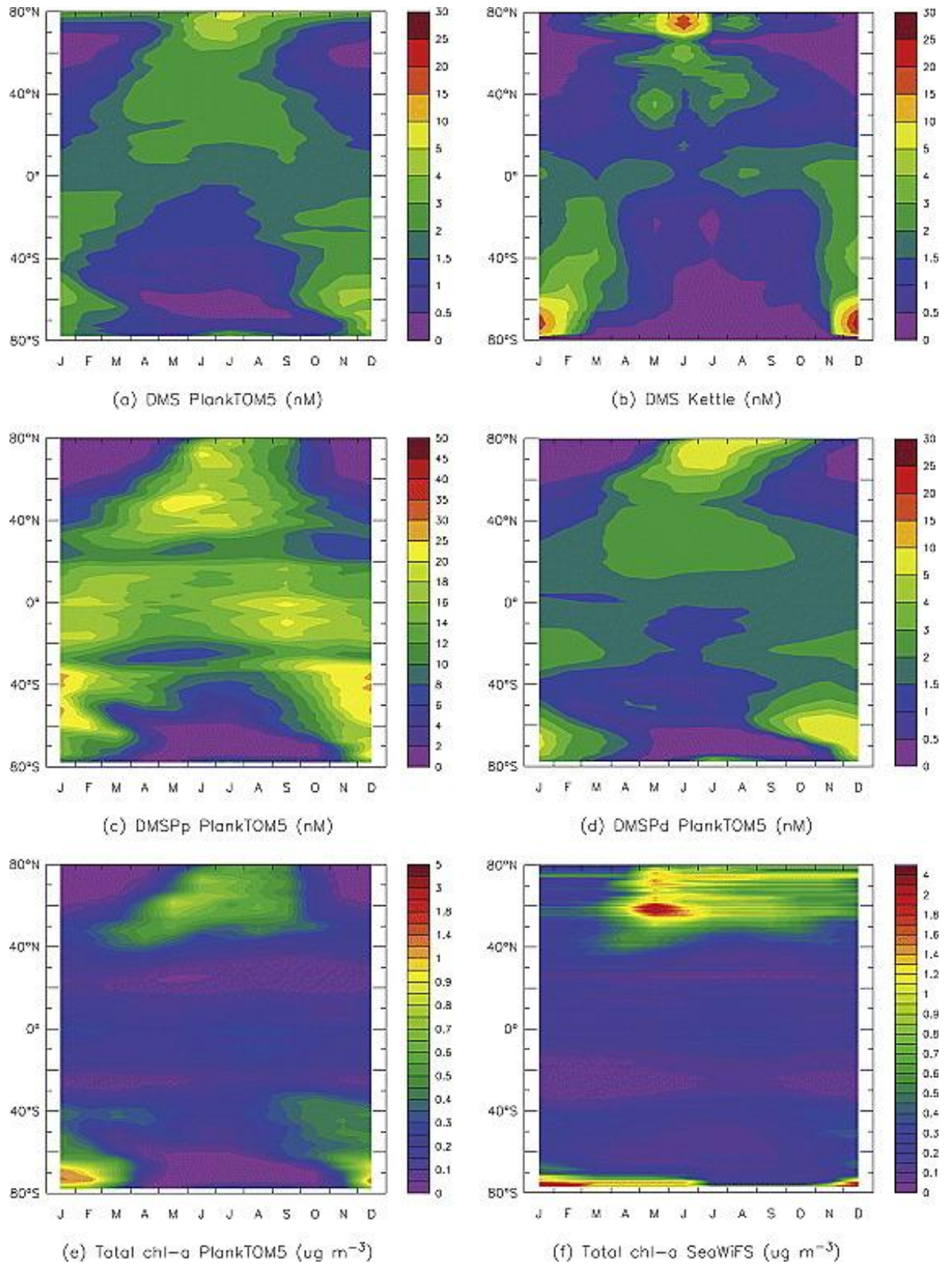


Figure 5.2 Modelled global DMS, DMSPp and DMSPd across an annual cycle. Modelled (a) DMS, (c) DMSPp, (d) DMSPd, and (e) chlorophyll from DMS-PlankTOM (SEP) and compared to interpolated (b) DMS (from Kettle and Andreae, 2000) and (f) Chl-a from SeaWiFS. Note the double DMS and DMSP maxima between 40°N and 40°S, despite the year-round low Chl-a concentrations. Source: Vogt et al. (2010).

5.2 Seasonal DMS/P trends: Benthic primary producers

Knowledge of seasonal trends in benthic primary producers (i.e. macroalgae and corals) is extremely limited, highlighting the need for further research to better understand the natural variability of DMSP dynamics in the coastal zone.

The invasive macroalga *Codium fragile* exhibits a strong seasonal trend in intracellular DMSP (DMSPi) concentrations in Nova Scotia, Canada (Lyons et al., 2010; Lyons et al., 2007). Maximum DMSPi concentrations are observed in late winter and early spring - attributed to the cryoprotective properties of DMSP and reduced DMSP-lyase activity (water temperatures around the coast of Nova Scotia can drop below 0°C in winter) (Lyons et al., 2010; Lyons et al., 2007). A 1°C rise in water temperature causes a 0.09% decline in intracellular DMSP concentration, resulting in an autumn minima, with concentrations half that observed in late winter (Lyons et al., 2010). Peak concentrations of dimethylated sulphur compounds (DMS, DMSP and dimethylsulphoxide, DMSO) on the Great Barrier Reef are observed in the summer months, but the relative contributions from phytoplankton, corals and macroalgae are currently unclear (Broadbent and Jones, 2006).

5.3 Aims of this chapter

Our understanding of the natural variability in DMS/P production by benthic habitats is limited to a few studies on coral reefs and fleshy macroalgae. DMS/P concentrations in coralline algae beds, despite their worldwide distribution and high intracellular DMSP concentrations (Kamenos et al., 2008b), has not yet been studied across a temporal scale. The aim of this chapter was to quantify the natural variability of DMS/P production by a coralline algal habitat on the west coast of Scotland. Specifically, this chapter assessed:

1. The seasonal production of DMSPi by free-living red coralline algae.
2. The seasonal production of dissolved and particulate DMS/P (DMSd, DMSPd, DMSPp) in the water column overlying the coralline algal bed and potential flux of DMS to the atmosphere.

3. The relationships between DMSPi, DMSd, DMSPd and DMSPp to abiotic variables including water temperature, cloud cover and daylength.

The growth of coralline algae is known to be extremely sensitive to water temperature (e.g. Kamenos and Law, 2010) and light (Burdett et al., 2011), and coralline algal DMSPi is reduced under high light (Rix et al., 2012). Thus, it was hypothesised that water column DMS/P and coralline algal DMSPi concentrations would be highest in the summer and that water temperature and light availability would be the primary driving factors. Additionally, it was hypothesised that the coralline algal habitat would influence the DMS/P concentration of the overlying water column.

5.4 Methods

5.4.1 Study site and sample collection

The study site was a coralline algal aggregation (a maerl bed) in Loch Sween, on the west coast of Scotland (56° 01.99'N, 05° 36.13'W). All samples were collected at slack tide using SCUBA at two to three monthly intervals from March 2010 to February 2012 (average time between sampling was 10 weeks). Sample collections were taken at irregular intervals to avoid inadvertently following algal circadian rhythms. In Loch Sween, the maerl bed lies in the centre of an 80 m wide channel. Tidal currents are strongest in the centre of the channel, minimising sedimentation over the maerl bed. Water samples were taken from four locations within the loch (Figure 5.3):

1. At the sea floor, at the maerl bed (MB), depth: 6 m.
2. Mid-water above the maerl bed (AB) , depth: 3 m.
3. At the sea floor, to the bed side (sand / gravel bottom) (BS), depth: 6 m.
4. Mid-water above the bed side (ABS) , depth: 3 m.

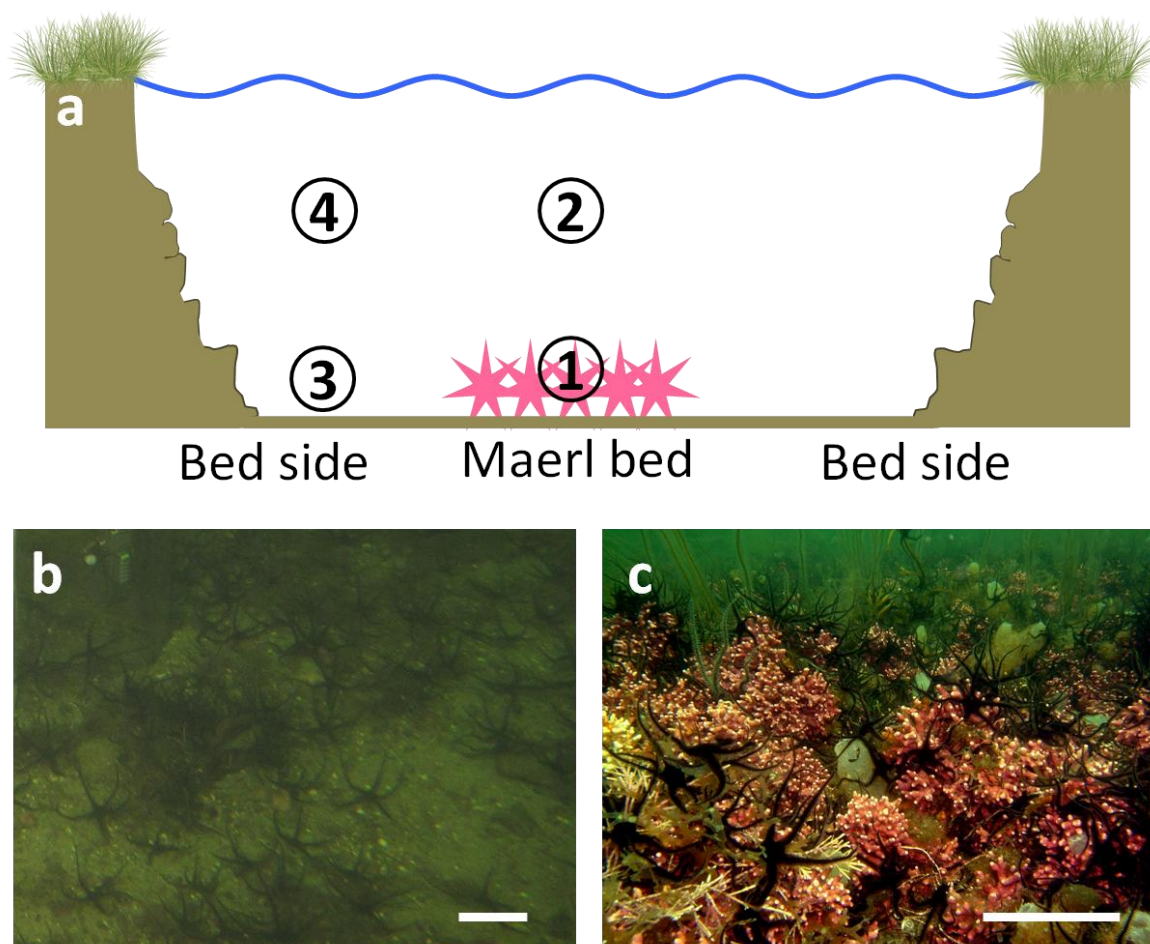


Figure 5.3 Sampling locations in Loch Sween, west coast of Scotland. (a) Diagrammatic cross-section of Loch Sween and the locations of the four water sampling sites (not to scale) – 1: Maerl Bed, 2: Above Maerl Bed, 3: Bed Side, 4: Above Bed Side, (b) photo of the bed side, (c) photo of the maerl bed. Scale bar = 80 mm. Photos: N. Kamenos.

Water samples ($n = 5$) from each location were taken for dissolved DMS (DMSd), dissolved DMSP (DMSPd) and particulate DMSP (DMSPp) determination, according to the methodologies described in Chapter 2. In addition, DMSPi of the dominant maerl-forming species in Loch Sween, *Lithothamnion glaciale*, was determined by collecting coralline algal samples ($n = 20$) from the maerl bed at each sampling timepoint. From March 2010 to March 2011, algal branches were patted dry before being fixed for DMS/P, but excess debris was not actively removed. From May 2011 to February 2012, two sets of samples were analysed: those treated as before (not cleaned) and those which were gently cleaned with a toothbrush prior to fixing to remove heavy fouling and excess detritus. This allowed the DMSP content of the fouling / detritus to also be determined. The full sampling regime is presented in Table 5.1.

Table 5.1 DMS/P sampling regime in Loch Sween, Mar 2010 – Feb 2012.

Samples were collected during 11 sampling campaigns from March 2010 to February 2012.

✓ indicates a complete sampling collection: intracellular DMSP (cleaned and not-cleaned) and water samples (dissolved DMS, DMSd, dissolved DMSP, DMSPd and particulate DMSP, DMSPp). On the first two sampling campaigns DMSPd and DMSd were not differentiated (total DMSPd+DMSd, DMS/Pd). NC = not cleaned.

Sampling Date	Intracellular DMSP	Water column sampling			
		Maerl Bed	Above Bed	Bed Side	Above Bed Side
10 Mar 2010	NC only	DMS/Pd+p only	DMS/Pd+p only	DMS/Pd+p only	DMS/Pd+p only
27 Apr 2010	NC only	DMS/Pd+p only	DMS/Pd+p only	DMS/Pd+p only	DMS/Pd+p only
28 Jul 2010	NC only	✓	✓	✓	✓
20 Sep 2010	NC only	✓	✓	✓	✓
9 Nov 2010	NC only	✓	✓	✓	✓
25 Jan 2011	NC only	✓	✓	✓	✓
9 Mar 2011	NC only	✓	✓	✓	None
27 May 2011	✓	✓	✓	✓	✓
30 Aug 2011	✓	✓	✓	✓	✓
30 Nov 2011	✓	No DMSPp	No DMSPp	No DMSPp	No DMSPp
7 Feb 2012	✓	✓	✓	✓	✓

5.4.2 Abiotic variables

Free-living red coralline algae are known to be highly sensitive to changes in water temperature (Kamenos, 2010; Kamenos and Law, 2010; Kamenos et al., 2008a) and light availability (Rix et al., 2012) and cloud cover (Burdett et al., 2011). Thus, to examine the drivers behind any observed patterns in DMS/P within the coralline algal habitat, the following abiotic parameters were considered:

1. *In situ* water temperature (T, °C) at the maerl bed was logged hourly throughout the sampling period using Gemini TinyTag TGI-3080 data loggers. For statistical modelling, the mean temperature from the week prior to sampling was used.
2. Cloud cover (CC, oktas) for the area was obtained from the ICOADS database as a monthly average, at a 1° x 1° spatial resolution (Woodruff et al., 2011). The ICOADS dataset is a compilation of surface observational records from ships, buoys and other platforms. For statistical modelling, the mean cloud cover in the month prior to sampling was used.

3. **Daylength (DL, hours)** was taken as the time between sunrise and sunset in Glasgow, UK. Data was obtained from the *Astronomical Almanac*, published annually by the UK Hydrographic Office and the United States Naval Observatory. For statistical analysis, the daylength on the day of sampling was used.

5.4.3 Statistical analyses

Generalised Additive Models (GAMs) were used to assess which abiotic factor(s) drove the annual patterns of DMS/P within the maerl bed system at Loch Sween. GAMs are generalised linear models where the linear predictor is dependent on numerous smooth functions. The exact parametric form of the smoothing functions is unknown. Thus, a number of linear regressions are incorporated into one additive model, making GAMs highly flexible. Such flexibility is particularly useful when dealing with non-linear relationships, high variance or a large number of independent variables (Wood, 2003).

DMSPi, DMSd, DMSPd and DMSPp concentrations (all \log_{10} transformed) were modelled against the abiotic variables T, CC and DL. All analyses were conducted in R V2.14.2 using the following steps (annotated R code may be found in Appendix A):

1. Cross-correlations between the mean of each measurement group (DMSd, DMSPd and DMSPp at each loch location and DMSPi, at each timepoint) against all abiotic variables to identify any significant (95%) correlations using the `ccf` function. Where a lagged correlation was identified, only positive lags were considered as negative lags are not ecologically relevant (abiotic factors cannot affect DMS/P concentrations that have already occurred). This also allowed any autocorrelation in the dataset to be identified. No autocorrelation was observed in any dataset (DMS/P or abiotic variables), perhaps due to the time between each sampling timepoint (between 8 and 12 weeks).
2. Ensure the (lagged) DMS/P measurements (using individual replicates) responded to abiotic variables independently from one

another using the `coplot` function. No interactions were identified.

3. Perform GAMs of all measurements (\log_{10} transformed) against all combinations of abiotic variables (including interactions where identified) using the `gam` function in the `mgcv` package (Family: Gaussian, link function: identity).
4. Use `gam.check` and `summary()` to retrieve the model diagnostics and model data.
5. Compare the models (95% significance) from each measurement set using the `anova()` function. Where two or more models had the same `anova` result, the model with the lowest Generalised Cross Validation (GCV) score and highest percentage deviance explained was chosen as the most parsimonious (Wood, 2006).

All GAMs were based on a Gaussian distribution for fitting, using a thin-plate regression spline (TPRS) basis as the smoothing function. In TPRS, the ‘wiggly’ components of the full thin-plate spline are optimally truncated whilst components with ‘zero wiggleness’ are left unchanged (Wood, 2003). This makes TPRS computationally expensive compared to other GAM bases such as cubic splines or p-splines, but TPRS do allow multiple predictor variables to be considered and have reduced subjectivity as knot locations (i.e. where the splines join) are not manually specified (Wood, 2003).

The GCV score is the weighted mean of the square of the error in predicting a value at n by fitting the model to all points prior to n (Wood, 2006). The GCV score is increased when the model order is (1) too low so the model does not fit the data well or (2) too high so data noise is fitted.

5.5 Results

5.5.1 Abiotic parameters

Water temperature was characterised by a strong seasonal pattern (Figure 5.4a). The warmest water temperatures were in July 2010 (17.3°C), whilst the

coldest water temperature was in January 2011 (3.5°C). The winters of 2009/10 and 2010/11 were particularly cold across the whole of the UK; the winter of 2011/12 was much warmer. CC was variable throughout the sampling period, ranging from one to eight oktas (Figure 5.4b). As with water temperature, DL was characterised by a strong seasonal pattern, ranging from 6.9 hours in mid-December, to 17.5 hours in mid-June (Figure 5.4c).

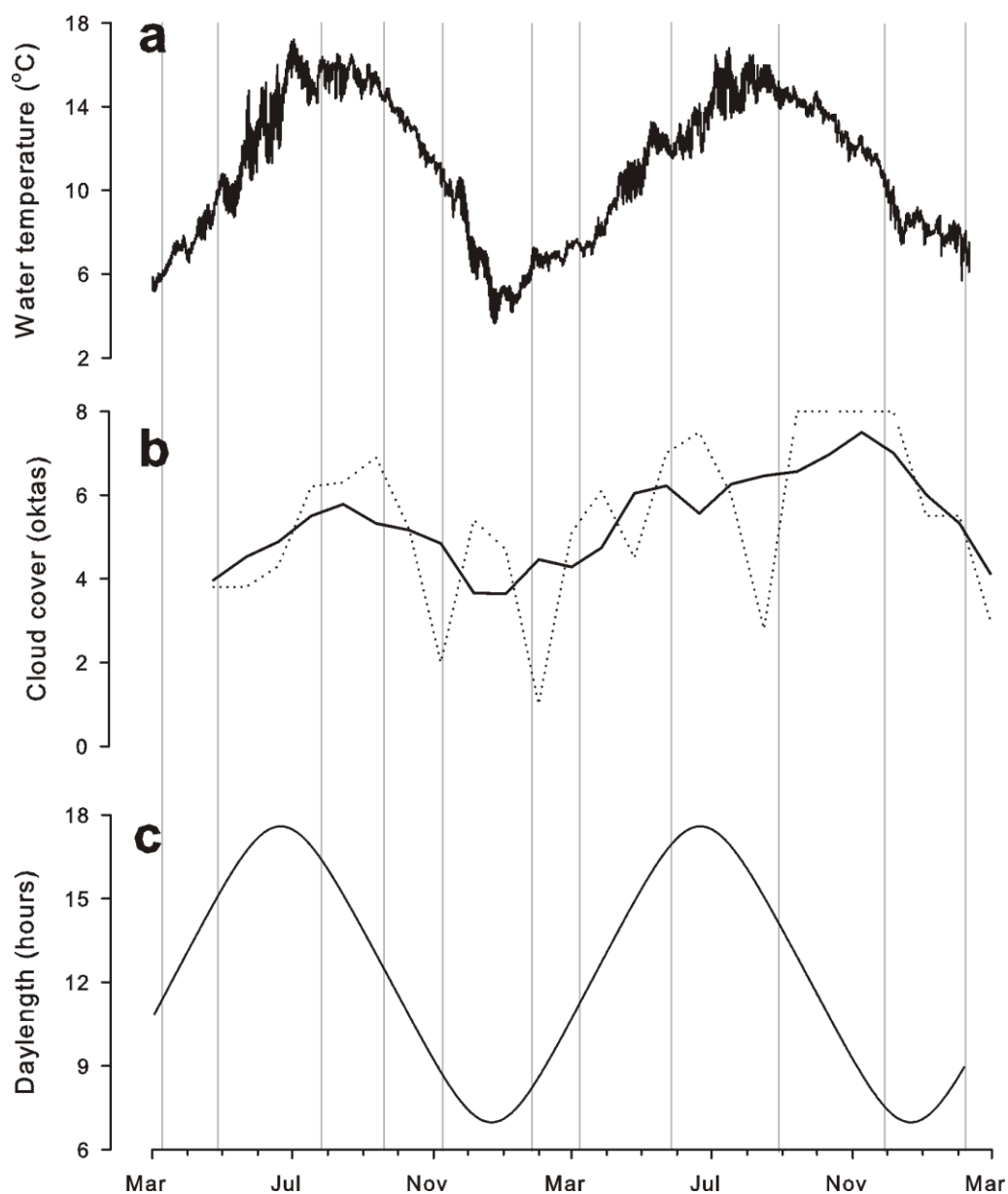


Figure 5.4 Abiotic variables in Loch Sween, March 2010 – March 2012.

(a) hourly water temperature ($^{\circ}\text{C}$) from data loggers at the maerl bed, (b) cloud cover (oktas) presented as a monthly average from the ICOADS database (dotted line) and a 5-month moving average (black line) and (c) daylength from the Astronomical Almanac (hours). Grey vertical lines indicate when water and algal sampling was undertaken (11 sampling points over a 24 month period).

5.5.2 DMS/P measurements

DMS_P was generally $<0.5 \text{ mg S g}^{-1}$ throughout the year (Figure 5.5b). The exceptions were small peaks in April 2010 (0.60 mg S g^{-1}) and May 2011 (0.79 mg S g^{-1}) and a larger peak in September 2010 (1.64 mg S g^{-1} , Figure 5.5b).

DMS_d concentrations were characterised by a maximum in July 2010 (up to 51 nmol L^{-1} at the MB site), followed by a decline to a minimum in winter of 1 – 2 nmol L^{-1} (Figure 5.5c). The autumnal decrease in **DMS_d** was rapid at the MB site (the concentration of **DMS_d** was 2.5 nmol L^{-1} by September 2010), whilst the

AB site had a slower decline, not reaching a minimum until January 2011. In 2011, summer peaks were less well-defined, with concentrations generally <5 nmol L^{-1} (Figure 5.5c). Peaks in DMSd were observed at the ABS site in May 2011 (24.9 nmol L^{-1} , although this was characterised by a high variability) and August 2011 at the AB site (10.4 nmol L^{-1}). In general, the AB site had the highest DMSd concentrations (overall average = 15.4 nmol L^{-1}), whilst the other three sites were similar (overall average ~ 10 nmol L^{-1}).

DMSPd concentrations were characterised by peaks in July - September 2010 and August 2011 (Figure 5.5d). At the MB site, DMSPd concentrations peaked in July 2010 (97.7 nmol L^{-1}), followed by a rapid decline to 3.5 nmol L^{-1} in September 2010. The AB site also peaked in July 2010 (66.4 nmol L^{-1}), but, as with DMSd, was characterised by a gentle decline to a minimum in January 2011 (9.6 nmol L^{-1}). The BS and ABS sites peaked later, in September 2010 (64.6 nmol L^{-1} and 61.4 nmol L^{-1} respectively), followed by a decline to <7 nmol L^{-1} by January 2011. From November 2010 - January 2011, DMSPd concentrations at the MB site were higher than at the other three sites (>16 nmol L^{-1} compared to <10 nmol L^{-1}). A peak in DMSPd was observed in August 2011 at the AB site (58.7 nmol L^{-1}); the summer peak in DMSPd was not as distinct at the MB, BS and ABS sites (all <32 nmol L^{-1}). In general, DMSPd concentrations were slightly lower at the BS site (overall average = 18.0 nmol L^{-1}) compared to the MB, AB and ABS sites (overall average = $21 - 22$ nmol L^{-1}).

DMSPp concentrations followed a similar pattern to DMSPd, but with more pronounced summer peaks (Figure 5.5e). As with DMSPd, maximum DMSPp concentrations at the MB and AB sites were in July 2010 (232 and 111 nmol L^{-1} respectively). Maximum DMSPp concentrations at the BS and ABS sites were observed as a plateau from July - September 2010 (110 and 130 nmol L^{-1} respectively). DMSPp concentrations at the MB rapidly decreased to a minimum in September 2010, rising slightly to $20 - 40$ nmol L^{-1} throughout the winter (Figure 5.5e). DMSPp at the other sites were lower during the winter at ~ 10 nmol L^{-1} . A steady increase in DMSPp was observed at all sites from March 2011, to a maximum in August 2011. The AB site was highest (198 nmol L^{-1}), whilst the other sites were lower (~ 110 nmol L^{-1}). The BS site had the lowest overall average (46 nmol L^{-1}), followed by AB (52 nmol L^{-1}), MB (55 nmol L^{-1}) and ABS (61 nmol L^{-1}).

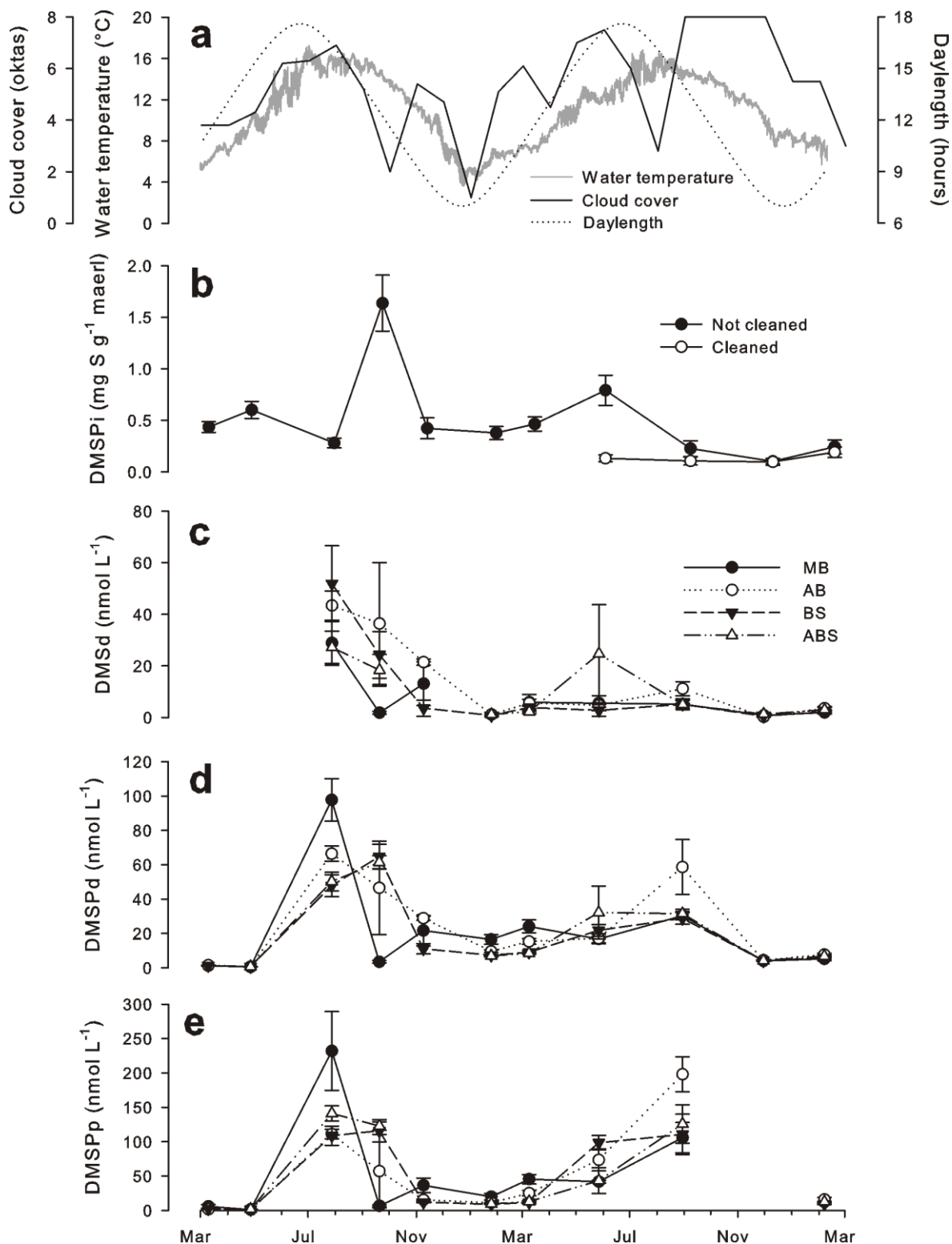


Figure 5.5 DMS/P measurements in Loch Sween.

Measurements taken from March 2010 to February 2012. (a) Abiotic variables from Figure 5.4 for reference: water temperature ($^{\circ}\text{C}$, grey line), cloud cover (oktas, black line) and daylength (hours (dotted line), (b) intracellular DMSP (DMSPi) of *Lithothamnion glaciale*, not cleaned (black circles) and gently cleaned to remove detritus (open circles), (c) dissolved DMS (DMSd), (d) dissolved DMSP (DMSPd) and (e) particulate DMSP (DMSPP) from four locations within Loch Sween: at the maerl bed (MB, black circles), above the maerl bed (AB, open circles), at the bed side (BS, black triangles) and above the bed side (ABS, open triangles). DMS/P data presented as mean \pm SE.

5.5.3 GAM modelling

GAM modelling was used to evaluate the relationships between T, CC and DL and DMS/P concentrations. The majority of the most parsimonious models included T and CC as explanatory variables; only DMSPi and BS DMSd used DL as the sole explanatory variable (Table 5.2). MB and BS DMSPd and DMSPp were modelled well using T and CC, all had >93% of their deviance explained. BS DMSPp required only T for 97.4% of the deviance to be explained. T and CC also fitted to AB and ABS DMSPd and DMSPp well, with 83 - 89% of their deviance explained by the two variables. DMSd was not so well-described by T, CC or DL, with 47 - 70% of the deviance explained, the most parsimonious models used CC only (except BS DMSd which used only DL). T was not included in any of the DMSd models. The most parsimonious model for DMSPi used DL with a lag of one timepoint (10 weeks), but this still only described 42.5% of the deviance. The other models in Table 5.2 had no lagging associated with them. None of the most parsimonious models required interaction terms between the abiotic variables.

Table 5.2 Most parsimonious GAM models from the mgcv package in R. Modelled measurements include maerl intracellular DMSP (DMSPi) and water samples from four locations in Loch Sween: at the maerl bed, above the maerl bed, at the bed side and above the bed side, split into dissolved DMS (DMSd), dissolved DMSP (DMSPd) and particulate DMSP (DMSPp). GAMs were constructed using the abiotic variables water temperature (T), cloud cover (CC) and daylength (DL). DL+1 indicates a one timepoint lag in daylength correlation (equivalent to a 10 week lag). A gaussian fit was assumed throughout, with a thin-plate regression spline fitted to each parameter. Estimated degrees of freedom (Est. df), GCV score, adjusted R^2 , % deviance explained (Dev. exp.) and the number of observations (n) are presented in the table. Models were run for all measurements with all abiotic variables; only the most parsimonious model for each DMS/P measurement is presented.

Location	GAM formula	Est. df	GCV score	Adj. R^2	Dev. exp. (%)	n
Maerl	DMSPi ~ s(DL+1)	8.97	0.179	0.403	42.5	217
Maerl Bed	DMSd ~ s(CC)	9.46	0.251	0.604	68.6	42
	DMSPd ~ s(T) + s(CC)	10.92	0.031	0.942	95.3	52
	DMSPp ~ s(T) + s(CC)	10.92	0.053	0.913	93.1	47
Above Maerl Bed	DMSd ~ s(CC)	9.77	0.224	0.617	70.1	41
	DMSPd ~ s(T) + s(CC)	8.79	0.097	0.802	83.0	56
Bed Side	DMSPp ~ s(T) + s(CC)	10.39	0.103	0.861	88.9	49
	DMSd ~ s(DL)	7.90	0.274	0.588	66.7	37
Above Bed Side	DMSPd ~ s(T) + s(CC)	10.55	0.017	0.966	97.2	53
	DMSPp ~ s(T)	9.84	0.020	0.968	97.4	50
	DMSd ~ s(CC)	9.77	0.224	0.617	70.1	41
	DMSPd ~ s(T) + s(CC)	8.79	0.097	0.802	83.0	56
	DMSPp ~ s(T) + s(CC)	10.39	0.103	0.861	88.9	49

5.6 Discussion

DMS/P concentrations at a maerl bed in Loch Sween were quantified over a 24-month period at the sea bed and mid-water, at the maerl bed and over a gravel substrate to the side of the bed. This research has provided valuable information on (1) the seasonal concentrations of water column DMS/P and coralline algal DMSPi within this habitat, (2) which abiotic factors drove the observed DMS/P patterns and (3) the influence the maerl bed has on the water column DMS/P concentrations within Loch Sween.

5.6.1 Seasonal cycle of DMS/P concentrations

As has been observed in other regions around the British Isles and further afield, a clear seasonal cycle in DMSPd and DMSPp was observed in Loch Sween, with maximum concentrations in the late summer, and minimum concentrations in the winter. DMSd concentrations observed in Loch Sween were very high (up to 60 nmol L^{-1}) in the summer of 2010 compared to other studies from shelf-seas, including the SLE (around 15 nmol L^{-1} , Michaud et al., 2007; Leck et al., 1990; Turner et al., 1988) and the open ocean (up to 23 nmol L^{-1} , Archer et al., 2009). DMSd concentrations in Loch Sween in the summer of 2011 were lower than 2010, but still comparable to previous studies. DMSPd and DMSPp were comparable to Loch Creran (Hatton and Wilson, 2007), another Scottish sea loch 60 km north of Loch Sween, and the St Lawrence Estuary in Canada (Michaud et al., 2007), but higher than the western English Channel (Archer et al., 2009). These results highlight how important the coastal ocean may be for the marine sulphur cycle and the global sulphur budget, and how variable DMS/P concentrations can be on an annual timescale.

In the open ocean, phytoplankton blooms (which are the primary source of DMS/P) occur in the spring due to increased light and water column stratification and in the autumn due to increased vertical mixing (Findlay et al., 2006). This research suggests that spring blooms may not be important for DMS/P concentrations within Loch Sween - peaks in DMS/P were only observed in August and September. In contrast, two peaks in DMSPd concentrations were observed in Loch Creran in 1999 (Hatton and Wilson, 2007), attributed to spring and autumn phytoplankton blooms. A combination of increased land run-off

(supplying nutrients), a breakdown in water-column stratification and a degradation of opportunistic seasonal macroalgae towards the end of the summer may have caused the observed peak in DMS/P concentrations in Loch Sween. In terms of DMS/P concentrations, these data provide no evidence for a spring bloom in Loch Sween. Opportunistic macroalgal growth (e.g. *Chorda filum*) does not begin in the loch until mid-summer. Phytoplankton community composition can be a major factor affecting bloom DMS/P production (Townsend and Keller, 1996). If a spring bloom did occur in Loch Sween, but was dominated by diatoms (typically low DMSP producers), the effect on DMS/P concentrations may have been lower than from a dinoflagellate or prymnesiophyte bloom. This has been observed in other coastal areas, such as the Gulf of Maine (Townsend and Keller, 1996).

5.6.1.1 Decoupling of dimethyl sulphur species

The observed seasonal pattern in DMSPd and DMSPp was, to some extent, reflected in DMSd concentrations, but not in DMSPi, suggesting a decoupling of DMSPd and DMSPp from DMSd and DMSPi. DMSd concentrations can be affected by microbial populations present in the system, as microbes use DMS to meet their sulphur and carbon requirements (Pinhassi et al., 2005; Kiene et al., 2000) and from sea to air flux (Turner et al., 1996).

5.6.1.2 Coralline algal DMSPi

The continued production of DMSPi within algal cells is energetically costly. Thus, it may be beneficial for coralline algae to continually maintain a high concentration of DMSPi within their cells, at a level that will not be significantly impacted if DMSP is required for cellular protection (against salinity stress, for example). This may reduce the need for continued, rapid DMSPi production and minimise overall energy outlay. In addition, the detritus and fouling that may be found within the branches of *L. glaciale* contained some DMSP, thus the peaks in DMSPi in September 2010 and May 2011 (when the thalli were not cleaned) may be a reflection of changes in the DMSP content of detritus and fouling on the maerl thalli rather than an up-regulation of DMSP production by the coralline algae itself. The detritus may have been sourced from the water column particulate phase, the peak of which was two months

earlier than peak DMSPi concentrations in 2010. Fallout of DMSP-containing detrital material, phytoplankton and terrestrial particles may significantly influence the DMSP concent of material located between the maerl branches. Continued temporal comparisons of cleaned / not cleaned maerl samples would provide more information on the partitioning of DMSP within the maerl thallus between detritus and coralline algal cells.

5.6.2 The impact of the maerl bed on DMS/P pools

The maerl bed appeared to have a direct influence on DMS/P pools at the MB site and, to a lesser extent, at the AB site. This suggests that when phytoplankton are not dominant, the maerl bed may be an important component of the DMS/P cycle in Loch Sween. Maximum concentrations of DMSPd and DMSPp at the MB and AB sites in 2010 were observed in July, whilst the BS and ABS sites peaks were in September, and lower than at the MB and AB sites. This suggests that the MB may be more responsive to environmental changes (such as rising water temperature) and act as a source of DMSPd, DMSPp and DMSP-containing detritus in the early summer. This was not observed in 2011, but may be due to the differing sample timings (May and August rather than July and September).

5.6.2.1 Summer phytoplankton blooms

The maerl bed may provide nutrients for the growth of phytoplankton, and continued bioturbation may transfer DMSP-containing particles into the water column and contribute to the DMSPp pool. A subsequent migration and / or growth of phytoplankton further up the water column may have reduced the amount of light available at the seabed, leading to the observed sudden drop in DMSPd and DMSPp at the MB site. DMSP and DMS are important carbon and sulphur sources for marine bacteria (Hatton et al., 2012a); the production of DMS/P by phytoplankton growth may have stimulated the growth of bacteria and the removal of DMS/P from the water column, observed as a gentle decrease in DMS/P at the AB site from September 2010 to January 2011.

5.6.2.2 Autumnal decay of seasonal macroalgae

The low DMSPd and DMSPp concentrations at the MB site in September may have also been influenced by the growth of seasonal macroalgae associated with the maerl bed (e.g. *C. filum*). From November 2010 - March 2011, DMSPd and DMSPp concentrations were highest at the MB site, suggesting that the maerl bed ecosystem may also act as a source of DMSP during the winter months, perhaps from the autumnal decay of seasonal macroalgae such as *C. filum*.

5.6.2.3 Ecosystem function

The high biodiversity of maerl beds (BIOMAERL et al., 2003) may allow for a continued turnover of DMS/P compounds within the maerl bed system at numerous trophic levels. DMS/P concentrations are high within the maerl bed system compared to the bed side, particularly in early summer and during the winter. DMS/P appeared to be generally recycled within the maerl bed system, characterised by high DMSPd and DMSPp concentrations in the water column at the MB site, followed by high maerl DMSPi concentrations (which may partly reflect the settlement and accumulation of detritus on the maerl thalli). This has been observed in other habitats such as seagrass and coralligène in the Mediterranean (see Chapter 4) and suggests that DMSP may be an important compound for ecosystem function within coastal habitats, sustaining microbial populations and perhaps acting as a settlement cue for juvenile invertebrates. Only when concentrations were highest (e.g. in the summer) did the production of DMS/P within the maerl bed appear to influence DMS/P concentrations further up the water column.

5.6.3 Temperature and cloud cover are driving factors

T and CC cover affect the growth of coralline algae (Burdett et al., 2011; Kamenos and Law, 2010; Kamenos et al., 2008a). This research has shown that T and CC are also crucial in driving the DMSPd+p pools within the maerl bed system in Loch Sween. In contrast, DMSd and DMSPi could not be well explained by T, CC or DL, further highlighting the decoupling of DMSd and DMSPi from DMSPd and DMSPp. This also suggests that other explanatory variables may drive the observed patterns in DMSd and DMSPi. When temperature was modelled against DMSPi and BS DMSd (which were most parsimonious with DL, Table 5.2),

a reduction in explained deviance was observed compared to DL (DMSPi: 22.9%, BS DMSd: 54.6%). This may include abiotic factors such as salinity, dissolved oxygen, sea-to-air flux and nutrient availability (all of which may be affected by storm activity) or biotic factors such as the composition of the microbial and / or phytoplankton populations or the growth, spread and decay of opportunistic and seasonal macroalgae such as *Codium* sp., *Ulva* sp. (both high in DMSPi, see Chapter 5) or *Chorda filum* (low in DMSPi, see Chapter 5).

5.6.4 Implications for the future

To minimise the error associated with model projections, it is not advised to make projections further than two or three times the length of a dataset (Wood, 2003). Thus, whilst long-term projections for the future cannot be made with the information presented in this chapter, qualitative expectations may be proposed. Projected increases in atmospheric CO₂ over the next century are likely to affect the oceans by increasing water temperature and storm activity and reducing oceanic pH, surface salinity and dissolved oxygen (Melzner et al., 2012; Doney, 2010; IPCC, 2007). Thus, shallow coastal ecosystems, including maerl beds, are likely to be significantly impacted. As shown in this chapter, DMS/P concentrations within the maerl beds are a potentially major component of the marine sulphur cycle and may be crucial in maintaining ecosystem function. The research presented in this chapter shows that water temperature and cloud cover, two factors that may increase in the future, can be positively related to DMS/P concentrations in the maerl bed system. Further, an acute reduction in pH can increase DMSPi in *L. glaciale*, the coralline algal species that dominates the maerl bed at Loch Sween (Burdett et al., 2012a, and see Chapter 7). Thus, it may be postulated that the production, release and / or turnover of DMSPd and DMSPp will increase in the future. At present it is not possible to say how this may translate to DMS production and subsequent atmospheric flux as DMSd was poorly modelled by the abiotic factors considered in this research (T, CC and DL).

5.7 Wider significance

The biodiversity and ecosystem structure of the maerl bed at Loch Sween is typical for a temperate maerl bed unaffected by fishing practices such as

trawling. Additionally, no significant difference in DMSPi between the two primary maerl-forming species (*L. glaciale* and *Phymatolithon calcareum*) in Scotland has been observed (see Chapter 4). Thus, it may be assumed that the seasonal patterns of DMS/P concentrations observed in Loch Sween are representative of similar maerl bed sites, such as those found throughout northern Europe. This has significant implications for coastal DMS/P cycling given the widespread distribution of maerl beds in this area. Where maerl beds have been damaged by trawling, biodiversity is much lower (BIOMAERL et al., 2003), thus we may expect to see reduced cycling of DMS/P within these ecosystems and a reduced influence on the overlying water column DMS/P concentrations.

5.8 Conclusions

This chapter aimed to quantify the natural variability in DMS/P concentrations within the ecologically and economically important maerl bed habitat on the west coast of Scotland, UK. Water and macroalgal samples were taken throughout a 24 month period from March 2010 to February 2012, and analysed for DMSPi, DMSd, DMSPd and DMSPp. Water column DMS/P concentrations were high compared to the shelf-seas and open ocean, particularly in the summer of 2010. The maerl bed habitat appeared to exert a subtle, but observable, effect on water column DMS/P concentrations, perhaps driven by the enhanced productivity in the area compared to the bed side. Seasonal patterns in DMSPd and DMSPp were clearly evident, and influenced predominantly by T and CC. DMSd and DMSPi, however, were not characterised by distinct seasonal patterns and could not be well described by T, CC or DL, suggesting an influence of other explanatory parameters (e.g. nutrients, salinity, microbial activity or sea-to-air flux) and a decoupling of DMSPd and DMSPp from DMSd and DMSPi.

6

Environmental pressures: Reduction in salinity

Coastal algae experience a naturally variable salinity regime. The salinity of coastal waters is affected by freshwater inputs from precipitation (on land and directly over the coastal ocean) and ice melt. These factors may occur over short (hours to days), long (days to weeks) or permanent timescales, and changes from the current state are projected for the future under IPCC climate change scenarios. Dimethylsulphoniopropionate (DMSP) has been postulated to act as an algal osmolyte or compatible solute. Thus, knowledge of the intracellular regulation of DMSP production by algae will provide crucial information on survival strategies that may be adopted under future ocean salinity regimes.

6.1 DMSP and osmotic regulation

A number of cellular functions have been postulated for intracellular DMSP (DMSP_i), perhaps most notably as a compatible solute (Kirst, 1996; Challenger, 1959). DMSP is comparable in structure and chemical behaviour to other plant osmolytes such as glycine, betaine or proline, indicating that DMSP may have similar enzyme-protective properties (Kiene et al., 2000). The role of DMSP as an osmo-acclimation compound appears to be most important in long-term, high salinity situations; less so as a short-term shock response (Kirst, 1989).

In order to survive in highly saline conditions such as seawater, marine autotrophs must produce osmolytes and organic solutes to maintain a sufficiently

high internal osmotic pressure without inhibiting metabolic functions (Stefels, 2000). Many compatible solutes are direct photosynthesis products (e.g. sucrose, mannitol, sorbitol, glycerol), but other compounds are also used (e.g. betaines, proline, DMSP) (Stefels, 2000). It has been suggested that the production of DMSP is an adaptation to oligotrophic conditions, where essential nutrients such as phosphorus and nitrogen may be limiting (Koop et al., 2001). While other osmolytes are more effective than DMSP (e.g. proline or betaine) (Kirst, 1996), their production under oligotrophic conditions is energetically costly as many contain nitrogen (Andreae, 1990). Thus, it may be favourable to produce a sulphur osmolyte (e.g. DMSP) and use nitrogen for other purposes, such as amino acid synthesis (Andreae, 1990).

Despite the potential advantage of using nitrogen-free DMSP to regulate osmotic balance, algae tend to use other osmolytes to cope with acute changes in salinity such as mannitol, proline or sucrose (Edwards et al., 1988; Edwards et al., 1987). Often, DMSP concentrations change only after prolonged exposure to altered salinity (e.g. Reed, 1983), although the majority of experiments have considered only increases in salinity. The *Enteromorpha* genus, for example, can tolerate a wide range of salinities and exhibits osmolyte-function responses for DMSP over long (35 day) time scales (Edwards et al., 1988; Edwards et al., 1987). In the hypersaline Salton Lake, southern California (salinity ~ 48), the phytoplankton community is composed of high-DMSP producers such as dinoflagellates and coccolithophores (Reese and Anderson, 2009). Some studies have, however, shown a rapid DMSP response to salinity (Vairavamurthy et al., 1985; Dickson et al., 1982), and the response may be related to the speed of salinity change (Dickson et al., 1982). Thus, the importance of DMSPi as a compatible solute may be species specific.

Increased precipitation resulted in a measurable freshening of the North Atlantic eastern subpolar gyre from the 1960s - 1990s (Bindoff et al., 2007; Josey and Marsh, 2005), highlighting the importance of freshwater inputs in determining ocean salinity at decadal timescales. Thus, an understanding of the short- and longer-term forcings associated with freshwater input into the oceans is essential if we are to make biogeochemical and biological projections for the future. Given the worldwide distribution of coralline algae (Foster, 2001), it is crucial to ascertain the importance of DMSP production by coralline algae under

hyposaline conditions, as this could have significant implications on the coastal marine sulphur cycle.

6.2 Global precipitation patterns

Atmospheric temperatures are projected to increase by up to 6 °C by the year 2100 (Figure 6.1) due to anthropogenic forcing (IPCC, 2007). Such increases in temperature are projected to increase the ‘moisture-holding capacity’ of the atmosphere by ~7% for every 1 °C (Trenberth et al., 2007). This, combined with radiative forcing (incoming minus outgoing energy in the atmosphere) and sensible heating (heat exchange because of changes in temperature), may significantly alter the global hydrological cycle, global precipitation patterns (Trenberth et al., 2003) and, ultimately, ocean salinity.

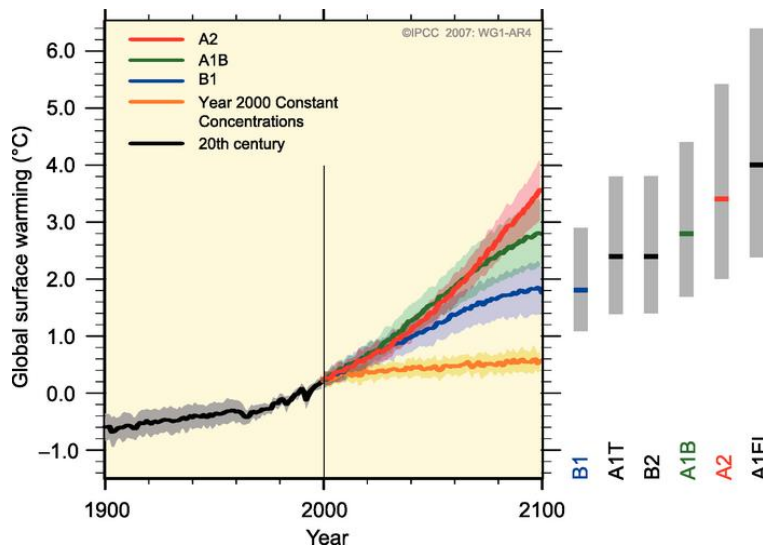


Figure 6.1 Global surface warming projections to year 2100. Multi-model global averages of surface warming relative to the 1980 – 1999 mean for A2 (red line), A1B (green line), B1 (blue line) and a year 2000 continuation (orange line) emission scenarios. Shading represents ± 1 SD of the individual model annual averages. Grey bars indicate the likely range of warming associated with each scenario outlined by IPCC, including results from atmosphere-ocean general circulation models, independent models and observational constraints. Source: IPCC (2007).

Precipitation over land north of 30° N has generally increased from 1900 – 2005, despite a drier period in the early 1990s (Trenberth et al., 2007; Josey and Marsh, 2005). This has been confirmed by an apparent increase in summer surface (top 1 m) soil moisture content over the past few decades in Ukraine, China, Mongolia, India and the USA (Robock et al., 2005; Robock et al., 2000). An increase in soil moisture can decrease water absorption by soil, increasing

freshwater inputs to the coastal zone, reducing coastal salinity and impacting coastal organisms.

6.2.1 Extreme events

Since 2000, an ‘exceptional number’ of extreme heat and precipitation events have been recorded worldwide, attributed to a rise in global temperatures (Coumou and Rahmstorf, 2012). This has caused ‘intense human suffering’ and financial damage (Coumou and Rahmstorf, 2012). Extreme precipitation events will cause significant amounts of freshwater to enter the coastal zone, directly and from land run-off. The contribution of extreme precipitation events to total annual rainfall has increased in many areas since the 1950s, and particularly since the late 1980s (Figure 6.2) (Trenberth et al., 2007). In addition, the frequency of high-intensity hurricanes has increased since the 1970s, and is projected to continue to increase over the next century (e.g. Bender et al., 2010), increasing freshwater input into the coastal zone through land run-off. For more information on hurricane activity, see Chapter 8.

6.2.2 Cloud formation

An increase in tropospheric water vapour and surface specific humidity has been observed over the past few decades, causing a general increase in cloud cover, in line with higher atmospheric temperatures (reviewed by Trenberth et al., 2007) and further increasing precipitation potential. An increase in cloud cover has been observed to have an effect on the growth of the coralline alga *Lithothamnion glaciale* in the western North Atlantic (Burdett et al., 2011), and may impact DMSP concentrations in coastal ecosystems (see Chapter 5).

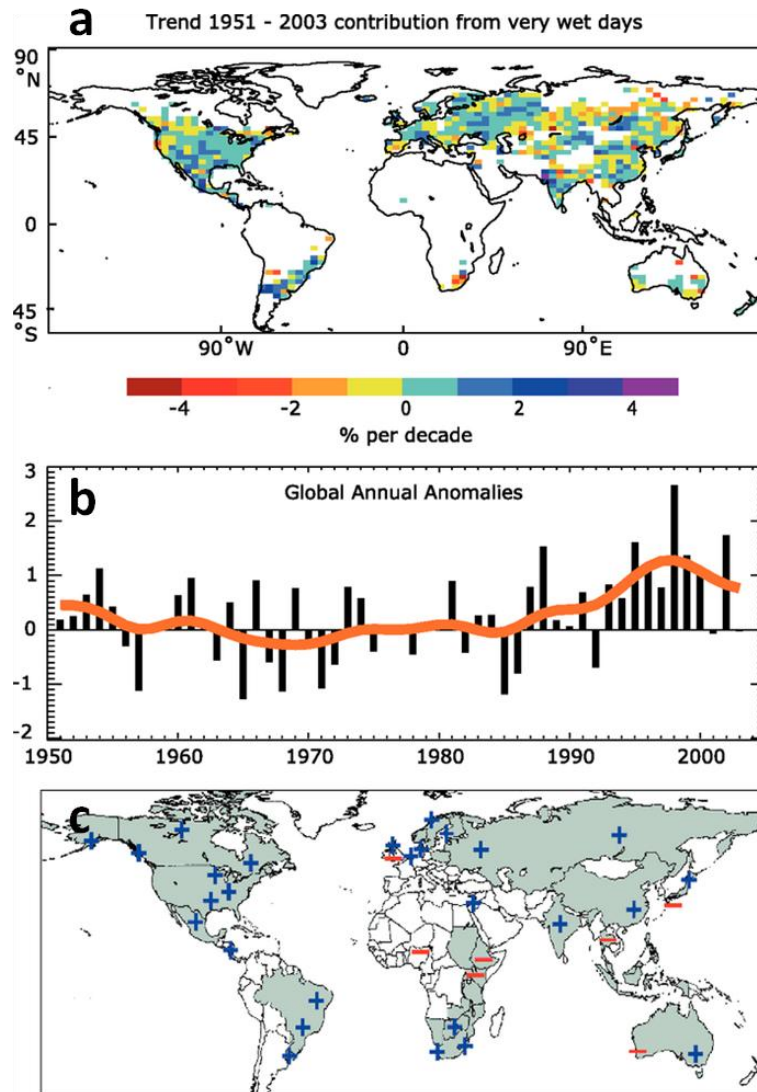


Figure 6.2 Global trends of very wet days since 1951.

(a) Contribution of very wet days (95th percentile) to total precipitation 1951 - 2003 (% change per decade) from 40+ year time series data sets. White areas had insufficient data. (b) % change in the frequency of very wet days relative to the 1961 – 1990 mean. Smooth curve is the decadal trend. (c) Shaded areas indicate regions which have experienced a significant increase (+) or decrease (-) in extreme precipitation events over the past 50 years. Source: Trenberth et al. (2007).

6.3 Ice melt

Increased seasonal and longer-term ice melt could become a major contributor to salinity variations in the polar coastal ocean as atmospheric temperatures rise. The majority of research into ice sheet melting has focused on sea level rise (e.g. Shepherd et al., 2012), but the melting of floating ice has no effect on sea level. Such events will, however, increase freshwater inputs into the ocean, which could affect ocean circulation patterns (Kwok and Comiso, 2002) and promote long-term oceanic freshening. Melting sea ice can also help

to accelerate the movement of land-based glaciers, further encouraging ice melt (Bindschadler et al., 2011) and reducing salinity in the coastal zone.

The Antarctic Ice Sheet (AIS), the world's largest ice sheet (30 million km³) represents a primary source of freshwater to the oceans under a melting scenario, equivalent to 70 m of water depth to the entire ocean (BAS, 2012). There are two Antarctic coastal areas that are likely to be most affected by ice melt - the western Antarctic Peninsula, one of the most rapidly warming regions in the world (Vaughan et al., 2003), and Pine Island Bay, where warm coastal waters underneath the ice shelf is accelerating melting (Bindschadler et al., 2011).

The Greenland Ice Sheet (GIS) contains 10% of the world's ice (2.5 million km³, Coumou and Rahmstorf, 2012). Using satellite gravity measurements and radar interferometry data, the melting rate over Greenland is currently between -239 ± 23 to -224 ± 41 km³ per year, primarily in East Greenland and exhibiting an accelerated warming since 2004 (Coumou and Rahmstorf, 2012; Schubert et al., 2006). Runoff records are scarce in Greenland, but recent proxy data using the coralline alga *L. glaciale* suggests that freshwater runoff into the Søndrestrom fjord has increased since the 1930s (reducing salinity to at least 8m depth), and is correlated with an increase in atmospheric warming (Kamenos et al., 2012).

6.4 Regional focus: west coast of Scotland

Low or variable salinity habitats are a priority marine feature of the UK (JNCC, 2012) due to their diverse, yet specialised, species range. The majority of these habitats are located in Scotland, primarily along the west coast, the western Isles and the northern Isles (Figure 6.3).

The west coast of Scotland is characterised by a fjordic environment: steep slopes, thin soils and high soil moisture (Gillibrand et al., 2005), which facilitates freshwater run-off into sea lochs. The majority of the lochs also have a shallow sill at their entrance, restricting water exchange with the open ocean. As such, the salinity of Scottish sea lochs may vary according to the frequency and intensity of precipitation events. Loch salinity may also be affected by more

North Atlantic climatic forcings such as the North Atlantic Oscillation - an inter-annual climatic oscillation determined by the pressure difference between the Icelandic Low and Azores High (Gillibrand et al., 2005).

In the eastern North Atlantic, the red coralline alga *L. glaciale* is typically found in fjordic environments, from 55 - 80°N (Teichert et al., 2012; Foster, 2001), and is therefore thought to be tolerant to variable salinity regimes (Connor et al., 2004). Following five weeks of incubation, no change in quantum efficiency (F_v/F_m) was observed at a salinity of 15, but F_v/F_m did decrease at a salinity of 3 (Wilson et al., 2004). The effects of reduced salinity on *L. glaciale* in Scotland may be representative of more northerly *L. glaciale* populations (as sampling logistics are difficult in polar regions), where snow and glacial melt may affect the seasonal and longer-term salinity of the coastal zone.

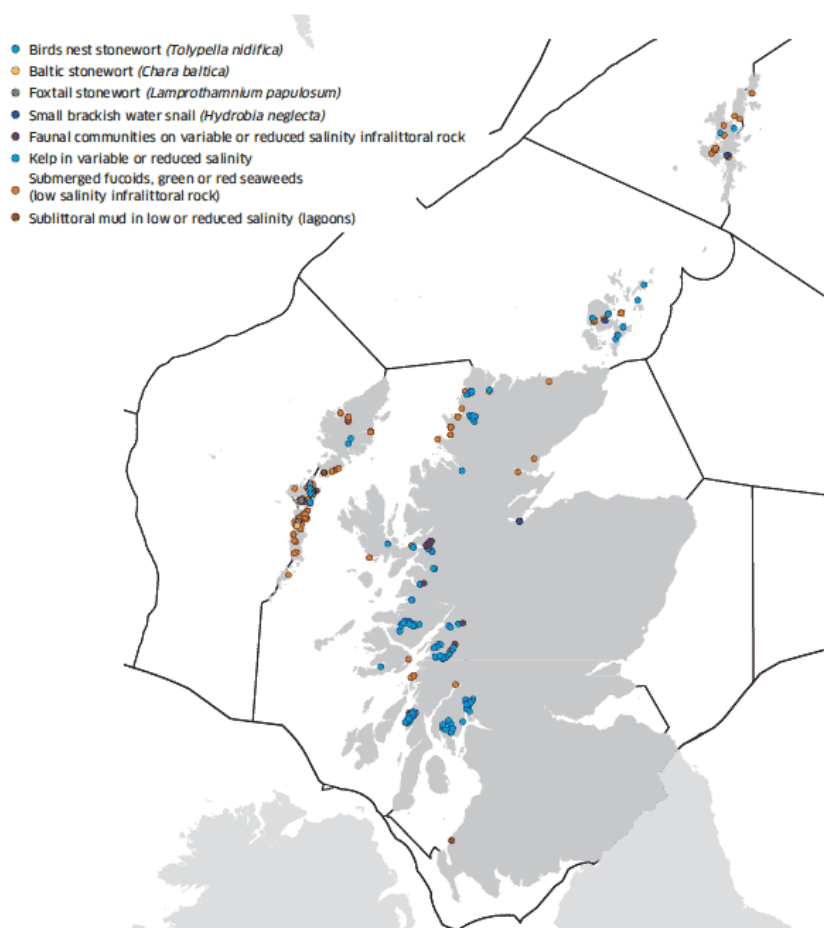


Figure 6.3 Location of low and variable salinity habitats in Scotland. Only those areas identified to harbour a priority marine feature or rare endemic species are shown. Source: Baxter et al. (2011).

6.5 Regional focus: Central Chilean coast

The salinity of the Chilean coastal ocean is governed by upwelling, storm activity and river outflow. Well-described climatic processes affect the degree of deep-water upwelling and storm activity in this region, thus impacting the salinity of the coastal zone:

El Niño Southern Oscillation (ENSO): ENSO events are a coupled ocean-atmosphere phenomenon in the South Pacific Ocean (Trenberth et al., 2007). During an El Niño phase, a prolonged weakening of the easterly trade winds affects atmospheric tropical circulation and precipitation patterns, warming the tropical Pacific surface waters from near the International Date Line to the west coast of South America. This weakens the usually strong sea surface temperature (SST) gradient across the equatorial Pacific, deepening the oceanic thermocline, reducing upwelling and increasing storms (therefore periodically reducing salinity) along the west coast of South America. Historically, El Niño events occur every three to seven years and alternate with La Niña phases (characterised by below average temperatures in the eastern tropical Pacific Ocean).

Decadal oscillations: The Inter-decadal Pacific Oscillation (IPO) and Pacific decadal oscillation (PDO) are related to observed decadal variations in atmospheric and oceanic circulation and SST in the Pacific basin. IPO and PDO may be longer-term El Niño-like climate variability (Evans et al., 2001) or residual ENSO variability (Newman et al., 2003) but may not be solely related to ENSO (Folland et al., 2002). Both scenarios affect SST, upwelling and storm activity (and therefore salinity) on the west coast of South America.

The central Chilean coast is known to experience short-term reductions in salinity throughout the year due to river outflow (e.g. Figure 6.4). For example, the Maipo River (33° 37'S, 71° 38'W), has a measurable effect on local hydrography. The drainage basin of the Maipo River covers >15 000 km², running from the Andes to the coast for ~250 km. Maximum river discharge occurs in the spring (glacial meltwater from the Andes) and during winter (high precipitation in the coastal area). During the spring, salinity of the surface water in the nearby area may not be correlated to river discharge, but driven by a diurnal

cycle related to wind patterns (Piñones et al., 2005). Despite this, reductions in surface salinity as a result of river discharge may be observed as far away as Las Cruces, 12 km north of the outflow (Piñones et al., 2005). Reductions in salinity typically last for 2 - 3 days (Figure 6.4) with minimum salinity values of around 27 at Las Cruces (R. Finke, pers. comm., 2012).

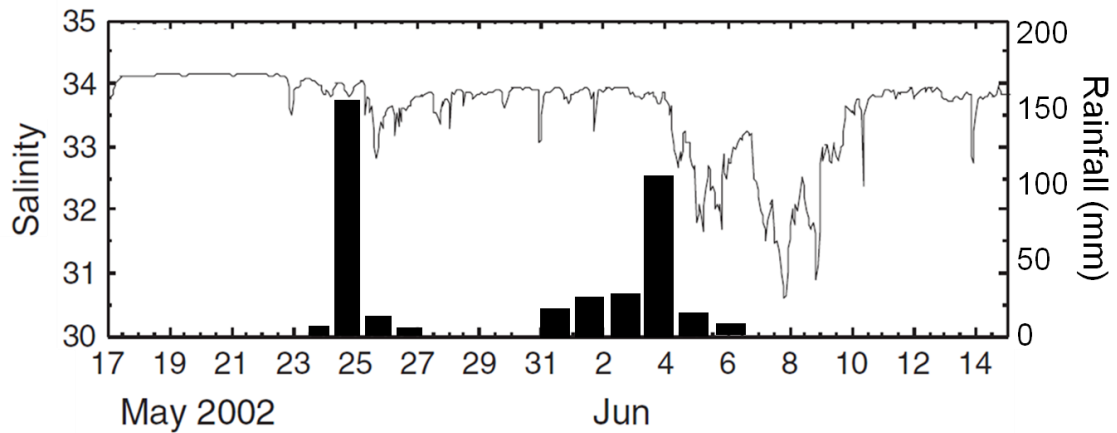


Figure 6.4 Surface salinity at Las Cruces, central Chile, during a storm. *In situ* salinity recordings (black line) and daily rainfall (black bars) from May – June 2002. The second rainfall event caused a large increase in river flow from the 4th – 8th June, resulting in the observed reduction in coastal salinity. Source: Piñones et al. (2005).

6.6 Aims of this chapter

Projections for increased storm intensity (see Chapter 8) and ice melt may significantly increase coastal salinity variability in the future. Thus, the compatible solute role of DMSPi may become more prominent. Specifically, this chapter will address:

1. The effect of chronic (weeks) salinity reduction on *L. glaciale* in a Scottish sea loch. The restricted water exchange within Scottish sea lochs can allow for prolonged salinity reductions following a large run-off event. *L. glaciale* may be found in polar waters, where ice melt will contribute to seasonal salinity reductions, which may be more extreme in the future due to global warming, so represents an excellent species to study.
2. The effect of acute (days) salinity reduction on intertidal and subtidal coralline algae from central Chile. The coastal salinity of central Chile is affected by El Niño-induced storms and upwelling

and seasonal ice melt from the Andes, thus representing an ideal location for assessing the short-term effect of hyposalinity on coralline algae.

To provide a more holistic understanding of the effects of salinity reduction on coralline algae, photosynthetic acclimation and pigment composition were also considered. It was hypothesised that:

1. The regulation of DMSPi in response to salinity changes will be observed only under a chronic, longer-term scenario, in line with previous literature.
2. Photosynthetic characteristics will be affected by acute and chronic reductions in salinity as photosynthetic regulation in coralline algae can be rapid (see Chapter 3).

6.7 Methods: Chronic salinity reduction, Scotland

6.7.1 Experimental set up

Free-living *L. glaciale* thalli were collected from Loch Sween (56° 01.99'N, 05° 36.13'W), transported to the University of Glasgow in seawater and transferred to 120 litre re-circulating seawater tanks (Aquael Brillux 80 aquaria, 800 x 350 x 400 mm) maintained at ambient temperature (12 °C), salinity (32) and light (40 $\mu\text{mol photons m}^{-2} \text{s}^{-1}$, artificial lights) (Figure 6.5). Seawater was made by mixing freshwater with TropicMarin Reef-Pro marine salt. Thalli were acclimated to laboratory conditions for one to two weeks before the experiment was started. Water flow was constantly maintained using a Rio400 Aqua pump (250 L water hr^{-1}) and an Aquael Fan2plus filter (200 L water hr^{-1}). The water was UV-treated using a Vecton² 120 Nano UV Aquarium steriliser prior to temperature regulation with a Teco TR15 Refrigerator (± 0.5 °C). Dissolved oxygen concentrations were maintained using an AquaHabitats H₂Air60 air pump (60 L air hr^{-1}). Salinity, temperature and dissolved oxygen (DO, salinity compensated) were monitored using a YSI Pro2030 probe.

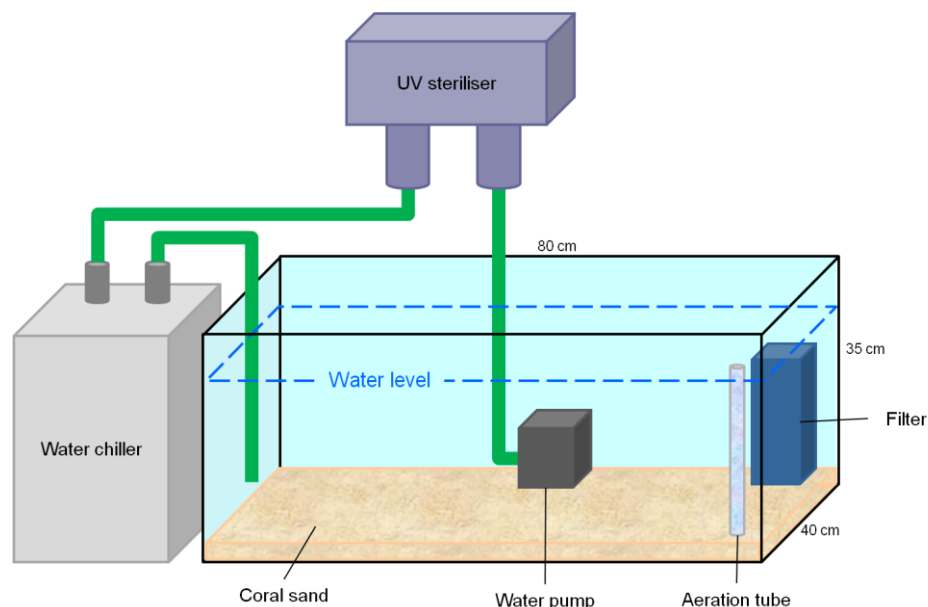


Figure 6.5 Aquarium set-up for chronic salinity reduction experiment.

Three salinity treatments were used to assess the effect of chronic reductions in salinity: control (C, target salinity: 32), low (L, target salinity: 22, representative of a typical salinity reduction period in an upper Scottish sea loch, e.g. Allen and Simpson, 1998) and very low (VL, target salinity: 12, representing an extreme salinity reduction period). The salinity of the two low salinity treatments was gradually reduced over a seven day period by performing daily water changes with a mix of freshwater and seawater. Target salinities were maintained for a further 14 days. Three aquarium set-ups (as per Figure 6.5) were available, thus each treatment was performed in each aquarium to account for any tank effects (Table 6.1). Ten replicates were sampled at each time point from each treatment, yielding 30 replicates per timepoint within the nested design. No repeat sampling of thalli was performed.

Table 6.1 Target salinities for the 21-day experiment.
21-day salinity reduction experiment with three salinity treatments – control (salinity of 32), low (salinity of 22) and very low (salinity of 12); target salinities were reached from the control value over a 7-day reduction period. Each salinity treatment was performed in three aquaria to allow tank effects to be assessed.

Date	Tank 1	Tank 2	Tank 3
June 2011	12	22	32
July 2011	22	32	12
August 2011	32	12	22

6.7.2 Sample measurements

DMSPi: Algal samples ($n = 5$ per timepoint, per treatment) were fixed and analysed for DMSPi using the headspace method described in Chapter 2 at T0, T3, T7, T14 and T21 days. Samples were gently cleaned with a soft toothbrush prior to fixing to remove macrofoulers and detritus.

Photosynthetic characteristics: Rapid Light Curves (RLCs) were performed on coralline algal thalli at T0, T3, T7, T14 and T21 days using a Diving-PAM (Heinz Walz GmbH) equipped with a 5 mm fibre optic probe 10 mm from the algal surface ($n = 5$ per timepoint, per treatment). RLCs were performed in the tanks, thus thalli were not cleaned prior to conducting the RLCs. Thalli were fully dark adapted for five minutes before the RLC was performed. RLC step intensities were: 2, 23, 67, 135, 230, 346, 493, 731 and 997 $\mu\text{mol photons m}^{-2} \text{s}^{-1}$ for 10 s duration. Details on performing RLCs and calculation of the photosynthetic parameters are found in Chapter 2.

Pigment composition: To quantify changes in thallus pigmentation (as a result of fouling or senescence), the optical reflectance of the coralline algal thalli ($n = 5$ per timepoint, per treatment) was measured at T0 and T21 using the Ocean Optics spectrometer, as detailed in Chapter 2. Samples were not cleaned prior to measurements.

Epithelial cell morphology: ESEM secondary electron imaging (see Chapter 2 for methodological details) was used to assess changes in epithelial cell morphology between the three treatments groups. Algal branches from each treatment ($n = 5$) were imaged at T21 days. Samples were not cleaned prior to imaging.

6.7.3 Statistical analyses

All statistical comparisons were conducted using ANOVA general linear models. To achieve normality and homogeneity of variance the following data transformations were applied prior to testing: E_k : $\log_{10}(x)$, F_q'/F_m' : $x^{1/3}$, α : none required, $rETR_{\text{max}}$: $\log_{10}(x)$. DO could not be transformed to meet ANOVA test assumptions, thus a Kruskal-Wallis test was used. The DMSPi data could not be transformed to meet ANOVA test assumptions, thus a Scheirer-Ray-Hare non-

parametric test was used. This test involves conducting a two-way ANOVA on the ranked data and a cumulative Chi- X^2 test to define the statistical probability of differences between the data. No tank effects were observed for any of the measurements.

6.8 Methods: Acute salinity reduction, Chile

6.8.1 Experimental set-up

An investigation into the effects of acute salinity reduction on coralline algae was conducted at Estación Costera de Investigaciones Marinas, Las Cruces, central Chile (33°30'S, 71°38'W), 12 km north of the Maipo river outflow. Encrusting coralline algae (Figure 6.6) were collected from two locations:

1. Las Cruces (33°30'S, 71°38'W) - *Lithothamnion* sp., at the lower limit of the intertidal zone; naturally high environmental fluctuations and irradiance.
2. Punta del Tralca (33°25'S, 71°42'W) - *Mesophyllum* sp., 14 m depth (subtidal); more stable natural conditions and lower irradiance.

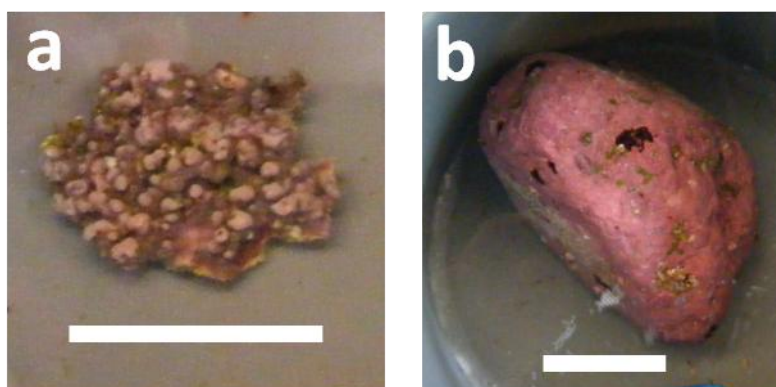


Figure 6.6 Encrusting coralline algae from central Chile. Example thalli from (a) the upper limit of low tide at Las Cruces and (b) at 14 m depth at Punta del Tralca. Scale bar = 20 mm.

Algae from Las Cruces were collected by hand at low tide, while the algae from Punta del Tralca were collected using SCUBA. All algae specimens were transported to the laboratory in seawater. Experiments were conducted in a shaded, outdoor seawater facility. All coralline algae were maintained in flow-through seawater tanks for two to three days to acclimatise to experimental

conditions, using seawater pumped directly from Las Cruces bay. For experimentation, each algal thallus was transferred to individual, aerated tubs (800 ml volume, 106 mm diameter, aeration: 5 L air hr⁻¹, Figure 6.7). Regular water changes (four times daily) with aerated water at ambient temperature were performed to maintain water quality. The temperature of the tubs was maintained at ambient temperature using a flow through water bath with seawater pumped from Las Cruces bay (Figure 6.7).

Two experimental treatments were considered (Figure 6.7): control (ambient salinity) and run-off (nine hour reduction in salinity, followed by a 22 hour recovery), representative of a storm event in the area (e.g. Figure 6.4). Salinity in the runoff treatment was adjusted by using a mix of seawater and de-chlorinated freshwater during the water changes. Salinity measurements were taken before and after each water change using a handheld refractometer. Ambient photosynthetically active radiation (PAR, $\mu\text{mol photons m}^{-2} \text{s}^{-1}$) was recorded at each sampling point with the Diving-PAM PAR meter.

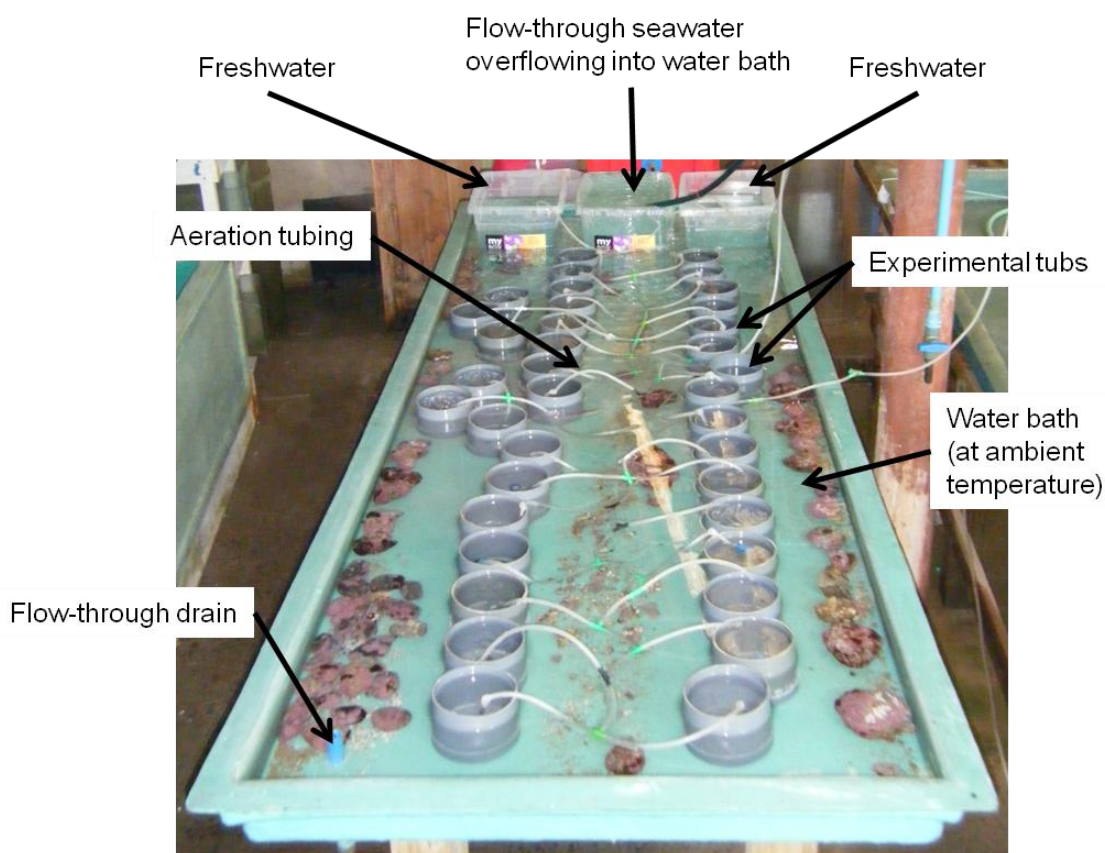
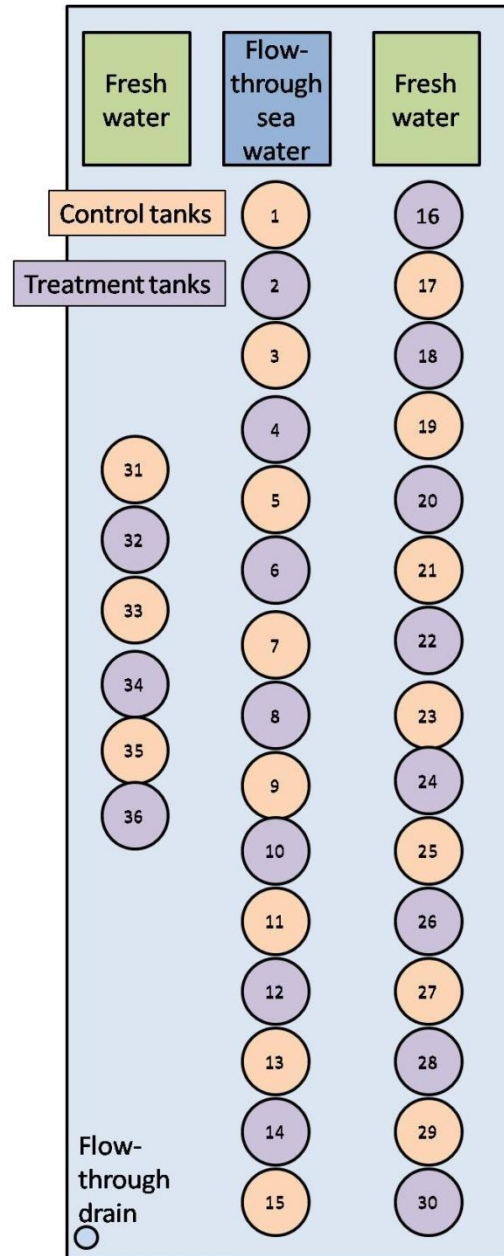


Figure 6.7 Experimental set-up for acute salinity reduction. Photo of the experimental set-up (this page) and diagrammatic representation (next page).



6.8.2 Sample measurements

DMSPi: fragments from each thallus ($n = 15$ per treatment) were fixed and analysed for DMSP according to the headspace methodology in Chapter 2. Thalli in tubs 31 - 36 (Figure 6.7) were not sampled for *DMSPi* and acted as photosynthetic controls to assess the effect of repeat sampling for *DMSPi* quantification on the quantum efficiency of the algae. Fouling by macroalgae was not visible, so samples were not cleaned prior to fixing. *DMSPi* samples were taken at T7, T17, T32, T40 and T64 hours (relative to 00:00 of experimental day one). Due to limited sample mass, for T40 (subtidal), $n = 11$ in the control and $n = 13$ in the runoff treatment, whilst for T64 (subtidal), $n = 6$ in the control and $n = 10$ in the runoff treatment.

Quantum efficiency: Quantum efficiency measurements were taken from each thallus at T7, T11, T17, T32, T40 and T64 (relative to 00:00 of experimental day one) using a Diving-PAM equipped with a 5 mm fibre optic probe. The algae were quasi-dark adapted by using the surface holder attachment (Burdett et al., 2012b, and see Chapter 2), thus measurements represented maximum quantum efficiency, F_v/F_m . Additional measurements were taken irregularly throughout the experiment (as the technique is non-invasive) to assess the diurnal pattern, as distinct diurnal trends may be observed in coralline algae (see Chapter 3). Logistical constraints prevented the monitoring of any other photosynthetic parameters.

Table 6.2 Acute salinity reduction sampling regime.

Sampling hour relative to 00:00 on day one. Number of samples (n) taken for intracellular DMSP (DMSPi) and quantum efficiency (F_v/F_m) from control (salinity of 35) and treatment (salinity reduction to 27 by hour 17 followed by a recovery to a salinity of 35) groups.

Sampling hour	DMSPi		F_v/F_m	
	n (control)	n (treatment)	n (control)	n (treatment)
7	15	15	15	15
17	15	15	15	15
32	15	15	15	15
40	11	13	15	15
64	6	10	15	15

6.8.3 Statistical analysis

Changes in DMSPi and quantum efficiency were statistically analysed using a repeated measure ANOVA and individuals were repeatedly sampled for DMSPi and F_v/F_m . To achieve normality and homogeneity of variance the following data transformations were applied prior to testing: DMSPi: $\log_{10}(x+1)$, quantum efficiency: x^3 .

6.9 Results: Chronic salinity reduction, Scotland

6.9.1 Abiotic parameters

The salinity of the control treatment remained constant throughout the experimental period (Figure 6.8). The salinity of the low (L) and very low (VL) treatments was gradually reduced over the course of seven days to a new salinity baseline of ~22 or ~12 respectively. The percentage of DO in the

experimental tanks gradually rose over the course of the experiment, although the range was small (<14%, Figure 6.8). DO was lower in the L treatment than the other treatments from day eight to 12 (Kruskall-Wallis test, $p = 0.02$). Mean (\pm SD) DO percentage throughout the experiment in all treatments was $104 \pm 3.5\%$.

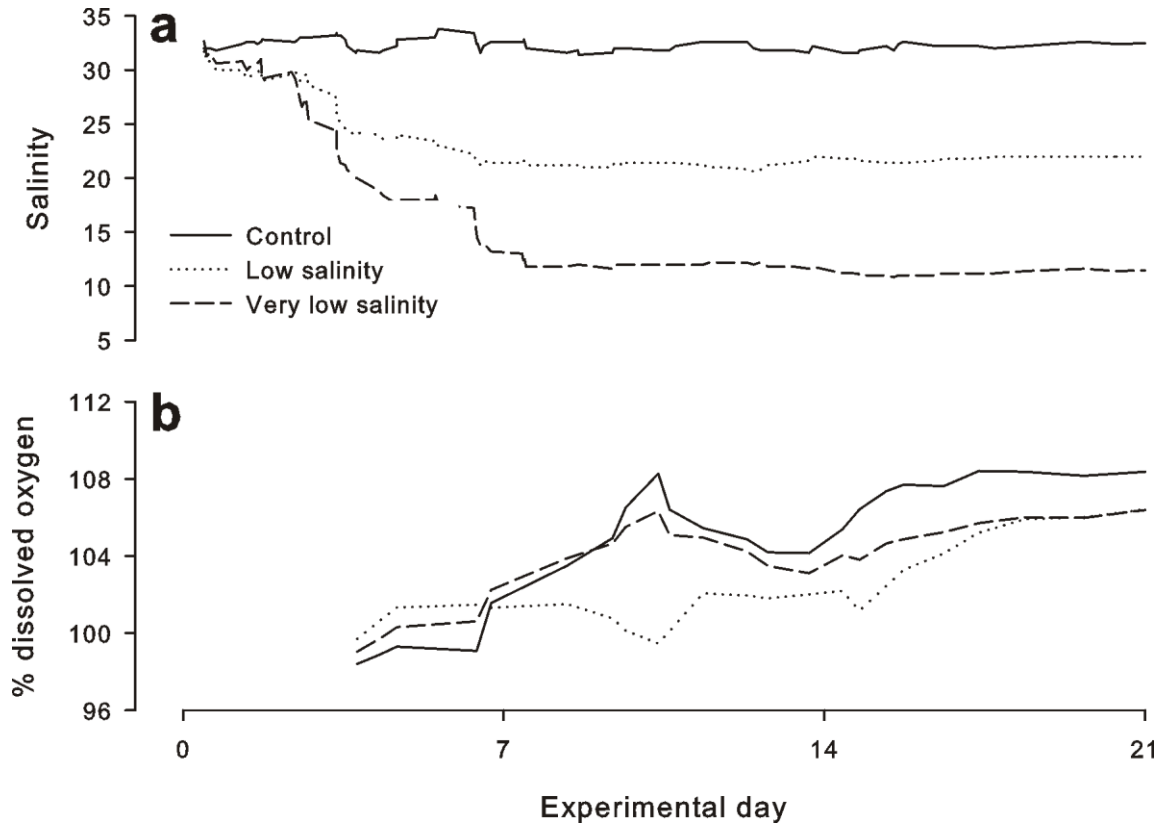


Figure 6.8 Abiotic parameters of the 21 day salinity experiment.

(a) Salinity and (b) dissolved oxygen (%) in control (black line), low (fine dashed line), and very low (thick dashed line) treatments. Data presented as a 5-point moving average from three runs of the 21 day experimental period.

6.9.2 Visual observations

Extensive fouling by green macroalgae was observed in both L and VL treatments by the end of the experiment (Figure 6.9). The fouling was mostly present on the upper side of the thalli, which had been exposed to direct light throughout the experiment (thalli were not turned during the 21 day experimentation period). Little fouling was observed in the control group.

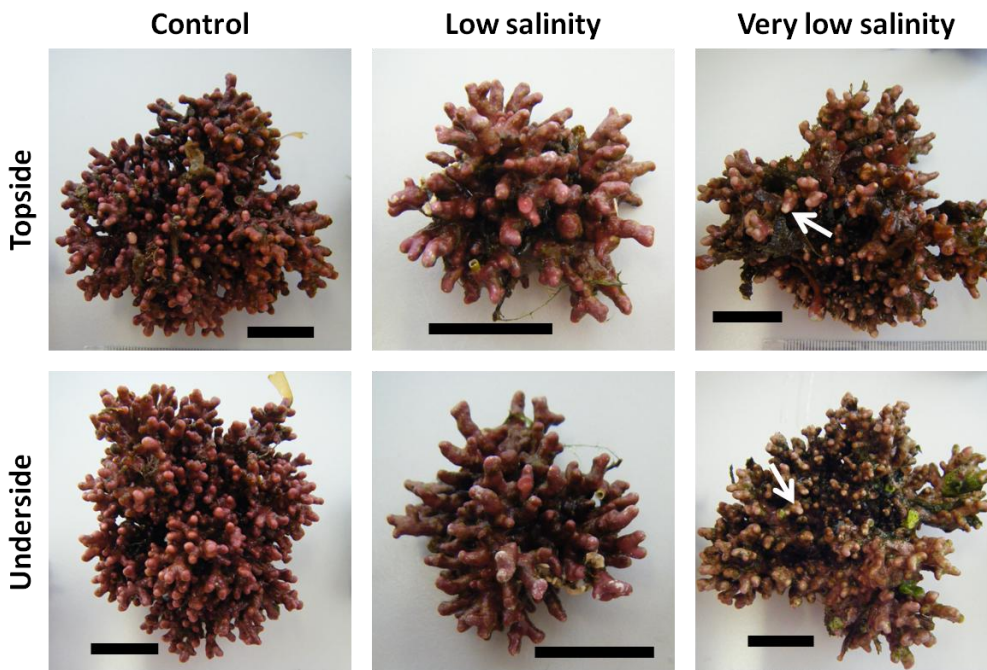


Figure 6.9 Thalli at the end of the 21-day salinity experiment. Topside (1st row) and underside (2nd row) of thalli from control (1st column, salinity = 32), low (2nd column, salinity = 22) and very low (3rd column, salinity = 12) salinity treatments after a 21 day incubation (target salinities reached at day seven). Fouling was most evident in the low salinity treatments. In the very low salinity treatment, branch tips began to lose their pigment (examples indicated by the white arrows). Scale bar = 20 mm. Photos: H. Burdett.

6.9.3 Intracellular DMSP

A significant difference in DMSPi was found between treatments ($p = 0.002$), with the VL salinity treatment lower than the C and L salinity treatments after 14 days (Figure 6.10; 30.6 ± 8.3 , 113.0 ± 28.0 and $76.9 \pm 22.1 \mu\text{g S g}^{-1}$ respectively). The C and L salinity treatments were characterised by a high variability, particularly in the first seven days. Variability in the VL treatment was small from day seven (Figure 6.10).

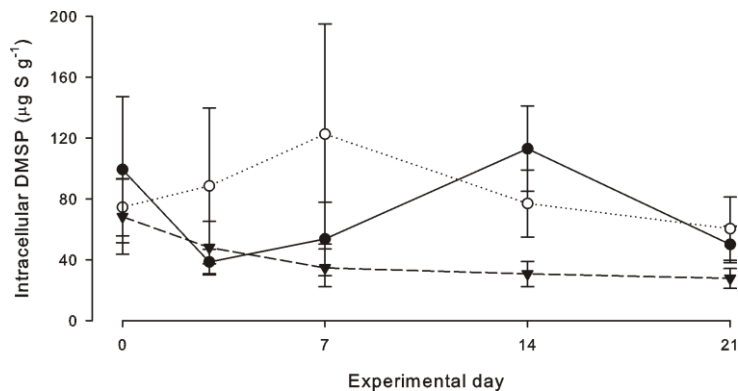


Figure 6.10 Intracellular DMSP concentrations in *L. glaciale*. DMSP determined from thalli maintained in control (salinity = 32, black circle), low (salinity = 22, open circle) and very low (salinity = 12, black triangle) salinities. Salinities were reduced from 32 to target salinities from day 0 – day 7. Data presented as mean \pm SE.

6.9.4 Photosynthetic parameters

Minimum saturating intensity (E_k) rose to a maximum of $\sim 45 \mu\text{mol photons m}^{-2} \text{s}^{-1}$ in the C and L treatments whilst E_k in the VL treatment remained $\sim 25 \mu\text{mol photons m}^{-2} \text{s}^{-1}$ throughout the experiment. ($F_2 = 6.80$, $p = 0.001$, Figure 6.11a). No difference between treatments was observed in maximum effective quantum efficiency ($F_q'/F_{m' \max}$, between 0.55 - 0.62, $F_2 = 0.15$, $p = 0.857$, Figure 6.11b). The light dependent gradient (α) was significantly higher in the VL treatment (up to 0.11 ± 0.01 , $F_2 = 3.03$, $p = 0.051$, Figure 6.11c). A similar pattern was observed in maximum relative electron transport rate ($rETR_{\max}$) ($7.28 \pm 1.37 \mu\text{mol electrons m}^{-2} \text{s}^{-1}$, $F_2 = 4.73$, $p = 0.010$, Figure 6.11d). However, differences in E_k , α and $rETR_{\max}$ were not observed until day 14, where $C < L < VL$ in all three parameters (Figure 6.11).

A reduction in salinity had little effect on the photochemical characteristics of *L. glaciale* (Figure 6.12). F_v/F_m and photochemical quenching (qP) rapidly reduced to almost zero as the light reached super-saturating intensities (> 10 times E_k) at both day one and day 21 (Figure 6.12). At day 21, qP was slightly higher in the control treatment compared to the L and VL salinity treatments. At the start of the experiment, $rETR$ rose to a maximum of $2 \mu\text{mol electrons m}^{-2} \text{s}^{-1}$ when $E/E_k = 2$, followed by a plateau at this level (Figure 6.12). By day 21, $rETR$ was higher in all three treatments, although this was characterised by a high variability. The VL treatment had the highest rates of $rETR$, peaking at $E/E_k = 15$, followed by a decline at the last light intensity. The L treatment peaked at $E/E_k = 11$, while the C treatment peaked at $E/E_k = 20$ (Figure 6.12).

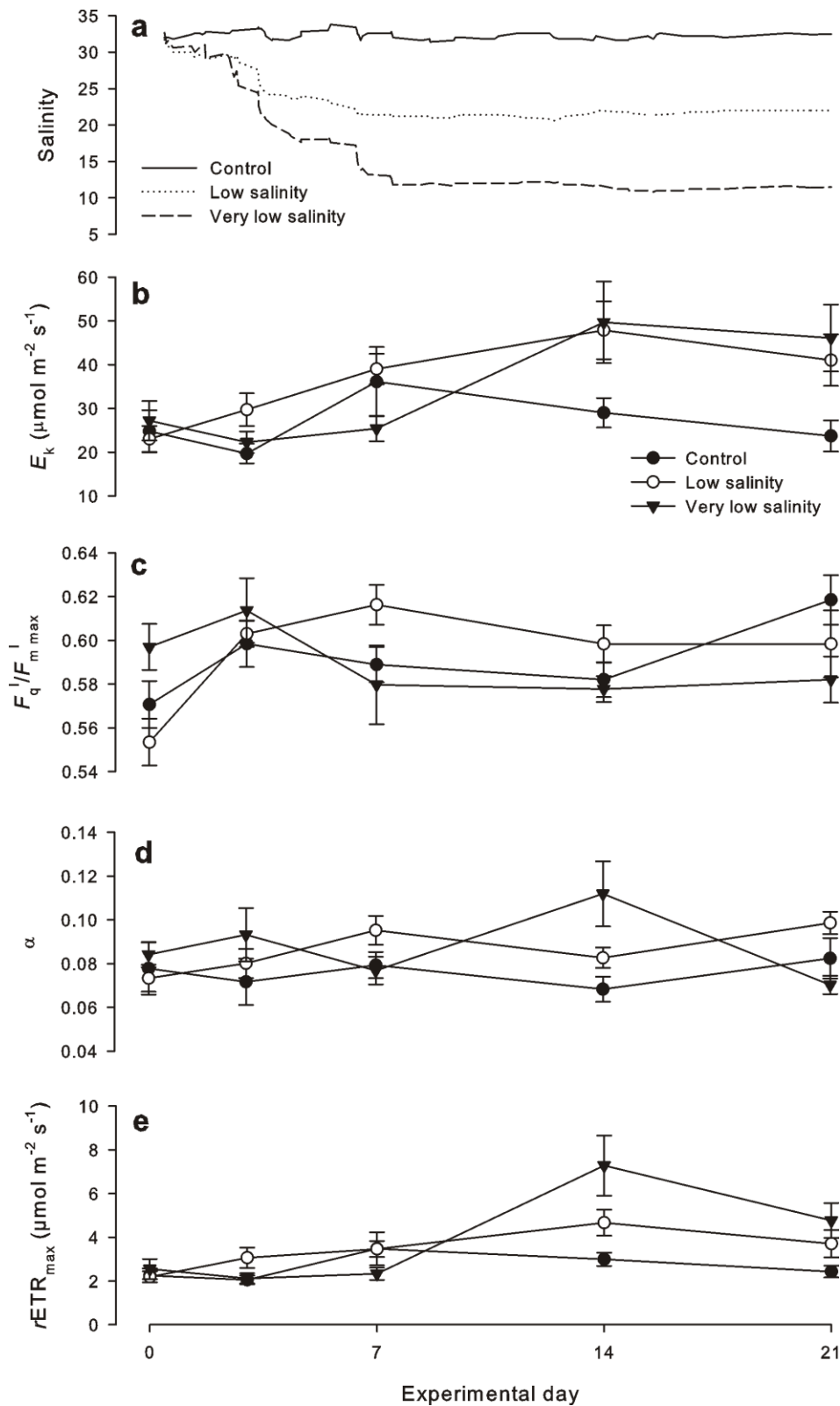


Figure 6.11 Photosynthetic parameters of *L. glaciale*.

(a) Salinity profiles for each treatment (control: black line, low salinity: dotted line, very low salinity: dashed line) as a reference, (b) E_k ($\mu\text{mol photons m}^{-2} \text{s}^{-1}$), (c) $F_q'/F_m' \max$, (d) α and (e) $rETR_{\max}$ ($\mu\text{mol electrons m}^{-2} \text{s}^{-1}$) from thalli maintained in control (salinity = 32, black circle), low (salinity = 22, open circle) and very low (salinity = 12, black triangle) salinities. Salinities were reduced from 32 to target salinities from day 0 – day 7. Photosynthetic data presented as mean \pm SE.

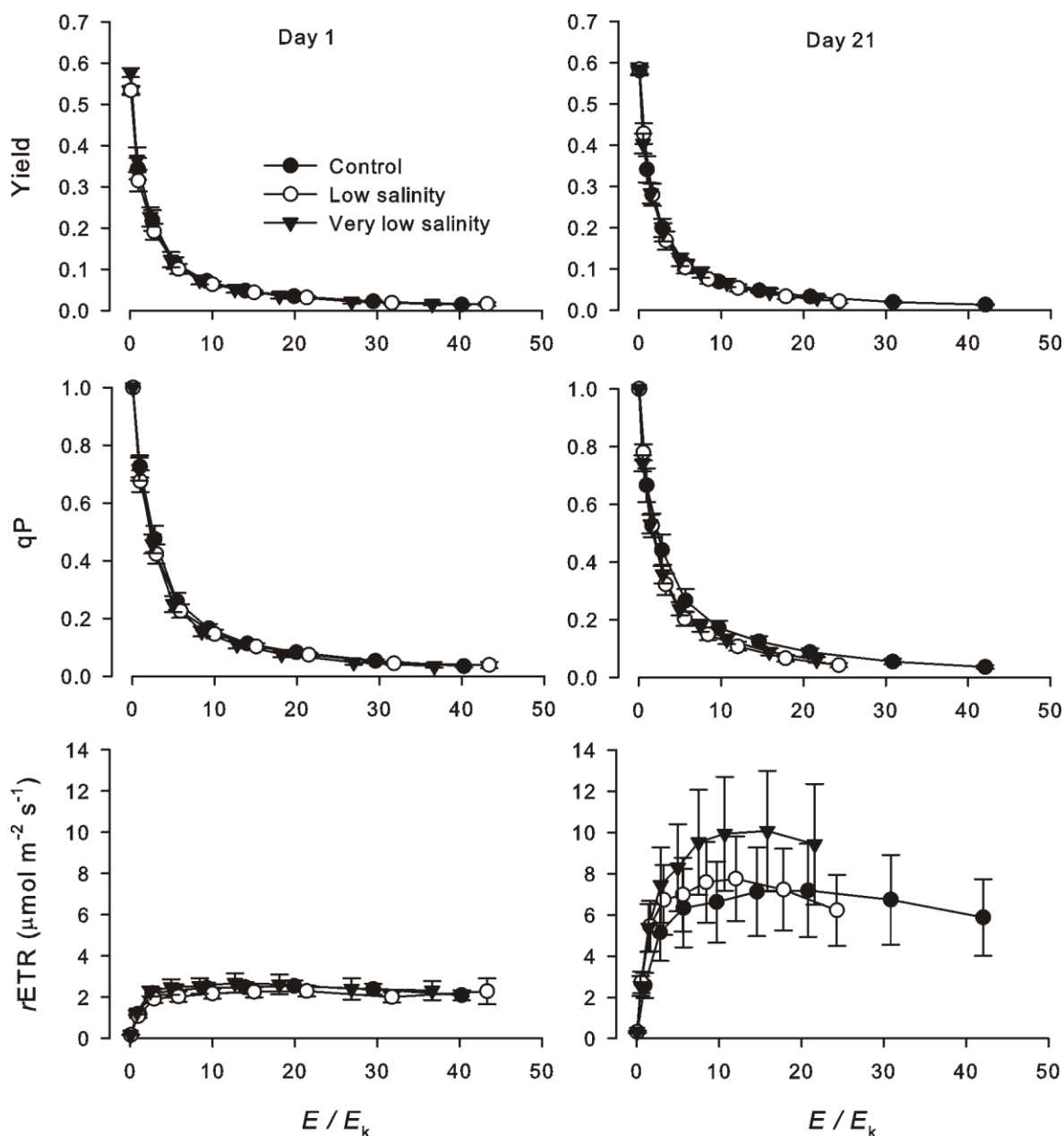


Figure 6.12 Photochemical response of *L. glaciale*.

Quantum efficiency (yield, top row), photochemical quenching (qP) (middle row) and relative electron transport rate (rETR, $\mu\text{mol electrons m}^{-2} \text{s}^{-1}$) (bottom row) at the start (left column) and end (right column) of a 21-day salinity reduction experiment. Treatments were control (black circles), low salinity (14 days at ~ 22 salinity, open circles) and very low salinity (14 days at ~ 12 salinity, black triangles). Data normalised to E/E_k and presented as mean \pm SE.

6.9.5 Photoprotective characteristics

As with the photochemical characteristics, a reduction in salinity did not induce a response in non-photochemical quenching (NPQ and qN) in *L. glaciale* (Figure 6.13). On day one, NPQ rose rapidly to ~ 0.4 during the first two light intensities, with a less steep increase in NPQ when $E/E_k > 10$ to a maximum of 0.7 - 0.8. A plateau in NPQ was not observed at the end of the RLC (Figure 6.13). A similar pattern was observed at day 21, although the magnitude of NPQ was reduced by 0.1 - 0.2 units. qN followed a similar pattern to NPQ on day one

(rapid increase to 0.50 - 0.55, followed by a continued rise to a maximum of ~0.6) and a small reduction in values by day 21 (<0.55). Little difference was observed between treatments, the exception being day one VL, where a lower 1-qN was measured, although this was characterised by a higher variability than the C and L treatment groups (Figure 6.13).

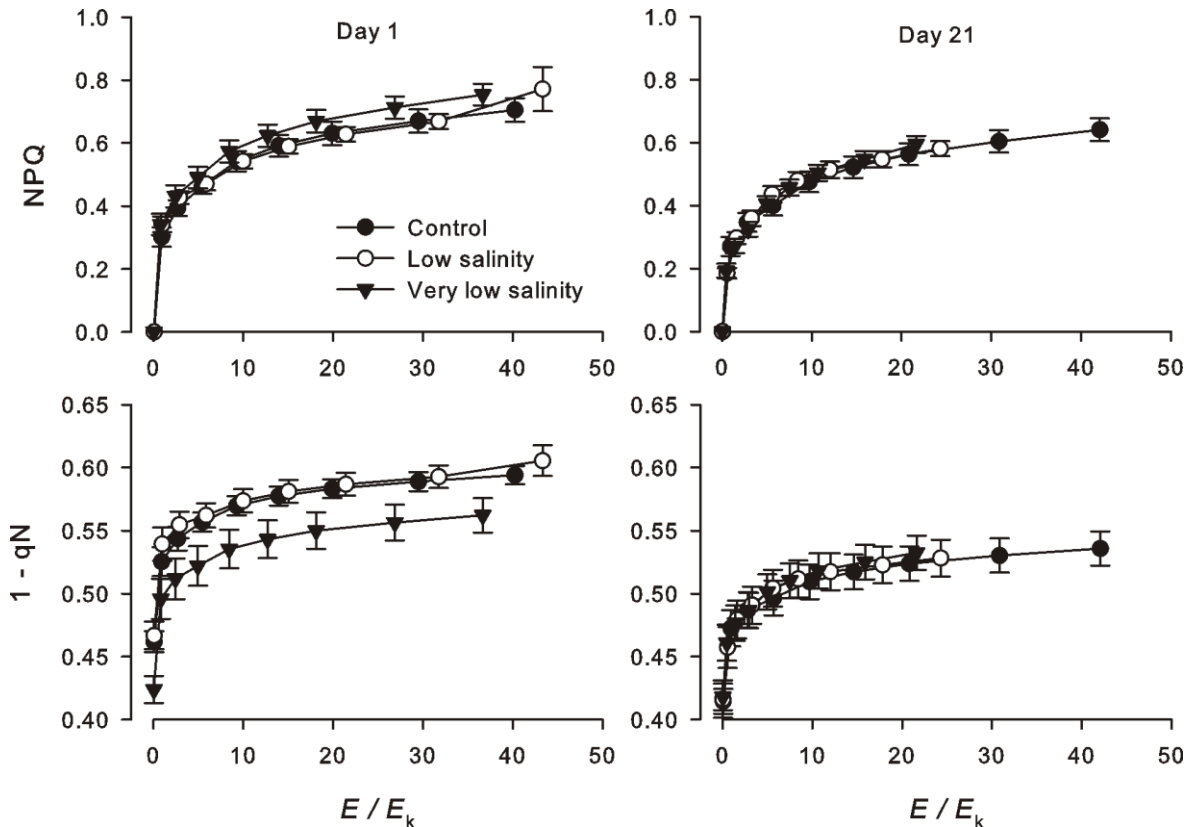


Figure 6.13 Photoprotective response of *L. glaciale*.

Non-photochemical quenching: NPQ (top row) and 1 - qN (bottom row) at the start (left column) and end (right column) of a 21-day salinity reduction experiment. Treatments were control (black circles), low salinity (14 days at ~22 salinity, open circles) and very low salinity (14 days at ~12 salinity, black triangles). Data normalised to E/E_k and presented as mean \pm SE.

6.9.6 Pigment composition

In reflectance data, a trough in reflectance indicates a peak in absorbance by pigments within the cells. The reflectance spectra from all treatments at day one and day 21 were similar in terms of peaks and troughs, although the absolute % reflectance varied (Figure 6.14). Peaks in absorbance occurred at wavelengths expected for Rhodophyta pigments: Chlorophyll-a (435 nm), phycoerythrin (488, 546, 576 nm), phycocyanin (613 nm) and allophycocyanin (652 nm). An absorbance peak at 405 nm was also observed in all spectra (Figure 6.14), but has not yet been identified. Little change in % reflectance was seen in C group throughout the experiment. However, by day

21, an 11% and 15% reduction in overall reflectance was observed in the L and VL treatments respectively (Figure 6.14). The variation in reflectance also increased with decreased salinity by the end of the experiment, as shown by the wider lines at day 21 in the L and VL treatments of Figure 6.14. The reflectance of the white tips ($n = 3$) was generally higher than the pink epithelia. This was, however, characterised by a relatively high variability, comparable to VL day 21. The spectral profile of the white tips was flatter, with less pronounced peaks and troughs, particularly for phycoerythrin (576 nm, Figure 6.14).

6.9.7 Epithelial cell morphology

The use of ESEM for secondary electron imaging prevented the formation of desiccation artefacts associated with thallus drying (see Chapter 6, ocean acidification). The calcite cell walls between each cell remained intact in all three treatments. However, sinking and deformation of the epithelial cell membrane was widespread in L and VL groups after 21 days of treatment (Figure 6.15).

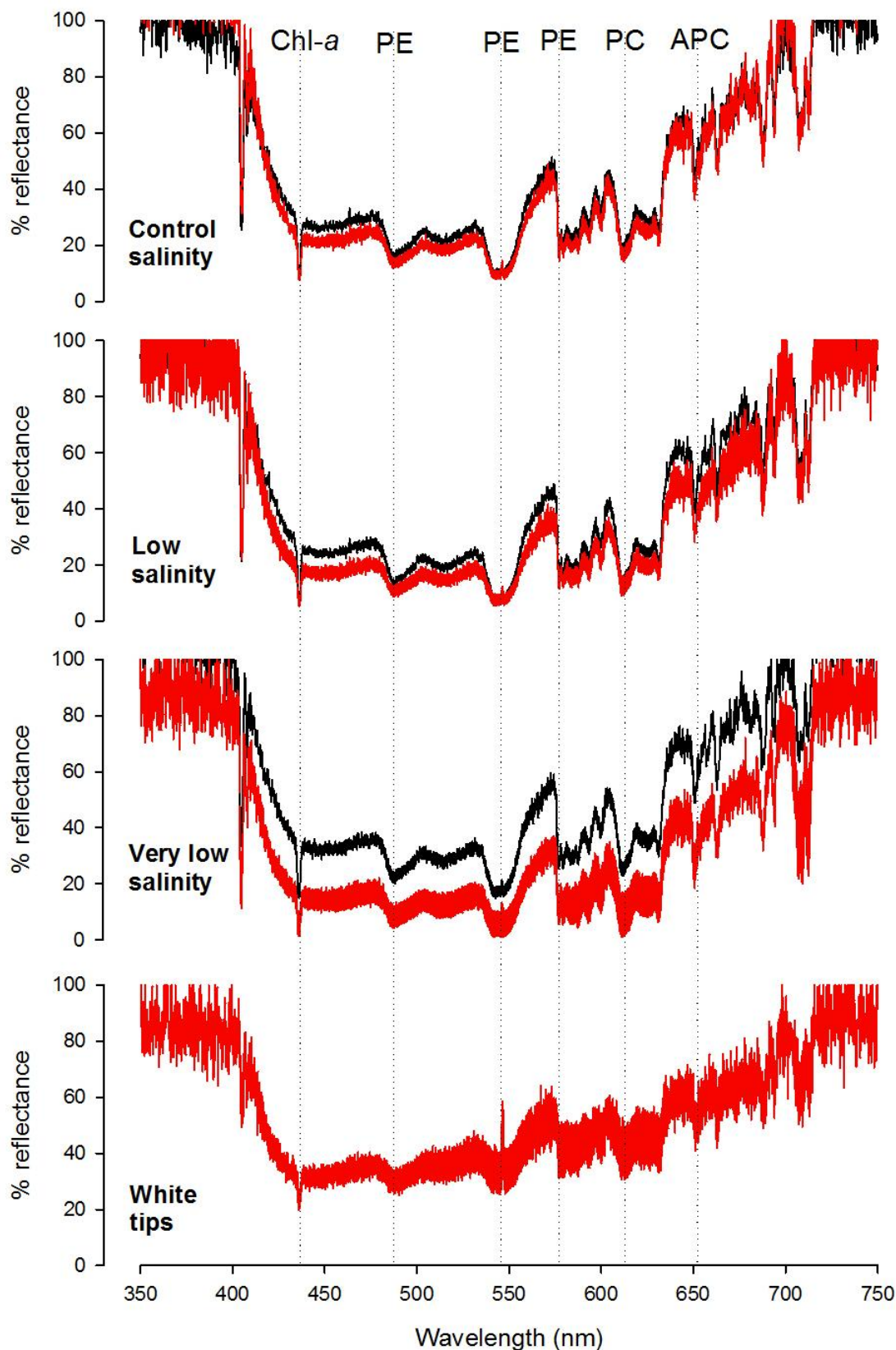


Figure 6.14 Pigment composition of *L. glaciale*.

Pigment composition determined by optical reflectance. Measurements taken at T0 (black line) and T21 days (red line) from samples at control (32), low (22) and very low (12) salinities. Bottom graph is reflectance from white thalli tips from the very low salinity treatment at T21. Width of the line represents mean \pm SD, $n=5$ for all except the white tips where $n=3$. Dotted lines indicate the absorption wavelength of the key Rhodophyta pigments: Chlorophyll-a (Chl-a), phycoerythrin (PE), phycocyanin (PC) and allophycocyanin (APC).

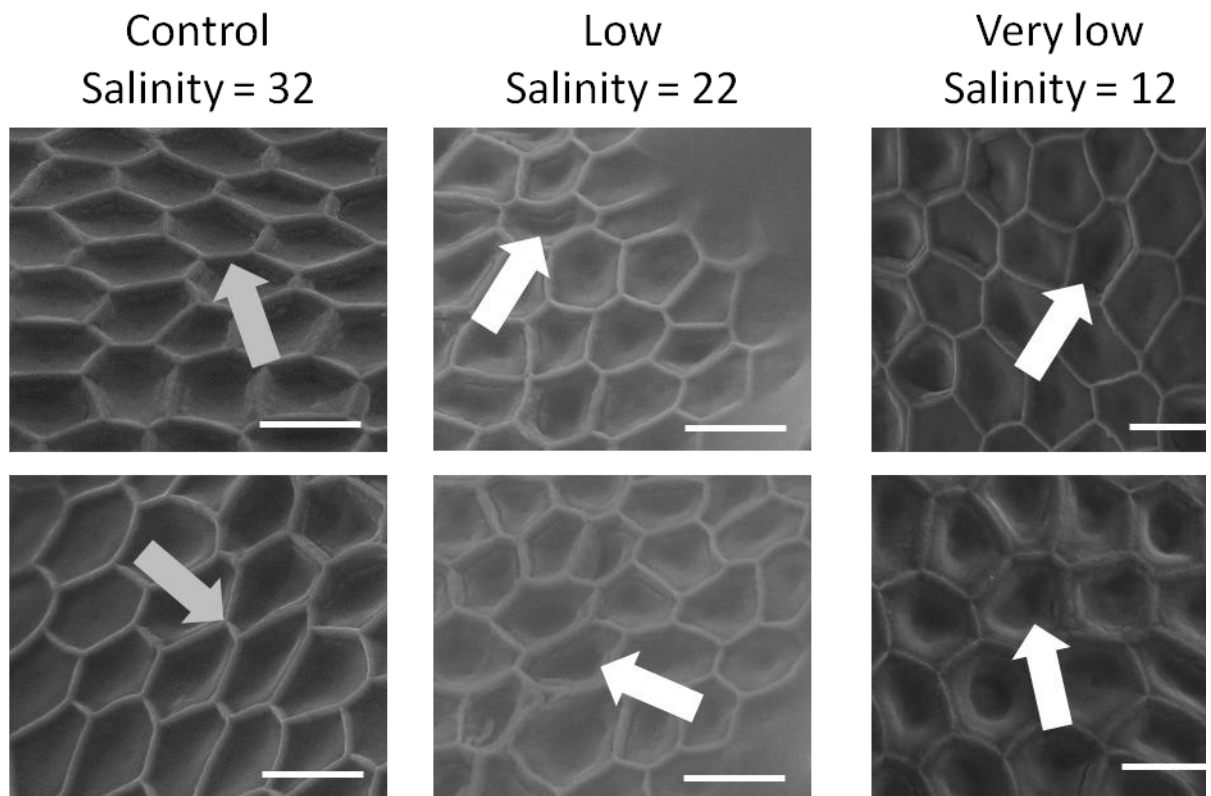


Figure 6.15 ESEM images of the epithelial cells of *L. glaciale*. Images produced after 21 days at control (salinity = 32 throughout), low (salinity = 22 for 14 days) and very low (salinity = 12 for 14 days). Each cell membrane is surrounded by a calcite cell wall (indicated by the grey arrows). Sinking and deformation of the cells occurred in the two low salinity treatments (examples indicated by the white arrows). Blurring in the corners of the low salinity images is surface water. Scale bar = 10 μm , magnification = 4000X.

6.10 Results: Acute salinity reduction, Chile

6.10.1 Abiotic parameters

Water temperature in the experimental tubs ranged from 17 - 19°C throughout the 64 hour experimental period (Figure 6.16a). Salinity in the control tubs remained at 35 throughout the experimental period (Figure 6.16b). The freshwater runoff simulation treatment was characterised by a salinity decline from 35 to ~27 in salinity over a nine hour period, followed by a 22 hour recovery to 35 (Figure 6.16b). Maximum PAR observed was at 14:00 on day one (25 $\mu\text{mol photons m}^{-2} \text{s}^{-1}$, Figure 6.16c).

6.10.2 Intracellular DMSP

Intertidal coralline algae contained significantly higher DMSPi concentrations compared to the subtidal samples throughout the experimental period (2.58 ± 0.45 and $1.35 \pm 0.81 \text{ mg g}^{-1}$ respectively, Figure 6.16d, $F_1 = 71.78$, p

< 0.001). There was no difference in DMSPi concentrations between the two treatments for intertidal or subtidal algae ($F_1 = 0.33$, $p = 0.564$), apart from T32 where intertidal DMSPi in the runoff treatment (mid recovery, salinity = 30) was higher than the intertidal control (3.41 ± 0.58 and $2.21 \pm 0.21 \text{ mg g}^{-1}$ respectively, Figure 6.16d).

6.10.3 Maximum quantum efficiency, F_v/F_m

Subtidal algae exhibited a significantly higher F_v/F_m than the intertidal algal type throughout the experimental period (Figure 6.16e, $F_1 = 16.37$, $p < 0.001$). Statistically, no difference between salinity treatment within algal groups was observed ($F_1 = 2.84$, $p = 0.093$), although the subtidal runoff group was significantly higher than the two intertidal groups (Tukey's comparison, $p < 0.001$).

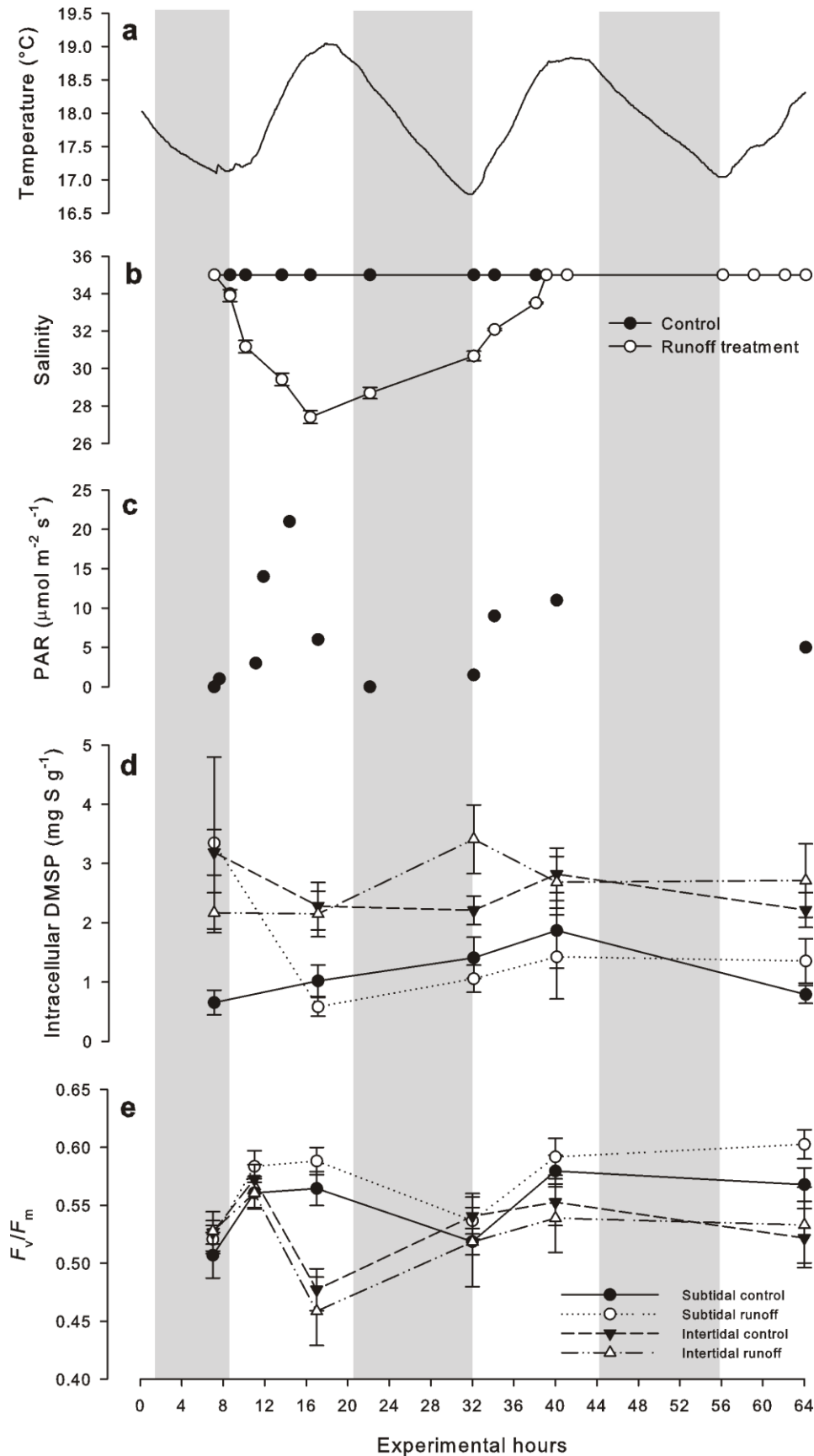


Figure 6.16 Results from the 64 hour runoff simulation experiment. (a) Water temperature ($^{\circ}\text{C}$), (b) salinity, (c) PAR ($\mu\text{mol photons m}^{-2} \text{s}^{-1}$), (d) DMSPi (mg S g^{-1}), (e) photochemical quantum efficiency (F_v/F_m) of subtidal (circles) and intertidal (triangles) coralline algae under control (solid symbols) and freshwater runoff (open symbols) conditions. Only F_v/F_m measurements that match DMSPi sampling are shown (see Figure 6.17). Grey shading bounds sunset and sunrise. Data presented as mean \pm SE.

6.10.4 Diurnal variation in F_v/F_m

Both algal types (subtidal and intertidal) were characterised by a general increase throughout the morning and a decrease in the evening (Figure 6.17). An exception to this was the 22:00 intertidal no sampling control group, although these measurements were associated with a high variability. The intertidal algae exhibited a larger range in F_v/F_m than the subtidal algae throughout the diurnal cycle (0.45 - 0.65 compared to 0.51 - 0.62, Figure 6.17). Sampling for DMSPi did not appear to result in any notable changes in F_v/F_m and little difference was observed between control and runoff groups (Figure 6.17).

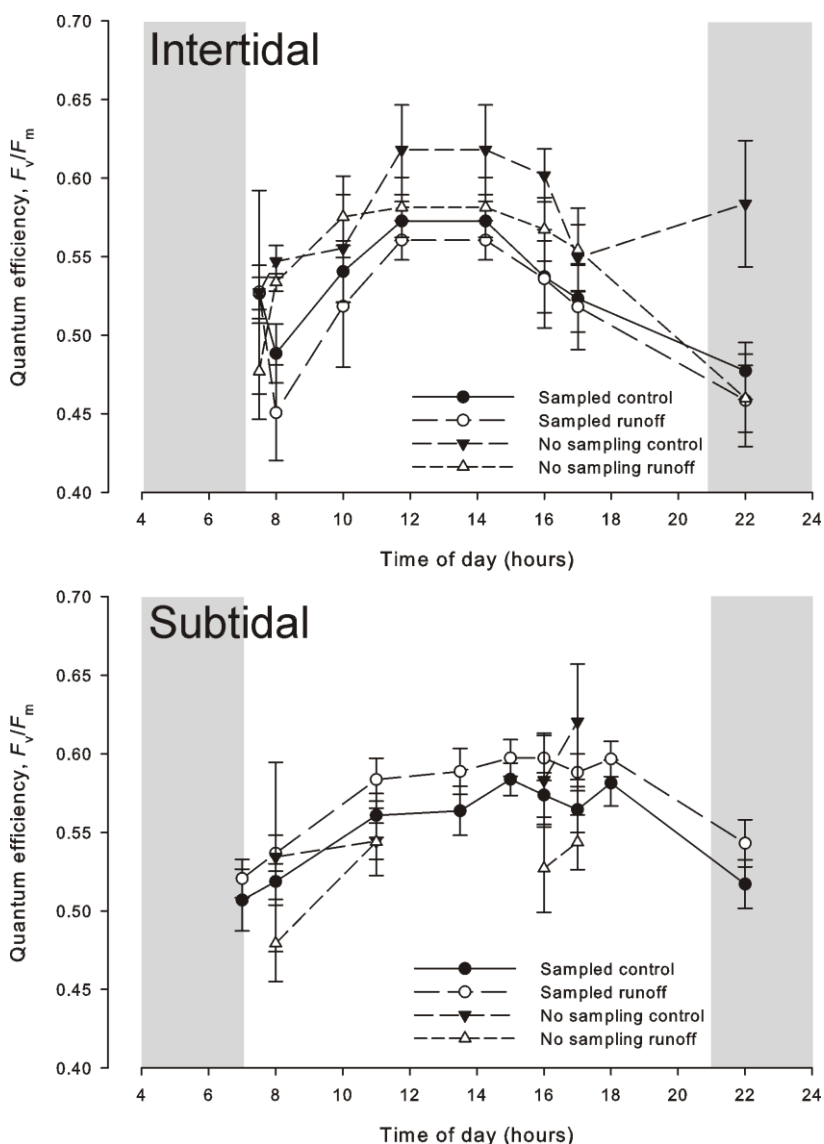


Figure 6.17 Diurnal variation in F_v/F_m in coralline algae at Las Cruces, Chile.

F_v/F_m from sunrise to sunset (bounded by the grey shading) for intertidal (top) and subtidal (bottom) coralline algae in control (solid symbols) and runoff (open symbols) treatments. Composite of measurements over several diurnal cycles. Algal samples which were also destructively sampled for intracellular DMSP (DMSPi) are denoted by circles ($n=20$); those not sampled for DMSPi are denoted by triangles ($n=3$). Data presented as mean \pm SE.

6.11 Discussion

Climate projections suggest that the coastal ocean may experience more severe and more prolonged periods of freshening in the future. Through two laboratory experiments, the effect of reduced salinity on DMSPi in coralline algae from two different climatic regimes was assessed. Such information is particularly useful when considering the widely accepted role of DMSP as a compatible solute in algal cells.

6.11.1 DMSPi as a compatible solute in red coralline algae

The results from the two experiments suggest that DMSPi is only important for controlling cellular osmotic balance over the longer-term - no effect was seen in the acute experiment in Chile and a significant down-regulation of DMSPi was only observed in Scotland after 14 days exposure. This will have reduced the effective salt concentration in the cell, equilibrating it to the surrounding environment. The observed down-regulation in DMSPi only after chronic exposure to salinity change is in agreement with previous literature (e.g. Stefels, 2000) and is to be expected given the energy outlay required to both produce and remove DMSP from algal cells. It appears that regulation of DMSP does not provide complete protection against osmotic stress: the presence of white branch tips in the VL treatment of the chronic experiment suggests that the cells had begun to lose their pigmentation, which may have ultimately led to cell death if treatment conditions had prevailed. However, the VL treatment was an extreme case, which may not be often observed in the natural environment.

Other secondary metabolites may have also been impacted by the reduced salinity regimes of the experiments, both at acute and chronic timescales. Betaine and sucrose are known to be important, short-term osmotic regulators in phytoplankton (Kirst, 1996), thus it may be proposed that coralline algae also use these compounds to maintain osmotic balance, at least when nitrogen is not limiting (which, in the coastal zone, is unlikely).

6.11.2 The impact of reduced salinity on photosynthesis

As with DMSPi, there appeared to be no effect of reduced salinity on the photosynthetic characteristics of the coralline algal species tested in this research. While coralline algae are generally considered to be low-light adapted (see Chapter 3), PAR levels during the acute experiment in Chile were probably lower than the natural conditions. This may have had some impact on the photosynthetic response and future work should address the impact of reduced salinity at light levels similar to the *in situ* conditions (which could not be measured during the experimental period).

In the L and VL treatments of the chronic experiment in Scotland, fouling by green algae was observed across the whole of the topsides of all thalli by the end of the experiment. Unfortunately, logistical constraints prevented the identification of this fouling species. However, photosynthetic measurements (from RLCs) remained similar for all treatments throughout the experiment, suggesting that fluorescence from *L. glaciale* remained dominant despite epithelial fouling. Had the foulers become dominant, a shift in photosynthetic characteristics may have been observed. Prolonged periods of fouling may be severely detrimental to red coralline algal thalli, reducing light quality and increasing competition for nutrients. Red coralline algae are, however, known to be able to survive periods of sedimentation, with reduced light availability and water movement (Rix et al., 2012). Thus, thalli may be able to recover from the observed fouling if salinities return to normal before cell senescence occurs. This could be established through further experimental work that included a recovery phase within the experimental design. A shift in the microbial community associated with the thallus surface, as a direct result of the reduction in salinity or a change in antifoulant compound production by the coralline algae may have been the trigger for the settling and growth of macrofoulants. Characterisation of the associated microbial community during environmental change experiments may indicate 'early warning' signs of thallus stress and impending fouling by other macroalgae.

6.11.3 Characterisation of red coralline algal pigments in *L. glaciale*

This is the first time that the pigment composition of *L. glaciale* has been characterised, and the Ocean Optics optical reflectance technique proved suitable for pigment identification in this alga. This study confirmed the presence of the four primary pigments associated with Rhodophyta in *L. glaciale*: Chlorophyll-*a*, phycoerythrin, phycocyanin and allophycocyanin, all of which remained detectable throughout the experiment, suggesting that photosynthetic ability was maintained, backing-up the fluorescence results. The reduction in reflectance by the end on the experiment in the L and VL treatments quantifiably confirms the presence of surface green and brown macrofoulers on the surface of *L. glaciale*, but the Rhodophyta pigments remained dominant.

6.11.4 The effect of reduced salinity on cell morphology

The use of ESEM imaging, although technically challenging, was extremely useful in comparing surface cell morphology of *L. glaciale* in the chronic experiment because of the extent of drying artefacts associated with traditional SEM practices (see Chapter 7, ocean acidification).

Cell expansion in response to rising osmotic pressure may be restricted in coralline algae due to their highly calcified structure. Thus, coralline algal cells may burst the high osmotic pressure of a low-salinity environment. Thalli of *L. glaciale* exposed to reduced salinity for a 21 day period exhibited significant amounts of cell deformation and sinking. The large shift in osmotic potential relative to the control treatment may have caused the cells to stretch and / or burst causing the observed changes in surface morphology. If the cells were damaged to such an extent as to compromise the cell membrane, intracellular substances, including DMSP, would be able to escape into the water column. Thus, damage to cell membranes may be a contributing factor to the observed reductions in DMSPi in the VL treatment. All observations are, at present, qualitative only. Quantitative SEM assessment (e.g. number of damaged cells per unit area) would improve conclusion made regarding the effects of reduced salinity on the epithelial cell morphology of *L. glaciale*.

An increase in osmotic potential may have also impacted the internal cell structure of the thalli as these are connected to the outer epithelial cells via pores and pit connections (Foster, 2001; Freiwald and Henrich, 1994; Bosence, 1976). These internal cell connections are believed to act as pathways for metabolite distribution around the thallus and as storage areas for starch reserves (Foster, 2001). Thus, changes in the connectivity of this network might significantly impact an alga's ecophysiology and survivability. The internal cell structure (elemental composition and morphological) could be investigated using quantitative SEM and Raman spectroscopy techniques.

6.11.5 Diurnal variation in quantum efficiency

As presented in Chapter 3, coralline algae can exhibit a clear diurnal response in quantum efficiency, characterised by a midday suppression in F_v/F_m . A diurnal response was observed in the two Chilean algal species of the acute experiment, although these species were characterised by a midday maximum - the reverse of what was expected. A similar pattern was observed in the lichen *Anaptychia ciliaris* under shade conditions (Valladares et al., 1995), suggesting that the low light regime of the acute salinity reduction experiment may have affected the photochemical response of the coralline algae. Under shade conditions, F_v/F_m may be increased during the day by reducing F_o in an attempt to maximise the available photon energy.

6.11.6 Species-specific natural variability

DMSPi was significantly higher in the intertidal algae than the subtidal algae. The production of DMSP requires a lot of energy, thus it may be beneficial to maintain low DMSPi concentrations if DMSP is not often required. However, DMSP has many intracellular functions other than for osmotic balance, for example as an antioxidant (Sunda et al., 2002), a grazing deterrent (Van Alstyne et al., 2001) or cryoprotectant (Karsten et al., 1996). The functional priority of DMSP within algal cells is not known, thus while low DMSPi concentrations may save energy, external environmental factors may necessitate the need for high DMSPi concentrations. In Chile, the antioxidant function of DMSP may be important as UV radiation is high (Huovinen et al., 2006). Organisms directly exposed to the high radiation at, for example, low tide, will have evolved

defence mechanisms to minimise oxidative damage (Huovinen et al., 2006). Incoming radiation may also be enhanced in shallow waters by wave refraction and light flashes from the sea surface (Payri et al., 2001), further increasing the intertidal algae's exposure to harmful UV rays. Subtidal algae will be exposed to far lower levels of UV radiation and overall irradiance. Unfortunately, it was not possible to quantify the UV exposure to the algae *in situ* but previous work have suggested a down-regulation of DMSP in temperate coralline algae in response to high light (Rix et al., 2012). It may be postulated that DMSPi regulation in the Chilean intertidal algae is prioritised towards antioxidant requirements rather than salinity regulation.

The Chilean intertidal algae also exhibited a larger range in diurnal F_v/F_m , suggesting a wider ability to photoacclimate to changing light regimes which may be experienced *in situ* in the intertidal zone. The subtidal algae will experience a smaller range in natural diurnal radiation, thus forgoing the need for a highly reactive photoacclimation strategy, whereas an efficient photoprotective response by the intertidal algae would help to minimise photosystem damage in the intertidal zone where light and UV radiation are higher.

6.12 Conclusions

Storm runoff events and prolonged coastal freshening are projected to become more extreme in the future due to global change. Based on two laboratory experiments, an environment with reduced salinity does not seem to affect intracellular DMSPi concentrations or photosynthetic characteristics in coralline algae unless the conditions are maintained for at least 14 days. This is despite the widely accepted intracellular role of DMSP as a compatible solute in algal cells. However, surface fouling and epithelial cell deformation was observed following longer-term exposure to reduced salinity; factors that may need to be overcome in areas of high freshwater input. Interestingly, results suggested that DMSP's other cellular functions (e.g. as an antioxidant) may be prioritised under certain environmental conditions. Such 'functional prioritisation' of DMSPi is yet to be investigated in detail in macro- or microalgae.

7

Environmental pressures: Ocean acidification

Oceanic pH has begun to decrease from pre-industrial levels as more carbon dioxide (CO₂) dissolves into the oceans and is projected to continue to decrease in the future. This may have significant morphological and biochemical effects on marine calcifying organisms. The physiological effect (e.g. calcification and growth rates) of reduced pH on marine calcifiers is relatively well understood, but the impact on biogeochemical cycles, particularly the sulphur cycle, has not been well researched.

7.1 Ocean acidification

The pH of the oceans is regulated by a carbonate equilibrium that is driven by the dissolution of atmospheric CO₂ into the oceans (Figure 7.1). Between 30 - 50% of the CO₂ released from the burning of fossil fuels, cement production and deforestation have been absorbed by the oceans (Sabine et al., 2004). Once dissolved in the oceans, CO₂ forms carbonic acid (H₂CO₃), which can dissociate into (bi)carbonate (HCO₃⁻ and CO₃²⁻) and hydrogen ions (H⁺) (Figure 7.1). An increase in atmospheric CO₂ causes a shift in the oceanic carbonate equilibrium, favouring the formation of H⁺, which controls oceanic pH by the relationship:

The bicarbonate ion (CO₃²⁻) may be released by the dissolution of calcium carbonate (Figure 7.1), providing CO₃²⁻ ions to the carbonate buffer system. The

carbonate saturation state (Ω) describes the thermodynamic potential for calcium carbonate to precipitate or dissolve and is defined by:

Where K is the carbonate mineral solubility product, which is specific to each carbonate polymorph: low-Mg calcite is the most thermodynamically stable, followed by aragonite. High-Mg calcite is the least stable polymorph of calcium carbonate found in the shells and skeletons of some marine organisms, including coralline algae.

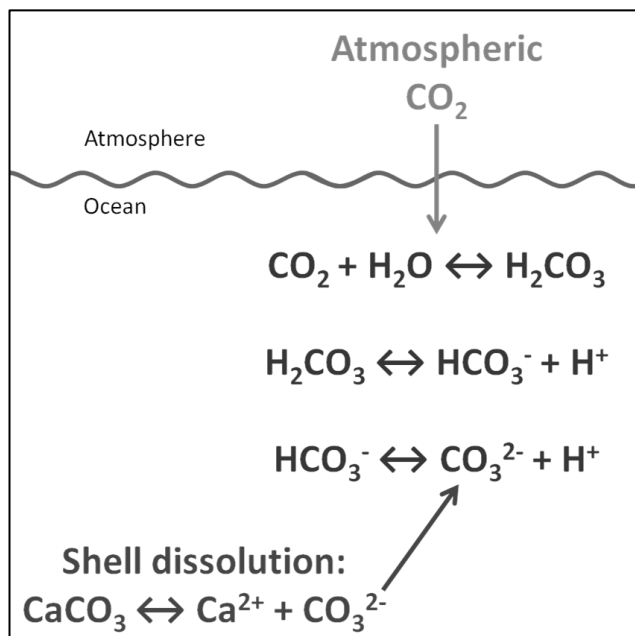


Figure 7.1 The oceanic carbonate equilibrium.

Since the Industrial Revolution, atmospheric CO_2 has increased from 280 ppm to ~390 ppm (Figure 7.2) (NOAA, 2012c), the highest levels for 650 000 years (IPCC, 2007). Since 2000, the average rate of increase in atmospheric CO_2 has been $\sim 2 \text{ ppm yr}^{-1}$; atmospheric CO_2 at Mauna Loa, Hawaii, in February 2013 was 396.80 ppm, compared to 393.54 ppm in February 2012 (NOAA, 2012c).

A 0.09 unit drop in the pH of the surface ocean has been observed in Hawaii since 1990 (Figure 7.2) - a process known as ocean acidification (OA). It is projected that continued anthropogenic emissions of CO_2 will cause the pH of the oceans to drop by 0.3 - 0.5 units by 2100 (Caldeira and Wickett, 2005), with potentially detrimental effects on calcifying marine organisms. Over geological

timescales, the dissolution of oceanic carbonate (e.g. shells) may balance the equilibrium shift and lower H^+ concentrations (Figure 7.1), but this is not expected to be fast enough to counteract the effect of anthropogenic CO_2 emissions (Basso, 2012). Cold polar waters are projected to be most rapidly affected, becoming under-saturated with respect to aragonite by 2100 (Meehl et al., 2007).

Present-day conditions already represent an extreme environment for calcifying organisms compared to the past 800 000 years. By analysing air bubbles trapped in Antarctic ice cores, it has been revealed that interglacial - glacial cycles only caused oceanic pH to vary between 8.1 - 8.3 (Luthi et al., 2008), a stability that has probably been maintained for ~2 million years (Pelejero et al., 2010). Oceanic pH has not been at the level predicted for 2100 for ~40 million years (Tripathi et al., 2009; Pearson and Palmer, 2000). The rate of change projected for the next century is ~100 times faster than that experienced during glacial terminations (Pelejero et al., 2010), raising concerns about the ability of calcifying organisms to adapt to such rapidly changing conditions.

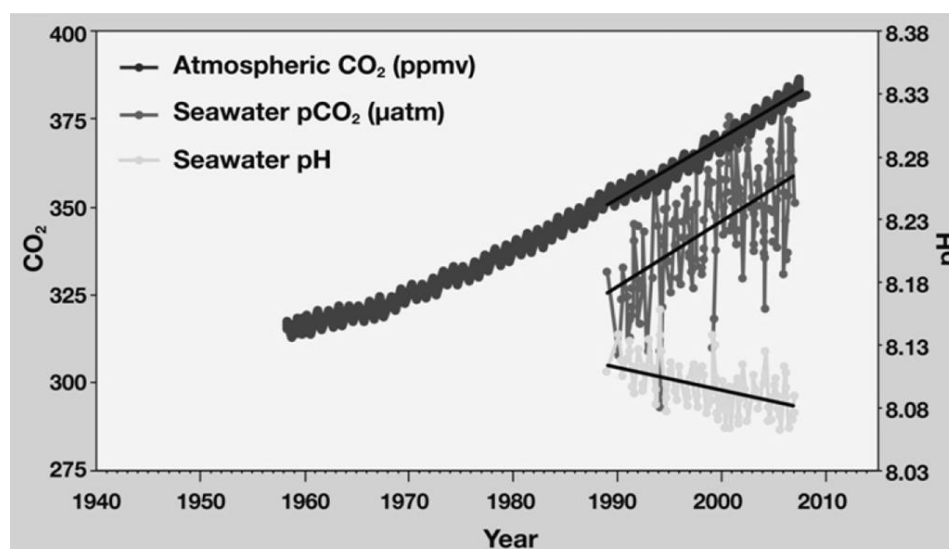


Figure 7.2 Observed atmospheric and oceanic CO_2 and oceanic pH. Data from the Mauna Loa Observatory, Hawaii. Source: NOAA (2012b).

7.1.1 Natural variability in the coastal ocean

The coastal ocean is characterised by more extreme natural variability in pH compared to the open ocean and is related to diurnal and seasonal cycles of biological and physical processes (Pelejero et al., 2010). The effects of OA will

be ‘superimposed on the natural variability of the ocean carbonate system, resulting in new extremes and ranges of oceanic pH’ (Pelejero et al., 2010). Thus, it is important to understand current natural variability in the coastal ocean in order to accurately project the effects of a future OA scenario.

7.1.1.1 CO₂ vents

Shallow marine CO₂ vents have been used as *in situ* field sites for high CO₂ experimentation (e.g. Ischia island, Italy; Hall-Spencer et al., 2008). A reduction in the abundance of calcified organisms (e.g. urchins and calcified algae, both high Mg-calcite) and an increase in the abundance of non-calcified organisms (e.g. fleshy macroalgae and seagrass) has been observed in areas where pH was often very low (Porzio et al., 2011; Hall-Spencer et al., 2008). However, the pH across CO₂ vent regions is highly variable over short temporal scales due to changes in CO₂ seepage rates and water circulation. This makes it difficult to project effects from vent studies to an OA scenario where pH is predicted to be low but (relatively) stable (Hall-Spencer et al., 2008; Riebesell, 2008).

7.1.1.2 Upwelling zones

Eastern boundary upwelling systems (EBUS, e.g. the California Current and Canary Current systems) may expose shelf-sea and coastal organisms (pelagic and benthic) to waters under-saturated with respect to calcite and aragonite (Gruber et al., 2012; Gruber, 2011; Hauri et al., 2009; Feely et al., 2008) and lead to a net sea - air flux of CO₂ (Lachkar and Gruber, 2013). An increase in the frequency of upwelling-favourable winds because of increased land-sea gradients has been observed (Bakun, 1990) and is predicted to continue to increase in the future (Diffenbaugh et al., 2004; Snyder et al., 2003). Along the California Current system, under-saturated waters were at a depth of 40 - 120 m in most areas but reached the surface in one area (Feely et al., 2008). Under both high (A2) and low (B1) IPCC emission scenarios, aragonite under-saturation is projected to occur in the upper 60 m throughout the summer along the California current system within the next 30 years (Gruber et al., 2012). By 2050, the aragonite saturation state (Ω_{Ar}) in nearshore waters (within 10 km of the coast) will be less than 1.5 throughout the year, with much of the area less than one (i.e. under-saturated) (Gruber et al., 2012). At saturation states <1,

dissolution of carbonate minerals is thermodynamically favoured. This will have implications for benthic calcifying marine organisms such as coralline algae, which grow from the intertidal zone to depths of 250 m (Foster, 2001).

7.1.1.3 Coral reefs

It has been suggested that coral reefs may act as an alkalinity sink and potential atmospheric CO₂ source due to carbonate precipitation and land run-off (Suzuki and Kawahata, 2003). In terms of carbonate chemistry, spatial heterogeneity may be observed on coral reef systems, with reef flats and lagoons more variable than fringing forereefs, due to biological (benthos composition) and physical (wave action and residence time) parameters (Gray et al., 2012; Zhang et al., 2012; Anthony et al., 2011; Kleypas et al., 2011; Smith and Price, 2011; Gagliano et al., 2010; Kleypas and Langdon, 2006). Similarly, surface *p*CO₂ in atoll and barrier reef lagoons is often higher than offshore waters in the Indo-Pacific (Suzuki and Kawahata, 2003). Net calcification may be observed during the day on coral reefs, whilst net dissolution is often observed at night (Zhang et al., 2012; Yates and Halley, 2006; Chisholm, 2000), affecting the carbonate chemistry of the water column. Seasonal patterns in carbonate chemistry have also been observed (Bates et al., 2010), but this may be seasonally de-coupled from reef calcification due to the maintenance of threshold saturation levels during the winter (Falter et al., 2012). Spatial variability may also be observed within the reef, with those dominated by filamentous turf algae having the highest pH (i.e. least acidic; Smith and Price, 2011; Gagliano et al., 2010). It has been suggested that corals which are exposed to a natural variability in temperature may be more thermally tolerant than those from stable conditions (Oliver and Palumbi, 2011). Thus, it may be expected that calcifying reef organisms (e.g. corals or calcifying algae) may be more tolerant of carbonate system variability in the more variable reef flats and lagoons compared to the forereef.

7.1.2 Carbon capture and storage

In order to reduce the rate of rise in atmospheric CO₂, a number of mitigation strategies have been considered. This includes carbon capture and storage (CCS), where CO₂ is pumped into bedrock cavities (from gas and oil

extraction for example), both on land and in the oceans. However, concerns have been raised over the risk of oceanic CO₂ leakage from CCS infrastructure (Blackford et al., 2009). Modelling of chronic and acute CO₂ release scenarios suggest that, on a regional scale (10s km), the effects of CCS leakage will be minor in comparison to OA effects (Blackford et al., 2009), but effects may be substantial on a finer scale. However, organism dynamics under these acute high-CO₂ scenarios have yet to be fully coupled with oceanographic CCS models so the impact of CCS leaks on marine ecosystems is still largely unknown (Blackford et al., 2009). In May 2012, an *in situ* experiment was conducted on the west coast of Scotland to simulate the release of CO₂ from a CCS leak (<http://www.bgs.ac.uk/qics/home.html>). The impact of this experiment on the benthic ecosystem has not yet been published but results are expected from 2013.

7.1.3 Ocean acidification and calcifying macroalgae

Calcifying macroalgae habitats (e.g. maerl beds, coral reefs, coralligène) can act as a sink for atmospheric CO₂ (Bensoussan and Gattuso, 2007; Short et al., 2007). However, their response to changing environmental conditions, such as that posed by OA, may be species and location specific (Nelson, 2009), highlighting the need for a continued effort to understand the potential effects of global change on calcifying benthic macroalgae.

The response of calcified organisms to projected OA is varied. Organisms whose carbonate structure is not covered by an external organic layer (e.g. conchs, periwinkles and scallops) appear to be least resilient to elevated CO₂ conditions (Ries et al., 2009) whereas organisms that can maintain a high pH calcifying fluid (e.g. corals) appear to be more resistant to elevated CO₂ levels (Ries et al., 2009). Photosynthetic organisms (e.g. macroalgae) may benefit from elevated CO₂ conditions as they utilise CO₂ for photosynthesis (Ries et al., 2009), which might lead to a phase shift towards algal dominance on coral reefs (Hoegh-Guldberg et al., 2007).

The negative effect of low pH / high CO₂ on coralline algal calcification has been well reported; the high-Mg calcite skeleton of red coralline algae (typically 7.7 - 28.8 mol%, Kamenos et al., 2009; Chave, 1954) makes these algae

particularly susceptible to high CO₂ compared to other marine calcifiers (Martin et al., 2008). The concentration of Mg in the calcite skeleton is proportional to water temperature (Kamenos and Law, 2010; Kamenos et al., 2009; Kamenos et al., 2008a) and, at geological timescales, the concentration of Mg in the water column (Stanley et al., 2002). During the winter, net calcification in the temperate / polar coralline alga *Lithothamnion glaciale* was significantly reduced at high CO₂ (750, 950 and 1500 ppm), whilst in summer, only the very high CO₂ treatment (1500 ppm) induced a decrease in calcification (Büdenbender et al., 2011). Growth rates of *L. glaciale* may also be reduced at high CO₂ (1020 µatm), although the microstructure may be affected at much lower (589 µatm) CO₂ levels (Ragazzola et al., 2012). Calcification in *Hydrolithon* sp. may be reduced after just five days at high CO₂ (0.09mbar CO₂-enriched air, Semesi et al., 2009). After a 1 year exposure to high CO₂ conditions (700 ppm), net dissolution exceeded net calcification in *Lithophyllum cabiochae* (Martin and Gattuso, 2009). Furthermore, when combined with high temperature (+ 3°C) more algal necroses, death and dissolution were observed (Martin and Gattuso, 2009). Spore production, growth and recruitment of the Corallinaceae is also inhibited by high CO₂ conditions (550 - 760 ppm, Cumani et al., 2010; Jokiel et al., 2008; Kuffner et al., 2008). Calcification of the geniculate coralline alga *Corallina pilulifera* may be inhibited under high CO₂ conditions (1250 ppm) (Gao et al., 1993). High CO₂ (1000 ppm) and UV radiation (particularly UVB) may also act synergistically to inhibit growth, photosynthetic O₂ evolution and calcification in *Corallina sessilis* (Gao and Zheng, 2010).

Padina spp. (Ochrophyta: Dictyoaceae), one of only two known calcifying brown algae, appear to thrive in CO₂ vent systems, albeit with reduced calcification in the more acidified areas (Johnson et al., 2012). This apparent success has been attributed to the lower abundance of grazing sea urchins in acidified areas and enhanced photosynthesis from higher CO₂ availability (Johnson et al., 2012). Red coralline algae, despite their high Mg content, may also take advantage of an increase in CO₂ for photosynthetic benefit (606 and 903 ppm, Ries et al., 2009). Experimental reef studies (which were dominated by macroalgae) suggest that although calcification appears to decline under high CO₂ conditions, net organic production does not change (Langdon et al., 2003; Langdon et al., 2000). However, current studies are not wholly conclusive and

more detailed investigations into the biochemical and morphological effects of low pH / high CO₂ on calcifying benthic macroalgae are still required.

7.1.4 DMSP and ocean acidification

Only one paper is currently available on the effect of OA on the secondary metabolite dimethylsulphoniopropionate (DMSP) in macroalgae: Intracellular DMSP (DMSPi) concentrations were not affected by elevated CO₂ in the green macroalgae *Ulva lactuca* and *U. clathrata* (Kerrison et al., 2012). The effects of high CO₂ (low pH) on phytoplankton DMSP production are varied. Higher dissolved dimethylsulphide (DMS) concentrations were observed under high CO₂ (760 / 1150 ppm) (Wingenter et al., 2007b) and an up-regulation of DMSPi has been observed in *Emiliana huxleyi* under high temperature and CO₂ (+4 °C and 1000 ppm: Arnold et al., 2012; +6 °C, 790 ppm: Spielmeyer and Pohnert, 2012). In contrast, dissolved DMS and DMSP concentrations were reduced under high CO₂ (750 ppm) (Avgoustidi et al., 2012; Hopkins et al., 2010) and DMSPi was reduced in *Thalassiosira pseudonana* (diatom) and *Phaeodactylum tricornutum* (prymnesiophyte) under high temperature (+6 °C) and CO₂ (790 ppm) (Spielmeyer and Pohnert, 2012). Further, Vogt et al. (2008) has recorded no overall change in dissolved DMSP or DMS under high CO₂ (700 / 1050 ppm). The varying results have been attributed to the different phytoplankton communities used in each study (Hopkins et al., 2010). These species-specific DMSP responses are also likely to extend to other algae, highlighting the need for detailed studies assessing the impact of low pH / high CO₂ on calcifying macroalgae, a poorly-researched group of macroalgae.

7.2 Aims of this chapter

Previous OA studies on calcifying algae have suggested that they may have some resilience towards low pH / high CO₂ conditions. The impact low pH may have on DMS/P production in coralline algae is unknown and requires testing, especially given the apparently species-specific response of phytoplankton to DMSP production under OA scenarios. Laboratory-based experiments, whilst providing useful information, are not representative of the natural environment due to the problems of replicating natural conditions in a controlled laboratory environment. Different responses may thus be observed in field-based OA

conditions compared to laboratory studies. In this chapter, laboratory and field studies were used to assess the impact of OA on DMSPi in calcifying algae.

Specifically this included:

1. A controlled laboratory-based OA experiment, designed to assess the impact of OA and sudden increases in $p\text{CO}_2$ (e.g. from a CCS leak or upwelling event) on DMSPi and epithelial cell morphology in the temperate free-living coralline alga *Lithothamnion glaciale*.
2. *In situ* field measurements of DMSPi in tropical calcifying macroalgae on a fringing coral reef in the Red Sea, Egypt over a diurnal cycle, from the environmentally stable reef crest and more variable reef flat (see section 7.1.1.3).

It was hypothesised that DMSPi would increase in *L. glaciale* under high $p\text{CO}_2$ conditions and that the epithelial cell morphology would be affected by the low pH environment. In the field, it was hypothesised that algae in the more variable reef flat would continually regulate DMSPi in response to the changing environment.

7.3 Methods: Laboratory study, UK

7.3.1 Experimental set-up

Thalli (40 - 60 mm in diameter) were collected by hand using SCUBA from Loch Sween (56° 01.99'N, 05° 36.13'W) in November 2009 from a depth of 7 m. Thalli were maintained in aerated seawater at approximately 10°C during transportation to Plymouth Marine Laboratory (PML) and were transferred to a 3000 litre flow-through seawater system within one day of collection. Approximately 400 g of *L. glaciale* thalli were separated into 12 experimental microcosms (6 L volume, 280 x 190 x 160 mm), acting as pseudoreplicates. Thalli were acclimated to the system for one week (water temperature $11.63 \pm 0.32^\circ\text{C}$, salinity 34.9 ± 0.36 [$X \pm \text{SD}$]), prior to the commencement of the experiment. The experiment was managed and maintained by the benthic research team at PML.

Initially, two pH treatments over an 80-day experiment were planned: a control (normal seawater pH ~ 8.1) and a low-pH treatment (~7.7, representing

IPCC 2100 projections). However, midway through the experiment, a failure in the CO₂ delivery system led to a sudden decline in pH in half of the low-pH treatment mesocosms. To take this unintended experimental factor into account, for the purposes of data analysis three pH conditions over the 80-day period were considered, using the method developed by Findlay et al. (2008) detailed below (Figure 7.3): control (pH 8.18, n = 6), low pH (pH 7.70, n = 3) representing the A1F1 IPCC year 2100 scenario (IPCC, 2007) and low, acutely spiked pH (pH 7.75 with an additional reduction in pH to 6.6 on day 47, n = 3). The acute spiked treatment was regarded as being representative of the sudden reduction in pH associated with a sudden injection of CO₂ from a CCS leak, natural CO₂ vent systems or areas of upwelling (see Table 7.1 for carbonate chemistry parameters).

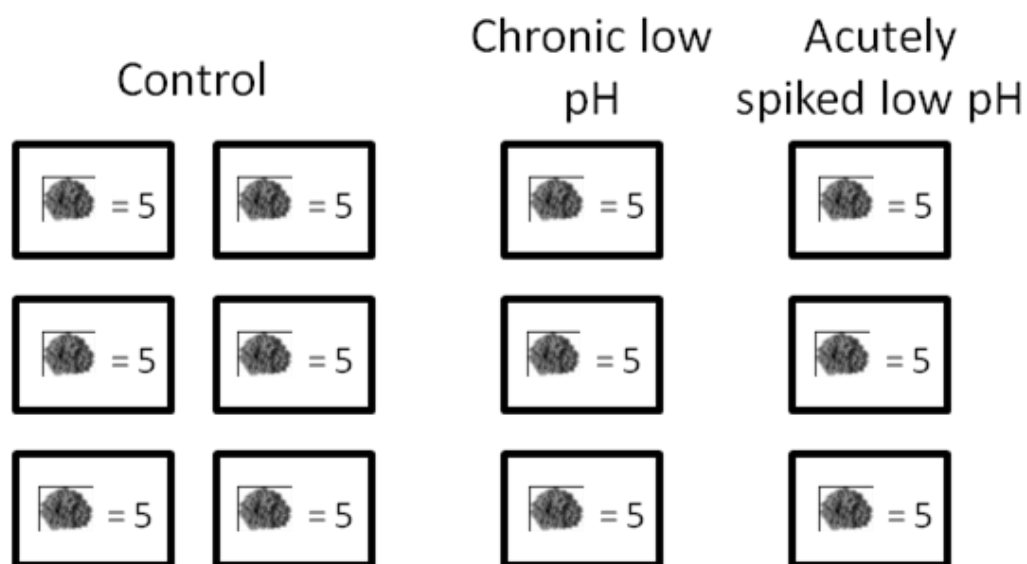


Figure 7.3 Mesocosm set-up for laboratory OA experiment.

Experiment was run for 80 days with three pH treatments: control (pH 8.1), chronic low (pH 7.7) and acutely spiked low (pH 7.7, plus a decrease to 6.6 from day 47 – 51). Pseudo-replication was accounted for by taking the mean of each mesocosm.

Low pH was achieved by aerating each mesocosm with ambient or pre-mixed high-CO₂ air, allowing water pCO₂ levels to equilibrate. Reduced pH levels in two low pH treatments were achieved by gradually increasing the bubbling of CO₂ in the mesocosms over a ten day period to minimise shock responses. Seawater temperature, salinity (WTW LF187 combination temperature and salinity probe), pH (Metrohm, 826 pH mobile with a Metrohm glass electrode) and dissolved oxygen (1302 Oxygen Electrode, Strathkelvin Instruments) were monitored daily, while nutrient concentrations (nitrate, nitrite, phosphate, silicate and ammonium) and total alkalinity were monitored weekly by the PML

benthic and nutrient teams to ensure seawater quality was maintained. Mesocosms were maintained at ambient temperature (11.63 ± 0.32 °C, mean \pm SD) and light ($90 \mu\text{mol photons m}^{-2} \text{ s}^{-1}$; 10h light: 14 h dark). Nutrients samples were analysed by an autoanalyser (Branne & Luebbe Ltd., AAIII) using standard methods (Jia-Zhong and Chi, 2002; Kirkwood, 1989; Mantoura and Woodward, 1983; Grasshoff, 1976; Brewer and Riley, 1965). Alkalinity was measured by poisoning 100 ml water samples with HgCl_2 according to Dickson et al. (2007) then analysing via potentiometric titration using an Apollo SciTech Alkalinity Titrator Model AS-ALK2 and Batch 100 certified reference materials from Andrew Dickson. TA, DIC, salinity and temperature measurements were used to calculate additional carbonate system parameters - pH, $p\text{CO}_2$, alkalinity, calcite (ΩCa) and aragonite (ΩAr) saturation states and HCO_3^- and CO_3^{2-} concentrations - using CO2SYS (Pierrot et al., 2006) with dissociation constants from Mehrbach et al. (1973) refit by Dickson and Millero (1987) and $[\text{KSO}_4]$ using Dickson (1990).

7.3.2 Sampling protocol

After 80 days exposure, *L. glaciale* thalli and water from control and treatment mesocosms were sampled for:

1. *DMSPi concentrations*: Thalli branches were prepared and analysed according to the headspace protocol described in Chapter 2; $n = 5$ per mesocosm, total pseudoreplicates = 28 (control, 2 were lost during preparation) and $n = 15$ (both low pH treatments). Branches were not cleaned prior to DMSP fixation as no discernible fouling of the thalli was evident.
2. *Total dissolved DMS+DMSP (DMS/Pd) concentrations*: Mesocosm water samples were prepared and analysed according to the liquid protocol described in Chapter 2; $n = 1$ per mesocosm, total replicates = 6 (control) and $n = 3$ (both low pH treatments).
3. *Outer epithelial cell morphology*: Thalli ($n = 3$ per treatment) were rinsed with Mill-Q ultrapure water and air-dried for SEM imaging; methodologies are detailed in Chapter 2.

4. *Percentage biomass*: The mass of air-dried algal samples ($n = 6$ per treatment) was recorded before and after overnight storage in 10M sodium hydroxide (NaOH) to break down the cells. The difference in mass represented the biomass of the samples.

In addition to the experimental samples, field controls were used: *L. glaciale* and water samples from Loch Sween under a similar oceanographic regime (12°C , salinity: 35, light: $90\ \mu\text{mol photons m}^{-2}\ \text{s}^{-1}$) to the experimental conditions were also analysed for DMSPi and DMS/Pd. All field samples were prepared within 2 hours of collection according to the methodology in Chapter 2 for liquid (water) and headspace (algae) DMS analyses.

7.3.3 Statistical analyses

DMSPi and DMS/Pd data could not be transformed to achieve normality and homogeneity of variance, therefore results were compared using a non-parametric test: a nested ANOVA of the ranked data (assumptions met, Conover and Iman, 1981). The mean of each mesocosm pseudoreplicate was used in the analysis. Analyses were conducted using Minitab V15.

7.4 Methods: *In situ* field study, Egyptian Red Sea

7.4.1 Field site

The field research was conducted on the Suleman reef, Gulf of Aqaba, northern Red Sea, Egypt ($28^{\circ}28'\text{N}$, $34^{\circ}30'\text{W}$). This fringing reef, approximately 120 m wide, is characterised by four distinct zones overlying a carbonate palaeo-reef structure (see Figure 7.4 for a species list):

1. Seagrass beds - seagrass and small free-living coralline algae, depth 0.2 - 0.85 m (low / high tide), nearest the shore.
2. Reef flat - fleshy macroalgae and free-living coralline algae, depth 0.4 - 1.05 m (low / high tide), 40 - 60 m from the shore.

3. Reef crest - branching corals, fleshy macroalgae and encrusting coralline algae, depth 0.8 - 1.55 m (low / high tide), 100 - 120 m from the shore.
4. Reef slope - high % coral cover (massive and branching species), depth up to 10 m, >120 m from the shore.

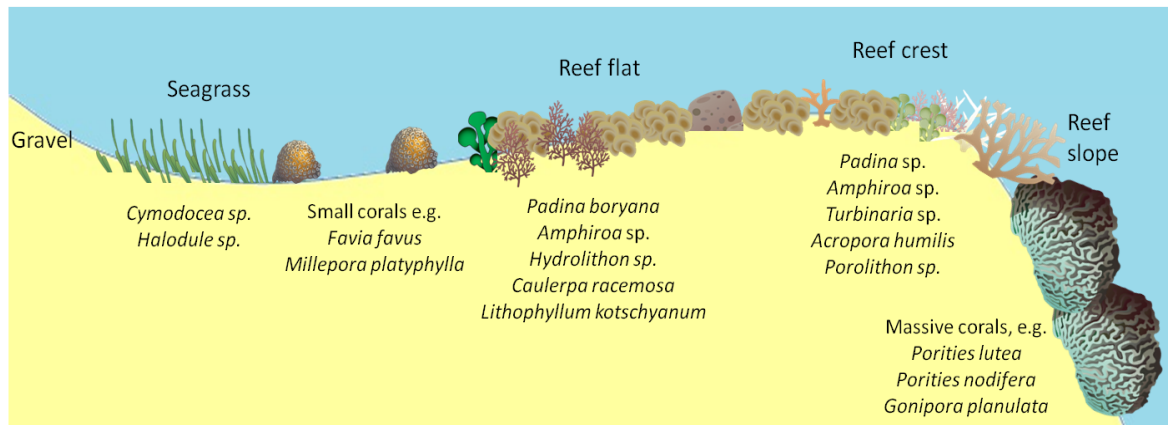


Figure 7.4 Cross-section of Suleman reef, Gulf of Aqaba, Egypt.

Four distinct zones are present on the reef – seagrass beds nearest the shore, reef flat (dominated by macroalgae), reef crest (small corals and encrusting coralline algae) and reef slope (dominated by massive and branching corals). Distance from shore to reef crest is ~120 m. Underlying substrate is a carbonate palaeo-reef.

7.4.2 Sampling regime

Water parameters and algal samples were taken over two 45 hour periods, at T14, T21, T29, T38 and T45 hours (relative to 00:00 on day one) at the reef crest and the reef slope.

Photosynthetically active radiation (PAR) was measured *in situ* using an Apogee QSO-E underwater quantum sensor (adjusted for electric light calibration) and a Gemini voltage data logger. PAR readings were recorded as the hourly average from each sampling timepoint at the reef crest and reef flat. Temperature, salinity and dissolved oxygen (salinity adjusted) were measured *in situ* using a YSI Pro2030 at each sampling timepoint at the reef crest and reef flat.

Water samples from each site were collected for carbonate system parameter determination by P. Donohue at the Scottish Association for Marine Science. 12 ml seawater samples were poisoned with $MgCl_2$ (40 μ l of a 50% saturated solution, Dickson et al., 2007) to stop biological activity and stored in

the dark at 4°C until analysed for DIC and TA. DIC was determined using a CO₂ Coulometer (CM5014 v.3, UIC Ltd.) with acidification module (CM5130 v.2, UIC Ltd.) and methods described by Dickson et al. (2007). TA was determined using the open-cell titration method (Dickson et al., 2007). Seawater was placed in an open cell and titrated with HCl in a two-stage process: (1) using a single aliquot of titrant the seawater was acidified to pH 3.5 and (2) after stirring for 40 s to allow evolved CO₂ to escape, the titration was continued with 0.5 µl drops of acid until pH 3.0 was attained. Additional carbonate parameters were calculated using CO2SYS, as described in section 7.3.1.

Water samples (n = 5 per location) were also collected for dissolved and particulate DMS/P (DMS/Pd and DMS/Pp), which were prepared and analysed according to the liquid methodology described in Chapter 2. Logistical constraints limited DMS/Pd and DMS/Pp sample collections to the first 45 hour sampling period only.

Algal samples (n = 10 per species, per location) were collected by hand using snorkelling and prepared and analysed for DMSPi using the headspace methodology described in Chapter 2. Three macroalgal species were analysed for DMSPi: *Padina* sp. (Ochrophyta: Dictyotales), *Amphiroa* sp. (Rhodophyta: Corallinales) and *Turbinaria* sp. (Ochrophyta: Fucales) (Figure 7.4), hereafter referred to using their genus names only. Calcification occurs in at least two of these macroalgae: *Padina* deposits bands of aragonitic crystals on the upper surface of the thalli to form concentric bands (Okazaki et al., 1986), whilst *Amphiroa* deposits high-Mg calcite in its cell walls (Figure 7.4). *Turbinaria*, despite its rigidity, may not be calcified as only two calcifying Ochrophyta genera have currently been identified - *Padina* and *Newhousia* (Kraft et al., 2004). *Padina* and *Amphiroa* were found at the reef crest and reef flat (Figure 7.4), whilst *Turbinaria* was found only at the reef crest (Figure 7.4). The distinct boundary of *Turbinaria* sp. growth was considered the boundary between the reef crest and flat. The mass of samples from *Padina* and *Amphiroa* was recorded before and after storage in 10M NaOH. The mass remaining represented percent calcification. However, percent calcification of *Amphiroa* from the crest could not be calculated as the samples completely broke down in the NaOH. An export permit could not be obtained for non-geniculate coralline algae at the quantity required for this study, thus were not included. DMSPi concentrations

from seven *Lithophyllum kotschyianum* specimens, a free-living coralline alga found on the reef flat (Figure 7.4), are presented in Chapter 3.

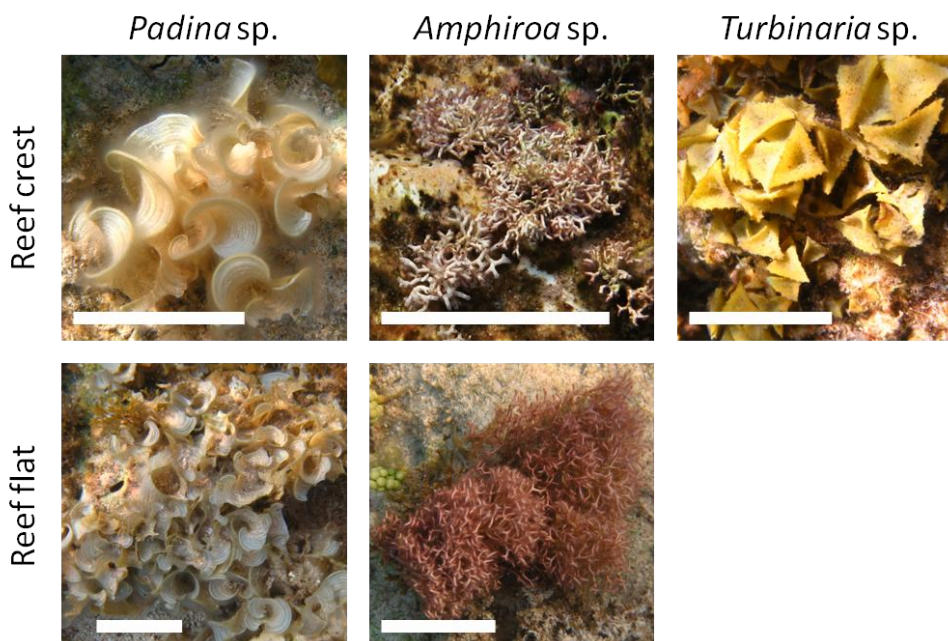


Figure 7.5 Examples of the macroalgae sampled at Suleman reef, Egypt. Samples of *Padina*, *Amphiroa* and *Turbinaria* on the reef crest reef flat; *Turbinaria* was not found on the reef flat. The concentric bands of calcification on *Padina* can be seen on the upper surface of the thalli. Scale bar = 5 mm. Photos: N. Kamenos.

7.4.3 Statistical analyses

DMSPi measurements could not be transformed to achieve normality and homogeneity of variance, thus a non-parametric multi-comparison Kruskal-Wallis test was performed to compare the data sets. DMS/Pd and DMS/Pp on the reef crest and flat were compared using t-tests. Analyses were conducted using Minitab V15.

7.5 Results: Laboratory study, UK

7.5.1 Water chemistry

pH levels in the control were stable throughout the experiment ($\text{pH } 8.18 \pm 0.102 / 498 \pm 161 \mu\text{atm pCO}_2$, mean \pm SD). pH in the low pH treatment also remained stable ($\text{pH } 7.70 \pm 0.139 / 1081 \pm 488 \mu\text{atm pCO}_2$, $n = 3$, Table 7.1). The acute, spiked pH ($n = 3$) treatment was stable until day 52 when an acute CO_2 injection was introduced, inducing a pH minimum of 6.49, returning to \sim pH 7.8 after 5 days (mean variability is described in Table 7.1). This acute pH treatment

had a similar magnitude and recovery time as the modelled high input, point source leak described by Blackford et al. (2009): -1 pH unit for ~5 days, thus representing a realistic future CCS leak scenario. Carbonate system values are provided in Table 7.1. Mean Ω_{Ca} and Ω_{Ar} were lowest in the acutely spiked pH treatment (1.74 ± 0.94 and 1.11 ± 0.60 respectively, Table 7.1). Both Ω_{Ca} and Ω_{Ar} were <1 during the low pH spike phase, favouring dissolution of the high-Mg calcite skeleton of *L. glaciale*. As is expected in a re-circulating system, nutrient concentrations gradually increased throughout the experiment; final concentrations are given in Table 7.2.

Table 7.1 Carbonate system parameters for the laboratory OA experiment. Carbonate system values over the 80 day experimental period for measured temperature (n = 80), salinity (n = 80), pH (n = 80) and alkalinity (n = 12) and calculated pCO_2 , dissolved inorganic carbon (DIC), calcite saturation state (Ω_{Ca}) and aragonite saturation state (Ω_{Ar}) for the three pH treatments. Data presented as mean \pm SD.

Parameter	Control	Low pH	Low, acute pH
pH (NBS)	8.18 ± 0.10	7.70 ± 0.14	7.75 ± 0.40
pCO_2 (μatm)	498 ± 161	1081 ± 488	2778 ± 4047
Alkalinity ($\mu mol kg^{-1}$)	2975 ± 443	2964 ± 467	2991 ± 414
DIC ($\mu mol kg^{-1}$)	2717 ± 420	2850 ± 489	3023 ± 556
Ω_{Ca}	4.7 ± 1.3	2.62 ± 0.6	1.74 ± 0.9
Ω_{Ar}	3.0 ± 0.8	1.67 ± 0.4	1.11 ± 0.6
Temperature ($^{\circ}C$)	11.74 ± 0.34	11.51 ± 0.28	11.64 ± 0.33
Salinity	34.9 ± 0.3	35.0 ± 0.3	34.9 ± 0.4

Table 7.2 Nutrient concentrations at the end of the OA experiment. Measurements for dissolved nitrite, nitrite+nitrate, ammonium, silicate and phosphate (μM) for the three pH treatments (see Table 7.1) at the end of the 80-day experiment. All nutrients were characterised by a general increase throughout the experiment. Data presented as mean \pm SD.

Parameter	Control	Low pH	Low, acute pH
Nitrite	0.45 ± 0.00	0.45 ± 0.00	0.45 ± 0.01
Nitrite+nitrate	31.57 ± 0.12	31.20 ± 0.15	31.38 ± 0.18
Ammonium	0.32 ± 0.03	0.28 ± 0.05	0.27 ± 0.08
Silicate	17.52 ± 0.03	17.67 ± 0.02	17.76 ± 0.29
Phosphate	7.22 ± 0.03	7.18 ± 0.04	7.12 ± 0.08

7.5.2 Percentage biomass and DMS/P measurements

No significant difference in % biomass was observed between the three pH treatments at the end of the 80-day experiment (mean % biomass = $3.50 \pm 0.47\%$, $F_3 = 0.30$, $p = 0.824$). Calculation of the biomass allowed DMSPi to be expressed in relation to biomass. Median \pm median absolute deviation (MAD) DMSPi in *L. glaciale* was lowest in the field control (4.01 ± 1.59 mg S as DMSP g^{-1} biomass, n =

18) (Figure 7.6a). In the experimental treatments, DMSPi was lowest in the control ($6.15 \pm 1.12 \text{ mg S g}^{-1}$ biomass, $n = 6$), slightly higher in the low pH treatment ($6.33 \pm 2.23 \text{ mg S g}^{-1}$ biomass, $n = 3$) and highest in the acute, spiked pH treatment ($8.13 \pm 1.80 \text{ mg S g}^{-1}$ biomass, $n = 3$) (Figure 7.6a). DMSPi was significantly higher in the acute, spiked pH condition than the control ($F_2 = 3.85$, $p = 0.028$) whilst other comparisons did not differ. A similar pattern was observed in the water samples (Figure 7.6b) where DMS/Pd was lowest in the field control ($1.40 \pm 0.14 \text{ nmol DMS/Pd L}^{-1}$, $n = 5$). DMS/Pd in the acute, spiked pH treatment was 121% greater than the treatment control (4.45 ± 0.83 and $2.24 \pm 0.63 \text{ nmol DMS/Pd L}^{-1}$ respectively; $F_2 = 4.42$, $p = 0.046$, Tukey's comparison, $p = 0.0414$), whilst the low pH treatment was not significantly higher than the treatment control ($3.13 \pm 1.19 \text{ nmol DMS/Pd L}^{-1}$, Tukey's comparison, $p = 0.9099$).

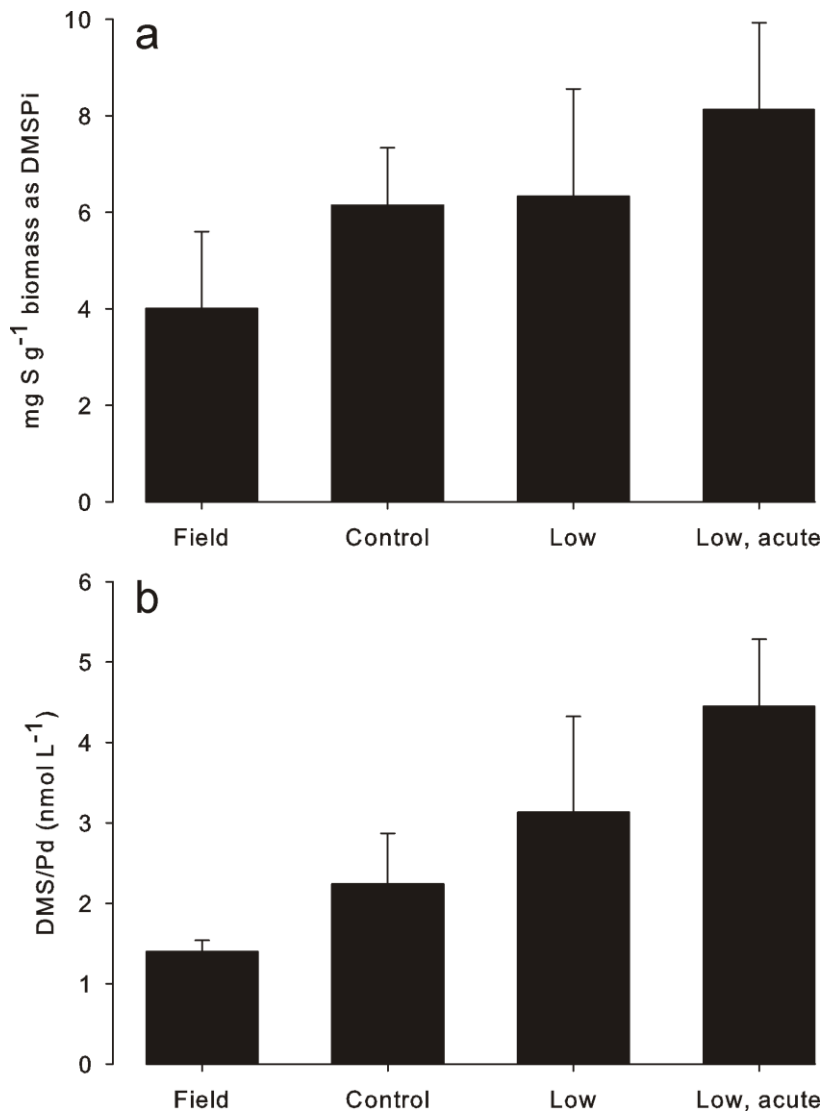


Figure 7.6 DMS/P at the end of the laboratory OA experiment. (a) Intracellular DMSP (mg S g^{-1} algal biomass as DMSPi) in *Lithothamnion glaciale* and (b) dissolved DMS and DMS (DMS/Pd) (nmol L^{-1}) from field (Loch Sween) and laboratory mesocosms following 80 days exposure to control ($\text{pH } 8.18 \pm 0.10$), low pH ($\text{pH } 7.70 \pm 0.14$) and low, acute pH ($\text{pH } 7.75 \pm 0.40$) treatments. Data presented as median \pm MAD.

7.5.3 Outer epithelial cell morphology

SEM micrographs of *L. glaciale* indicated that each cell was surrounded by a high-Mg calcite cell wall, forming a honeycomb-like structure (Figure 7.7), as described by Irvine and Chamberlain (1994). In the control treatment, all cell walls were joined to the next by the middle lamellae, a layer of organic material between each cell (Figure 7.7 a,b). This structure was consistent with the field controls. In both low pH treatments, some areas of visually healthy epithelial cells appeared to lose their organic ‘glue’ and cracks developed between the calcite cell walls (Figure 7.7 c-f). Across some of the epithelia, lesions were observed between the cell and cell wall (e.g. Figure 7.7 a,b). This was observed

in thalli from all treatments and is desiccation damage from drying the algae prior to SEM micrography.

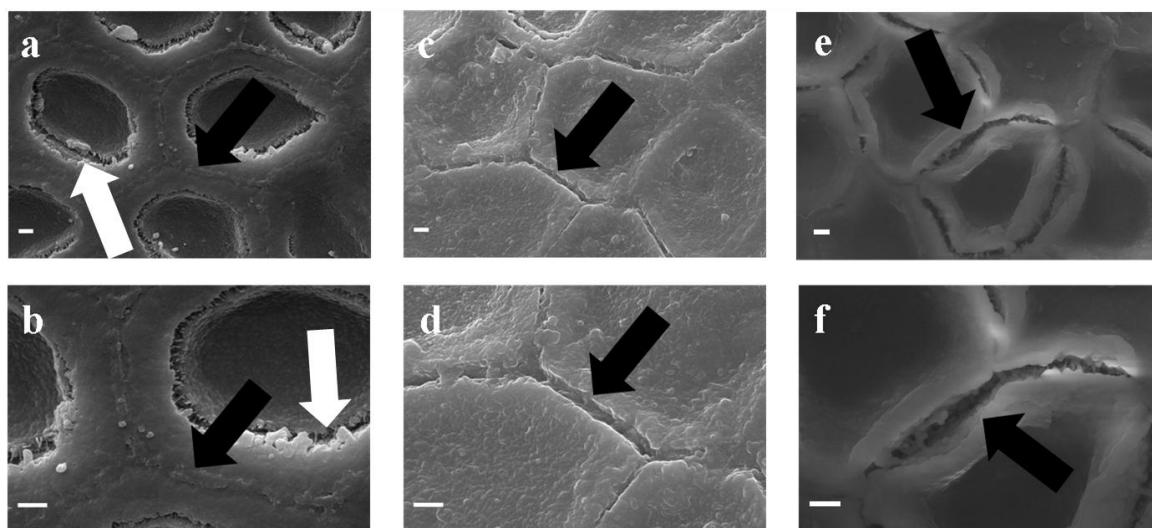


Figure 7.7 Surface epithelial cells of *L. glaciale*. Surface epithelial cells imaged following 80 days exposure to (a,b) control (pH 8.18±0.10), (c,d) low pH (pH 7.70±0.14) and (e,f) and low, acute pH (pH 7.75±0.40). All scale bars represent 1 μm. Micrographs of a thallus from each treatment are presented at two magnifications: 12,000X (a,c,e) and 24,000X (b,d,f). Black arrows indicate the connections between cell walls: organic ‘glue’ is present in the control (a,b), cracks are seen in both low pH treatments (c-f). Desiccation damage from sample preparation, which was observed in all thalli, are indicated by the white arrows (a,b).

7.6 Results: *In situ* field study, Egyptian Red Sea

7.6.1 Water chemistry

7.6.1.1 Physical parameters

Both the reef crest and reef flat exhibited a diurnal trend in water temperature. Highest temperatures were in the afternoon and lowest temperatures were at dawn (Figure 7.8a). Maximum temperatures were higher on the reef flat than the reef crest (29.1°C compared to 27.5°C), resulting in the reef flat being more variable than the reef crest (temperature range: 3.15°C and 1.5°C respectively, Figure 7.8a). A diurnal trend in dissolved oxygen was also observed on both the reef crest and reef flat, with the highest percentage at 14:00 (crest: 109%, flat: 159%) and the lowest during the night and at dawn (crest: 73%, flat: 63%, Figure 7.8b). No difference between the reef crest and reef flat was observed in terms of PAR (Figure 7.8c), which reached a maximum of 1542 μmol photons m⁻² s⁻¹ at 14:00. Salinity on the reef crest was stable (~42.6) throughout the experimental period, except for hour 38, when a drop to

40.6 was observed (Figure 7.8c). In contrast, the reef flat remained slightly higher than the reef crest throughout, with a small range of 42.9 - 43.4 (Figure 7.8d).

7.6.1.2 Carbonate parameters

Diurnal patterns were observed for all carbonate parameters on the reef crest and flat (Figure 7.9) although the magnitude of diurnal variation was generally larger on the reef flat (except CO_3^{2-} , ΩCa and ΩAr , Figure 7.9). TA did not exhibit a strong diurnal trend on the reef crest (2422 - 2681 $\mu\text{mol kg}^{-1}$) or flat (2433 - 2574 $\mu\text{mol kg}^{-1}$, Figure 7.9a). DIC on the reef flat (<2000 $\mu\text{mol kg}^{-1}$) was lower than the reef crest (~2100 $\mu\text{mol kg}^{-1}$) at all daytime sampling points; at night (21h and 45h) DIC on the flat and crest were similar (2100 - 2200 $\mu\text{mol kg}^{-1}$, Figure 7.9a). pH was highest in the day (8.4 - 8.6), lowest at night (8.2, Figure 7.9b) and generally higher on the reef crest (Figure 7.9b). $p\text{CO}_2$ was lowest in the day (76 - 85 μatm on the flat, 137 - 154 μatm on the crest) and higher at night (maximum of 266 μatm on the flat and 236 μatm on the crest). CO_3^{2-} was highest in the day (221 - 405 $\mu\text{mol kg}^{-1}$ on the crest, 327 - 345 $\mu\text{mol kg}^{-1}$ on the flat) and lower at night (minimum of 168 $\mu\text{mol kg}^{-1}$ on the crest and 163 $\mu\text{mol kg}^{-1}$ on the flat, Figure 7.9d). HCO_3^- was lowest in the day (minimum of 1684 $\mu\text{mol kg}^{-1}$ on the crest and 1587 $\mu\text{mol kg}^{-1}$ on the flat) and highest at night / dawn (maximum of 2033 $\mu\text{mol kg}^{-1}$ on the crest and 20874 $\mu\text{mol kg}^{-1}$ on the flat, Figure 7.9e). Saturation states were highest in the day (maximum ΩCa : 9.3 on the crest and 7.8 on the flat; ΩAr : 5.9 on the crest and 4.9 on the flat) and lowest at night / dawn (minimum ΩCa : 3.9 on the crest and 3.7 on the flat; ΩAr : 2.4 on the crest and 2.3 on the flat, Figure 7.9f).

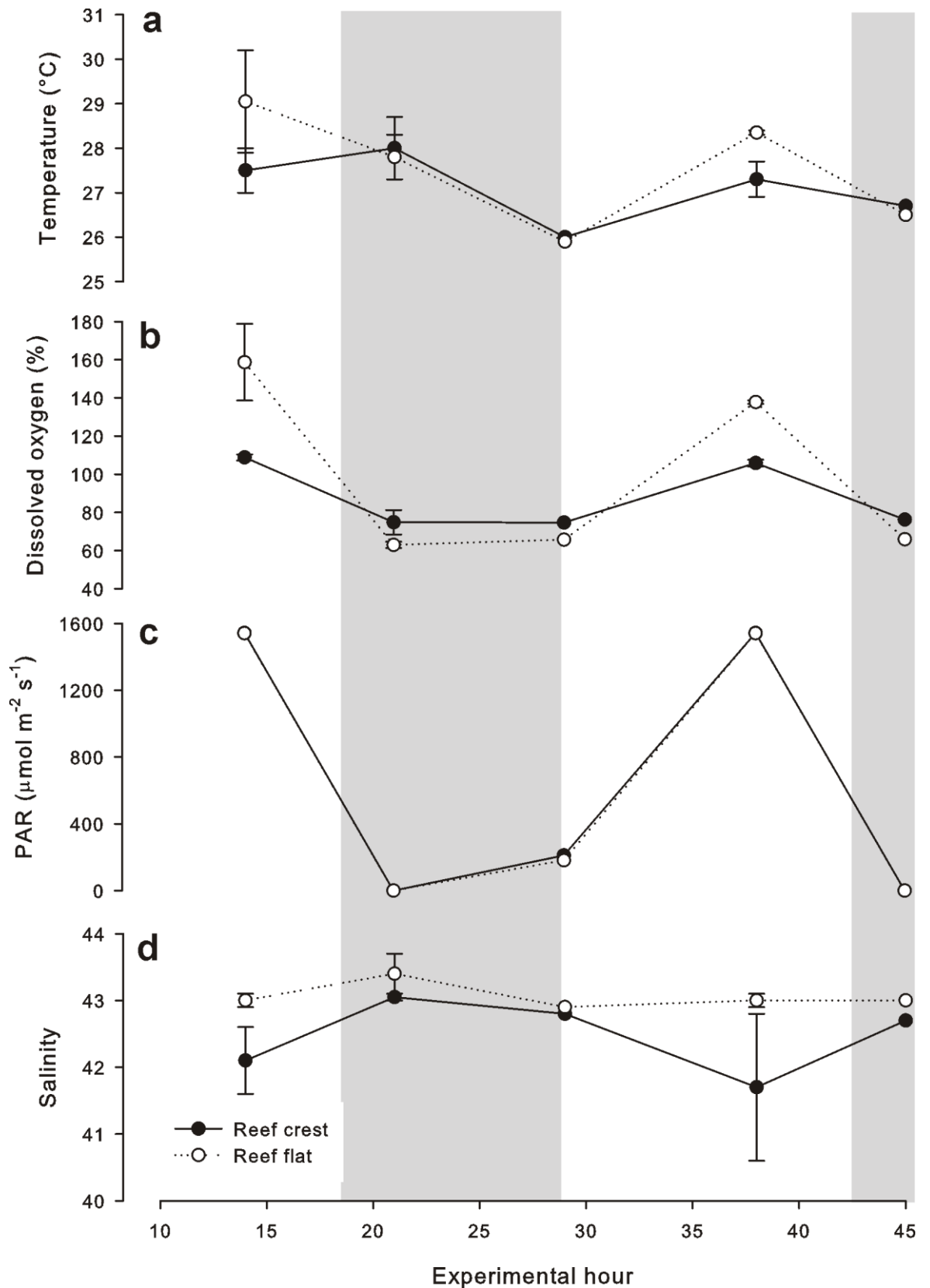


Figure 7.8 Abiotic parameters from Suleman reef, Egypt. *In situ* (a) water temperature ($^{\circ}\text{C}$), (b) dissolved oxygen (%), (c) PAR ($\mu\text{mol photons m}^{-2} \text{s}^{-1}$) and (d) salinity at the reef crest (black circles) and reef flat (open circles) over a 45 hour period. Grey shading indicates night-time (sunset – sunrise). Data presented as mean $\pm 1/2$ range of two experimental runs.

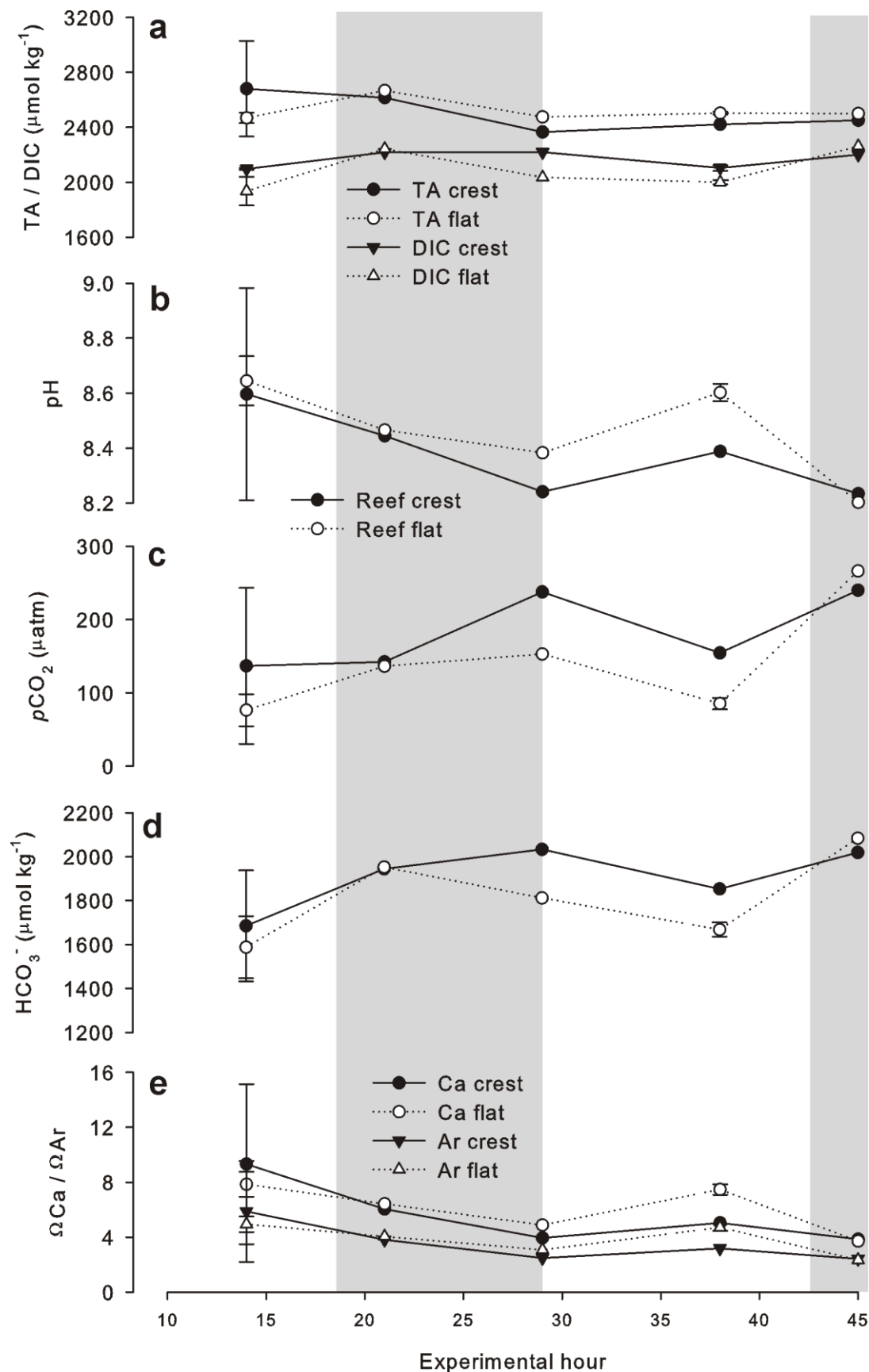


Figure 7.9 Carbonate system parameters from Suleman reef, Egypt.

In situ (a) TA and DIC ($\mu\text{mol kg}^{-1}$), (b) pH, (c) $p\text{CO}_2$ (μatm), (d) CO_3^{2-} ($\mu\text{mol kg}^{-1}$), (e) HCO_3^- ($\mu\text{mol kg}^{-1}$) and (f) calcite (Ω_{Ca}) and aragonite (Ω_{Ar}) saturation states on the reef crest (black symbols) and reef flat (open symbols) over a 45 hour period. Grey shading indicates night-time (sunset – sunrise). Data presented as the mean \pm 1/2 range of two experimental runs.

7.6.2 Percentage calcification

Percent calcification could not be computed for *Amphiroa* as the algae completely broke down in NaOH. However, *Amphiroa* from the crest was visibly more calcified than on the flat (Figure 7.4). In contrast, there was no significant difference in % calcification between *Padina* from the crest or the flat ($T_1 = 0.30$, $p = 0.816$, Table 7.3).

Table 7.3 Percent calcification of macroalgae from Suleman Reef, Egypt.

Genus	Reef location	% calcification
<i>Amphiroa</i>	Crest	na
	Flat	43.57±5.00
<i>Padina</i>	Crest	56.50±16.00
	Flat	51.54±4.70

na: not available – could not calculate % calcification.

7.6.3 Macroalgal and water column DMS/P

A general diurnal trend was observed for most DMS/P measurements: high DMS/P concentrations at 21:00 and low concentrations at 14:00 (Figure 7.10). An exception to this was *Padina* on the crest (no diurnal trend, Figure 7.10a).

A significant decline in DMSPi was observed in *Padina* on the reef flat from T29 (07:00, 17.07±1.78 mg S g⁻¹, mean±SE), to T38 (14:00, 5.71±0.74 mg S g⁻¹, $Z = 3.95$, $p < 0.001$, Figure 7.10a). No statistical difference was observed between *Padina* DMSPi on the flat and crest except at T29 ($Z = 3.41$, $p < 0.001$, Figure 7.10a). Although a diurnal trend in *Amphiroa* DMSPi on the flat was observed (<9 mg S g⁻¹ at 14:00, >14 mg S g⁻¹ at 21:00, Figure 7.10b), the changes in DMSPi were not significant ($Z < 3.40$). *Amphiroa* DMSPi on the flat was significantly lower than the crest (24.9±8.2 mg S g⁻¹ compared to 12.6±5.5 mg S g⁻¹, mean±SD, $Z = 4.73$, $p < 0.001$, Figure 7.10b), with a significant diurnal trend of low DMSPi at 14:00 and high DMSPi at 21:00 ($Z = 4.63$, $p < 0.001$) (Figure 7.10b). A diurnal trend was also evident in *Turbinaria* (<0.3 mg S g⁻¹ at 14:00, > 0.5 mg S g⁻¹ at 21:00), although this was not significant ($Z < 3.40$) and was characterised by a relatively high variability at 21:00 and 07:00 (Figure 7.10c).

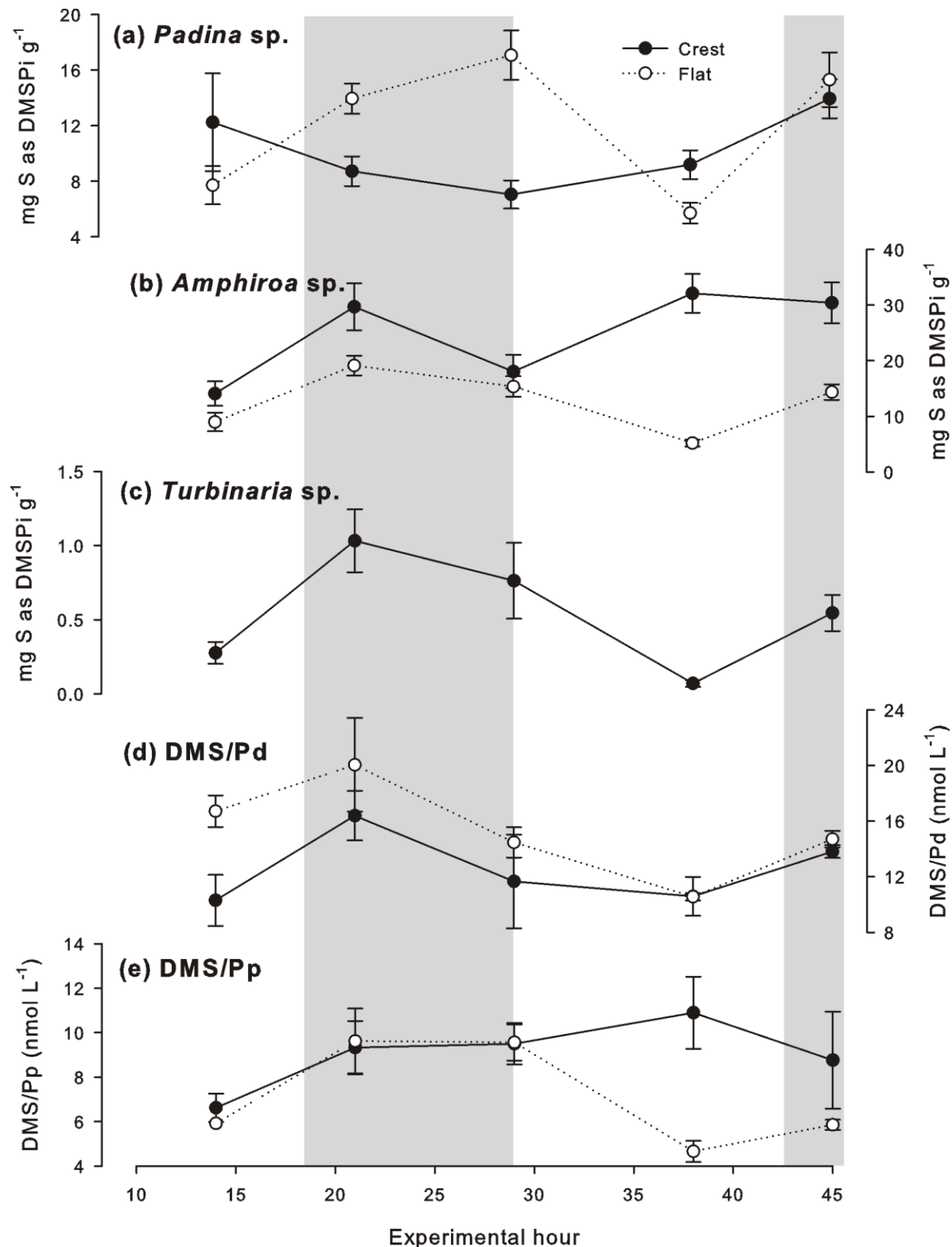


Figure 7.10 DMS/P on the reef flat and crest of Suleman Reef, Egypt. Intracellular DMSP (mg S g⁻¹ algae as DMSPi) of (a) *Padina* sp., (b) *Amphiroa* sp. and (c) *Turbinaria* sp. and (d) dissolved DMS/P (DMS/Pd, nmol L⁻¹) and (e) particulate DMS/P (DMS/Pp, nmol L⁻¹) on the reef crest (black circles) and reef flat (open circles) over the 45 hour experimental period. Grey shading indicates night-time (sunset – sunrise). Data presented as mean±SE. Note the different y-axes on all the graphs.

DMS/Pd did not differ significantly between the crest and flat ($T_{23} = 1.64$, $p = 0.114$), but there was suggestion of a diurnal trend, with elevated concentrations at 21:00 (12.31 ± 1.05 nmol L⁻¹) compared to 14:00 (9.46 ± 0.85

nmol L⁻¹). A significant difference in DMS/Pp was observed between the crest and flat ($T_{24} = 2.27$, $p = 0.033$), although this was driven only by differences observed at T38 (14:00, crest: 4.65 ± 0.48 nmol L⁻¹, flat: 10.89 ± 1.62 nmol L⁻¹).

7.7 Discussion

It has been proposed that coralline algal dissolution may exceed calcification by the end of the 21st century due to OA (Martin and Gattuso, 2009). However, the effect of OA on calcifying algae biochemical processes (e.g. intracellular production of DMSP) is not well understood. The aim of this research was to investigate the effect of reduced and variable pH on DMSPi concentrations in temperate coralline algae under controlled laboratory conditions and in tropical macroalgae at a naturally variable field site in the Gulf of Aqaba in the Red Sea.

7.7.1 Regulation of intracellular DMSP

The production of DMSP is energetically costly (Stefels, 2000), so the regulation of DMSP in response to environmental change is often slow (e.g. reduced salinity, Chapter 6). However, under low or variable pH conditions, DMSP appears to be rapidly up-regulated in calcifying macroalgae. In the laboratory experiment, DMSPi was only significantly increased under low, acutely spiked, conditions, suggesting a stress response to the rapidly changing environment and / or the excessive physical damage to cell structure caused by the low carbonate saturation states. In the field, continual regulation of DMSPi in the three macroalgae and water column DMS/Pd and DMS/Pp concentrations was observed throughout the sampling period in response to diurnal changes in carbonate chemistry, temperature, light and dissolved oxygen. Maximum DMSPi, DMS/Pp and DMS/Pd concentrations occurred at night, when carbonate saturation states were low. It is likely that if temperature and light were driving DMSPi, maximum concentrations would occur in the day, when these factors were highest. Dissolved oxygen was lowest at night (~60% saturation), but this is above the level suggested for hypoxic impact (~30% saturation, Doney, 2010).

The observed enhancement in DMSPi suggests that DMSP may be an important compound in calcifying macroalgae for building resistance to low or variable pH environments. Under an OA regime, the availability of CO₂ is

increased, so photosynthetic organisms (e.g. algae and seagrass) may benefit from a moderate increase in CO₂ (Ries et al., 2009). An increase in photosynthetic output may increase intracellular methionine, which may be subsequently moderated by an up-regulation of DMSPi, acting as an overflow mechanism in a similar manner to that described for nitrogen deficiency (Stefels, 2000). Additionally, enhanced photosynthesis will form damaging reactive oxygen species (ROS). It has been suggested that DMSP and its associated breakdown products can act as an antioxidant cascade (Sunda et al., 2002). Thus, DMSPi may be up-regulated to 'mop up' ROS and minimise cellular oxidative damage. A lag in the DMSPi response to enhanced photosynthesis may explain why the DMSPi was enhanced during the night. DMSPi may also play some role in helping to maintain cellular function whilst under low carbonate saturation conditions. The role of DMSP in the calcification process is unknown, but many calcifying phytoplankton (e.g. *Emiliana huxleyi*) also contain high DMSPi concentrations. This research supports a putative role of DMSPi in algal calcification and structural maintenance. If excess DMSPi is actively transported out of the cells into the water column (as was implied in the laboratory experiment) this may facilitate the cycling of DMS/P compounds within the ecosystem. This will make more DMSP available to bacteria, thus increasing the potential for DMS production and subsequent atmospheric emission. Tracer studies would allow monitoring of the production and release of DMS/P within these systems.

7.7.2 Species-specific response to ocean acidification

DMSPi concentrations were determined in four macroalgae - *L. glaciale* (temperate), *Padina*, *Amphiroa* and *Turbinaria* (tropical). Control DMSPi concentrations in *L. glaciale* were similar to other research presented in Chapters 4, 5, 6 and 8, with a significant increase under low, acutely spiked, pH conditions. DMSPi concentrations for the tropical macroalgae were higher than previously published results from Australia (Broadbent et al., 2002) and the Caribbean (Dacey et al., 1994). Due to the restricted circulation within the Gulf of Aqaba, oceanographic conditions are more extreme than other tropical reef sites; the Red Sea is one of the warmest and most saline seawater bodies in the world (Chiffings, 2003). To survive in such extreme conditions, organisms must have effective mechanisms to cope with high salinity, irradiance, temperature

and carbonate chemistry. In phytoplankton, DMSP is known to be up-regulated under these conditions (Sunda et al., 2002; Karsten et al., 1996; Karsten et al., 1992), thus may be especially important for Red Sea macroalgae.

However, inter and intra-species differences in DMSPi concentrations were observed in Suleman reef, with *Amphiroa* (crest) > *Amphiroa* (flat) > *Padina* (crest and flat) > *Turbinaria* (crest). These inter and intra-specific differences may be a reflection of palatability and grazing pressure, as macroalgal DMSPi is known to be important in invertebrate grazing activity (Van Alstyne et al., 2009; Van Alstyne and Houser, 2003; Van Alstyne et al., 2001; and see Chapter 8). *Amphiroa* and *Padina* (thin thalli, not heavily calcified compared to non-geniculate red coralline algae) may be targeted by grazers, so they may maintain high DMSPi concentrations as a grazing deterrent. This may be particularly important during the night when grazing pressure is highest. If *Amphiroa* is a preferential food source for grazers, this may necessitate a requirement for higher DMSPi on crest compared to the flat (as was observed). In contrast, *Turbinaria*, which was robust and rigid, may not be preferentially targeted by grazers, hence the low DMSPi concentrations. Annual patterns in macroalgal growth and calcification and grazer densities may lead to strong seasonal, as well as diurnal, patterns in macroalgal DMSPi concentrations.

7.7.3 Biological control on carbonate chemistry

The carbonate chemistry of Suleman reef was within the range cited for other tropical reef systems (Kleypas and Langdon, 2006). Biological processes, namely calcification / dissolution and photosynthesis / respiration probably exerted a strong influence on the carbonate chemistry of Suleman reef. This has also been observed in other reef environments (Zhang et al., 2012; Anthony et al., 2011; Smith and Price, 2011; Gagliano et al., 2010; Kleypas and Langdon, 2006), and is most pronounced in shallow waters (like Suleman reef) due to the reduced surface area to volume ratio (Kleypas and Langdon, 2006). In general, the reef flat was more variable than the reef crest, likely due to the greater disparity in CO₂ utilisation in the day for photosynthesis (which reduces DIC) and CO₂ release at night by respiration (which increases DIC). This was also reflected in the dissolved oxygen measurements. Minimum pH and carbonate

saturation states were observed at night on the reef crest, where there was a higher proportion of fauna (e.g. urchins; Burdett, pers. obs.).

7.7.4 Structural sensitivity to ocean acidification

This research suggests that the structural integrity of calcifying algal cells under low or variable pH regimes may be compromised, particularly for high-Mg calcite structures. SEM micrographs of the surface epithelial cells of *L. glaciale* indicated a possible pathway for DMSP release that has not been previously described. In the control group, the calcite cell walls were adhered together, mediated via an organic material (the middle lamellae). In some areas of the low pH thalli epithelia (both chronic and acute), the organic material was absent and cracks had formed between the cells. Such structural damage would likely also cause damage to cell membranes, thereby allowing DMSP to leak from the cells into the water column, facilitating DMSP / DMS cycling. Cell lysis through grazing activity is thought to be the primary mechanism for the release of DMSP into the water column (Yoch, 2002), as DMSP cannot readily pass across cell membranes. However, no grazers were present in the laboratory experiment. DMSP production may be up-regulated in response to increased methionine concentrations (Stefels, 2000; Gröne and Kirst, 1992), followed by active export of excess DMSP out of the cell (Stefels, 2000). This pathway has primarily been associated with nitrogen deficiency (Stefels, 2000) (not a limiting factor in the laboratory experiment), but may also result from increased photosynthesis under high-CO₂ conditions.

In the field, calcification was visibly reduced in *Amphiroa* on the reef flat (high-Mg calcite), but this could not be quantitatively confirmed. Red coralline algae may start dissolving at an aragonite saturation state of 1.7 (Langdon et al., 2000), which may explain the apparent decline in *Amphiroa* calcification from the stable reef crest to the more variable reef flat. In contrast, the calcification of *Padina* (aragonite) was not significantly different between the reef flat and crest, despite previous reports of decalcified *Padina* in naturally low pH environments (Johnson et al., 2012). Minimum aragonite saturation state on the reef during the sampling period ($\Omega_{Ar} = 2.3$) appeared to be sufficiently high to maintain an aragonite structure.

7.7.5 Laboratory and field experiments

Physical parameters are well controlled in the laboratory, but the conditions do not accurately mimic the natural environment. As such, stress responses associated with laboratory experiments should be considered, particularly when conducting climate change experiments over a short time scale such as the 80-day laboratory experiment in this chapter. The use of field and laboratory controls and longer-term experiments allow for a more thorough understanding of the effects of experimental practice and environmental change on organisms. This research suggests that a DMSPi response is only observed following acute spikes in $p\text{CO}_2$ (laboratory experiment) or in a naturally variable environment. This highlights concerns that have been raised over the use of CO_2 vents as OA field experimentation sites; such areas are extremely variable and conclusions based solely on these field areas may lead to inaccurate conclusions (Hall-Spencer et al., 2008; Riebesell, 2008).

Knowledge that acute changes in $p\text{CO}_2$ enhance DMSPi and impact cell structures may be useful for projecting the effect of future climate change. Additional sources of CO_2 to the natural environment, such as CCS leaks and upwelling events, may become more important in the future as CCS infrastructure grows and oceanic circulation changes. Thus, caution should be taken when extrapolating results from high CO_2 / low pH experiments to the natural world. Further experiments should be conducted to assess the recovery of calcifying organisms to acute and variable CO_2 conditions.

7.7.6 Wider implications

An up-regulation in DMSPi because of increased CO_2 may affect the function of coralline algal habitats, with implications for the important service provisions (e.g. fisheries recruitment) provided by these ecosystems. For example, coralline algae are important for the settlement of invertebrate larvae (e.g. Steller and Cáceres-Martinez, 2009; Huggett et al., 2006), and increased CO_2 has been shown to reduce the settlement of coral larvae (Doropoulos and Diaz-Pulido, 2013; Webster et al., 2013). DMSPi may be an important component of macroalgal settlement cues (Steinberg and De Nys, 2002). DMSPi is also important in herbivorous grazing, acting as an attractant or a deterrent (e.g.

Seymour et al., 2010; Van Alstyne and Houser, 2003; see Chapter 8 for more details). Further, calcifying macroalgae will not be the only organisms to be affected by OA. Previous literature suggests that calcifying invertebrates such as urchins, the tests of which are composed of high-Mg calcite, may be detrimentally affected by OA conditions (Johnson et al., 2012; Stumpp et al., 2011a; Stumpp et al., 2011b; O'Donnell et al., 2009; Todgham and Hofmann, 2009; Hall-Spencer et al., 2008). This will impact the food web dynamics of the reef ecosystem, allowing macroalgae (particularly uncalcified species) to proliferate, with the potential to induce a phase shift from coral to macroalgal dominance (Dudgeon et al., 2010). A reduction in calcifying organisms will also affect the biogeochemical carbon cycle by reducing carbonate production; maerl beds are currently important sediment sources to seagrass beds in the Mediterranean (Martin et al., 2008). If calcifying organisms suffer under an OA regime, sediment supplies may be depleted.

The effect of OA on coastal microbial communities has not been well studied, despite their importance in facilitating the cycling of nutrients (Arrigo, 2005), carbon (Jiao et al., 2011) and DMS/P (Moran et al., 2012). Some studies observed no change in coral-associated microbial structure under varying pH regimes (Meron et al., 2012), whilst others have observed an increase in the abundance of the pathogenic community (Vega Thurber et al., 2009), as has been observed under other environmental stressors (e.g. elevated temperature, Thomas et al., 2010). Microbial biofilms may increase their production under naturally high-CO₂ conditions (Lidbury et al., 2012) and the abundance of Flavobacteriales (Bacteroidetes) may increase; bacteria which may be important in DMS/P breakdown and release (Hatton et al., 2012a; Green et al., 2011).

7.8 Conclusions

Rising atmospheric CO₂ levels are projected to cause a shift in the carbonate chemistry of the oceans towards a more acidic environment. Previous research suggests that calcifying organisms, particularly those with aragonitic or high-Mg calcitic structures may be most affected. The research presented in this chapter assessed the impact of a low or variable pH environment on macroalgal DMSPi production under controlled laboratory conditions and in the field. In the laboratory, DMSPi in red coralline algae was elevated in all treatments relative

to the field control, highlighting the benefits of combining laboratory and field-based investigations to better understand the likely response of organisms to projected climatic changes. Relative to the laboratory control, DMSPi was elevated in the low, variable conditions only and epithelial cell damage was observed. Similarly, macroalgal DMSPi and water column DMS/Pd and DMS/Pp were highest at night and dawn when carbonate saturation states were lowest. These results suggest that DMSPi may be important for maintaining cellular function during periods of low or variable pH.

8

Environmental pressures: Grazing-hurricane interactions

Herbivorous grazing has been described as a major release mechanism for dimethylsulphoniopropionate (DMSP) from algal cells into the surrounding water column. This was first investigated by Dacey and Wakeham (1986), who observed that copepod grazing of dinoflagellates led to a release of the climatically important compound, dimethylsulphide (DMS), thus explaining why oceanic DMS emissions were sometimes decoupled from phytoplankton biomass. This so called ‘sloppy feeding’ by zooplankton is an important ecological process that facilitates the release of DMSP from phytoplankton for subsequent breakdown into DMS (Yoch, 2002).

8.1 DMS and DMSP as a grazing defence

The cleavage of DMSP was first postulated as a microalgal activated defence mechanism in *Emiliana huxleyi* by Wolfe et al. (1997; 1996). They hypothesised that DMSP and DMSP-lyase, usually separated within cells, are mixed at the onset of a physical or chemical attack on cell membranes, producing DMS and acrylic acid which deter protozoan predators.

An activated chemical defence mechanism has also been identified in macroalgae, perhaps most extensively in the ulvoid algae of the north-eastern Pacific. Four lines of defence have been proposed in support of this hypothesis:

1. The algae contain high levels of intracellular DMSP (DMSPi) relative to other chemical defences, at concentrations ~ 25 - 125 $\mu\text{mol g}^{-1}$ fresh mass (Van Alstyne et al., 2007; Van Alstyne et al., 2001).
2. *Ulva lactuca*, an important ulvoid in the region, contains DMSP-lyase, the primary mechanism for cleavage of DMSP to DMS and acrylic acid (Van Alstyne et al., 2001).
3. When grazed by green sea urchins (*Strongylocentrotus droebachiensis*), the algae release DMS. Algae that have low DMSPi concentrations (primarily brown kelp species) do not release DMS when grazed (Van Alstyne and Houser, 2003).
4. DMS and acrylic acid are superior to DMSP as herbivore deterrents, reducing feeding rates in green and purple (*S. purpuratus*) sea urchins (Van Alstyne and Houser, 2003; Van Alstyne et al., 2001).

The success of the invasive macroalga *Codium fragile* on the eastern coast of Canada has been attributed to its year round high DMSP concentrations (Lyons et al., 2010; Lyons et al., 2007) and the alga's apparent ability to up-regulate DMSP production during grazing (Lyons et al., 2010; Lyons et al., 2007).

8.2 DMSP as a grazer attractant

DMSP-based activated chemical defences are not effective towards all predators. Some plankton (bacteria, phytoplankton and zooplankton) are attracted towards DMSP (Seymour et al., 2010). Littorinid snails (*Littorina sikana*) preferentially consume macroalgae that are high producers of DMSP (and which do exhibit a DMSP-activated defence mechanism, including *U. lactuca* and *U. linza*) in order to meet its nutritional requirements (Van Alstyne et al., 2009). High-DMSP containing algae and DMS / acrylic acid production do not deter grazing by the tropical sea urchin *Echinometra lucunter* (Erickson et al., 2006). These urchins are, however, less tolerant of another algal metabolite (caulerpenyne) than reef fish, thus providing *E. lucunter* with a feeding niche within the reef environment (Erickson et al., 2006).

DMSP can also act as a foraging cue for predators, indicating the location of prey. Planktivorous reef fish 'eavesdrop on trophic interactions' using DMSP as a marker (De Bose et al., 2008) whilst the high DMSPi concentrations in the salt marsh grass *Spartina alterniflora* attract the snail *Littoraria irrorata*, signalling refugia and food locations (Kiehn and Morris, 2010). DMS is also an important olfactory foraging cue for Procellariiform seabirds (albatrosses, petrels and shearwaters) (Nevitt, 2011; Nevitt, 2008; Bonadonna et al., 2006; Nevitt and Bonadonna, 2005; Nevitt, 2000), penguins (Amo et al., 2013; Wright et al., 2011; Cunningham et al., 2008), harbour seals (Kowalewsky et al., 2006) and perhaps basking sharks (Sims and Quayle, 1998). Strom et al. (2003a; 2003b) observed a reduction in protist grazing activity in DMSP-enhanced conditions but not when DMS and / or acrylate were enhanced. This led to another hypothesis that DMSP (non-toxic) can act as a warning molecule for grazers, indicating the presence of toxic compounds in their prey (such as DMS and acrylic acid) (Strom et al., 2003a; Strom et al., 2003b). These complex attractant / deterrent interactions suggest that DMSP production and breakdown is vital for ecosystem function as well as for the production of the climatically important gas DMS.

8.3 Regional focus: The eastern Canadian kelp forests

The shallow marine benthos along the coast of Nova Scotia is characterised by two habitat types: kelp forests (kelp canopy and coralline algae-encrusted substrate) and coralline barrens (primarily coralline algae only). The spatial coverage of these habitats is mediated by the grazing activity of the green sea urchin, *S. droebachiensis* (Scheibling, 1986). High density urchin aggregations form destructive 'grazing fronts' that initiate rapid (months - years) phase shifts from kelp beds to coralline barrens (Scheibling, 1986; Miller, 1985). Under stormy conditions, the urchin front is considerably reduced (Figure 8.1), temporarily reducing the effective grazing urchin population.

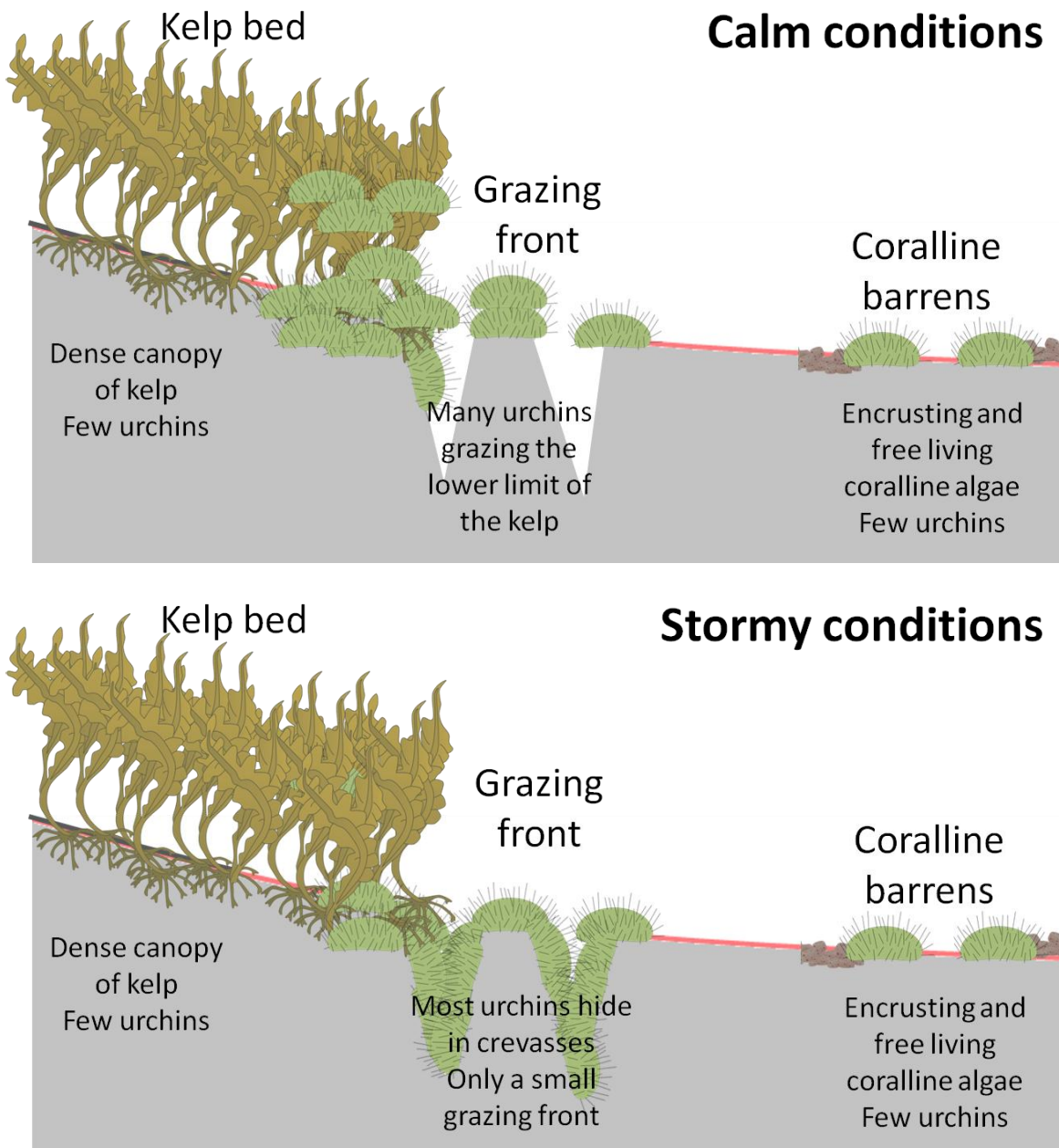


Figure 8.1 Structure of the kelp forest ecosystem in Nova Scotia. Note the well developed grazing front under calm conditions (top panel) compared to a smaller grazing front under stormy conditions (lower panel).

The two major algal components of kelp forest systems (kelp and coralline algae) have very different DMSPi concentrations: DMSPi in kelp is low compared to other macroalgae, often below detection limits (Lyons et al., 2007; Van Alstyne and Puglisi, 2007; also see chapter 5), whilst non-geniculate coralline algae have high DMSPi concentrations (Burdett et al., 2012a; Rix et al., 2012; also see chapter 5; Kamenos et al., 2008b). This concentration disparity and the hypothesised grazing deterrent mechanism of DMSP may contribute to the overall ecosystem function of this habitat by encouraging urchin grazing at the kelp / coralline barren interface.

Since 1980, numerous mass mortality events of *S. droebachiensis* in eastern Canada have been consistently observed following hurricane passage (Feehan et al., 2012; Scheibling and Lauzon-Guay, 2010; Scheibling, 1986; Jones and Scheibling, 1985). A fatal infection by the amoeba *Paramoeba invadens*, associated with hurricane presence, has been attributed as the cause of these mortality events (Jones and Scheibling, 1985). It is still not clear whether hurricanes transport the amoeba northwards or whether the rise in SST associated with hurricanes stimulates dormant amoebic cysts to become active (Scheibling and Lauzon-Guay, 2010). Urchin populations around the coast of Nova Scotia have significantly declined since mass mortality events began, leading to a collapse of the once lucrative urchin fishery (Miller and Nolan, 2008), raising concerns for the future of *S. droebachiensis* in Nova Scotian coastal waters.

8.3.1 The role of kelp forests in biogeochemical cycles

The primary production of kelp forests is high (Delille et al., 2009) and their importance in coastal biogeochemical cycling notable. Faecal production by urchins during periods of high grazing activity provides an important source of carbon and nitrogen within the kelp bed ecosystem (Sauchyn and Scheibling, 2009a; Sauchyn and Scheibling, 2009b; Soares et al., 1997). The horizontal transport of faecal material may also contribute to deep water carbon supply (Sauchyn and Scheibling, 2009a; Sauchyn and Scheibling, 2009b).

Kelp species are vital components of the iodine biogeochemical cycle, with tissue concentrations often > 50 mM (Küpper et al., 1998). A significant atmospheric flux of iodine from kelp systems has been observed (Carpenter et al., 2000), providing a source of cloud condensation nuclei and an ozone removal mechanism (Küpper et al., 2008). Similarly, kelp are key components of the bromine biogeochemical cycle, producing large quantities of bromoform (CHBr₃) and methylene bromide (CH₂Br₂) (Manley et al., 1992).

In contrast, the dynamics of the sulphur biogeochemical cycle within kelp forests is not well understood, perhaps because of the low DMSPi concentrations within kelp, and thus an apparent lack of DMSP-driven grazing defence mechanisms (Van Alstyne and Houser, 2003).

8.4 Aims of this study

The low DMSPi concentrations found within kelp (Lyons et al., 2007; Van Alstyne and Puglisi, 2007; also see Chapter 5) mean that the effect of grazing on kelp forest system DMS/P dynamics has not yet been studied, despite the importance of DMSP for grazing in other benthic systems (Van Alstyne et al., 2001). Eastern Canadian kelp forests provide an ideal location to investigate the effect of grazing on DMS/P dynamics due to the well-defined grazing front. Thus, the aims of this chapter were to assess the:

1. Influence urchin grazing has on dissolved DMS+DMSP (DMS/Pd) concentrations in a kelp forest in Nova Scotia, Canada *in situ*.
2. Effect of stormy conditions on the DMS/Pd concentrations within the Nova Scotian kelp forest system *in situ*.
3. Influence of urchin grazing on DMS/P release from kelp and coralline algae and DMSPi in coralline algae from the Nova Scotian kelp bed system using laboratory based experiments.

It was hypothesised that urchin grazing would facilitate the release of DMSP from kelp and coralline algae, and, based on the activated defence hypothesis, grazing would stimulate an up-regulation of DMSPi in coralline algae.

8.5 Methods: *In situ* field sampling

8.5.1 Sample collection

Water samples were collected using SCUBA at Splitnose Point, Nova Scotia, Canada (44°28'37"N, 63°32'48"W) for DMS/Pd determination. For comparison between calm and stormy conditions, water samples were taken on two occasions:

1. Calm conditions: wind speeds of <20 km h⁻¹ with no storm activity for one week prior to sampling.

2. Stormy conditions: wind speeds of $>50 \text{ km h}^{-1}$ with a visibly reduced grazing front - taken one day before Hurricane Earl made landfall on Nova Scotia in September 2010.

Water samples ($n = 5$ per location) were collected using SCUBA in glass bottles at the seabed along a transect 90° to the shoreline. Samples were taken at set distances from the urchin front (= lower limit of kelp growth): -10 m, -5 m (both in the kelp bed), 0m (at the urchin front), +5m, + 10m, +20m, +40m (all in the coralline barrens). Logistical constraints prevented a full sample collection during stormy conditions: only -5m, 0m, +20m and +40m water samples were collected. Water samples were prepared and analysed for DMS/Pd as described in Chapter 2.

8.5.2 Hurricane Earl

On the day of sampling in stormy conditions, hurricane Earl was classified as a category 1 hurricane, having been downgraded from a maximum of category 4 in the western Atlantic (Figure 8.2). At landfall in Nova Scotia, maximum one-minute surface winds of 115 km h^{-1} were reported (Cangialosi, 2011).

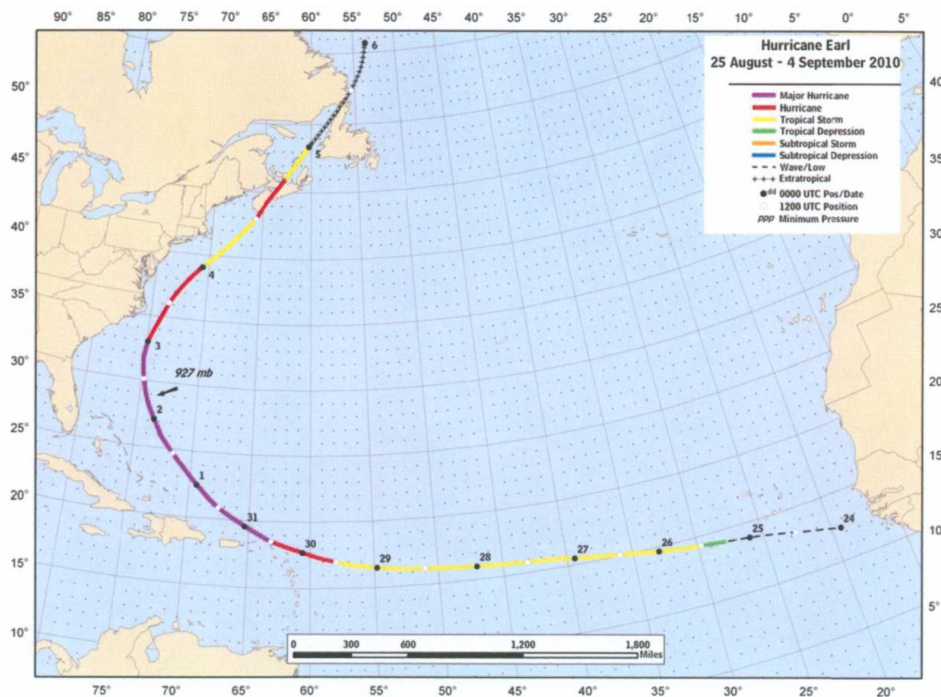


Figure 8.2 Hurricane Earl track, 25th August – 4th September 2010. Source: Cangialosi (2011) [NOAA hurricane report].

8.5.3 Statistical analyses

General linear models and Tukey's pairwise comparisons in Minitab V15 were used to identify differences between ecosystem zones and between calm and stormy conditions. Square-root data transformation of both calm and stormy data sets was required to meet test assumptions of normality and homogeneity of variance.

8.6 Methods: Laboratory experiment

8.6.1 Sample collection

The primary components of the Nova Scotian kelp bed ecosystem - *Saccharina longicruris* (kelp), *Lithothamnion glaciale* (coralline algae) and *S. droebachiensis* (urchins) were collected by hand using SCUBA and transported to Dalhousie University's seawater facility in seawater maintained at $\sim 14^{\circ}\text{C}$. Free-living *L. glaciale* thalli were collected from Eagle Head ($44^{\circ}04'05''\text{N}$, $64^{\circ}36'44''\text{W}$) at a depth of 3 m (thalli approx. 40 - 60 mm in diameter). *S. longicruris* thalli were collected from Splitnose ($44^{\circ}28'37''\text{N}$, $63^{\circ}32'48''\text{W}$) at a depth of 5 m. *S. droebachiensis* were collected from Bear Cove ($44^{\circ}32'13''\text{N}$, $63^{\circ}32'36''\text{W}$) at a depth of 6 m (tests ~ 100 mm in diameter). Within two hours of collection, thalli and urchins were transferred to flow-through holding tanks maintained at ambient conditions and allowed to acclimatise for one week. Urchins were not fed during this time to ensure equal starvation levels.

8.6.2 Mesocosm set-up

Three experiments were conducted to assess the effect of urchin grazing on DMS/Pd and DMSPi concentrations in kelp and coralline algae.

Experiment 1: The effect of kelp grazing on water column DMS/Pd

24 mesocosms (300 mm diameter, 7 litre water volume, 14°C , 35 salinity) were arranged over two treatments of high ($8 \mu\text{mol photons m}^{-2} \text{s}^{-1}$, $n = 12$) and low ($1 \mu\text{mol photons m}^{-2} \text{s}^{-1}$, $n = 12$) photosynthetically active radiation (PAR, 14h:10h light:dark cycle) using shading. Within each light level, four grazing

treatments were randomly assigned to the 12 mesocosms, thus creating three independent replicates per treatment, per light level (Figure 8.3):

1. Control - no biota present, water only (n = 3).
2. Kelp - one 100 x 150 mm frond section (n = 3).
3. Urchin - one urchin (n = 3).
4. Both - one kelp section and one urchin (n = 3) (Figure 8.5a).

Mesocosms had continuous flow-through circulation for two days before removing the flow-through component and covering the mesocosms with cling-film to minimise DMS loss by atmospheric flux. After six hours, water samples were taken from each mesocosm for DMS/Pd analysis following the methodology detailed in Chapter 2.

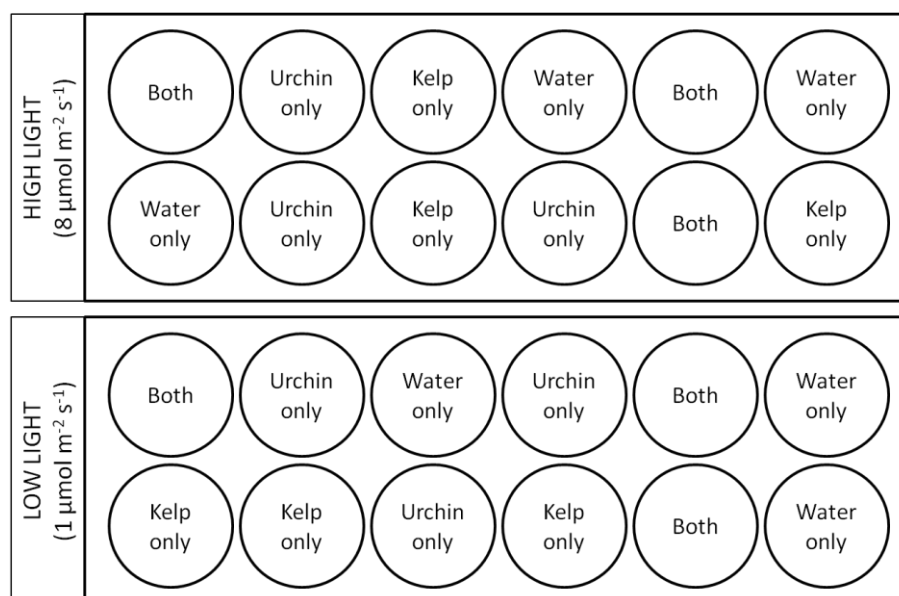


Figure 8.3 Mesocosm set-up for kelp DMS/Pd experiment. Four grazing treatments were considered: water only, kelp (unfouled) only, urchins only and both kelp and urchins at high and low light levels.

Experiment 2: The effect of coralline algae grazing on water column DMS/Pd

24 mesocosms (300 mm diameter, 7 litre water volume, 14°C, 35 salinity) were arranged over two treatments of high ($8 \mu\text{mol photons m}^{-2} \text{s}^{-1}$, n = 12) and low ($1 \mu\text{mol photons m}^{-2} \text{s}^{-1}$, n = 12) PAR (14h:10h light:dark cycle) using shading.

Within each light level, four grazing treatments were randomly assigned to the 12 mesocosms, thus creating three independent replicates per treatment, per light level (Figure 8.4):

1. Control - no biota present, water only (n = 4).
2. Coralline algae - 14 free-living coralline algal thalli evenly distributed (n = 3).
3. Urchin - one urchin (n = 3).
4. Both - 14 coralline algal thalli and one urchin (n = 3) (Figure 8.5b).

Mesocosms had continuous flow-through circulation for two days before removing the flow-through component and covering the mesocosms with cling-film to minimise DMS loss by atmospheric flux. After six hours, water samples were taken from each mesocosm for DMS/Pd analysis following the methodology detailed in Chapter 2.

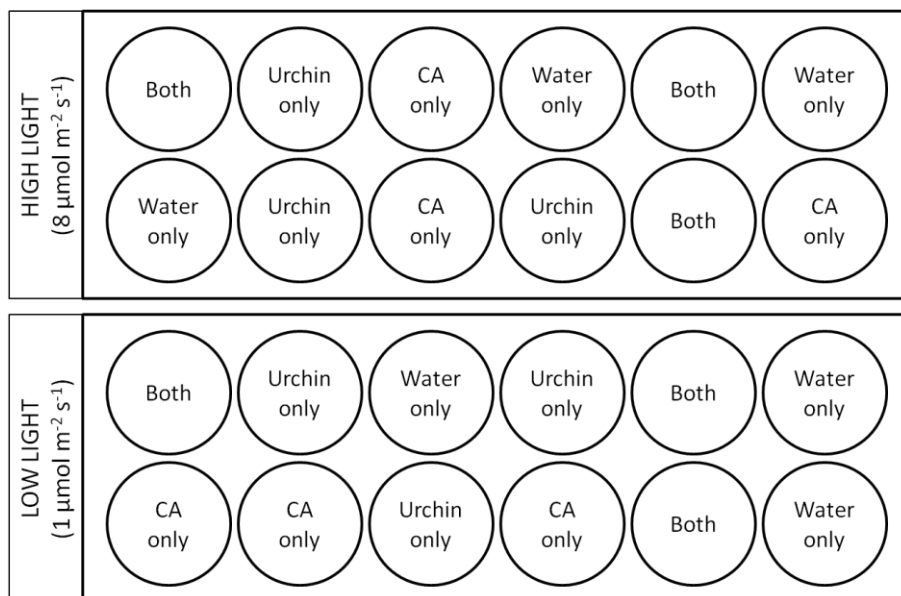


Figure 8.4 Mesocosm set-up for coralline algae (CA) DMS/Pd experiment. Four grazing treatments were considered: water only, CA only, urchins only and both CA and urchins at high and low light levels.

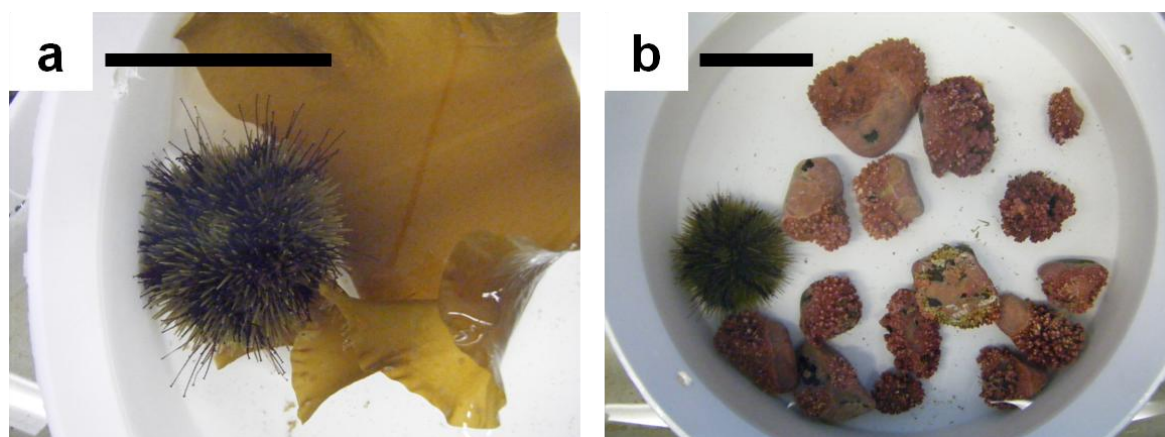


Figure 8.5 Examples of (a) kelp and (b) coralline algae mesocosms. Mesocosm set-up for grazing treatment four in experiments one and two: both algae and urchins. Scale bar = 100 mm.

Experiment 3: The effect of urchins on coralline algal DMSPi

24 flow-through mesocosms (300 mm diameter, 7 litre water volume, 14°C, 35 salinity) were arranged over two treatments of high ($8 \mu\text{mol photons m}^{-2} \text{s}^{-1}$, $n = 12$) and low ($1 \mu\text{mol photons m}^{-2} \text{s}^{-1}$, $n = 12$) PAR (14h:10h light:dark cycle) using shading. Within each light level, three grazing treatments were randomly assigned to the 12 mesocosms, thus creating four independent replicates per treatment, per light level (Figure 8.6 and Figure 8.7):

1. Control - six coralline algae thalli only ($n = 4$).
2. Free urchins - six coralline algae thalli and two urchins free to graze ($n = 4$).
3. Caged urchins - six coralline algae thalli and two urchins held in perforated containers to prevent grazing but with maintained water flow ($n = 4$) (Figure 8.7b).

Coralline algae samples were taken after two and four days ($n = 3$ per mesocosm, per timepoint, thus creating a nested design). There was no repeat sampling of thalli. Branch tips were prepared and analysed for DMSPi as detailed in Chapter 2.

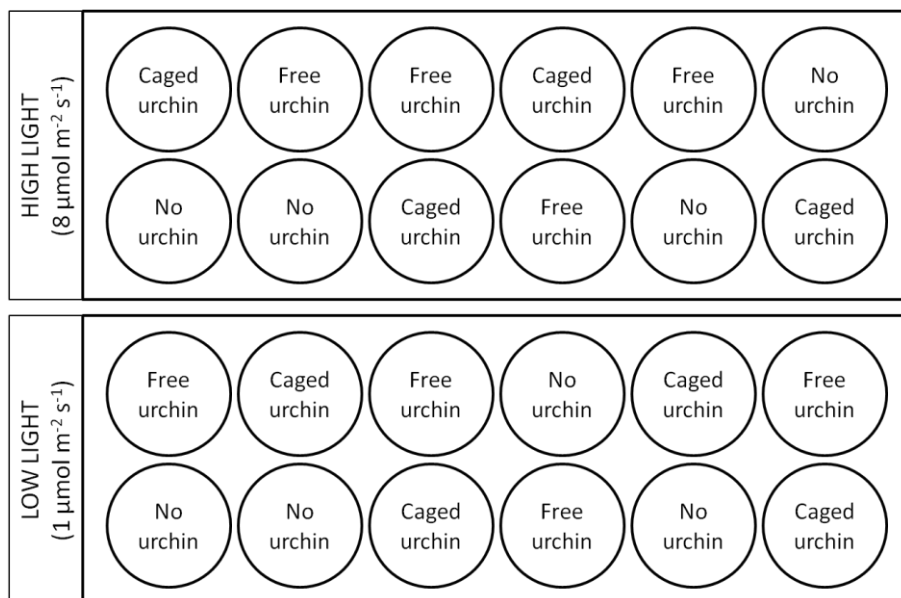


Figure 8.6. Experimental set-up for coralline algal DMSPi experiment.

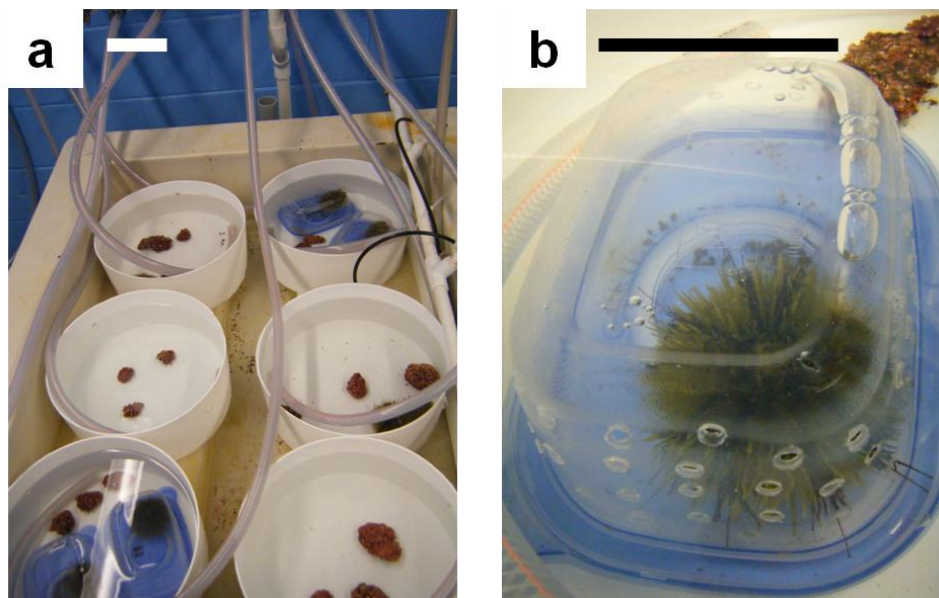


Figure 8.7. Examples of experiment three set-up. (a) Six mesocosms from the high light regime; (b) one of two cages per 'caged urchin' treatment used to prevent grazing activity. Scale bar = 100 mm.

8.6.3 Statistical analyses

All data were analysed using General Linear Models; each experiment was analysed independently. In order to meet test assumptions of normality and homogeneity of variance, the DMS/Pd (kelp) data were $\log_{10}(x+1)$ transformed (where x is the data point) and the coralline algal DMSPi data were \log_{10} transformed. The DMS/Pd (coralline) data did not require transformation. All analyses were conducted in Minitab V15.

8.7 Results: *In situ* sampling

During calm conditions, an elevation in DMS/Pd concentrations to >15 nmol L⁻¹ was observed across a 15 m wide area spanning the grazing front, from 5 m within the kelp forest to 10 m into the coralline barrens (Figure 8.8). A significant decline in DMS/Pd was observed at the +20 m site (in the coralline barrens) ($F_6 = 4.15$, $p = 0.005$, Figure 8.8). A slight rise in DMS/Pd concentration was observed at +40m, although this was characterised by relatively high variability. DMS/Pd concentrations during stormy conditions, although smaller in magnitude, followed a similar trend, with a significant increase at the urchin front (0m) compared to the coralline barrens (+20m and +40m) ($F_3 = 6.35$, $p = 0.005$, Figure 8.8).

DMS/Pd concentrations were significantly higher during calm conditions compared to stormy conditions ($F_1 = 6.43$, $p = 0.015$, Figure 8.8). An overall difference in sampling location was also observed ($F_6 = 3.63$, $p = 0.005$), with the highest concentrations centred around the grazing front.

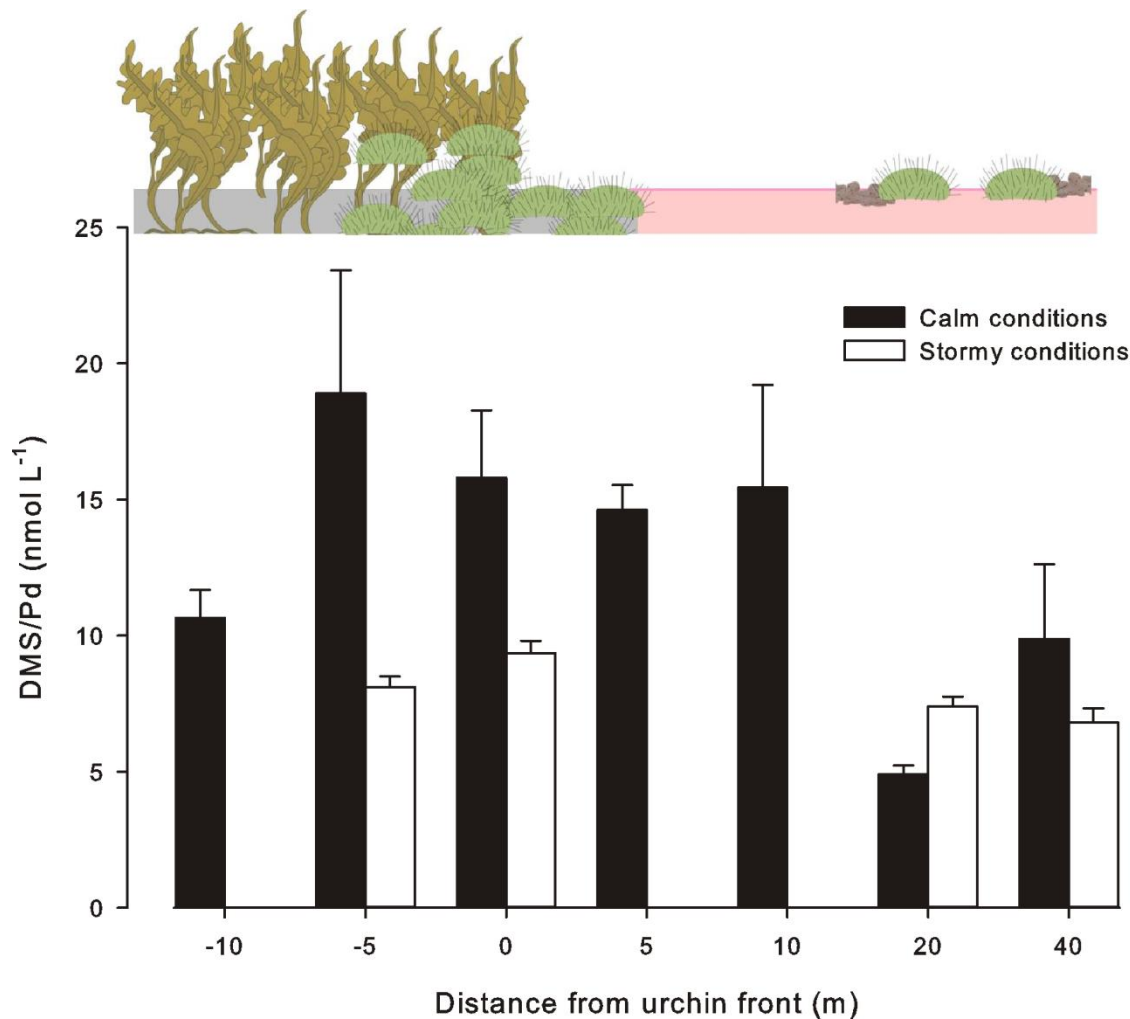


Figure 8.8 Dissolved DMS/P (nmol L⁻¹) within the kelp bed ecosystem. Samples were taken at defined distances from the urchin front during calm (<20 km h⁻¹, black bars) and stormy (>50 km h⁻¹, white bars) conditions. Negative distances are within the kelp bed, positive distances are within the coralline barrens, as represented by the image above the graph. Data presented as mean ± SE.

8.8 Results: Laboratory experiment

8.8.1 Dissolved DMS/P

In the *S. longicuris* (kelp) experiment, significantly higher DMS/Pd concentrations were observed under the low-light regime, irrespective of grazing treatment ($F_1 = 22.16$, $p = 0.002$, Figure 8.9a). DMS/Pd concentrations in urchin-only treatments were significantly higher than the kelp-only treatment when both light regimes considered together ($F_3 = 5.06$, $p = 0.030$). However, DMS/Pd concentrations did not differ significantly between grazing treatments within each light regime (high PAR: $F_3 = 0.98$, $p = 0.46$; low PAR: $F_3 = 1.82$, $p = 0.24$).

In the *L. glaciale* (coralline algae) experiment, no significant differences were observed between grazing ($F_3 = 0.69$, $p = 0.58$) or light ($F_1 = 0.19$, $p = 0.67$) treatments (Figure 8.9b).

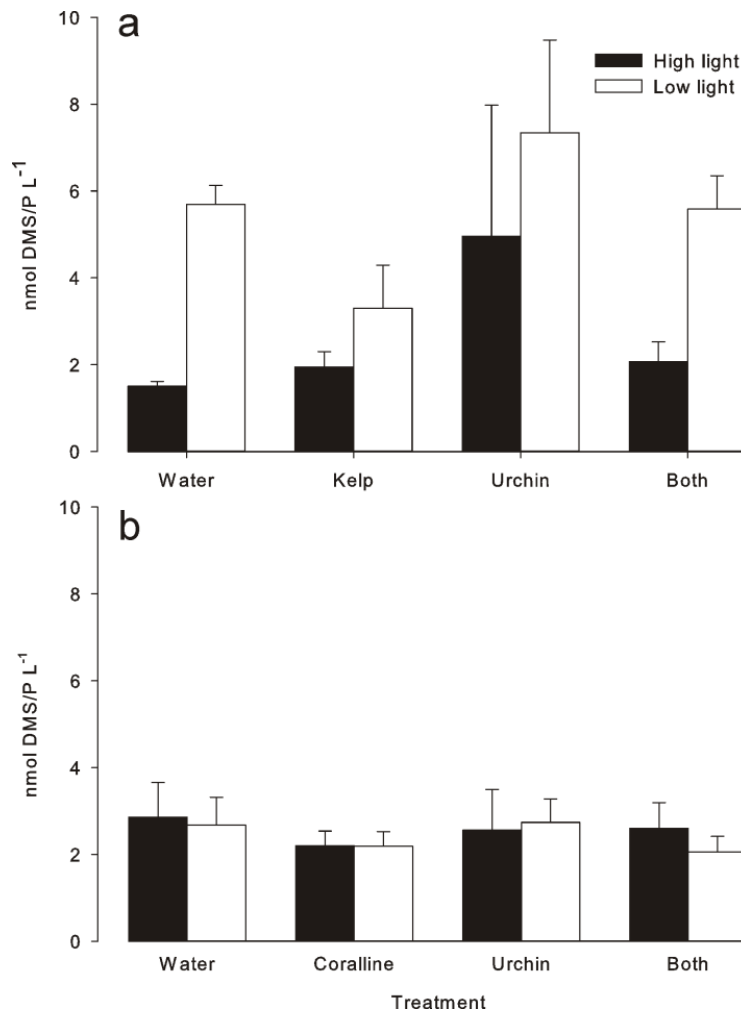


Figure 8.9. Dissolved DMS/P (nmol L⁻¹) following two days incubation. Four treatments of (1) water only, (2) algae only, (3) urchins only and (4) both algae and urchins at high (8 μmol photons m⁻² s⁻¹, black bars) and low (1 μmol photons m⁻² s⁻¹, white bars) PAR levels using a) *S. longicuris* (kelp) and b) *L. glaciale* (coralline algae). Data presented as mean ± SE.

8.8.2 Intracellular DMSP

Light regime did not have a significant impact on DMSPi concentrations in *L. glaciale* ($F_1 = 3.00$, $p = 0.086$, Figure 8.10). Urchin treatment, however, exhibited a significant effect ($F_2 = 5.70$, $p = 0.004$): no significant difference was observed between the no-urchin and free-urchin treatments, whilst the caged treatment was significantly higher. A significant increase in DMSPi concentrations from day 2 - 4 was observed ($F_1 = 20.77$, $p < 0.001$, Figure 8.10), except in the low light / free urchin treatment.

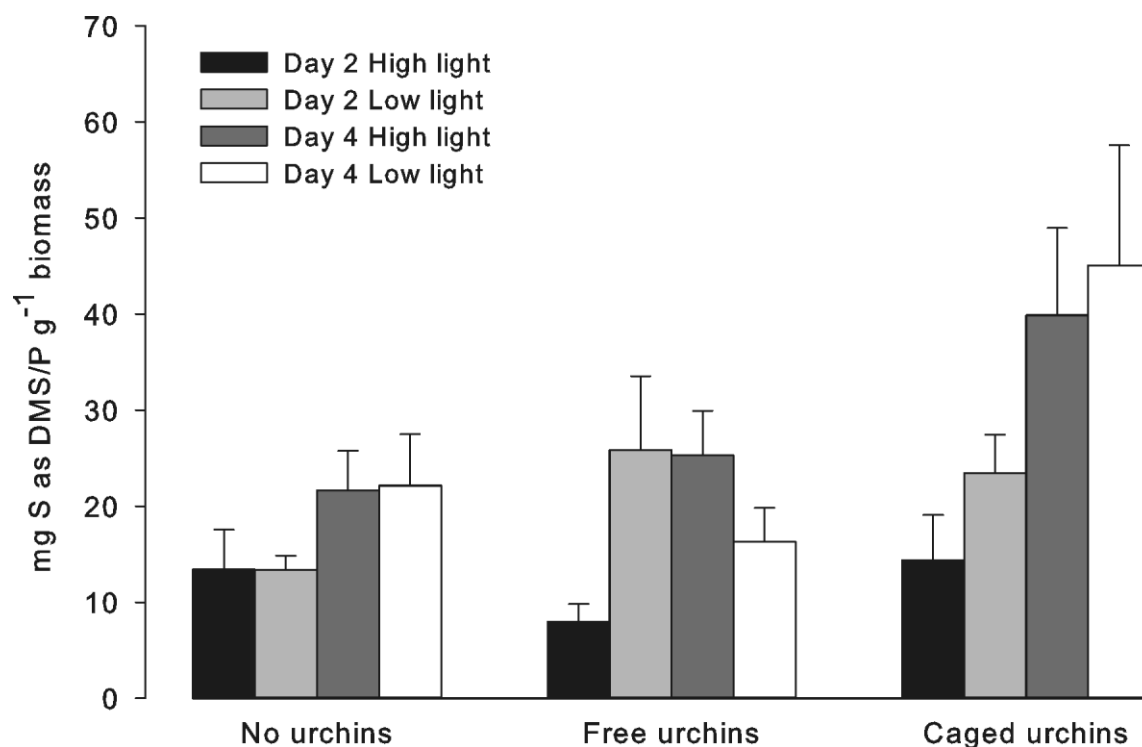


Figure 8.10. Coralline algal DMSPi (mg S g⁻¹ biomass as DMS/P). Concentrations determined after exposure to (1) no urchins, (2) free urchins and (3) caged urchins. Samples were taken after two (black and light grey bars) and four (dark grey and white bars) days incubation under high (8 $\mu\text{mol photons m}^{-2} \text{s}^{-1}$, black and dark grey bars) and low (1 $\mu\text{mol photons m}^{-2} \text{s}^{-1}$, light grey and white bars) PAR levels. Data presented as mean \pm SE.

8.9 Discussion

Kelp forests are an important habitat in the marine environment, harbouring a high biodiversity, providing ecosystem services and provisions and may be crucial in the biogeochemical cycling of macro and micronutrients. This research aimed to investigate the effect urchin grazing may have on DMSPi in kelp and coralline algae and on water column DMS/P concentrations. A clear pattern in DMS/Pd concentrations were observed in the field, although this was not fully supported by laboratory experiments, highlighting a requirement for further investigations to fully elucidate the role of urchin grazing on the production and release of DMS/P from the kelp forest system.

8.9.1 The grazing front as a source of DMS/Pd

In the field, the urchin grazing front provided a significant source of DMS/Pd to the water column during calm and stormy conditions, suggesting that high-density urchin grazing may be important in facilitating the cycling of DMS/P in the kelp forest ecosystem. Urchin grazing in this habitat appears to facilitate

the release of DMS/P into the water column, probably in a similar manner to the previously described 'sloppy feeding' mechanism of zooplankton (Yoch, 2002). The production of urchin faecal pellets may also have contributed to the elevated DMS/Pd at the urchin front. Zooplankton faecal pellets produced during pelagic plankton blooms are characterised by a high DMS/P content (up to 33 mM, Kwint et al., 1996), thus it may be postulated that urchin faecal pellets are important sources of DMS/P in the coastal zone. If sufficiently maintained into the upper water column, kelp grazing may be a significant source of DMS to the atmosphere around the coast of Nova Scotia and in other areas where kelp bed grazing occurs (e.g. *Macrocystis pyrifera* beds along the eastern coast of the USA). Future investigations, profiling DMSP, DMS and dimethylsulphoxide (DMSO) concentrations throughout the water column and across the kelp bed ecosystem would help to more fully understand the sulphur dynamics within the kelp forest habitat. Urchin grazing may also be important in DMS/P cycling in other ecosystems such as coral reefs (see Chapter 4), highlighting the requirement for further research into the ecosystem effects of herbivorous grazing.

Despite the clear pattern in the field, when the impact of urchin grazing was tested in the laboratory results were inconclusive - urchin grazing did not appear to have an effect on DMS/Pd concentrations. The laboratory light conditions were low, but not below the PAR tolerance of kelp nor coralline algae (Roleda, 2009; Adey, 1970). However, in the low-light kelp experimental groups, the natural planktonic community appeared to elevate DMS/Pd concentrations (although this was highly variable). The planktonic community within the experimental mesocosms was not characterised thus it is not known which species were dominant. However, in the open ocean, a wide range of DMS/P metabolising bacterial species are known (Hatton et al., 2012b), including the α -*Proteobacteria* which degrade DMSP to DMS and oxidise DMS to DMSO (Zubkov et al., 2002; Gonzalez et al., 2000; Gonzalez et al., 1999). Laboratory conditions cannot accurately mimic the natural world, thus all laboratory studies have some degree of error associated with them. Mesocosm studies have been shown to cause an elevation in DMSPi production in coralline algae (Burdett et al., 2012a, and see Chapter 7). Thus, the inconclusive laboratory results of this research may have been driven by artefacts inherent with laboratory studies.

8.9.2 Chemical signals

DMSPi in coralline algae was enhanced only whilst urchins were caged. The urchins' restricted environment may have stimulated the production of a waterborne chemical cue that the coralline algae responded to by up-regulating DMSPi. DMSP has, until now, been described as a herbivore defence only activated by direct grazing activity (Van Alstyne and Houser, 2003). Anti-herbivore defences in response to waterborne cues have been previously observed in algae (e.g. Toth, 2007; Macaya et al., 2005; Toth and Pavia, 2000) and other plants (Dicke and Bruin, 2001; Baldwin and Schultz, 1983). This research suggests a similar pre-emptive defence mechanism for coralline algae may be present, utilising DMSPi (and perhaps its associated breakdown products) as the defence compound.

8.9.3 Impact of storm activity on DMS/Pd

During stormy conditions, when the grazing front was depleted, DMS/Pd concentrations were lower and the peak of DMS/Pd release less pronounced. Two primary factors may have acted to reduce DMS/Pd concentrations during stormy conditions:

1. A depleted grazing front: reduced grazing pressure on the kelp may have reduced the importance of sloppy feeding by urchins as a release mechanism for DMSPi from the kelp.
2. Increased atmospheric flux of DMS: wind speed is the primary factor driving air-sea gas exchange (Liss and Merlivat, 1986). Bubble penetration may reach >20 m depth during a storm (Zhang et al., 2006), further enhancing gas exchange.

These factors may have led to a reduced input of DMS/Pd from the kelp and an increased export of DMSd to the atmosphere, reducing observed DMS/Pd. Knowledge of the proportions of DMSd and DMSPd in the water column would have allowed the importance of these processes to be assessed.

8.9.4 North Atlantic hurricanes

Hurricanes are classified using the Saffir-Simpson Hurricane Wind Scale (Table 8.1), based on maximum 1-minute sustained wind speeds. Potential damage to land rises by a factor of four for every rise in category (NOAA, 2012a).

North Atlantic hurricanes form from ‘seedlings’ - persistent rain disturbances 200 - 600 km wide - in the eastern Atlantic that migrate westwards in the trade winds (Simpson and Riehl, 1981). Hurricanes rarely develop where ocean sea surface temperature (SST) is less than ca. 26°C, so the majority of hurricanes occur in August and September, when SSTs are warmest (NOAA, 2012a; Simpson and Riehl, 1981). North Atlantic hurricanes are characterised by an anticlockwise storm rotation and slight northwards path across the central Atlantic (Figure 8.11). At around 30°N, general atmospheric circulation reverses, causing the hurricanes to recurve north and eastwards along the eastern coast of North America towards Nova Scotia (Figure 8.11). The drop in SST at higher latitudes causes a weakening and eventual cessation of hurricane storms at around 45°N (Figure 8.11).

Table 8.1 The Saffir-Simpson Hurricane Wind Scale.

Wind speeds correspond to peak 1-minute sustained speeds at a height of 10m. This table includes the minor modifications of category 3/4 and 4/5 boundaries established in 2012 (NOAA, 2012a).

Category	Wind speed (km h ⁻¹)	Summary
1	119 – 153	Very dangerous winds, will produce some damage
2	154 – 177	Extremely dangerous winds, will cause extensive damage
3	178 – 208	Devastating damage will occur
4	209 – 251	Catastrophic damage will occur
5	252+	Catastrophic damage will occur

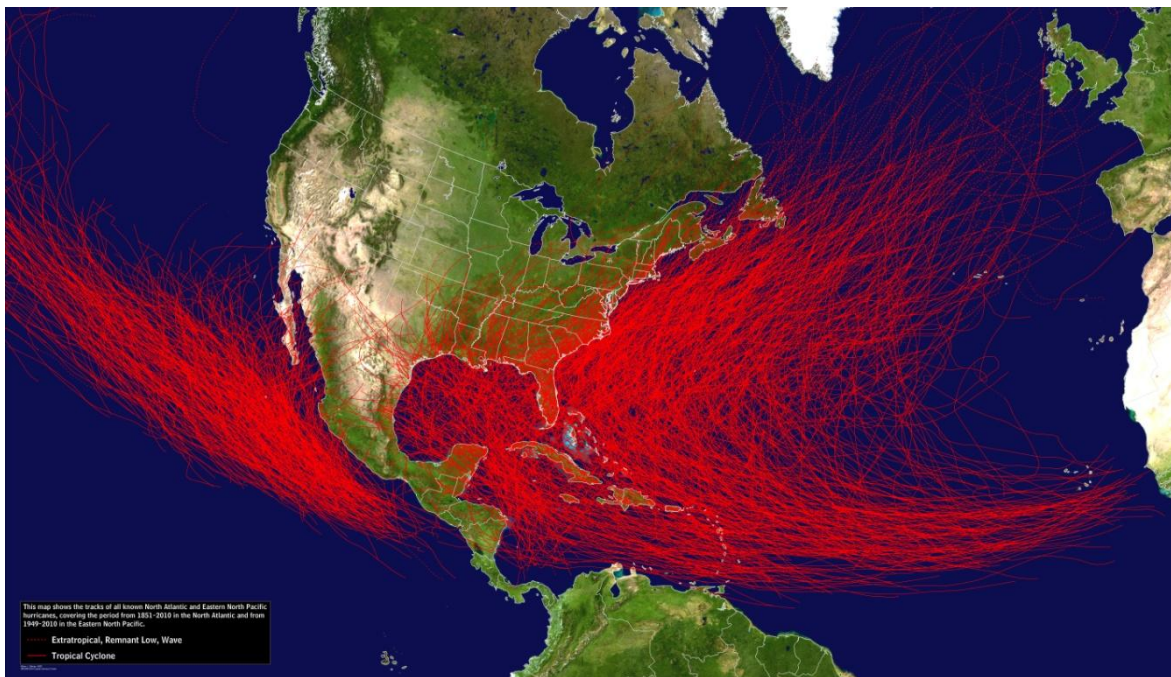


Figure 8.11 Hurricane tracks in the eastern Pacific and north Atlantic. Data from 1949 - 2010 in the Pacific and 1851 - 2010 in the Atlantic. Source: NOAA National Hurricane Center (2012a).

8.9.4.1 Future hurricane projections

The climate of the North Atlantic is influenced by numerous climatic oscillations that result in large natural variations in hurricane activity (Knutson et al., 2010), including the:

1. Atlantic Meridonal Oscillation (AMO): 65 - 70 year oscillation in SST owing to changes in the thermohaline circulation (Schlesinger and Ramankutty, 1994).
2. North Atlantic Oscillation (NAO): decadal oscillations of the location of the Icelandic low and Azores high pressure systems; the NAO may affect Atlantic storm tracks (Hurrell, 1995).
3. El Niño - Southern Oscillation (ENSO): Sub-decadal oscillations in the surface pressure of the western tropical Pacific; El Niño years may suppress Atlantic hurricane activity (Philander, 1983).
4. Stratospheric quasi-biennial oscillation (QBO): 26 - 28 month oscillation of the equatorial stratospheric (30mb) wind; westerly QBO increases hurricane activity (Gray, 1984).

There appears to have been an increase in hurricane frequency over the 20th century in the north Atlantic (Holland and Webster, 2007; Mann and Emanuel, 2006) that has been linked to both natural variability (Shanahan et al., 2009) and anthropogenic warming (Gillett et al., 2008; Mann and Emanuel, 2006). Presently, scientific consensus projects that the number of hurricanes in the north Atlantic will not change, or may even decline, over the next century due to a weakening of the tropical circulation patterns, but that the frequency of category 4 and 5 hurricanes could double by 2100 (Bender et al., 2010; Knutson et al., 2010; Knutson et al., 2008). Thus, the frequency and severity of hurricanes along the coast of Nova Scotia may increase in the future, impacting the shallow coastal zone where the kelp forests are located.

8.9.5 Impact of hurricanes on kelp forests

Kelp thalli are engineered to withstand the significant drag forces associated with the shallow coastal zone (water currents and wave action) (Gaylord and Denny, 1997). However, thalli can be damaged, dislodged and broken during high intensity storm events (Krumhansl et al., 2011). If thalli are broken at the holdfast or stipe, mortality of that plant will occur (Seymour et al., 1989). If only the fronds are damaged the thallus may not die, but habitat biomass is reduced (Krumhansl and Scheibling, 2011). Grazing and encrustation damage (lesions, excavations and perforations) significantly increases the likelihood of thallus damage during the high wave activity associated with storm events (Krumhansl et al., 2011).

High orbital velocities, breaking waves and entanglement has been attributed to the mortality of the Pacific giant kelp *Macrocystis pyrifera* during storm events (Seymour et al., 1989). However, the fast growth rate of this kelp allows full recovery from storm damage within two years, faster than the average frequency of high intensity storms along the coast of California (currently 3.5 years) (Graham et al., 1997). Significant changes to the kelp forest ecosystem structure could occur if high intensity storms became more frequent in the future (Byrnes et al., 2011), creating a less diverse food web as species become locally extinct, particularly from high trophic levels (Byrnes et al., 2011).

8.9.6 Impact of hurricanes on ocean circulation

Nova Scotia is subject to upwelling events which may be induced by wind (Petrie et al., 1987), tide (Tee et al., 1993) or currents (Garrett and Loucks, 1976). Upwelled water, although nutrient-rich, may contain high levels of dissolved CO₂ (Gruber et al., 2012), perhaps reducing carbonate saturation states below one at the surface (Feely et al., 2008). An increase in hurricane frequency and intensity may instigate periodic upwelling events, exposing the kelp forest ecosystem to acute pulses of low-pH water, as is predicted globally under a future ocean acidification scenario (see Chapter 7). The morphology and DMSPi concentrations of *L. glaciale* are affected by acute exposure to low-pH conditions (Burdett et al., 2012a; and see chapter 7) and urchins have been reported to undergo significant, negative alterations at the genomic and larval level (e.g. O'Donnell et al., 2009; Todgham and Hofmann, 2009; Kurihara, 2008) under high CO₂ conditions. In contrast, fleshy macroalgae (such as kelp) may benefit from an increase in CO₂, by enhancing photosynthesis.

North Atlantic hurricanes transport warm water northwards towards the coast of Nova Scotia. The rise in temperature appears to stimulate the proliferation of an amoeba that is fatal to urchins (Jones and Scheibling, 1985) and has caused numerous urchin mass mortality events since the 1980s (Scheibling and Lauzon-Guay, 2010; Jones and Scheibling, 1985). As mass mortality events become more widespread, the Nova Scotian population of *S. droebachiensis* (and therefore their grazing potential) is predicted to decline (Feehan et al., 2012; Scheibling and Lauzon-Guay, 2010).

8.9.7 Implications for the future

With reduced grazing pressure and periodic increases in CO₂ and temperature, the coverage of kelp will be able to extend seawards (Feehan et al., 2012; Scheibling and Lauzon-Guay, 2010) (Figure 8.12), forcing the coralline barrens to deeper waters. In the absence of an urchin front, the primary DMSP release mechanisms from kelp would likely be cell senescence and lysis (Yoch, 2002), which may occur during storms because of physical damage to kelp fronds - a factor that would not be important for the release of DMSP from

phytoplankton in the water column. High intensity storms will increase air-sea gas exchange of DMS, leading to pulsed releases of DMS into the atmosphere.

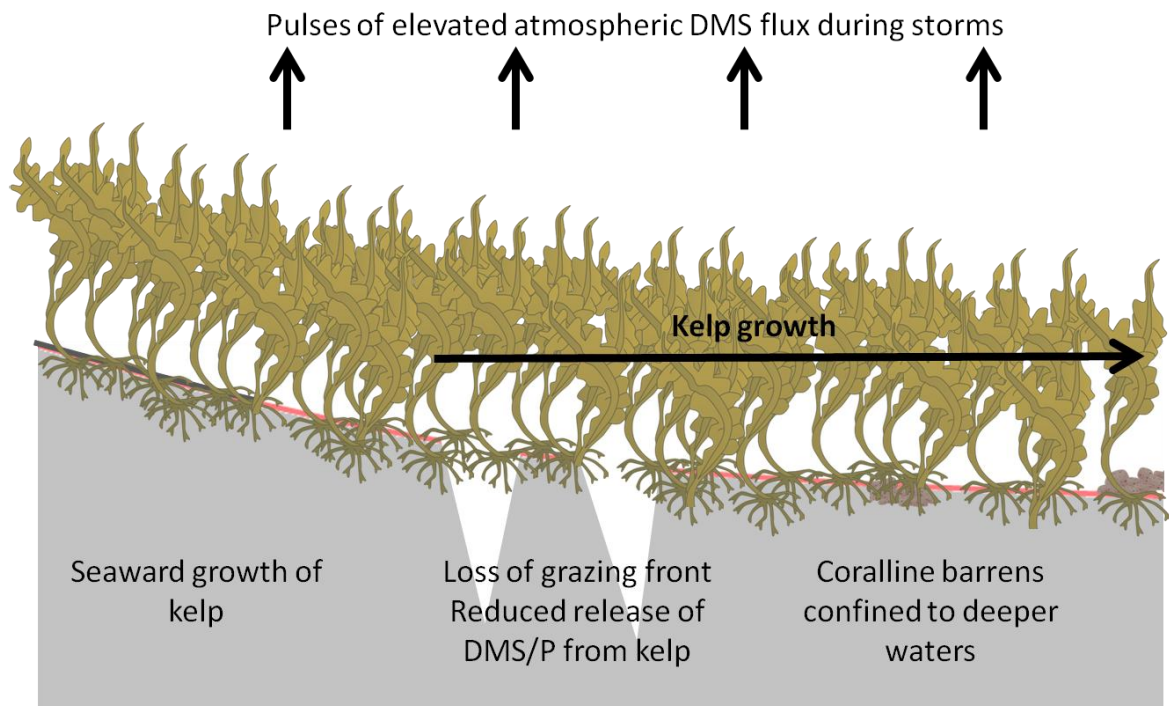


Figure 8.12 Proposed future kelp forest ecosystem. Changes in grazing activity and ocean chemistry may result in changes to the ecosystem structure and sulphur biogeochemical cycle in the kelp forest ecosystem.

Kelp bed ecosystems are important for the biogeochemical cycling of the macronutrients (carbon and nitrogen, Sauchyn and Scheibling, 2009a; Sauchyn and Scheibling, 2009b; Soares et al., 1997), iodine (Küpper et al., 2008; Carpenter et al., 2000; Küpper et al., 1998) and bromine (Manley et al., 1992). The proposed ecosystem phase shift, towards a prolonged kelp bed state, may therefore also impact the coastal biogeochemical cycling of elements other than sulphur:

1. Carbon and nitrogen: reduced horizontal and vertical transport of grazed biomass and faecal pellets alongshore and to deeper waters, although thallus damage by storms may provide periodic supplies of biomass.
2. Iodine and bromine: increased production by kelp across a larger area and increased atmospheric flux, peaking during storms; enhanced iodine production in particular may increase the production of coastally-derived cloud condensation nuclei.

8.10 Conclusions

The kelp forest habitats of eastern Canada are ecologically and economically important, and are involved in a number of biogeochemical cycles. In areas of high-density grazing activity (i.e. at the urchin grazing front), an increase in water column DMS/Pd was observed, perhaps in a similar manner to the 'sloppy feeding' mechanism of zooplankton. This was also observed during stormy conditions, when grazing pressure is reduced and mixing of the water column is increased, highlighting the potential importance of the urchin front in releasing DMS/P from the macroalgae. Laboratory experiments to further investigate this effect were not wholly conclusive, but did suggest that urchin 'stress' may result in an up-regulation of DMSPi in the coralline alga *L. glaciale*, perhaps via water-borne chemical cues. Projected climate change may cause the dynamics of the kelp forest ecosystem to change in the future, perhaps favouring prolonged kelp-bed dominance, with storm-driven pulsed releases of DMSPi into the water column and DMS flux into the atmosphere.

9

Discussion and conclusion

The production and release of dimethylsulphoniopropionate (DMSP) by algae is a major component of the marine sulphur cycle, accounting for $\sim 50 \times 10^{12}$ moles of sulphur per year (Sievert et al., 2007). The subsequent formation of dimethylsulphide (DMS) may help to regulate local climate by promoting the formation of clouds (Kocsis et al., 1998; Charlson et al., 1987). Dimethylated sulphur compounds are also important in maintaining marine ecosystem function, acting as a cryoprotectant (Karsten et al., 1996), antioxidant (Sunda et al., 2002), compatible solute (Stefels, 2000), grazing deterrent (Dacey and Wakeham, 1986) and attractant (Seymour et al., 2010) and microbial energy source (Hatton et al., 2012a; Green et al., 2011). However, our knowledge of the sulphur cycle in the coastal ocean is limited, despite the high intracellular DMSP (DMSPi) concentrations of some coastal macroalgae.

By area, the open ocean represents around 90% of the oceans (Lana et al., 2012; Costanza et al., 1997). However, ecosystem services provided by the coastal ocean (such as nutrient cycling, food production and recreation) are some of the most valuable in the world (Costanza et al., 1997). The overall global value of coastal habitats (including estuaries, coral reefs, seagrass meadows and macroalgal beds) is similar to the entire open ocean ($\sim \$8400 \times 10^9 \text{ yr}^{-1}$, Costanza et al., 1997). Red coralline algae are often major components of these coastal habitats. Their high DMSPi concentrations (Burdett et al., 2012a; Rix et al., 2012; Kamenos et al., 2008b; and see Chapters 3 - 8) may therefore be important in the coastal marine sulphur cycle, influencing ecosystem function (and therefore service provision and value) and potential climate regulation through DMS emissions.

Previous macroalgal DMSP studies have focused on the Chlorophyta (e.g. Lyons et al., 2010; Van Alstyne, 2008; Lyons et al., 2007; Van Alstyne et al., 2007; Van Alstyne and Puglisi, 2007). Coralline algal habitats (including maerl beds, seagrass meadows, coral reefs and kelp forests) are globally ubiquitous in the coastal ocean, yet are under-researched in terms of DMSP+DMS (DMS/P) production and release. Using a variety of techniques in the field and the laboratory, this research aimed to provide a better understanding of:

1. The cellular photosynthetic characteristics of coralline algae (Chapter 3), as the precursor to DMSPi is methionine, an indirect product of, and facilitator to, the photosynthetic pathway.
2. The spatial (Chapter 4) and temporal (Chapter 5) natural variability of DMS/P production and release by coralline algal habitats.
3. The impact environmental and biological forcing may have on DMS/P production by coralline algal habitats, including reduced salinity (Chapter 6), reduced and variable pH (Chapter 7) and herbivorous grazing (Chapter 8).

9.1 The photosynthetic characteristics of coralline algae

Methionine, the intracellular precursor to DMSPi (Greene, 1962), is an indirect product of photosynthesis and an essential component of the proteins involved in photosynthesis (Wirtz and Droux, 2005). Thus, an understanding of algal photosynthetic characteristics enables a more detailed insight into potential DMSPi production. Detailed analyses of the photosynthetic characteristics of temperate and tropical coralline algae were conducted *in situ* and in the laboratory using Pulse Amplitude Modulation (PAM) fluorometry (Chapter 3).

9.1.1 Light saturation mechanisms

Using optical reflectance techniques, five photosynthetic pigments were identified in tropical (*Lithophyllum kotschyannum*) and temperate (*Lithothamnion glaciale*) coralline algae: chlorophyll-*a*, α -carotenoids (both ubiquitous photosynthetic pigments), phycoerythrin, phycocyanin and

allophycocyanin (pigments unique to Rhodophyta and cyanobacteria). PAM fluorometry research suggested that, in shallow water (< 6 m), coralline algae (specifically *L. kotschy anum*, *Porolithon* sp. and *L. glaciale*) are acclimated to an optimum light level (E_k) that is equal to, or below, ambient light (Chapter 3). Thus, it is highly probable that shallow-water coralline algae are regularly exposed to saturating light conditions and may explain why coralline algae can successfully grow at the lower limit of the photic zone (Foster, 2001). The results presented in Chapters 3, 4 and 7 suggest that coralline algae harbour efficient mechanisms for minimising oxidative damage from photosynthetically-derived reactive oxygen species, including:

1. Photoprotection appears to include regulation of both minimal and maximal light-acclimated fluorescence (F_o' and F_m') (Chapter 3).
2. DMSPi was up-regulated in thalli exposed to high irradiance (Chapters 3 and 6) and high CO₂ (Chapter 7), suggesting that DMSPi may be used as an antioxidant, as described by Sunda et al (2002).
3. Presence of α -carotenoids, which have been associated with photoprotective strategies (Schubert and García-Mendoza, 2008; Wilson et al., 2006).

9.1.2 Diurnal trends

Strong diurnal trends in quantum efficiency were observed in tropical coralline algae exposed to a large range in diurnal irradiance (topsides of free-living thalli and encrusting morphotypes, Chapter 3), similar to other macroalgae (Edwards and Kim, 2010; Figueroa et al., 2009; Häder et al., 1998). In contrast, thalli exposed to a small diurnal irradiance range (e.g. the undersides of tropical thalli) exhibited little photosynthetic trend throughout the day. Intra-thallus heterogeneity was also observed in the temperate species *L. glaciale* (Chapter 3): thallus branch tips were higher light-adapted than branch bases due to self-shading, despite the small branch length (<20 mm). This suggests that coralline algae are able to photoacclimate to changing light regimes. This may be beneficial in the future as species distributions shift in response to global environmental change (e.g. poleward migration of organisms to follow the

thermoclines) as light regime is one factor not affected by global change (Saikkonen et al., 2012).

9.2 Natural variability of coralline algal habitats

Anthropogenic perturbations (e.g. ocean acidification) are overlain on the natural variability of a system (Pelejero et al., 2010). Thus, to make accurate projections for the future, we must understand present-day natural variability. This research has identified some key trends in DMS/P production and release by, and within, coralline algal habitats.

9.2.1 Spatio-temporal variability

DMS/P concentrations in coralline algal habitats were characterised by a high natural spatiotemporal variability (Chapters 4 and 5). Annually averaged dissolved DMS (DMSd) and DMSP (DMSPd) in the open ocean is estimated at 1 - 5 nmol L⁻¹ (Lana et al., 2011) and 2.8 nmol L⁻¹ (Kiene and Slezak, 2006) respectively. DMSd is less than 2 nmol L⁻¹ in 50% of the surface ocean (upper 10 m) (Lana et al., 2011). It was hypothesised that DMS/P concentrations in the coastal ocean would be higher due to the higher productivity in coastal ecosystems. DMSPd, DMSd and particulate DMSP (DMSPp) were measured at four sites around a Scottish maerl bed over a 24 month period (Chapter 5): at the maerl bed (6 m depth), above the maerl bed (3 m depth), at the bed side (6 m depth) and above the bed side (3 m depth). Annually averaged concentrations were considerably higher than open ocean estimates (average across all sites - DMSd: 11.7±1.5 nmol L⁻¹, DMSPd: 19.8±1.7 nmol L⁻¹, DMSPp: 53.3±4.9, mean±SE; Figure 9.1). These results suggest that, despite the small area of the coastal ocean, the region may significantly contribute to the global marine sulphur cycle throughout the year.

The ecosystem dynamics associated with the maerl bed at Loch Sween (e.g. stimulation of spring phytoplankton blooms and autumnal decay of fleshy macroalgae) allowed the maerl bed to seasonally act as a sink and a source of dissolved DMS+DMSP (DMS/Pd) and DMS/Pp, most notably in the summer months (Chapter 5). The DMSPi concentration of coralligène in southwest France was relatively high (Chapter 4), thus could potentially act as a source of DMSP to the

water column. However, DMS/P appeared to be rapidly recycled and the ecosystem in fact acted as a sink for DMS/P. In contrast, DMS/Pd concentrations at Suleman Reef, Egypt were highest in areas dominated by seagrass and macroalgae (Chapter 4). On coral reefs, there is strong biological control on the carbonate chemistry (Zhang et al., 2012; Anthony et al., 2011; Smith and Price, 2011; Gagliano et al., 2010; Kleypas and Langdon, 2006, also see Chapter 7), the strength of which is, in part, determined by water depth and residence time (Kleypas and Langdon, 2006). These factors may also affect the apparent production and release of dimethylated sulphur compounds from coastal ecosystems: in shallow water ecosystems with restricted water exchange (e.g. Suleman reef), DMS/P released from the benthic ecosystems may not be readily mixed with low-concentration oceanic water, allowing the ecosystem to act as a DMS/P source to the water column and atmosphere.

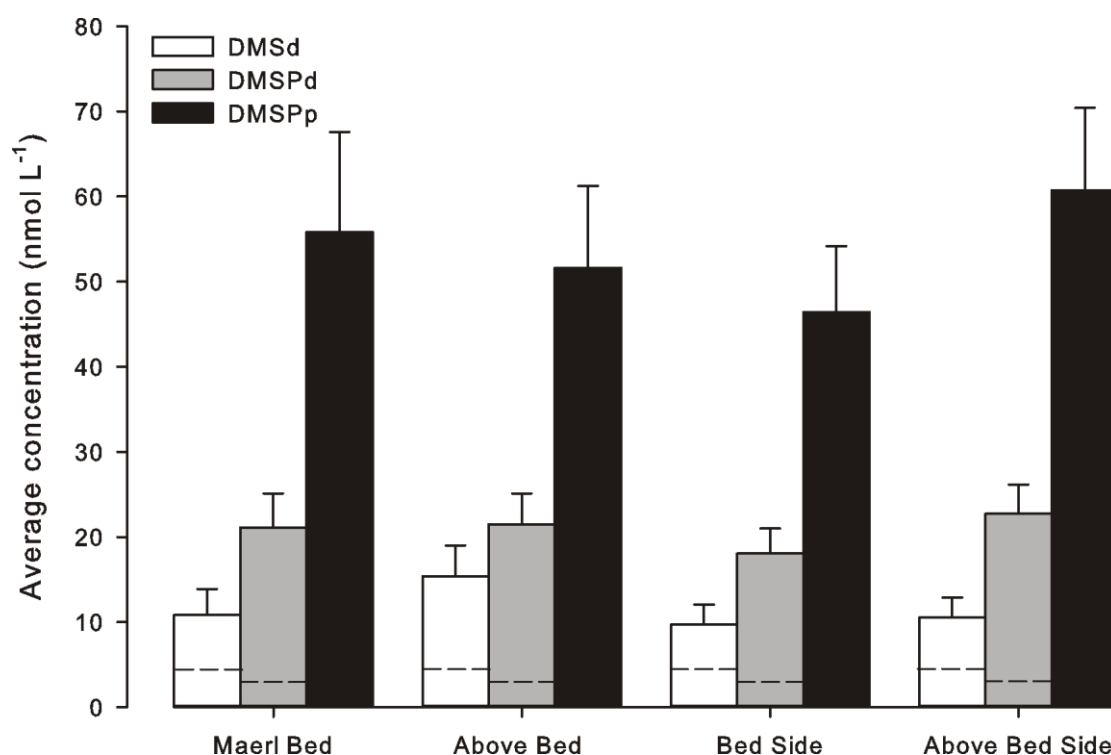


Figure 9.1 Annually averaged DMS/P in Loch Sween, Scotland. Averaged dissolved DMS (white bars), dissolved DMSP (grey bars) and particulate DMSP (black bars) over a 24 month sampling period at a maerl bed in Loch Sween, west coast of Scotland, from March 2010 – February 2012 at four sampling sites: at the maerl bed, above the maerl bed, at the bed side and above the bed side. See Chapter 5 for more information. Data presented as mean \pm SE. Dotted lines represent the global estimate for annual averages for DMSd (up to 5 nmol L⁻¹, Lana et al., 2011) and DMSPd (2.8 nmol L⁻¹, Kiene and Slezak, 2006).

9.2.2 Phylum-specific trends

It has been suggested that DMSPi concentrations follow a phylum-specific trend, where Chlorophyta > Ochrophyta (formally Phaeophyta) > Rhodophyta, perhaps due to evolutionary and ecological factors (Van Alstyne and Puglisi, 2007). However, these conclusions were based on a dataset heavily biased towards Chlorophyta. In this research, a transatlantic comparison of macroalgal DMSPi was conducted (Chapter 4), consisting of one Chlorophyta species, eight Ochrophyta species and six Rhodophyta species (coralline and fleshy). Despite a high within-Phylum variability, the general trend suggested by Van Alstyne and Puglisi (2007) was confirmed. While a number of intracellular functions for DMSP have been postulated (see Chapters 1 and 3 - 8), the genetic control on algal DMSPi is still unknown.

9.2.3 Latitudinal trends

DMSPi appears to increase with increasing latitude in the fleshy Chlorophyta *Ulva* spp. (Van Alstyne et al., 2007; Van Alstyne and Puglisi, 2007). In contrast, this research suggests that, in red coralline algae, DMSPi increased with decreasing latitude (Chapter 4). Sampling at a finer resolution is required before any firm conclusions are made (this research had only six sampling locations), but this may highlight the differing functional prioritisation of DMSPi between *Ulva* spp. and red coralline algae. *Ulva* spp. are opportunistic, fast-growing macroalgae that need to maintain constant metabolism; the algae may increase DMSPi in response to colder conditions (higher latitude) to prevent a slowing of metabolic pathways. In contrast, coralline algae are extremely slow growing (Foster, 2001) and may often become light saturated in shallow waters (this research, Chapter 3). In lower-latitude coralline algae, DMSPi may be used in an antioxidant pathway (Sunda et al., 2002) to quench reactive oxygen species created during cascade. The antioxidant function of DMSPi in coralline algae was also implied from the species-specific variability between two coralline algae species from Chile (where natural UV radiation at the Earth's surface is high, Huovinen et al., 2006): DMSPi in *Lithothamnion* sp., found at the lower limit of the tidal range, was significantly higher than *Mesophyllum* sp., found at 14 m depth (Chapter 6).

9.2.4 Abiotic drivers

Temperature and cloud cover were major drivers in the seasonal patterns of DMS/P in the Loch Sween maerl bed (Chapter 5). High light has been shown to induce a down-regulation of DMSPi in *Lithothamnion glaciale* (Rix et al., 2012). Temperature and cloud cover also affect the growth of *L. glaciale* (Burdett et al., 2011). In this research, the environmental regime exerted strong control on DMS/P concentrations in coralline algal habitats, suggesting that projected climate change may cause significant changes to coastal DMS/P concentrations in the future.

9.3 The effect of environmental and biological perturbations

The continued rise in atmospheric CO₂ since the Industrial Revolution is projected to cause significant alterations in the global climate over the next 100 years (IPCC, 2007). An enhanced greenhouse effect is projected to induce a 1.5 - 4.0°C rise in sea surface temperature (IPCC, 2007), leading to ice melt and reduced salinity in surface waters (Curry and Mauritzen, 2005; Curry et al., 2003; Munk, 2003), increased frequency of high intensity storms (Bender et al., 2010; Knutson et al., 2010), increased water column stratification and oxygen depletion in surface waters (Melzner et al., 2012; Doney, 2010) and a breakdown in the thermohaline circulation (Clark et al., 2002). More CO₂ will be absorbed by the oceans, shifting the carbonate equilibrium towards more acidic conditions and causing a shoaling of the carbonate saturation horizon (Caldeira and Wickett, 2005).

The rate of change associated with these climate projections is ~100 times faster than glacial terminations (Pelejero et al., 2010). Such rapid changes in environmental conditions are expected to impact ecosystems worldwide (Doney, 2010). Research into the potential impact of climate change on marine organisms has increased exponentially over the past decade but there are still many unknowns. Research into the impact of climate change on marine DMS/P has only recently begun, but may be extremely important given the numerous ecological functions for DMSP and the potential role of DMS in climate regulation. Research presented in Chapters 6 - 8 provided new information on

the impact of reduced salinity, reduced and variable pH and herbivorous grazing on coralline algal DMSPi production and release.

9.3.1 Intracellular DMSP functions

Research presented in Chapter 6 confirms the long-term compatible solute function of DMSPi in algae (Reese and Anderson, 2009; Edwards et al., 1988; Edwards et al., 1987; Vairavamurthy et al., 1985; Dickson et al., 1982). During acute reductions in salinity (<2 days), no change in DMSPi or quantum efficiency was observed in *Lithothamnion* sp. and *Mesophyllum* sp. In contrast, a significant reduction in DMSPi was observed in *L. glaciale* when exposed to reduced salinity for 14 days.

The importance of DMSPi during grazing activity was also confirmed *in situ* in Canadian kelp forests. Laboratory experiments to further investigate this effect were not conclusive, although results did suggest that water-borne chemical signals from stressed urchins could induce an up-regulation of DMSPi in coralline algae. This is in contrast to the previously described DMSP 'activated defence mechanism' that responds to direct grazing activity (Van Alstyne and Houser, 2003).

A potentially new algal function for DMSPi has also been identified - as a mechanism for maintaining cellular function under low or variable pH conditions. When calcifying algae were exposed to such conditions (in the field and *in situ*), DMSPi was upregulated, perhaps in response to (1) increased photosynthesis (due to higher $p\text{CO}_2$), (2) increased metabolism, (3) subsequent over-production of methionine (the precursor to DMSP) and (4) the production of reactive oxygen species.

9.3.2 Structural integrity

Climate change, and in particular ocean acidification (OA), is predicted to significantly impact calcifying organisms because of the increased potential for carbonate dissolution (Caldeira and Wickett, 2005). Studies currently suggest that the method of calcification greatly influences OA susceptibility (Ries et al., 2009) and that photosynthetic organisms (e.g. macroalgae) may benefit from the increased CO_2 (Ries et al., 2009). This research suggests that the structural

integrity of *L. glaciale* may be compromised under different environmental regimes. Under low pH conditions, cracks developed between the cell walls, instead of the usual organic 'glue'. Further, during chronic (21 day) salinity reduction, widespread cell deformation and sinking was observed, perhaps caused by stretching and bursting of cells under the reduced osmotic potential. However, percent calcification of the calcifying brown alga *Padina* sp. was not significantly different between the environmentally stable reef crest and more variable (in terms of carbonate chemistry) reef flat, suggesting some resistance to *in situ* changes compared to laboratory experiments. This information provides evidence that, when exposed to slow rates of change, coralline algae may be able to maintain their calcitic skeleton. However, the energetic costs and long-term physiological viability associated with this is unknown and difficult to project.

9.3.3 Ecosystem shifts

Projected climate change is forecast to induce ecosystem phase shifts that favour fleshy macroalgae over calcifying organisms such as corals (Dudgeon et al., 2010). Further, hurricane-induced disease is predicted to cause widespread mortality of the green sea urchin, a keystone species in eastern Canada that regulates the growth of kelp (Feehan et al., 2012; Scheibling and Lauzon-Guay, 2010). This research suggests that although the structural integrity of coralline algae may be affected, biochemical responses (up or down-regulation of DMSPi or utilisation of increased CO₂) may help to minimise impacts, but their slow growth will restrict their expansion capability. In contrast, with reduced grazing pressure, east Canadian kelps may increase their spatial distribution, leading to a change in DMS/P cycling in the kelp forest ecosystem (Chapter 8). Storm-induced damage may increase, leading to periodic pulses of sea-air DMS emissions, in a similar manner to the present-day grazing front.

9.4 Future work and research direction

9.4.1 Intra-thallus heterogeneity

This research has identified significant intra-thallus photosynthetic heterogeneity in coralline algae due to self-shading. Whether this is reflected

in intracellular secondary metabolite concentrations (such as DMSPi) is currently unknown. X-ray absorption spectroscopy (e.g. X-ray Absorption Near Edge Structure, XANES) mapping could provide detailed sulphur speciation information within the thalli at the micrometre scale. Proteomic analyses could also be used to determine the intracellular production pathway for DMSPi in coralline algae. Only one algal pathway has been currently identified (Stefels, 2000, and see Chapter 1) and has been confirmed in only a few Chlorophyta species. This combined knowledge will help to constrain the reasons for the often large inter-thallus DMSPi variations (e.g. what is the effect of morphology and growth history).

9.4.2 The role of the microbial community

The microbial community is a major component of DMS/P cycling in the open ocean (Hatton et al., 2012a; Moran et al., 2012; Green et al., 2011). At present, there is a paucity of information available on the microbial communities associated with coralline algal habitats, with no data available on the role of these microbial communities in DMS/P cycling. Previous microbial research has focussed on sediment carbon sequestration potential in seagrass meadows (e.g. James et al., 2006; Devereux, 2005; Weidner et al., 2000), invertebrate larval settlement on coralline algae (e.g. Webster et al., 2012; Webster et al., 2011; Huggett et al., 2006; Negri et al., 2001) and secondary production in kelp forests (e.g. Bengtsson et al., 2012; Bengtsson et al., 2011; Bengtsson and Ovreas, 2010; Bengtsson et al., 2010). The majority of these studies have focused on cultivatable bacteria (which may be <1% of total diversity, Su et al., 2012), but now culture-independent next-generation sequencing techniques (e.g. 454, Illumina or SOLiD sequencing) are beginning to be utilised in environmental research. Characterisation of ecosystem metagenomes and the ability of the microbial community to utilise DMS/P substrates (by, for example, DNA Stable Isotope Probing) will elucidate the role of microbes in DMS/P production and release in coralline algal habitats.

9.4.3 Characterisation of associated compounds

Characterisation of the full suite of dimethylated sulphur compounds (including dimethylsulphoxide, DMSO) and associated breakdown products (e.g.

acrylate) would provide a more detailed understanding of the system dynamics. Isotopic labelling of DMSP (^{13}C or ^{35}S) for uptake by algae would elucidate the production, release and breakdown pathways. Natural stable isotopic fractionation ($\delta^{34}\text{S}_{\text{V-CDT}}$) of the algae, seagrass, invertebrates, seawater and phytoplankton would provide information on the sulphur sources and sinks to the ecosystems (terrestrial vs marine, Newton, 2010; Hoefs, 2009) and the sulphur-specific trophic dynamics (as sulphur fractionation is conserved up the food chain, Newton, 2010), including those specific to DMSP (Oduro et al., 2012; Oduro et al., 2011).

9.4.4 Photosynthesis of red algae

At present, the Diving-PAM is the only way to investigate the photosynthesis of marine plants and macroalgae *in situ*. This research has shown that the photosynthetic characteristics of coralline algae may be significantly altered under laboratory conditions, thus the Diving-PAM is an excellent tool for assessing the natural variability of photosynthesis in the field. The use of PAM fluorometry on Rhodophyta is more complex than Chlorophyta or Ochrophyta because of phycobilisomes (see Chapter 1). The application of a far-red light and five minute dark acclimation period prior to a saturating actinic pulse has been suggested to ensure that the electron transport chain is fully oxidised and the phycobilisomes are associated with PSII (Schubert et al., 2011). This function is not available on the Diving-PAM, but dark acclimation experiments presented in Chapter 3 suggest that just 10 s of 'quasi-dark acclimation' is sufficient to achieve at least 95% of full dark acclimation in red coralline algae.

The short illumination times associated with Rapid Light Curves (RLCs) does not allow a photosynthetic steady-state to be achieved and thus, does not describe optimal photosynthetic rate (Enríquez and Borowitzka, 2010). RLCs, do however, provide information on the actual, rather than optimal photosynthetic state and can act as a proxy for electron transport rate through PSII, provided standardised procedures are used, as in this research (Enríquez and Borowitzka, 2010; Ralph and Gademann, 2005). Complementary laboratory-based measurements of oxygen or carbon dioxide evolution would provide information on actual photosynthetic / respiration rate. Such data would help to substantiate the photosynthetic inferences outlined in this research. In addition,

the Ocean Optics spectrometer was a portable instrument that could be used in the field and proved a useful technique to qualitatively identify the photosynthetic pigments associated with coralline algae. However, the method could be made more robust by complementary laboratory assays that quantitatively assess pigment concentrations and determine the detection limit of the Ocean Optics optical reflectance technique.

9.5 Wider applications of this research

9.5.1 Habitat conservation and natural capital

The total value of coastal ecosystem services and products (terrestrial and marine) is estimated at almost \$26,000 billion per year globally (Martínez et al., 2007). The value of ecosystem services and natural capital supplied by the coastal ocean is estimated to be at least 40% of the global total (Costanza et al., 1997). Thus, it appears to be in our economic interest to maintain a healthy and diverse coastal ocean.

The importance of the coastal ocean in providing natural capital (e.g. Costanza et al., 1997) is calculated using various ecosystem services such as climate regulation, nutrient cycling, habitat formation and food production, for which the contribution by the coastal ocean is often not fully understood or is under-estimated (Beaumont et al., 2008; Beaumont et al., 2007; Beaumont and Tinch, 2003). Thus, the coastal ocean may actually contribute far more than 40% of our natural capital. This research has highlighted the importance of coralline algal habitats in the marine sulphur cycle, a factor that contributes to many ecosystem service provisions, including gas regulation (production of DMS), habitat formation (invertebrate settlement and refugia), nutrient cycling (recycling of sulphur within the ecosystem) and biological control (of carbonate chemistry and DMS/P release).

9.5.2 Algal biofuels and bioproducts

In 2010, the global market for macroalgal-derived products (energy, hydrocolloids, etc) was £4.6 billion, derived from ~1.6 million dry tonnes of macroalgae (Smith and Higson, 2012). However, there is still considerable uncertainty regarding the environmental impact (including the impact on the

natural biogeochemical sulphur cycle) of commercial macroalgal growth and use, a concern highlighted in a recent report commissioned by the UK Natural Environment Research Council / Technology Strategy Board Algal Bioenergy Special Interest Group (Smith and Higson, 2012). Coralline algal habitats support a number of commercially important species, many of which were investigated in this research (Chapters 4 and 8), including: *Laminaria* spp. (bioenergy and nutrition), *Ascophyllum nodosm* (alginate and fertiliser production), *Porphyra* spp. (nutrition) and *Lithothamnion* spp. (biomedical and agriculture), *Chondrus crispus* (carrageenan, nutrition), *Corallina* sp. (biomedical) and *Palmaria palamta* (nutrition, agriculture). Importantly, all of these macroalgae had detectable levels of DMSPi, thus have the potential to impact natural DMS/P cycling and atmospheric DMS flux if grown on commercially viable scales.

9.5.3 Climate modelling

Clouds represent one of the largest uncertainties in climate models (Solomon et al., 2007) and may be directly influenced by oceanic DMS emissions through the production of cloud condensation nuclei (Charlson et al., 1987). Although we can now quantify changes to the global climate since the Industrial Revolution (e.g. increased atmospheric pCO₂, NOAA, 2012c), there are still not enough data to attribute the effect of phytoplankton-derived DMS emissions to observed global change (Halloran et al., 2010). Consequently, it has been suggested that studies using empirical DMS data to investigate the impact of climate change on DMS production (e.g. Gunson et al., 2006; Kloster et al., 2006; Bopp et al., 2003) carry an unacceptably high degree of uncertainty (Halloran et al., 2010). Thus, it has been proposed that an analysis of inter-annual variability, which may be representative of future DMS emissions (Woodhouse et al., 2010), should be conducted to investigate spatial trends that may be translated to future climate projections (Halloran et al., 2010). However, the relative paucity of data available on DMS/P from benthic species compared to open-ocean phytoplankton makes such analyses currently impossible for the coastal ocean. This research presents the first regularly sampled, multi-year time series of DMS/P concentrations in the coastal ocean. Significant variation was observed between the two years, highlighting the importance of understanding present-day natural variability if projections of future climate are to become more accurate.

9.6 Conclusion

In the past, the coastal ocean has been neglected within dimethylated sulphur research under the assumption that its relatively small size (~10% of the total ocean surface area) would mean that it is not an important component of the global marine sulphur cycle. However, our continued exploitation of the coastal ocean necessitates a requirement to better understand the ecosystem processes in this region. This research focused on globally distributed coralline algal habitats (e.g. maerl beds, coralligène, coral reefs, seagrass meadows and kelp forests) and aimed to (1) investigate the photosynthetic characteristics of coralline algae (as this may affect DMSPi production), (2) quantify the natural variability of DMS/P production and (3) assess the impact environmental pressures (reduced salinity, reduced pH and herbivorous grazing) on DMS/P production. This research has shown that, compared to the open ocean, natural production of DMS/P within these habitats is very high, thus representing a potentially significant marine source of dimethylated sulphur compounds. However, extremely high biodiversity and strong environmental forcings may result in a recycling of the sulphur compounds within these habitats, maintaining ecosystem function and health but limiting DMS sea-to-air emissions. Thus, the potential for DMS emissions from these habitats is mediated by biological (e.g. community composition, grazing activity) and abiotic (e.g. depth, light intensity, temperature) factors that are more complex than the relatively stable open ocean environment. This research provides fundamental biogeochemical baseline data which may be used to inform further investigations into the possible evolution of the coastal marine sulphur cycle in the future.

References

- ACKLESON, S. G. 2003. Light in shallow waters: A brief research review. *Limnology and Oceanography*, 48, 323-328.
- ADEY, W. H. 1970. The Effects of Light and Temperature on Growth Rates in Boreal-Subarctic Crustose Corallines. *Journal of Phycology*, 6, 269-276.
- ADEY, W. H. & ADEY, P. 1973. Studies on the biosystematics and ecology of the epithilic crustose Corallinaceae of the British Isles. *British Phycological Journal*, 8, 1-60.
- AIKAWA, S., HATTORI, H., GOMI, Y., WATANABE, K., KUDOH, S., KASHINO, Y. & SATOH, K. 2009. Diel tuning of photosynthetic systems in ice algae at Saroma-ko Lagoon, Hokkaido, Japan. *Polar Science*, 3, 57-72.
- ALLEN, G. L. & SIMPSON, J. H. 1998. Deep Water Inflows to Upper Loch Linnhe. *Estuarine, Coastal and Shelf Science*, 47, 487-498.
- AMO, L., RODRIGUEZ-GIRONES, M. A. & BARBOSA, A. 2013. Olfactory detection of dimethyl sulphide in a krill-eating Antarctic penguin. *Marine Ecology Progress Series*, 474, 277-285.
- ANDREAE, M. O. 1990. Ocean-Atmosphere Interactions in the Global Biogeochemical Sulfur Cycle. *Marine Chemistry*, 30, 1-29.
- ANDREWS, J. E., BRIMBLECOMBE, P., JICKELLS, T. D., LISS, P. S. & REID, B. 2004. *An Introduction to Environmental Chemistry*, Oxford: Blackwell Science Ltd.
- ANSEDE, J. H., PELLECHIA, P. J. & YOCH, D. C. 2001. Nuclear Magnetic Resonance Analysis of ¹³C-Dimethylsulfoniopropionate (DMSP) and ¹³C-Acrylate Metabolism by a DMSP Lyase-Producing Marine Isolate of the α -Subclass of Proteobacteria. *Applied and Environmental Microbiology*, 67, 3134-3139.
- ANTHONY, K. R. N., A. KLEYPAS, J. & GATTUSO, J.-P. 2011. Coral reefs modify their seawater carbon chemistry – implications for impacts of ocean acidification. *Global Change Biology*, 17, 3655-3666.
- ARCHER, S., CUMMINGS, D., LLEWELLYN, C. & FISHWICK, J. 2009. Phytoplankton taxa, irradiance and nutrient availability determine the seasonal cycle of DMSP in temperate shelf seas. *Marine Ecology Progress Series*, 394, 111-124.
- ARNOLD, H. E., KERRISON, P. & STEINKE, M. 2012. Interacting effects of ocean acidification and warming on growth and DMS-production in the haptophyte coccolithophore *Emiliania huxleyi*. *Global Change Biology*, n/a-n/a.
- ARRIGO, K. R. 2005. Marine microorganisms and global nutrient cycles. *Nature*, 437, 349-355.
- ASLAM, M. N., BHAGAVATHULA, N., PARUCHURI, T., HU, X., CHAKRABARTY, S. & VARANI, J. 2009. Growth-inhibitory effects of a mineralized extract from the red marine algae, *Lithothamnion calcareum*, on Ca²⁺-sensitive and Ca²⁺-resistant human colon carcinoma cells. *Cancer Letters*, 283, 186-192.
- AVGOUSTIDI, V., NIGHTINGALE, P. D., JOINT, I., STEINKE, M., TURNER, S., HOPKINS, F. E. & LISS, P. S. 2012. Decreased marine dimethyl sulfide production under elevated CO₂ levels in mesocosm and in vitro studies. *Environmental Chemistry*, 9, 399-404.
- AYERS, G. P. & CAINEY, J. M. 2007. The CLAW hypothesis: a review of the major developments. *Environmental Chemistry*, 4, 366-374.
- BAKUN, A. 1990. Global Climate Change and Intensification of Coastal Ocean Upwelling. *Science*, 247, 198-201.
- BALDWIN, I. T. & SCHULTZ, J. C. 1983. Rapid Changes in Tree Leaf Chemistry Induced by Damage: Evidence for Communication Between Plants. *Science*, 221, 277-279.
- BALLESTEROS, E. 2006. Mediterranean coralligenous assemblages: A synthesis of present knowledge. *Oceanography and marine biology: an annual review*, 44, 123-195.
- BARATTOLO, F., BASSI, D. & ROMANO, R. 2007. Upper Eocene larger foraminiferal–coralline algal facies from the Klokova Mountain (southern continental Greece). *Facies*, 53, 361-375.
- BAS. 2012. *Ice sheets in Antarctica* [Online]. Available: http://www.bas.ac.uk/about_antarctica/geography/ice/sheets.php [Accessed 7th January 2013].
- BASSI, D. 2005. Larger foraminiferal and coralline algal facies in an Upper Eocene storm-influenced, shallow-water carbonate platform (Colli Berici, north-eastern Italy). *Palaeogeography, Palaeoclimatology, Palaeoecology*, 226, 17-35.
- BASSO, D. 2012. Carbonate production by calcareous red algae and global change. *Geodiversitas*, 34, 13-33.

- BATES, N. R., AMAT, A. & ANDERSSON, A. J. 2010. Feedbacks and responses of coral calcification on the Bermuda reef system to seasonal changes in biological processes and ocean acidification. *Biogeosciences*, 7, 2509-2530.
- BATES, T. S., LAMB, B. K., GUENTHER, A., DIGNON, J. & STOIBER, R. E. 1992. Sulfur emissions to the atmosphere from natural sources. *Journal of Atmospheric Chemistry*, 14, 315-337.
- BAUMANN, H. A., MORRISON, L. & STENGEL, D. B. 2009. Metal accumulation and toxicity measured by PAM--Chlorophyll fluorescence in seven species of marine macroalgae. *Ecotoxicology and Environmental Safety*, 72, 1063-1075.
- BAXTER, J. M., BOYD, I. L., COX, M., DONALD, A. E., MALCOLM, S. J., MILES, H., MILLER, B. & MOFFAT, C. F. (eds.) 2011. *Scotland's Marine Atlas: Information for the national marine Plan*, Edinburgh: Marine Scotland.
- BEAUMONT, N. J., AUSTEN, M. C., ATKINS, J. P., BURDON, D., DEGRAER, S., DENTINHO, T. P., DEROUS, S., HOLM, P., HORTON, T., VAN IERLAND, E., MARBOE, A. H., STARKEY, D. J., TOWNSEND, M. & ZARZYCKI, T. 2007. Identification, definition and quantification of goods and services provided by marine biodiversity: Implications for the ecosystem approach. *Marine Pollution Bulletin*, 54, 253-265.
- BEAUMONT, N. J., AUSTEN, M. C., MANGI, S. C. & TOWNSEND, M. 2008. Economic valuation for the conservation of marine biodiversity. *Marine Pollution Bulletin*, 56, 386-396.
- BEAUMONT, N. J. & TINCH, R. 2003. *Goods and services related to the marine benthic environment*. CSERGE Working Paper ECM 03-14.
- BEER, S. & AXELSSON, L. 2004. Limitations in the use of PAM fluorometry for measuring photosynthetic rates of macroalgae at high irradiances. *European Journal of Phycology*, 39, 1-7.
- BEER, S., VILENKIN, B., WEIL, A., VESTE, M., SUSEL, L. & ESHEL, A. 1998. Measuring photosynthetic rates in seagrasses by pulse amplitude modulated (PAM) fluorometry. *Marine Ecology Progress Series*, 174, 293-300.
- BELSHE, E. F., DURAKO, M. J. & BLUM, J. E. 2008. Diurnal light curves and landscape-scale variation in photosynthetic characteristics of *Thalassia testudinum* in Florida Bay. *Aquatic Botany*, 89, 16-22.
- BELSHE, E. F., DURAKO, M. J. & BLUM, J. E. 2007. Photosynthetic rapid light curves (RLC) of *Thalassia testudinum* exhibit diurnal variation. *Journal of Experimental Marine Biology and Ecology*, 342, 253-268.
- BENDER, M. A., KNUTSON, T. R., TULEYA, R. E., SIRUTIS, J. J., VECCHI, G. A., GARNER, S. T. & HELD, I. M. 2010. Modeled Impact of Anthropogenic Warming on the Frequency of Intense Atlantic Hurricanes. *Science*, 327, 454-458.
- BENGTSSON, M. & OVREAS, L. 2010. Planctomycetes dominate biofilms on surfaces of the kelp *Laminaria hyperborea*. *BMC Microbiology*, 10, 261.
- BENGTSSON, M., SJØTUN, K. & ØVREÅS, L. 2010. Seasonal dynamics of bacterial biofilms on the kelp *Laminaria hyperborea*. *Aquatic Microbial Ecology*, 60, 71-83.
- BENGTSSON, M. M., SJØTUN, K., LANZEN, A. & OVREAS, L. 2012. Bacterial diversity in relation to secondary production and succession on surfaces of the kelp *Laminaria hyperborea*. *ISME J*, 6, 2188-2198.
- BENGTSSON, M. M., SJØTUN, K., STORESUND, J. E. & ØVREÅS, L. 2011. Utilization of kelp-derived carbon sources by kelp surface-associated bacteria. *Aquatic Microbial Ecology*, 62, 191-199.
- BENSOUSSAN, N. & GATTUSO, J.-P. 2007. Community primary production and calcification in a NW Mediterranean ecosystem dominated by calcareous macroalgae. *Marine Ecology Progress Series*, 334, 37-45.
- BIGG, G. R. 1996. *The Oceans and Climate*, Cambridge: Cambridge University Press.
- BINDOFF, N. L., WILLEBRAND, J., ARTALE, V., CAZENAVE, A., GREGORY, J., GULEV, S., HANAWA, K., QUÉRÉ, C. L., LEVITUS, S., NOJIRI, Y., SHUM, C. K., TALLEY, L. D. & UNNIKRISHNAN, A. 2007. Observations: Oceanic Climate Change and Sea Level. In: SOLOMON, S., QIN, D., MANNING, M., CHEN, Z., MARQUIS, M., AVERYT, K. B., TIGNOR, M. & MILLER, H. L. (eds.) *Climate Change 2007: The Physical Science Basis. Contribution of Working Group I to the Fourth Assessment Report of the Intergovernmental Panel on Climate Change*. Cambridge: Cambridge University Press.
- BINDSCHADLER, R., VAUGHAN, D. G. & VORNBERGER, P. 2011. Variability of basal melt beneath the Pine Island Glacier ice shelf, West Antarctica. *Journal of Glaciology*, 57, 581-595.
- BIOMAERL, BARBERA, C., BORDEHORE, C., BORG, J. A., GLEMAREC, M., GRALL, J., HALL-SPENCER, J. M., DE LA HUZ, C., LANFRANCO, E., LASTRA, M., MOORE, P. G., MORA, J., PITA, M. E., RAMOS-ESPLA, A. A., RIZZO, M., SANCHEZ-MATA, A., SEVA, A., SCHEMBRI, P. J. & VALLE, C. 2003. Conservation and management of northeast Atlantic

- and Mediterranean maerl beds. *Aquatic Conservation: Marine and Freshwater Ecosystems*, 13, S65-S76.
- BLACKFORD, J., JONES, N., PROCTOR, R., HOLT, J., WIDDICOMBE, S., LOWE, D. & REES, A. 2009. An initial assessment of the potential environmental impact of CO₂ escape from marine carbon capture and storage systems. *Proceedings of the Institution of Mechanical Engineers, Part A: Journal of Power and Energy*, 223, 269-280.
- BLAKE, C. & MAGGS, C. A. 2003. Comparative growth rates and internal banding periodicity of maerl species (Corallinales, Rhodophyta) from northern Europe. *Phycologia*, 42, 606-612.
- BONADONNA, F., CARO, S., JOUVENTIN, P. & NEVITT, G. A. 2006. Evidence that blue petrel, *Halobaena caerulea*, fledglings can detect and orient to dimethyl sulfide. *Journal of Experimental Biology*, 209, 2165-2169.
- BOPP, L., AUMONT, O., BELVISO, S. & MONFRAY, P. 2003. Potential impact of climate change on marine dimethyl sulfide emissions. *Tellus B*, 55, 11-22.
- BOSENCE, D. 1976. Ecological studies on two unattached coralline algae from western Ireland. *Palaeontology*, 19, 365-395.
- BOSENCE, D. 1983. The occurrence and ecology of recent rhodoliths - a review. In: PERYT, T. M. (ed.) *Coated Grains*. Berlin: Springer-Verlag.
- BOSSCHER, H. 1992. *Growth Potential of Coral Reefs and Carbonate Platforms*. Thesis, Vrije Universiteit.
- BRATBAK, G., LEVASSEUR, M., MICHAUD, S., CANTIN, G., FERNÁNDEZ, E., HEIMDAL, B. & HELDAL, M. 1995. Viral activity in relation to *Emiliania huxleyi* blooms: a mechanism of DMSP release? *Marine Ecology Progress Series*, 128, 133-142.
- BREWER, P. G. & RILEY, J. P. 1965. The automatic determination of nitrate in seawater. *Deep Sea Research*, 12, 765-772.
- BRIMBLECOMBE, P., HAMMER, C., RODHE, H., RYABOSHAPKO, A. & BOUTRON, C. F. 1989. Human influence on the sulphur cycle. In: BRIMBLECOMBE, P. & LEIN, A. Y. (eds.) *Evolution of the global biogeochemical sulphur cycle*. Chichester: John Wiley & Sons.
- BROADBENT, A. & JONES, G. 2006. Seasonal and Diurnal Cycles of Dimethylsulfide, Dimethylsulfoniopropionate and Dimethylsulfoxide at One Tree Reef Lagoon. *Environmental Chemistry*, 3, 260-267.
- BROADBENT, A. D. & JONES, G. B. 2004. DMS and DMSP in mucus ropes, coral mucus, surface films and sediment pore waters from coral reefs in the Great Barrier Reef. *Marine and Freshwater Research*, 55, 849-855.
- BROADBENT, A. D., JONES, G. B. & JONES, R. J. 2002. DMSP in corals and benthic algae from the Great Barrier Reef. *Estuarine Coastal and Shelf Science*, 55, 547-555.
- BROWN, S. S. & STUTZ, J. 2012. Nighttime radical observations and chemistry. *Chemical Society Reviews*, 41, 6405-6447.
- BÜDENBENDER, J., U, R. & A, F. 2011. Calcification of the Arctic coralline red algae *Lithothamnion glaciale* in response to elevated CO₂. *Marine Ecology Progress Series*, 441, 79-87.
- BURDETT, H., KAMENOS, N. A. & LAW, A. 2011. Using coralline algae to understand historic marine cloud cover. *Palaeogeography, Palaeoclimatology, Palaeoecology*, 302, 65-70.
- BURDETT, H. L., ALOISIO, E., CALOSI, P., FINDLAY, H. S., WIDDICOMBE, S., HATTON, A. D. & KAMENOS, N. A. 2012a. The effect of chronic and acute low pH on the intracellular DMSP production and epithelial cell morphology of red coralline algae. *Marine Biology Research*, 8, 756-763.
- BURDETT, H. L., HENNIGE, S., FRANCIS, F., T.-Y. & KAMENOS, N. A. 2012b. The photosynthetic characteristics of red coralline algae, determined using pulse amplitude modulation (PAM) fluorometry. *Botanica Marina*, 55, 499-509.
- BUTTERFIELD, N., KNOLL, A. & SWETT, K. 1990. A bangiophyte red alga from the Proterozoic of arctic Canada. *Science*, 250, 104-107.
- BUTTERFIELD, N. J. 2000. *Bangiomorpha pubescens* n. gen., n. sp.: implications for the evolution of sex, multicellularity, and the Mesoproterozoic/Neoproterozoic radiation of eukaryotes. *Paleobiology*, 26, 386-404.
- BYRNES, J. E., REED, D. C., CARDINALE, B. J., CAVANAUGH, K. C., HOLBROOK, S. J. & SCHMITT, R. J. 2011. Climate-driven increases in storm frequency simplify kelp forest food webs. *Global Change Biology*, 17, 2513-2524.
- CALDEIRA, K. & WICKETT, M. E. 2005. Ocean model predictions of chemistry changes from carbon dioxide emissions to the atmosphere and ocean. *Journal of Geophysical Research*, 110, C09S04.
- CAMPBELL, D., HURRY, V., CLARKE, A. K., GUSTAFSSON, P. & ÖQUIST, G. 1998. Chlorophyll fluorescence analysis of cyanobacterial photosynthesis and acclimation. *Microbiology and Molecular Biology Reviews*, 62, 667-683.

- CANFIELD, D. E. 2005. The early history of atmospheric oxygen: Homage to Robert M. Garrels. *Annual Review of Earth and Planetary Sciences*, 33, 1-36.
- CANGIALOSI, J. P. 2011. *NOAA Tropical Cyclone Report: Hurricane Earl (AL072010)*.
- CAPALDO, K., CORBETT, J. J., KASIBHATLA, P., FISCHBECK, P. & PANDIS, S. N. 1999. Effects of ship emissions on sulphur cycling and radiative climate forcing over the ocean. *Nature*, 400, 743-746.
- CARPENTER, L. J., MALIN, G., LISS, P. S. & KÜPPER, F. C. 2000. Novel biogenic iodine-containing trihalomethanes and other short-lived halocarbons in the coastal east Atlantic. *Global Biogeochem. Cycles*, 14, 1191-1204.
- CARPENTER, L. W. & PATTERSON, M. R. 2007. Water flow influences the distribution of photosynthetic efficiency within colonies of the scleractinian coral *Montastrea annularis* (Ellis and Solander, 1786); implications for coral bleaching. *Journal of Experimental Marine Biology and Ecology*, 351, 10-26.
- CHALLENGER, F. 1959. *Aspects of the Organic Chemistry of Sulphur*, New York: Academic Press.
- CHALLENGER, F. & SIMPSON, I. 1948. Studies on biological methylation. Part XII. A precursor of the dimethyl sulphide evolved by *Polysiphonia fastigiata*. dimethyl-2-carboxyethylsulphonium hydroxide and its salts. *Journal of the Chemical Society*, 43, 1591-1597.
- CHARLSON, R. J., LOVELOCK, J. E., ANDREAE, M. O. & WARREN, S. G. 1987. Oceanic phytoplankton, atmospheric sulphur, cloud albedo and climate. *Nature*, 326, 655-661.
- CHAVE, K. E. 1954. Aspects of the Biogeochemistry of Magnesium 1. Calcareous Marine Organisms. *The Journal of Geology*, 62, 266-283.
- CHIFFINGS, A. 2003. Marine Region 11: Arabian Seas. A global representative system of Marine Protected Areas.
- CHISHOLM, J. R. M. 2000. Calcification by Crustose Coralline Algae on the Northern Great Barrier Reef, Australia. *Limnology and Oceanography*, 45, 1476-1484.
- CHISHOLM, J. R. M. 2003. Primary Productivity of Reef-Building Crustose Coralline Algae. *Limnology and Oceanography*, 48, 1376-1387.
- CLARK, P. U., PISIAS, N. G., STOCKER, T. F. & WEAVER, A. J. 2002. The role of the thermohaline circulation in abrupt climate change. *Nature*, 415, 863-869.
- COLMER, T. D., CORRADINI, F., CAWTHRAY, G. R. & OTTE, M. L. 2000. Analysis of dimethylsulphoniopropionate (DMSP), betaines and other organic solutes in plant tissue extracts using HPLC. *Phytochemical Analysis*, 11, 163-168.
- CONNOR, D. W., ALLEN, J. H., GOLDING, N., HOWELL, K. L., LIEBERKNECHT, L. M., NORTHERN, K. O. & REKER, J. B. 2004. *The Marine Habitat Classification for Britain and Ireland Version 04.05*, Peterborough: JNCC.
- CONOVER, W. J. & IMAN, R. L. 1981. Rank transformation as a Bridge between parametric and nonparametric statistics. *The American Statistician*, 35, 124-129.
- CONSTANZA, R., D'ARGE, R., DE GROOT, R., FARBER, S., GRASSO, M., HANNON, B., LIMBURG, K., NAEEM, S., O'NEILL, R. V., PARUELO, J., RASKIN, R. G., SUTTON, P. & VAN DE BELT, M. 1997. The value of the world's ecosystem services and natural capital. *Nature*, 387, 253-260.
- COPPER, P. 1994. Ancient reef ecosystem expansion and collapse. *Coral Reefs*, 13, 3-11.
- COSGROVE, J. & BOROWITZKA, M. 2006. Applying Pulse Amplitude Modulation (PAM) fluorometry to microalgae suspensions: stirring potentially impacts fluorescence. *Photosynthesis Research*, 88, 343-350.
- COSTANZA, R., D'ARGE, R., DE GROOT, R., FARBER, S., GRASSO, M., HANNON, B., LIMBURG, K., NAEEM, S., O'NEILL, R. V., PARUELO, J., RASKIN, R. G., SUTTON, P. & VAN DEN BELT, M. 1997. The value of the world's ecosystem services and natural capital. *Nature*, 387, 253-260.
- COUMO, D. & RAHMSTORF, S. 2012. A decade of weather extremes. *Nature Clim. Change*, 2, 491-496.
- CUMANI, F., BRADASSI, F., DI PASCOLI, A. & BRESSAN, G. 2010. Marine Acidification Effects on Reproduction and Growth Rates of Corallinaceae Spores (Rhodophyta). *CIESM Congress Proceedings*, 39, 735.
- CUNNINGHAM, G. B., STRAUSS, V. & RYAN, P. G. 2008. African penguins (*Spheniscus demersus*) can detect dimethyl sulphide, a prey-related odour. *Journal of Experimental Biology*, 211, 3123-3127.
- CURRY, R., DICKSON, B. & YASHAYAIEV, I. 2003. A change in the freshwater balance of the Atlantic Ocean over the past four decades. *Nature*, 426, 826-829.
- CURRY, R. & MAURITZEN, C. 2005. Dilution of the Northern North Atlantic Ocean in Recent Decades. *Science*, 308, 1772-1774.

- DACEY, J. W. H. & BLOUGH, N. V. 1987. Hydroxide decomposition of dimethylsulfoniopropionate to form dimethylsulfide. *Geophysical Research Letters*, 14, 1246-1249.
- DACEY, J. W. H., KING, G. M. & LOBEL, P. S. 1994. Herbivory by Reef Fishes and the Production of Dimethylsulfide and Acrylic-Acid. *Marine Ecology Progress Series*, 112, 67-74.
- DACEY, J. W. H. & WAKEHAM, S. G. 1986. Oceanic Dimethylsulfide: Production During Zooplankton Grazing on Phytoplankton. *Science*, 233, 1314-1316.
- DAMM, E., HELMKE, E., THOMS, S., SCHAUER, U., NÖTHIG, E., BAKKER, K. & KIENE, R. P. 2010. Methane production in aerobic oligotrophic surface water in the central Arctic Ocean. *Biogeosciences*, 7, 1099-1108.
- DE BOSE, J. L., LEMA, S. C. & NEVITT, G. A. 2008. Dimethylsulfoniopropionate as a Foraging Cue for Reef Fishes. *Science*, 319, 1356.
- DE GRAVE, S., FAZAKERLEY, H., KELLY, L., GUIRY, M. D., RYAN, M. & WALSHE, J. 2000. *A study of selected maerl beds in Irish waters and their potential for sustainable extraction.*: The Marine Institute.
- DEL VALLE, D. A., KIEBER, D. J., TOOLE, D. A., BISGROVE, J. & KIENE, R. P. 2009. Dissolved DMSO production via biological and photochemical oxidation of dissolved DMS in the Ross Sea, Antarctica. *Deep Sea Research Part I: Oceanographic Research Papers*, 56, 166-177.
- DELILLE, B., BORGES, A. V. & DELILLE, D. 2009. Influence of giant kelp beds (*Macrocystis pyrifera*) on diel cycles of pCO₂ and DIC in the Sub-Antarctic coastal area. *Estuarine, Coastal and Shelf Science*, 81, 114-122.
- DETHIER, M., VAN ALSTYNE, K. & DUGGINS, D. 2001. Spatial Patterns in Macroalgal Chemical Defenses. *Marine Chemical Ecology*. CRC Press.
- DEVEREUX, R. 2005. Seagrass rhizosphere microbial communities. *Interactions Between Macro and Microorganisms in Marine Sediments*. Washington, DC: AGU.
- DICKE, M. & BRUIN, J. 2001. Chemical information transfer between plants: back to the future. *Biochemical Systematics and Ecology*, 29, 981-994.
- DICKSON, A. G. 1990. Standard potential of the reaction: $\text{AgCl(s)} + 1/2\text{H}_2(\text{g}) = \text{Ag(s)} + \text{HCl(aq)}$, and the standard acidity constant of the ion HSO_4^- in synthetic sea water from 273.15 to 318.15 K. *The Journal of Chemical Thermodynamics*, 22, 113-127.
- DICKSON, A. G. & MILLERO, F. J. 1987. A comparison of the equilibrium constants for the dissociation of carbonic acid in seawater media. *Deep Sea Research Part A. Oceanographic Research Papers*, 34, 1733-1743.
- DICKSON, A. G., SABINE, C. L. & CHRISTIAN, J. R. (eds.) 2007. *Guide to best practices for ocean CO₂ measurements*.
- DICKSON, D. M. J., WHY JONES, R. G. & DAVENPORT, J. 1982. Osmotic adaptation in *Ulva lactuca* under fluctuating salinity regimes. *Planta*, 155, 409-415.
- DIERSSON, H. M., ZIMMERMAN, R. C., LEATHERS, R. A., DOWNES, T. V. & DAVIS, C. O. 2003. Ocean color remote sensing of seagrass and bathymetry in the Bahamas Banks by high-resolution airborne imagery. *Limnology and Oceanography*, 48, 444-455.
- DIFFENBAUGH, N. S., SNYDER, M. A. & SLOAN, L. C. 2004. Could CO₂-induced land-cover feedbacks alter near-shore upwelling regimes? *Proceedings of the National Academy of Sciences*, 101, 27-32.
- DONEY, S. C. 2010. The Growing Human Footprint on Coastal and Open-Ocean Biogeochemistry. *Science*, 328, 1512-1516.
- DOROPOULOS, C. & DIAZ-PULIDO, G. 2013. High CO₂ reduces the settlement of a spawning coral on three common species of crustose coralline algae. *Marine Ecology Progress Series*, 475, 93-99.
- DUDGEON, S., ARONSON, R., BRUNO, J. & PRECHT, W. 2010. Phase shifts and stable states on coral reefs. *Marine Ecology Progress Series*, 413, 201-216.
- DURAKO, M. J. 2012. Using PAM fluorometry for landscape-level assessment of *Thalassia testudinum*: Can diurnal variation in photochemical efficiency be used as an ecoindicator of seagrass health? *Ecological Indicators*, 18, 243-251.
- DURAKO, M. J. & KUNZELMAN, J. I. 2002. Photosynthetic characteristics of *Thalassia testudinum* measured *in situ* by pulse-amplitude modulated (PAM) fluorometry: methodological and scale-based considerations. *Aquatic Botany*, 73, 173-185.
- ECKMAN, J. E., DUGGINS, D. O. & SEWELL, A. T. 1989. Ecology of under story kelp environments. I. Effects of kelps on flow and particle transport near the bottom. *Journal of Experimental Marine Biology and Ecology*, 129, 173-187.
- EDWARDS, D. M., REED, R. H., CHUDEK, J. A., FOSTER, R. & STEWART, W. D. P. 1987. Organic solute accumulation in osmotically-stressed *Enteromorpha intestinalis*. *Marine Biology*, 95, 583-592.

- EDWARDS, D. M., REED, R. H. & STEWART, W. D. P. 1988. Osmoacclimation in *Enteromorpha intestinalis* long-term effects of osmotic stress on organic solute accumulation. *Marine Biology*, 98, 467-476.
- EDWARDS, M. S. & KIM, K. Y. 2010. Diurnal variation in relative photosynthetic performance in giant kelp *Macrocystis pyrifera* (Phaeophyceae, Laminariales) at different depths as estimated using PAM fluorometry. *Aquatic Botany*, 92, 119-128.
- ENRÍQUEZ, S. & BOROWITZKA, M. A. 2010. The use of the fluorescence signal in studies of seagrasses and macroalgae. In: SUGGETT, D. J., PRÁŠIL, O. & BOROWITZKA, M. A. (eds.) *Chlorophyll a Fluorescence in Aquatic Sciences: Methods and Applications*. Springer Netherlands.
- ERICKSON, A., PAUL, V., VAN ALSTYNE, K. & KWIATKOWSKI, L. 2006. Palatability of Macroalgae that Use Different Types of Chemical Defenses. *Journal of Chemical Ecology*, 32, 1883-1895.
- EVANS, M. N., CANE, M. A., SCHRAG, D. P., KAPLAN, A., LINSLEY, B. K., VILLALBA, R. & WELLINGTON, G. M. 2001. Support for tropically-driven pacific decadal variability based on paleoproxy evidence. *Geophysical Research Letters*, 28, 3689-3692.
- FALKOWSKI, P. G. & RAVEN, J. A. 2007. *Aquatic photosynthesis*, Princeton: Princeton University Press.
- FALTER, J. L., LOWE, R. J., ATKINSON, M. J. & CUET, P. 2012. Seasonal coupling and decoupling of net calcification rates from coral reef metabolism and carbonate chemistry at Ningaloo Reef, Western Australia. *Journal of Geophysical Research*, 117, C05003.
- FAZAKERLEY, H. & GUIRY, M. D. 1998. *The distribution of maerl beds around Ireland and their potential for sustainable extraction: phycological section.*, Report to the Marine Institute, Dublin. National University of Ireland, Galway.
- FEEHAN, C., SCHEIBLING, R. E. & LAUZON-GUAY, J. S. 2012. An outbreak of sea urchin disease associated with a recent hurricane: Support for the "killer storm hypothesis" on a local scale. *Journal of Experimental Marine Biology and Ecology*, 413, 159-168.
- FEELY, R. A., SABINE, C. L., HERNANDEZ-AYON, J. M., IANSON, D. & HALES, B. 2008. Evidence for Upwelling of Corrosive "Acidified" Water onto the Continental Shelf. *Science*, 320, 1490-1492.
- FIGUEROA, F., CONDE-ÁLVAREZ, R. & GÓMEZ, I. 2003. Relations between electron transport rates determined by pulse amplitude modulated chlorophyll fluorescence and oxygen evolution in macroalgae under different light conditions. *Photosynthesis Research*, 75, 259-275.
- FIGUEROA, F., MARTINEZ, B., ISRAEL, A., NEORI, A., MALTA, E., ANG, P. J., INKEN, S., MARQUARDT, R., RACHAMIM, T., ARAZI, U., FRENK, S. & KORBEE, N. 2009. Acclimation of Red Sea macroalgae to solar radiation: photosynthesis and thallus absorbance. *Aquatic Biology*, 7, 159-172.
- FIGUEROA, F. L., AGUILERA, J. & NIELL, F. X. 1995. Red and blue light regulation of growth and photosynthetic metabolism in *Porphyra umbilicalis* (Bangiales, Rhodophyta). *European Journal of Phycology*, 30, 11-18.
- FINDLAY, H. S., KENDALL, M. A., SPICER, J. I., TURLEY, C. & WIDDICOMBE, S. 2008. Novel microcosm system for investigating the effects of elevated carbon dioxide and temperature on intertidal organisms. *Aquatic Biology*, 3, 51-62.
- FINDLAY, H. S., YOOL, A., NODALE, M. & PITCHFORD, J. W. 2006. Modelling of autumn plankton bloom dynamics. *Journal of Plankton Research*, 28, 209-220.
- FOLLAND, C. K., RENWICK, J. A., SALINGER, M. J. & MULLAN, A. B. 2002. Relative influences of the Interdecadal Pacific Oscillation and ENSO on the South Pacific Convergence Zone. *Geophysical Research Letters*, 29, 1643.
- FOSLIE, M. 1907. *Antarctic and subantarctic Corallinaceae*, Stockholm: Lithographisches Institut des Generalstabs.
- FOSTER, M. S. 2001. Rhodoliths: Between rocks and soft places. *Journal of Phycology*, 37, 659-667.
- FOSTER, M. S., AMANDO-FILHO, G. M., KAMENOS, N. A. & RIOSMENA-RODRIGUEZ, R. In press. Rhodoliths and rhodolith beds. *Smithsonian Proceedings*.
- FRANTZ, B. R., KASHGARIAN, M., COALE, K. H. & FOSTER, M. S. 2000. Growth rate and potential climate record from a rhodolith using ¹⁴C accelerator mass spectrometry. *Limnology and Oceanography*, 45, 1773-1777.
- FREIWALD, A. & HENRICH, R. 1994. Reefal Coralline Algal Build-Ups within the Arctic-Circle - Morphology and Sedimentary Dynamics under Extreme Environmental Seasonality. *Sedimentology*, 41, 963-984.
- FRESTEDT, J., KUSKOWSKI, M. & ZENK, J. 2009. A natural seaweed derived mineral supplement (Aquamin F) for knee osteoarthritis: A randomised, placebo controlled pilot study. *Nutrition Journal*, 8, 7.

- FRESTEDT, J., WALSH, M., KUSKOWSKI, M. & ZENK, J. 2008. A natural mineral supplement provides relief from knee osteoarthritis symptoms: a randomized controlled pilot trial. *Nutrition Journal*, 7, 9.
- GAGE, D. A., RHODES, D., NOLTE, K. D., HICKS, W. A., LEUSTEK, T., COOPER, A. J. L. & HANSON, A. D. 1997. A new route for synthesis of dimethylsulphonioacetate in marine algae. *Nature*, 387, 891-894.
- GAGLIANO, M., MCCORMICK, M., MOORE, J. & DEPCZYNSKI, M. 2010. The basics of acidification: baseline variability of pH on Australian coral reefs. *Marine Biology*, 157, 1849-1856.
- GAO, K., ARUGA, Y., ASADA, K., ISHIHARA, T., AKANO, T. & KIYOHARA, M. 1993. Calcification in the Articulated Coralline Alga *Corallina pilulifera*, with Special Reference to the Effect of Elevated CO₂ Concentration. *Marine Biology*, 117, 129-132.
- GAO, K. & ZHENG, Y. 2010. Combined effects of ocean acidification and solar UV radiation on photosynthesis, growth, pigmentation and calcification of the coralline alga *Corallina sessilis* (Rhodophyta). *Global Change Biology*, 16, 2388-2398.
- GARRETT, C. J. R. & LOUCKS, R. 1976. Upwelling along Yarmouth shore of Nova Scotia. *Journal of the Fisheries Research Board of Canada*, 33, 116-117.
- GAYLORD, B. & DENNY, M. 1997. Flow and flexibility. I. Effects of size, shape and stiffness in determining wave forces on the stipitate kelps *Eisenia arborea* and *Pterygophora californica*. *Journal of Experimental Biology*, 200, 3141-64.
- GILLET, N. P., STOTT, P. A. & SANTER, B. D. 2008. Attribution of cyclogenesis region sea surface temperature change to anthropogenic influence. *Geophysical Research Letters*, 35, L09707.
- GILLIBRAND, P. A., CAGE, A. G. & AUSTIN, W. E. N. 2005. A preliminary investigation of basin water response to climate forcing in a Scottish fjord: evaluating the influence of the NAO. *Continental Shelf Research*, 25, 571-587.
- GOLDBERG, N. 2006. Age estimates and description of rhodoliths from Esperance Bay, Western Australia. *Journal of the Marine Biological Association of the United Kingdom*, 86, 1291-1296.
- GOLDSTEIN, J. I., ROMIG, A. D., NEWBURY, D. E., LYMAN, C. E., ECHLIN, P., FIORI, C., JOY, D. C. & LIFSHIN, E. 1992. *Scanning electron microscopy and x-ray microanalysis*, (2nd edn), New York: Plenum Press.
- GONZALEZ, J. M., KIENE, R. P. & MORAN, M. A. 1999. Transformation of Sulfur Compounds by an Abundant Lineage of Marine Bacteria in the alpha-Subclass of the Class *Proteobacteria*. *Applied and Environmental Microbiology*, 65, 3810-3819.
- GONZALEZ, J. M., SIMO, R., MASSANA, R., COVERT, J. S., CASAMAYOR, E. O., PEDROS-ALIO, C. & MORAN, M. A. 2000. Bacterial Community Structure Associated with a Dimethylsulfonylacetate-Producing North Atlantic Algal Bloom. *Applied and Environmental Microbiology*, 66, 4237-4246.
- GORHAM, J. 1986. Separation and quantitative estimation of betaine esters by high-performance liquid chromatography. *Journal of Chromatography A*, 361, 301-310.
- GRAHAM, M., HARROLD, C., LISIN, S., LIGHT, K., WATANABE, J. & FOSTER, M. 1997. Population dynamics of giant kelp *Macrocystis pyrifera* along a wave exposure gradient. *Marine Ecology Progress Series*, 148, 269-279.
- GRALL, J. & HALL-SPENCER, J. M. 2003. Problems facing maerl conservation in Brittany. *Aquatic Conservation: Marine and Freshwater Ecosystems*, 13, S55-S64.
- GRASSHOFF, K. 1976. *Methods of seawater analysis*, Weinheim: Verlag Chemie.
- GRAY, S. E. C., DEGRANDPRE, M. D., LANGDON, C. & CORREDOR, J. E. 2012. Short-term and seasonal pH, pCO₂ and saturation state variability in a coral-reef ecosystem. *Global Biogeochem. Cycles*, 26, GB3012.
- GRAY, W. M. 1984. Atlantic Seasonal Hurricane Frequency. Part I: El Niño and 30 mb Quasi-Biennial Oscillation Influences. *Monthly Weather Review*, 112, 1649-1668.
- GREEN, D. H., SHENOY, D. M., HART, M. C. & HATTON, A. D. 2011. DMS oxidation coupled to biomass production by a marine Flavobacterium. *Applied and Environmental Microbiology*, 77, 3137-3140.
- GREEN, E. P. & SHORT, F. T. 2003. *The World Atlas of Seagrasses*, Berkeley: University of California Press.
- GREENE, R. C. 1962. Biosynthesis of Dimethyl-β-propiothetin. *The Journal of Biological Chemistry*, 237, 2251-2254.
- GRÖNE, T. & KIRST, G. O. 1992. The effect of nitrogen deficiency, methionine and inhibitors of methionine metabolism on the DMSP contents of *Tetraselmis subcordiformis* (Stein). *Marine Biology*, 112, 497-503.

- GRUBER, N. 2011. Warming up, turning sour, losing breath: ocean biogeochemistry under global change. *Philosophical Transactions of the Royal Society A: Mathematical, Physical and Engineering Sciences*, 369, 1980-1996.
- GRUBER, N., HAURI, C., LACHKAR, Z., LOHER, D., FRÖLICHER, T. L. & PLATTNER, G.-K. 2012. Rapid Progression of Ocean Acidification in the California Current System. *Science*, 337, 220-223.
- GRÜBLER, A. 2002. Trends in global emissions: carbon, sulfur and nitrogen. In: DOUGLAS, I. (ed.) *Encyclopedia of global environmental change volume 3: Causes and consequences of global environmental change*. Chichester: John Wiley & Sons.
- GRZYMSKI, J., JOHNSEN, G. & SAKSHAUG, E. 1997. The significance of intracellular self-shading on the biooptical properties of brown, red and green macroalgae. *Journal of Phycology*, 33, 408-414.
- GUIRY, M. D. 2013. *AlgaeBase* [Online]. Available: www.algaebase.org [Accessed 19th February 2013].
- GUNSON, J. R., SPALL, S. A., ANDERSON, T. R., JONES, A., TOTTERDELL, I. J. & WOODAGE, M. J. 2006. Climate sensitivity to ocean dimethylsulphide emissions. *Geophysical Research Letters*, 33, L07701.
- HAAS, P. 1935. The liberation of methyl sulphide by seaweed. *Biochemical Journal*, 29, 1297-1299.
- HÄDER, D.-P., LEBERT, M., FIGUEROA, F. L., JIMÉNEZ, C., VIÑEGLA, B. & PEREZ-RODRIGUEZ, E. 1998. Photoinhibition in Mediterranean macroalgae by solar radiation measured on site by PAM fluorescence. *Aquatic Botany*, 61, 225-236.
- HALEVY, I., PETERS, S. E. & FISCHER, W. W. 2012. Sulfate Burial Constraints on the Phanerozoic Sulfur Cycle. *Science*, 337, 331-334.
- HALFAR, J., STENECK, R. S., JOACHIMSKI, M., KRONZ, A. & WANAMAKER JR, A. D. 2008. Coralline red algae as high-resolution climate recorders. *Geology*, 36, 463-466.
- HALFAR, J., WILLIAMS, B., HETZINGER, S., STENECK, R. S., LEBEDNIK, P., WINSBOROUGH, C., OMAR, A., CHAN, P. & WANAMAKER, A. D. 2011. 225 years of Bering Sea climate and ecosystem dynamics revealed by coralline algal growth-increment widths. *Geology*, 39, 579-582.
- HALFAR, J., ZACK, T., KRONZ, A. & ZACHOS, J. C. 2000. Growth and high-resolution paleoenvironmental signals of rhodoliths (coralline red algae): A new biogenic archive. *Journal of Geophysical Research*, 105.
- HALL-SPENCER, J. M., GRALL, J., MOORE, P. G. & ATKINSON, R. J. A. 2003. Bivalve fishing and maerl-bed conservation in France and the UK - retrospect and prospect. *Aquatic Conservation: Marine and Freshwater Ecosystems*, 13, S33-S41.
- HALL-SPENCER, J. M. & MOORE, P. G. 2000. Scallop dredging has profound, long term impacts on maerl habitats. *ICES Journal of Marine Science*, 57, 1407-1415.
- HALL-SPENCER, J. M., RODOLFO-METALPA, R., MARTIN, S., RANSOME, E., FINE, M., TURNER, S. M., ROWLEY, S. J., TEDESCO, D. & BUIA, M.-C. 2008. Volcanic carbon dioxide vents show ecosystem effects of ocean acidification. *Nature*, 454, 96-99.
- HALLORAN, P. R., BELL, T. G. & TOTTERDELL, I. J. 2010. Can we trust empirical marine DMS parameterisations within projections of future climate? *Biogeosciences*, 7, 1645-1656.
- HANELT, D. & NULTSCH, W. 1995. Field Studies of Photoinhibition Show Non-Correlations between Oxygen and Fluorescence Measurements in the Arctic Red Alga *Palmaria palmata*. *Journal of Plant Physiology*, 145, 31-38.
- HANSON, A. D., RIVOAL, J., PAQUET, L. & GAGE, D. A. 1994. Biosynthesis of 3-Dimethylsulfoniopropionate in *Wollastonia biflora* (L.) DC. (Evidence That S-Methylmethionine Is an Intermediate). *Plant Physiology*, 105, 103-110.
- HARVEY, A. S., BROADWATER, S. T., WOELKERLING, W. J. & MITROVSKI, P. J. 2003. Choreonema (Corallinales, Rhodophyta): 18S rDNA phylogeny and resurrection of the Hapalidiaceae for the subfamilies Choreonematoideae, Australithoideae and Melobesioideae. *Journal of Phycology*, 39, 988-998.
- HATTON, A., SHENOY, D., HART, M., MOGG, A. & GREEN, D. 2012a. Metabolism of DMSP, DMS and DMSO by the cultivable bacterial community associated with the DMSP-producing dinoflagellate *Scrippsiella trochoidea*. *Biogeochemistry*, 110, 131-146.
- HATTON, A. & WILSON, S. 2007. Particulate dimethylsulphoxide and dimethylsulphoniopropionate in phytoplankton cultures and Scottish coastal waters. *Aquatic Sciences - Research Across Boundaries*, 69, 330-340.
- HATTON, A. D. 2002. DMSP removal and DMSO production in sedimenting particulate matter in the northern North Sea. *Deep Sea Research Part II: Topical Studies in Oceanography*, 49, 3053-3065.

- HATTON, A. D., DARROCH, L. & MALIN, G. 2004. The Role of Dimethylsulphoxide in the Marine Biogeochemical Cycle of DMS. In: GIBSON, R. N., ATKINSON, R. J. A. & GORDON, J. D. M. (eds.) *Oceanography and Marine Biology: An Annual Review*. Boca Raton: CRC Press.
- HATTON, A. D., MALIN, G. & LISS, P. S. 1999. Distribution of biogenic sulphur compounds during and just after the southwest monsoon in the Arabian Sea. *Deep Sea Research Part II: Topical Studies in Oceanography*, 46, 617-632.
- HATTON, A. D., SHENOY, D. M., HART, M. C., MOGG, A. & GREEN, D. H. 2012b. Metabolism of DMSP, DMS and DMSO by the cultivable bacterial community associated with the DMSP-producing dinoflagellate *Scrippsiella trochoidea*. *Biogeochemistry*.
- HAURI, C., GRUBER, N., PLATTNER, G.-K., ALIN, S., FEELY, R. A., HALES, B. & WHEELER, P. A. 2009. Ocean acidification in the California Current System. *Oceanography*, 22, 60-71.
- HECK JR., K. L., HAYS, G. & ORTH, R. J. 2003. Critical evaluation of the nursery role hypothesis for seagrass meadows. *Marine Ecology Progress Series*, 253, 123-136.
- HEDLEY, J. D. & MUMBY, P. J. 2002. Biological and remote sensing perspectives of pigmentation in coral reef organisms. *Advances in Marine Biology*, 43, 277-317.
- HENNIGE, S., MCGINLEY, M., GROTTOLI, A. G. & WARNER, M. E. 2011. Photoinhibition of *Symbiodinium* spp. within the reef corals *Montastraea faveolata* and *Porites astreoides*: implications for coral bleaching. *Marine Biology*, 158, 2515-2526.
- HENNIGE, S., SMITH, D., PERKINS, R., CONSALVEY, M., PATERSON, D. & SUGGETT, D. 2008. Photoacclimation, growth and distribution of massive coral species in clear and turbid waters. *Marine Ecology Progress Series*, 369, 77-88.
- HENNIGE, S., SUGGETT, D., WARNER, M., MCDUGALL, K. & SMITH, D. 2009. Photobiology of *Symbiodinium* revisited: bio-physical and bio-optical signatures. *Coral Reefs*, 28, 179-195.
- HETZINGER, S., HALFAR, J., KRONZ, A., STENECK, R. S., ADEY, W. H., LEBEDNIK, P. A. & SCHONE, B. R. 2009. High-Resolution Mg/Ca Ratios in a Coralline Red Alga as a Proxy for Bering Sea Temperature Variations from 1902 to 1967. *Palaios*, 24, 406-412.
- HILL, R., SCHREIBER, U., GADEMANN, R., LARKUM, A. W. D., KÜHL, M. & RALPH, P. J. 2004. Spatial heterogeneity of photosynthesis and the effect of temperature-induced bleaching conditions in three species of corals. *Marine Biology*, 144, 633-640.
- HILY, C., POTIN, P. & FLOCH, J. Y. 1992. Structure of Subtidal Algal Assemblages on Soft-Bottom Sediments - Fauna / Flora Interactions and Role of Disturbances in the Bay of Brest, France. *Marine Ecology Progress Series*, 85, 115-130.
- HOCHBERG, E. J. & ATKINSON, M. J. 2000. Spectral discrimination of coral reef benthic communities. *Coral Reefs*, 19, 164-171.
- HOEFS, J. 2009. *Stable Isotope Geochemistry*: Springer Berlin Heidelberg.
- HOEGH-GULDBERG, O., MUMBY, P. J., HOOTEN, A. J., STENECK, R. S., GREENFIELD, P., GOMEZ, E., HARVELL, C. D., SALE, P. F., EDWARDS, A. J., CALDEIRA, K., KNOWLTON, N., EAKIN, C. M., INGLESIAS-PRIETO, R., MUTHIGA, N., BRADBURY, R. H., DUBI, A. & HATZIOLOS, M. E. 2007. Coral Reefs Under Rapid Climate Change and Ocean Acidification. *Science*, 318, 1737-1742.
- HOLLAND, G. J. & WEBSTER, P. J. 2007. Heightened tropical cyclone activity in the North Atlantic: natural variability or climate trend? *Philosophical Transactions of the Royal Society A: Mathematical, Physical and Engineering Sciences*, 365, 2695-2716.
- HOPKINS, F. E., TURNER, S. M., NIGHTINGALE, P. D., STEINKE, M., BAKKER, D. & LISS, P. S. 2010. Ocean acidification and marine trace gas emissions. *Proceedings of the Academy of Natural Sciences of Philadelphia*, 107, 760-765.
- HOWARD, A. G., FREEMAN, C. E., RUSSELL, D. W., ARBAB-ZAVAR, M. H. & CHAMBERLAIN, P. 1998. Flow injection system with flame photometric detection for the measurement of the dimethylsulphide precursor β -dimethylsulphoniopropionate. *Analytica Chimica Acta*, 377, 95-101.
- HUGGETT, M., WILLIAMSON, J., DE NYS, R., KJELLEBERG, S. & STEINBERG, P. 2006. Larval settlement of the common Australian sea urchin *Heliocidaris erythrogramma* in response to bacteria from the surface of coralline algae. *Oecologia*, 149, 604-619.
- HUOVINEN, P., GÓMEZ, I. & LOVINGREEN, C. 2006. A Five-year Study of Solar Ultraviolet Radiation in Southern Chile (39° S): Potential Impact on Physiology of Coastal Marine Algae? *Photochemistry and Photobiology*, 82, 515-522.
- HURRELL, J. W. 1995. Decadal Trends in the North Atlantic Oscillation: Regional Temperatures and Precipitation. *Science*, 269, 676-679.
- HURTGEN, M. T. 2012. The Marine Sulfur Cycle, Revisited. *Science*, 337, 305-306.
- HUSSNER, A., HOFSTRA, D. & JAHNS, P. 2011. Diurnal courses of net photosynthesis and photosystem II quantum efficiency of submerged *Lagarosiphon major* under natural light conditions. *Flora - Morphology, Distribution, Functional Ecology of Plants*, 206, 904-909.
- IPCC 2007. Summary for Policymakers. In: SOLOMON, S., QIN, D., MANNING, M., CHEN, Z., MARQUIS, M., AVERYT, K. B., M. TIGNOR & MILLER, H. L. (eds.) *Climate Change 2007*:

- The Physical Science Basis. Contribution of Working Group I to the Fourth Assessment Report of the Intergovernmental Panel on Climate Change.* Cambridge, UK, New York, USA: Cambridge University Press.
- IRVINE, L. M. & CHAMBERLAIN, Y. M. 1994. *Seaweeds of the British Isles: Volume 1 Rhodophyta, Part 2B Corallinales, Hildenbrandiales*, London: HMSO.
- IRVING, A., CONNELL, S., JOHNSTON, E., PILE, A. & GILLANDERS, B. 2005. The response of encrusting coralline algae to canopy loss: an independent test of predictions on an Antarctic coast. *Marine Biology*, 147, 1075-1083.
- IRVING, A. D., CONNELL, S. D. & ELSDON, T. S. 2004. Effects of kelp canopies on bleaching and photosynthetic activity of encrusting coralline algae. *Journal of Experimental Marine Biology and Ecology*, 310, 1-12.
- IVANOV, M. V. & FRENEY, J. R. (eds.) 1983. *The global biogeochemical sulfur cycle, SCOPE 19*, Chichester: John Wiley & Sons.
- JAMES, J., SHERMAN, T. & DEVEREUX, R. 2006. Analysis of Bacterial Communities in Seagrass Bed Sediments by Double-Gradient Denaturing Gradient Gel Electrophoresis of PCR-Amplified 16S rRNA Genes. *Microbial Ecology*, 52, 655-661.
- JASSBY, A. D. & PLATT, T. 1976. Mathematical formulation of the relationship between photosynthesis and light for phytoplankton. *Limnology and Oceanography*, 21, 540-547.
- JEAN, N., BOGE, G., JAMET, J.-L. & JAMET, D. 2006. Comparison of β -dimethylsulfoniopropionate (DMSP) levels in two mediterranean ecosystems with different trophic levels. *Marine Chemistry*, 101, 190-202.
- JIA-ZHONG, Z. & CHI, J. 2002. Automated analysis of nanomolar concentrations of phosphate in natural waters with liquid waveguide. *Environmental Science & Technology*, 36, 1048-1053.
- JIAO, N., AZAM, F. & SANDERS, S. (eds.) 2011. *Microbial carbon pump in the ocean: Science / AAAS Business Office.*
- JNCC. 2012. *Joint Nature Conservation Committee* [Online]. Available: <http://jncc.defra.gov.uk/> [Accessed 24 July 2012].
- JOHANSEN, H. W. 1981. *Coralline algae: a first synthesis*, Florida: CRC Press.
- JOHNSON, V. R., RUSSELL, B. D., FABRICIUS, K. E., BROWNLEE, C. & HALL-SPENCER, J. M. 2012. Temperate and tropical brown macroalgae thrive, despite decalcification, along natural CO₂ gradients. *Global Change Biology*, n/a-n/a.
- JOHNSTON, A. W. B., TODD, J. D., SUN, L., NIKOLAIDOU-KATSARIDOU, M. N., CURSON, A. R. J. & ROGERS, R. 2008. Molecular diversity of bacterial production of the climate-changing gas, dimethyl sulphide, a molecule that impinges on local and global symbioses. *Journal of Experimental Botany*, 59, 1059-1067.
- JOKIEL, P., RODGERS, K., KUFFNER, I., ANDERSSON, A., COX, E. & MACKENZIE, F. 2008. Ocean acidification and calcifying reef organisms: a mesocosm investigation. *Coral Reefs*, 27, 473-483.
- JONES, G., CURRAN, M., BROADBENT, A., KING, S., FISCHER, E. & JONES, R. 2007. Factors affecting the cycling of dimethylsulfide and dimethylsulfoniopropionate in coral reef waters of the Great Barrier Reef. *Environmental Chemistry*, 4, 310-322.
- JONES, G. M. & SCHEIBLING, R. E. 1985. *Paramoeba* sp. (Amoebida, Paramoebidae) as the Possible Causative Agent of Sea Urchin Mass Mortality in Nova Scotia. *The Journal of Parasitology*, 71, 559-565.
- JOSEY, S. A. & MARSH, R. 2005. Surface freshwater flux variability and recent freshening of the North Atlantic in the eastern subpolar gyre. *Journal of Geophysical Research*, 110, C05008.
- KAMENOS, N. A. 2010. North Atlantic summers have warmed more than winters since 1353 and the response of marine zooplankton. *Proceedings of the National Academy of Sciences*, 107, 22442-22447.
- KAMENOS, N. A., CUSACK, M., HUTHWELKER, T., LAGARDE, P. & SCHEIBLING, R. E. 2009. Mg-lattice associations in red coralline algae. *Geochimica et Cosmochimica Acta*, 73, 1901-1907.
- KAMENOS, N. A., CUSACK, M. & MOORE, P. G. 2008a. Coralline algae are global palaeothermometers with bi-weekly resolution. *Geochimica et Cosmochimica Acta*, 72, 771-779.
- KAMENOS, N. A., HOEY, T. B., NIENOW, P., FALLICK, A. E. & CLAVERIE, T. 2012. Reconstructing Greenland ice sheet runoff using coralline algae. *Geology*.
- KAMENOS, N. A. & LAW, A. 2010. Temperature controls on coralline algal skeletal growth. *Journal of Phycology*, 46, 331-335.
- KAMENOS, N. A., MOORE, P. G. & HALL-SPENCER, J. 2004a. The small-scale distribution of juvenile gadoids in shallow inshore waters; what role does maerl play? *ICES Journal of Marine Science*, 61, 422-429.

- KAMENOS, N. A., MOORE, P. G. & HALL-SPENCER, J. M. 2004b. Attachment of the juvenile queen scallop (*Aequipecten opercularis* (L.)) to maerl in mesocosm conditions; juvenile habitat selection. *Journal of Experimental Marine Biology and Ecology*, 306, 139-155.
- KAMENOS, N. A., MOORE, P. G. & HALL-SPENCER, J. M. 2004c. Nursery-area function of maerl grounds for juvenile queen scallops *Aequipecten opercularis* and other invertebrates. *Marine Ecology Progress Series*, 274, 183-189.
- KAMENOS, N. A., MOORE, P. G. & HALL-SPENCER, J. M. 2003. Substratum heterogeneity of dredged vs un-dredged maerl grounds. *Journal of the Marine Biological Association of the United Kingdom*, 83, 411-413.
- KAMENOS, N. A., STRONG, S. C., SHENOY, D. M., WILSON, S. T., HATTON, A. D. & MOORE, P. G. 2008b. Red coralline algae as a source of marine biogenic dimethylsulphonioacetate. *Marine Ecology Progress Series*, 372, 61-66.
- KARSTEN, U., KIRST, G. & WIENCKE, C. 1992. Dimethylsulphonioacetate (DMSP) accumulation in green macroalgae from polar to temperate regions: interactive effects of light versus salinity and light versus temperature. *Polar Biology*, 12, 603-607.
- KARSTEN, U., KUCK, K., VOGT, C. & KIRST, G. O. 1996. Dimethylsulphonioacetate production in phototrophic organisms and its physiological function as a cryoprotectant. In: KIENE, R. P., VISSCHER, P. T., KELLER, M. D. & KIRST, G. O. (eds.) *Biological Chemistry of DMSP and Related Sulfonium Compounds*. New York: Plenum Press.
- KARSTEN, U., WIENCKE, C. & KIRST, G. O. 1990. The effect of light intensity and daylength on the β -dimethylsulphonioacetate (DMSP) content of marine green macroalgae from Antarctica. *Plant, Cell and Environment*, 13, 989-993.
- KELLER, M. D., BELLOWS, W. K. & GUILLARD, R. L. 1989. Dimethyl Sulfide Production in Marine Phytoplankton. *Biogenic Sulfur in the Environment*. American Chemical Society.
- KERRISON, P., SUGGETT, D., HEPBURN, L. & STEINKE, M. 2012. Effect of elevated $p\text{CO}_2$ on the production of dimethylsulphonioacetate (DMSP) and dimethylsulfide (DMS) in two species of *Ulva* (Chlorophyceae). *Biogeochemistry*, 110, 5-16.
- KETTLE, A. J. & ANDREAE, M. O. 2000. Flux of dimethylsulfide from the oceans: A comparison of updated data sets and flux models. *Journal of Geophysical Research*, 105, 26793-26808.
- KETTLE, A. J., ANDREAE, M. O., AMOUROUX, D., ANDREAE, T. W., BATES, T. S., BERRESHEIM, H., BINGEMER, H., BONIFORTI, R., CURRAN, M. A. J., DITULLIO, G. R., HELAS, G., JONES, G. B., KELLER, M. D., KIENE, R. P., LECK, C., LEVASSEUR, M., MALIN, G., MASPERO, M., MATRAI, P., MCTAGGART, A. R., MIHALOPOULOS, N., NGUYEN, B. C., NOVO, A., PUTAUD, J. P., RAPSOMANIKIS, S., ROBERTS, G., SCHEBESKE, G., SHARMA, S., SIMÓ, R., STAUBES, R., TURNER, S. & UHER, G. 1999. A global database of sea surface dimethylsulfide (DMS) measurements and a procedure to predict sea surface DMS as a function of latitude, longitude, and month. *Global Biogeochem. Cycles*, 13, 399-444.
- KIEHN, W. M. & MORRIS, J. T. 2010. Variability in dimethylsulphonioacetate (DMSP) concentrations in *Spartina alterniflora* and the effect on *Littoraria irrorata*. *Marine Ecology Progress Series*, 406, 47-55.
- KIENE, R. P. & BATES, T. S. 1990. Biological removal of dimethyl sulphide from sea water. *Nature*, 345, 702-705.
- KIENE, R. P. & LINN, L. J. 2000. Distribution and Turnover of Dissolved DMSP and Its Relationship with Bacterial Production and Dimethylsulfide in the Gulf of Mexico. *Limnology and Oceanography*, 45, 849-861.
- KIENE, R. P., LINN, L. J. & BRUTON, J. A. 2000. New and important roles for DMSP in marine microbial communities. *Journal of Sea Research*, 43, 209-224.
- KIENE, R. P., LINN, L. J., GONZÁLEZ, J., MORAN, M. A. & BRUTON, J. A. 1999. Dimethylsulphonioacetate and Methanethiol Are Important Precursors of Methionine and Protein-Sulfur in Marine Bacterioplankton. *Applied and Environmental Microbiology*, 65, 4549-4558.
- KIENE, R. P. & SLEZAK, D. 2006. Low dissolved DMSP concentrations in seawater revealed by small-volume gravity filtration and dialysis sampling. *Limnology and Oceanography: Methods*, 4, 80-95.
- KIRK, J. T. O. 2011. *Light and photosynthesis in aquatic ecosystems*, (3rd edn), Cambridge: Cambridge University Press.
- KIRKWOOD, D. 1989. Simultaneous determination of selected nutrients in seawater. *International Council for the Exploration of the Sea (ICES)*, CM 1989/C:29.
- KIRST, G. 1996. Osmotic adjustment in phytoplankton and macroalgae: the use of dimethylsulphonioacetate (DMSP). In: KIENE, R. P., VISSCHER, P. T., KELLER, MAUREEN, D. & KIRST, G. (eds.) *Biological and Environmental Chemistry of DMSP and Related Sulfonium Compounds*. New York: Plenum Press.

- KIRST, G. 1989. Salinity tolerance of eukaryotic marine algae. *Annu. Rev. Plant Physiol. Plant Mol. Biol.*, 40, 21-53.
- KIRST, G. O., THIEL, C., WOLFF, H., NOTHNAGEL, J., WANZEK, M. & ULMKE, R. 1991. Dimethylsulfoniopropionate (DMSP) in icealgae and its possible biological role. *Marine Chemistry*, 35, 381-388.
- KLEYPAS, J. A., ANTHONY, K. R. N. & GATTUSO, J.-P. 2011. Coral reefs modify their seawater carbon chemistry – case study from a barrier reef (Moorea, French Polynesia). *Global Change Biology*, 17, 3667-3678.
- KLEYPAS, J. A. & LANGDON, C. 2006. Coral reefs and changing seawater carbonate chemistry. *Coral Reefs and Climate Change: Science and Management*. Washington, DC: AGU.
- KLOSTER, S., FEICHTER, J., MAIER-REIMER, E., SIX, K. D., STIER, P. & WETZEL, P. 2006. DMS cycle in the marine ocean-atmosphere system - a global model study. *Biogeosciences*, 3, 29-51.
- KNUTSON, T. R., MCBRIDE, J. L., CHAN, J., EMANUEL, K., HOLLAND, G., LANDSEA, C., HELD, I., KOSSIN, J. P., SRIVASTAVA, A. K. & SUGI, M. 2010. Tropical cyclones and climate change. *Nature Geosci*, 3, 157-163.
- KNUTSON, T. R., SIRUTIS, J. J., GARNER, S. T., VECCHI, G. A. & HELD, I. M. 2008. Simulated reduction in Atlantic hurricane frequency under twenty-first-century warming conditions. *Nature Geosci*, 1, 359-364.
- KOCSIS, M. G., NOLTE, K. D., RHODES, D., SHEN, T. L., GAGE, D. A. & HANSON, A. D. 1998. Dimethylsulfoniopropionate biosynthesis in *Spartina alterniflora* - Evidence that S-methylmethionine and dimethylsulfoniopropylamine are intermediates. *Plant Physiology*, 117, 273-281.
- KOOP, K., BOOTH, D., BROADBENT, A., BRODIE, J., BUCHER, D., CAPONE, D., COLL, J., DENNISON, W., ERDMANN, M., HARRISON, P., HOEGH-GULDBERG, O., HUTCHINGS, P., JONES, G. B., LARKUM, A. W. D., O'NEIL, J., STEVEN, A., TENTORI, E., WARD, S., WILLIAMSON, J. & YELLOWLEES, D. 2001. ENCORE: The effect of nutrient enrichment on coral reefs. Synthesis of results and conclusions. *Marine Pollution Bulletin*, 42, 91-120.
- KORHONEN, H., CARSLAW, K. S., SPRACKLEN, D. V., MANN, G. W. & WOODHOUSE, M. T. 2008. Influence of oceanic dimethyl sulfide emissions on cloud condensation nuclei concentrations and seasonality over the remote Southern Hemisphere oceans: A global model study. *Journal of Geophysical Research*, 113, D15204.
- KOWALEWSKY, S., DAMBACH, M., MAUCK, B. & DEHNHARDT, G. 2006. High olfactory sensitivity for dimethyl sulphide in harbour seals. *Biology Letters*, 2, 106-109.
- KRAFT, G. T., SAUNDERS, G. W., ABBOTT, I. A. & HAROUN, R. J. 2004. A uniquely calcified brown alga from Hawaii: *Newhousia inbricata* gen. et. sp. nov. (Dictyotales, Phaeophyceae). *Journal of Phycology*, 40, 383-394.
- KROMKAMP, J. & FORSTER, R. 2003. The use of variable fluorescence measurements in aquatic ecosystems: differences between multiple and single turnover measuring protocols and suggested terminology. *European Journal of Phycology*, 38, 103 - 112.
- KRUMHANSL, K. & SCHEIBLING, R. 2011. Detrital production in Nova Scotian kelp beds: patterns and processes. *Marine Ecology Progress Series*, 421, 67-82.
- KRUMHANSL, K. & SCHEIBLING, R. E. 2012. Detrital subsidy from subtidal kelp beds is altered by the invasive green alga *Codium fragile* ssp. *fragile*. *Marine Ecology Progress Series*, 456, 73-85.
- KRUMHANSL, K. A., LEE, J. M. & SCHEIBLING, R. E. 2011. Grazing damage and encrustation by an invasive bryozoan reduce the ability of kelps to withstand breakage by waves. *Journal of Experimental Marine Biology and Ecology*, 407, 12-18.
- KUFFNER, I. B., ANDERSSON, A. J., JOKIEL, P. L., RODGERS, K. U. S. & MACKENZIE, F. T. 2008. Decreased abundance of crustose coralline algae due to ocean acidification. *Nature Geoscience*, 1, 114-117.
- KUMAR, S. S., CHINCHKAR, U., NAIR, S., LOKA BHARATHI, P. A. & CHANDRAMOHAN, D. 2009. Seasonal dimethylsulfoniopropionate (DMSP) variability in Dona Paula bay. *Estuarine, Coastal and Shelf Science*, 81, 301-310.
- KÜPPER, F. C., CARPENTER, L. J., MCFIGGANS, G. B., PALMER, C. J., WAITE, T. J., BONEBERG, E.-M., WOITSCH, S., WEILLER, M., ABELA, R., GROLIMUND, D., POTIN, P., BUTLER, A., LUTHER, G. W., KRONECK, P. M. H., MEYER-KLAUCKE, W. & FEITERS, M. C. 2008. Iodide accumulation provides kelp with an inorganic antioxidant impacting atmospheric chemistry. *Proceedings of the National Academy of Sciences*, 105, 6954-6958.
- KÜPPER, F. C., SCHWEIGERT, N., AR GALL, E., LEGENDRE, J. M., VILTER, H. & KLOAREG, B. 1998. Iodine uptake in Laminariales involves extracellular, haloperoxidase-mediated oxidation of iodide. *Planta*, 207, 163-171.

- KURIHARA, H. 2008. Effects of CO₂-driven ocean acidification on the early developmental stages of invertebrates. *Marine Ecology Progress Series*, 373, 275-284.
- KUTSER, T., VAHTMAE, E. & L., M. 2006. Spectral library of macroalgae and benthic substrates in Estonian coastal waters. *Proceedings of the Estonian Academy of Sciences. Biology and Ecology*, 55, 329-340.
- KWINT, R., IRIGOIGEN, X. & KRAMER, K. 1996. Copepods and DMSP. In: KIENE, R. P., VISSCHER, P. T., KELLER MAUREEN, D. & KIRST, G. O. (eds.) *Biological and environmental chemistry of DMSP and related sulfonium compounds*. New York: Plenum Press.
- KWOK, R. & COMISO, J. C. 2002. Southern ocean climate and sea ice anomalies associated with the Southern Oscillation. *Journal of Climate*, 15, 487-501.
- LACHKAR, Z. & GRUBER, N. 2013. Response of biological production and air-sea CO₂ fluxes to upwelling intensification in the California and Canary Current Systems. *Journal of Marine Systems*, 109-110, 149-160.
- LANA, A., BELL, T. G., SIMÓ, R., VALLINA, S. M., BALLABRERA-POY, J., KETTLE, A. J., DACHS, J., BOPP, L., SALTZMAN, E. S., STEFELS, J., JOHNSON, J. E. & LISS, P. S. 2011. An updated climatology of surface dimethylsulfide concentrations and emission fluxes in the global ocean. *Global Biogeochem. Cycles*, 25, GB1004.
- LANA, A., SIMÓ, R., VALLINA, S. & DACHS, J. 2012. Re-examination of global emerging patterns of ocean DMS concentration. *Biogeochemistry*, 110, 173-182.
- LANGDON, C., BROECKER, W. S., HAMMOND, D. E., GLENN, E., FITZSIMMONS, K., NELSON, S. G., PENG, T.-H., HAJDAS, I. & BONANI, G. 2003. Effect of elevated CO₂ on the community metabolism of an experimental coral reef. *Global Biogeochem. Cycles*, 17, 1011.
- LANGDON, C., TAKAHASHI, T., SWEENEY, C., CHIPMAN, D., GODDARD, J., MARUBINI, F., ACEVES, H., BARNETT, H. & ATKINSON, M. J. 2000. Effect of calcium carbonate saturation state on the calcification rate of an experimental coral reef. *Global Biogeochem. Cycles*, 14, 639-654.
- LAVAUD, J., ROUSSEAU, B., VAN GORKOM, H. J. & ETIENNE, A.-L. 2002. Influence of the diadinoxanthin pool size on photoprotection in the marine planktonic diatom *Phaeodactylum tricornutum*. *Plant Physiology*, 129, 1398-1406.
- LECK, C., LARSSON, U., BÅGANDER, L. E., JOHANSSON, S. & HAJDU, S. 1990. Dimethyl Sulfide in the Baltic Sea: Annual Variability in Relation to Biological Activity. *Journal of Geophysical Research*, 95, 3353-3363.
- LEVY, O., DUBINSKY, Z., SCHNEIDER, K., ACHITUV, Y. & GORBUNOV, D. Z. M. Y. 2004. Diurnal hysteresis in coral photosynthesis. *Marine Ecology Progress Series*, 268, 105-117.
- LEWIS, N., BRECKELS, M., ARCHER, S., MOROZOV, A., PITCHFORD, J., STEINKE, M. & CODLING, E. 2011. Grazing-induced production of DMS can stabilize food-web dynamics and promote the formation of phytoplankton blooms in a multitrophic plankton model. *Biogeochemistry*, 1-11.
- LIDBURY, I., JOHNSON, V., HALL-SPENCER, J. M., MUNN, C. B. & CUNLIFFE, M. 2012. Community-level response of coastal microbial biofilms to ocean acidification in a natural carbon dioxide vent ecosystem. *Marine Pollution Bulletin*, 64, 1063-1066.
- LISS, P. S. & MERLIVAT, L. 1986. Air-sea gas exchange rates: Introduction and synthesis. In: BUAT-MENARD, P. (ed.) *The role of air-sea gas exchange in geochemical cycling*. Dordrecht: D. Reidel Publishing Company.
- LITTLER, M. M., LITTLER, D. S. & HANISAK, M. D. 1991. Deep-water rhodolith distribution, productivity, and growth history at sites of formation and subsequent degradation. *Journal of Experimental Marine Biology and Ecology*, 150, 163-182.
- LUBIN, D., LI, W., DUSTAN, P., MAZEL, C. H. & STAMNES, K. 2001. Spectral Signatures of Coral Reefs: Features from Space. *Remote Sensing of Environment*, 75, 127-137.
- LÜNING, K. 1990. *Seaweeds. Their environment, biogeography and ecophysiology.*, New York: Wiley Interscience.
- LUTHI, D., LE FLOCH, M., BEREITER, B., BLUNIER, T., BARNOLA, J.-M., SIEGENTHALER, U., RAYNAUD, D., JOUZEL, J., FISCHER, H., KAWAMURA, K. & STOCKER, T. F. 2008. High-resolution carbon dioxide concentration record 650,000-800,000 years before present. *Nature*, 453, 379-382.
- LYONS, D., SCHEIBLING, R. & VAN ALSTYNE, K. 2010. Spatial and temporal variation in DMSP content in the invasive seaweed *Codium fragile* ssp. *fragile*: effects of temperature, light and grazing. *Marine Ecology Progress Series*, 417, 51-61.
- LYONS, D., VAN ALSTYNE, K. & SCHEIBLING, R. 2007. Anti-grazing activity and seasonal variation of dimethylsulfoniopropionate-associated compounds in the invasive alga *Codium fragile* ssp. *tomentosoides*. *Marine Biology*, 153, 179-188.

- MACAYA, E. C., ROTHÄUSLER, E., THIEL, M., MOLIS, M. & WAHL, M. 2005. Induction of defenses and within-alga variation of palatability in two brown algae from the northern-central coast of Chile: Effects of mesograzers and UV radiation. *Journal of Experimental Marine Biology and Ecology*, 325, 214-227.
- MANLEY, S. L., GOODWIN, K. & NORTH, W. J. 1992. Laboratory Production of Bromoform, Methylene Bromide, and Methyl Iodide by Macroalgae and Distribution in Nearshore Southern California Waters. *Limnology and Oceanography*, 37, 1652-1659.
- MANN, M. E. & EMANUEL, K. A. 2006. Atlantic hurricane trends linked to climate change. *Eos Trans. AGU*, 87.
- MANTOURA, R. F. C. & WOODWARD, E. M. S. 1983. Optimisation of the indophenol blue method for the automated determination of ammonia in estuarine waters. *Estuarine Coastal and Shelf Science*, 17, 219-224.
- MARTIN, S. & GATTUSO, J. P. 2009. Response of Mediterranean coralline algae to ocean acidification and elevated temperature. *Global Change Biology*, 15, 2089-2100.
- MARTIN, S., RODOLFO-METALPA, R., RANSOME, E., ROWLEY, S., BUIA, M. C., GATTUSO, J. P. & HALL-SPENCER, J. 2008. Effects of naturally acidified seawater on seagrass calcareous epibionts. *Biology Letters*, 4, 689-692.
- MARTÍNEZ, M. L., INTRALAWAN, A., VÁZQUEZ, G., PÉREZ-MAQUEO, O., SUTTON, P. & LANDGRAVE, R. 2007. The coasts of our world: Ecological, economic and social importance. *Ecological Economics*, 63, 254-272.
- MAXWELL, K. & JOHNSON, G. N. 2000. Chlorophyll fluorescence—a practical guide. *Journal of Experimental Botany*, 51, 659-668.
- MEEHL, G. A., STOCKER, T., COLLINS, W., FRIEDLINGSTEIN, P., GAYE, A., GREGORY, J., KITOC, A., KNUITTI, R., MURPHY, J., NODA, A., RAPER, S., WATTERSON, I., WEAVER, A. & ZHAO, Z.-C. 2007. Global Climate Projections. In: SOLOMON, S., QIN, D., MANNING, M., CHEN, Z., MARQUIS, M., AVERYT, K. B., TIGNOR, M. & MILLER, H. L. (eds.) *Climate Change 2007: The Physical Science Basis. Contribution of Working Group I to the Fourth Assessment Report of the Intergovernmental Panel on Climate Change*. Cambridge: Cambridge University Press.
- MEHRBACH, C., CULBERSON, C. H., HAWLEY, J. E. & PYTKOWICZ, R. M. 1973. Measurement of the Apparent Dissociation Constants of Carbonic Acid in Seawater at Atmospheric Pressure. *Limnology and Oceanography*, 18, 897-907.
- MELZNER, F., THOMSEN, J., KOEVE, W., OSCHLIES, A., GUTOWSKA, M., BANGE, H., HANSEN, H. & KÖRTZINGER, A. 2012. Future ocean acidification will be amplified by hypoxia in coastal habitats. *Marine Biology*, 1-14.
- MERON, D., RODOLFO-METALPA, R., CUNNING, R., BAKER, A. C., FINE, M. & BANIN, E. 2012. Changes in coral microbial communities in response to a natural pH gradient. *ISME J*, 6, 1775-1785.
- MICHAUD, S., LEVASSEUR, M. & CANTIN, G. 2007. Seasonal variations in dimethylsulfoniopropionate and dimethylsulfide concentrations in relation to the plankton community in the St. Lawrence Estuary. *Estuarine, Coastal and Shelf Science*, 71, 741-750.
- MILLER, R. J. 1985. Succession in sea urchin and seaweed abundance in Nova Scotia, Canada. *Marine Biology*, 84, 275-286.
- MILLER, R. J. & NOLAN, S. C. 2008. Management Methods for a Sea Urchin Dive Fishery with Individual Fishing Zones. *Journal of Shellfish Research*, 27, 929-938.
- MOORE, C. M., LUCAS, M. I., SANDERS, R. & DAVIDSON, R. 2005. Basin-scale variability of phytoplankton bio-optical characteristics in relation to bloom state and community structure in the Northeast Atlantic. *Deep Sea Research Part I: Oceanographic Research Papers*, 52, 401-419.
- MORAN, M. A., REISCH, C. R., KIENE, R. P. & WHITMAN, W. B. 2012. Genomic Insights into Bacterial DMSP Transformations. *Annual Review of Marine Science*, 4, 523-542.
- MUNK, W. 2003. Ocean Freshening, Sea Level Rising. *Science*, 300, 2041-2043.
- NEGRI, A. P., WEBSTER, N. S., HILL, R. T. & HEYWARD, A. J. 2001. Metamorphosis of broadcast spawning corals in response to bacteria isolated from crustose algae. *Marine Ecology Progress Series*, 223, 121-131.
- NELSON, W. A. 2009. Calcified macroalgae – critical to coastal ecosystems and vulnerable to change: a review. *Marine and Freshwater Research*, 60, 787-801.
- NEVITT, G. A. 2011. The Neuroecology of Dimethyl Sulfide: A Global-Climate Regulator Turned Marine Infochemical. *Integrative and Comparative Biology*, 51, 819-825.
- NEVITT, G. A. 2000. Olfactory Foraging by Antarctic Procellariiform Seabirds: Life at High Reynolds Numbers. *Biological Bulletin*, 198, 245-253.
- NEVITT, G. A. 2008. Sensory ecology on the high seas: the odor world of the procellariiform seabirds. *Journal of Experimental Biology*, 211, 1706-1713.

- NEVITT, G. A. & BONADONNA, F. 2005. Sensitivity to dimethyl sulphide suggests a mechanism for olfactory navigation by seabirds. *Biology Letters*, 1, 303-305.
- NEWMAN, M., COMPO, G. P. & ALEXANDER, M. A. 2003. ENSO-Forced Variability of the Pacific Decadal Oscillation. *Journal of Climate*, 16, 3853-3857.
- NEWTON, J. 2010. Stable Isotope Ecology. eLS. John Wiley & Sons, Ltd.
- NIELSEN, H. & NIELSEN, S. 2008. Evaluation of imaging and conventional PAM as a measure of photosynthesis in thin- and thick-leaved marine macroalgae. *Aquatic Biology*, 3, 121-131.
- NOAA. 2012a. *NHC Data Archive* [Online]. Available: http://www.nhc.noaa.gov/pastall.shtml#tracks_all [Accessed 21st March 2012].
- NOAA. 2012b. *OA Observations and Data* [Online]. Available: <http://pmel.noaa.gov/co2/story/OA+Observations+and+Data> [Accessed 30th July 2012].
- NOAA. 2012c. *Trends in atmospheric carbon dioxide* [Online]. Available: <http://www.esrl.noaa.gov/gmd/ccgg/trends/mlo.html> [Accessed 8th March 2013].
- NOAA. 2012d. *Where are reef building corals found?* [Online]. Available: http://oceanservice.noaa.gov/education/tutorial_corals/coral05_distribution.html [Accessed 31st August 2012].
- NOORDKAMP, D. J. B., GIESKES, W. W. C., GOTTSCHAL, J. C., FORNEY, L. J. & RIJSSEL, M. V. 2000. Acrylate in *Phaeocystis* colonies does not affect the surrounding bacteria. *Journal of Sea Research*, 43, 287-296.
- NYBAKKEN, J. W. & BERTNESS, M. D. 2005. *Marine biology: an ecological approach*: Pearson/Benjamin Cummings.
- O'DONNELL, M., HAMMOND, L. & HOFMANN, G. 2009. Predicted impact of ocean acidification on a marine invertebrate: elevated CO₂ alters response to thermal stress in sea urchin larvae. *Marine Biology*, 156, 439-446.
- ODURO, H., KAMYSHNY JR, A., GUO, W. & FARQUHAR, J. 2011. Multiple sulfur isotope analysis of volatile organic sulfur compounds and their sulfonium precursors in coastal marine environments. *Marine Chemistry*, 124, 78-89.
- ODURO, H., VAN ALSTYNE, K. L. & FARQUHAR, J. 2012. Sulfur isotope variability of oceanic DMSP generation and its contributions to marine biogenic sulfur emissions. *Proceedings of the National Academy of Sciences*, 109, 9012-9016.
- OKAZAKI, M., PENTECOST, A., TANAKA, Y. & MIYATA, M. 1986. A study of calcium carbonate deposition in the genus *Padina* (Phaeophyceae, Dictyotales). *British Phycological Journal*, 21, 217-224.
- OLIVER, T. & PALUMBI, S. 2011. Do fluctuating temperature environments elevate coral thermal tolerance? *Coral Reefs*, 30, 429-440.
- ORTH, R. J., CARRUTHERS, T. J. B., DENNISON, W. C., DUARTE, C. M., FOURQUREAN, J. W., JR, K. L. H., HUGHES, A. R., KENDRICK, G. A., KENWORTHY, W. J., OLYARNIK, S., SHORT, F. T., WAYCOTT, M. & WILLIAMS, S. L. 2006. A Global Crisis for Seagrass Ecosystems. *Bioscience*, 56, 987-996.
- OXFORD, D. O. C. 2004. *Oxford Dictionary of Chemistry*, Oxford: Oxford University Press.
- PARRY, G. 1981. The meanings of r- and K-selection. *Oecologia*, 48, 260-264.
- PAYRI, C. E., MARITORENA, S., BIZEAU, C. & RODIÈRE, M. 2001. Photoacclimation in the tropical coralline alga *Hydrolithon onkodes* (Rhodophyta, Corallinaceae) from a French Polynesian reef. *Journal of Phycology*, 37, 223-234.
- PEARSON, P. N. & PALMER, M. R. 2000. Atmospheric carbon dioxide concentrations over the past 60 million years. *Nature*, 406, 695-699.
- PELEJERO, C., CALVO, E. & HOEGH-GULDBERG, O. 2010. Paleo-perspectives on ocean acidification. *Trends in Ecology & Evolution*, 25, 332-344.
- PEÑA, V. & BÁRBARA, I. 2008. Biological importance of an Atlantic European maërl bed off Benencia Island (northwest Iberian Peninsula). *Botanica Marina*, 51, 493-505.
- PETRIE, B., TOPLISS, B. J. & WRIGHT, D. G. 1987. Coastal upwelling and eddy development off Nova Scotia. *Journal of Geophysical Research*, 29, 12979-12991.
- PHILANDER, S. G. H. 1983. El Niño Southern Oscillation phenomena. *Nature*, 302, 295-301.
- PIANKA, E. R. 1970. On r- and K-Selection. *The American Naturalist*, 104, 592-597.
- PIERROT, D., LEWIS, E. & WALLACE, D. W. R. 2006. CO₂SYS DOS Program developed for CO₂ system calculations. ORNL/CDIAC-105. Carbon Dioxide Information analysis Center. Oak Ridge National Laboratory, US Department of Energy, Oak Ridge, TN.
- PINHASSI, J., SIMÓ, R., GONZÁLEZ, J. M., VILA, M., ALONSO-SÁEZ, L., KIENE, R. P., MORAN, M. A. & PEDRÓS-ALIÓ, C. 2005. Dimethylsulfoniopropionate Turnover Is Linked to the Composition and Dynamics of the Bacterioplankton Assemblage during a Microcosm Phytoplankton Bloom. *Applied and Environmental Microbiology*, 71, 7650-7660.
- PINIÁK, G. A. & STORLAZZI, C. D. 2008. Diurnal variability in turbidity and coral fluorescence on a fringing reef flat: Southern Molokai, Hawaii. *Estuarine, Coastal and Shelf Science*, 77, 56-64.

- PIÑONES, A., VALLE-LEVINSON, A., NARVÁEZ, D. A., VARGAS, C. A., NAVARRETE, S. A., YURAS, G. & CASTILLA, J. C. 2005. Wind-induced diurnal variability in river plume motion. *Estuarine, Coastal and Shelf Science*, 65, 513-525.
- PORZIO, L., BUIA, M. C. & HALL-SPENCER, J. M. 2011. Effects of ocean acidification on macroalgal communities. *Journal of Experimental Marine Biology and Ecology*, 400, 278-287.
- RAGAZZOLA, F., FOSTER, L. C., FORM, A., ANDERSON, P. S. L., HANSTEEN, T. H. & FIETZKE, J. 2012. Ocean acidification weakens the structural integrity of coralline algae. *Global Change Biology*, 18, 2804-2812.
- RAINA, J.-B., TAPIOLAS, D., WILLIS, B. L. & BOURNE, D. G. 2009. Coral-Associated Bacteria and Their Role in the Biogeochemical Cycling of Sulfur. *Applied and Environmental Microbiology*, 75, 3492-3501.
- RALPH, P. J. & GADEMANN, R. 2005. Rapid light curves: A powerful tool to assess photosynthetic activity. *Aquatic Botany*, 82, 222-237.
- REED, R. H. 1983. The osmotic responses of *Polysiphonia lanosa* (L.) Tandy from marine and estuarine sites: Evidence for incomplete recovery of turgor. *Journal of Experimental Marine Biology and Ecology*, 68, 169-193.
- REEF, R., KANIEWSKA, P. & HOEGH-GULDBERG, O. 2009. Coral Skeletons Defend against Ultraviolet Radiation. *PLoS ONE*, 4, e7995.
- REESE, B. K. & ANDERSON, M. A. 2009. Dimethyl sulfide production in a saline eutrophic lake, Salton Sea, California. *Limnology and Oceanography*, 54, 250-261.
- REISCH, C. R., STOUDEMAYER, M. J., VARALJAY, V. A., AMSTER, I. J., MORAN, M. A. & WHITMAN, W. B. 2011. Novel pathway for assimilation of dimethylsulphoniopropionate widespread in marine bacteria. *Nature*, 473, 208-211.
- RESHEF, L., KOREN, O., LOYA, Y., ZILBER-ROSENBERG, I. & ROSENBERG, E. 2006. The Coral Probiotic Hypothesis. *Environmental Microbiology*, 8, 2068-2073.
- RIEBESELL, U. 2008. Climate change: Acid test for marine biodiversity. *Nature*, 454, 46-47.
- RIES, J. B., COHEN, A. L. & MCCORKLE, D. C. 2009. Marine calcifiers exhibit mixed response to CO₂-induced ocean acidification. *Geology*, 37, 1131-1134.
- RIVERA, M. G., RIOSMENA-RODRIGUEZ, R. & FOSTER, M. S. 2004. Age and growth of *Lithothamnion muelleri* (Corallinales, Rhodophyta) in the southwestern Gulf of California, Mexico. *Ciencias Marinas*, 30, 235-249.
- RIX, L. N., BURDETT, H. L. & KAMENOS, N. A. 2012. Irradiance-mediated dimethylsulphoniopropionate (DMSP) responses of red coralline algae. *Estuarine, Coastal and Shelf Science*, 96, 268-272.
- ROBERTS, R. D., KÜHL, M., GLUD, R. N. & RYSGAARD, S. 2002. Primary Production of Crustose Coralline Red Algae in a High Arctic Fjord. *Journal of Phycology*, 38, 273-283.
- ROBOCK, A., MU, M., VINNIKOV, K., TROFIMOVA, I. V. & ADAMENKO, T. I. 2005. Forty-five years of observed soil moisture in the Ukraine: No summer desiccation (yet). *Geophysical Research Letters*, 32, L03401.
- ROBOCK, A., VINNIKOV, K. Y., SRINIVASAN, G., ENTIN, J. K., HOLLINGER, S. E., SPERANSKAYA, N. A., LIU, S. & NAMKHAI, A. 2000. The global soil moisture data bank. *Bulletin of the American Meteorological Society*, 81, 1281-1299.
- ROLEDA, M. Y. 2009. Photosynthetic response of Arctic kelp zoospores exposed to radiation and thermal stress. *Photochemical & Photobiological Sciences*, 8, 1302-1312.
- RUNCIE, J. W. & RIDDLE, M. J. 2006. Photosynthesis of marine macroalgae in ice-covered and ice-free environments in East Antarctica. *European Journal of Phycology*, 41, 223-233.
- SABINE, C. L., FEELY, R. A., GRUBER, N., KEY, R. M., LEE, K., BULLISTER, J. L., WANNINKHOF, R., WONG, C. S., WALLACE, D. W. R., TILBROOK, B., MILLERO, F. J., PENG, T.-H., KOZYR, A., ONO, T. & RIOS, A. F. 2004. The Oceanic Sink for Anthropogenic CO₂. *Science*, 305, 367-371.
- SAIKKONEN, K., TAULAVUORI, K., HYVONEN, T., GUNDEL, P. E., HAMILTON, C. E., VANNINEN, I., NISSINEN, A. & HELANDER, M. 2012. Climate change-driven species' range shifts filtered by photoperiodism. *Nature Clim. Change*, 2, 239-242.
- SAROUSI, S. & BEER, S. 2007. Alpha and quantum yield of aquatic plants derived from PAM fluorometry: Uses and misuses. *Aquatic Botany*, 86, 89-92.
- SARTORETTO, S., VERLAQUE, M. & LABOREL, J. 1996. Age of settlement and accumulation rate of submarine "coralligène" (-10 to -60 m) of the northwestern Mediterranean Sea; relation to Holocene rise in sea level. *Marine Geology*, 130, 317-331.
- SAUCHYN, L. & SCHEIBLING, R. 2009a. Degradation of sea urchin feces in a rocky subtidal ecosystem: implications for nutrient cycling and energy flow. *Aquatic Botany*, 6, 99-108.
- SAUCHYN, L. & SCHEIBLING, R. 2009b. Fecal production by sea urchins in native and invaded algal beds. *Marine Ecology Progress Series*, 396, 35-48.

- SCAVIA, D., FIELD, J., BOESCH, D., BUDDEMEIER, R., BURKET, V., CAYAN, D., FOGARTY, M., HARWELL, M., HOWARTH, R., MASON, C., REED, D., ROYER, T., SALLENGER, A. & TITUS, J. 2002. Climate change impacts on US coastal and marine ecosystems. *Estuaries*, 25, 149-164.
- SCHÄFER, H., MYRONOVA, N. & BODEN, R. 2010. Microbial degradation of dimethylsulphide and related C₁-sulphur compounds: organisms and pathways controlling fluxes of sulphur in the biosphere. *Journal of Experimental Botany*, 61, 315-334.
- SCHEIBLING, R. 1986. Increased macroalgal abundance following mass mortalities of sea urchins (*Strongylocentrotus droebachiensis*) along the Atlantic coast of Nova Scotia. *Oecologia*, 68, 186-198.
- SCHEIBLING, R. E. & LAUZON-GUAY, J. 2010. Killer storms: North Atlantic hurricanes and disease outbreaks in sea urchins. *Limnology and Oceanography*, 55, 2331-2338.
- SCHLESINGER, M. E. & RAMANKUTTY, N. 1994. An oscillation in the global climate system of period 65-70 years. *Nature*, 367, 723-726.
- SCHLITZER, R. 2011. *Ocean Data View*. <http://odv.awi.de>.
- SCHUBERT, N. & GARCÍA-MENDOZA, E. 2008. Photoinhibition in red algal species with different carotenoid profiles. *Journal of Phycology*, 44, 1437-1446.
- SCHUBERT, N., GARCIA-MENDOZA, E. & ENRIQUEZ, S. 2011. Is the photo-acclimatory response of Rhodophyta conditioned by the species carotenoid profile? *Limnology and Oceanography*, 56, 2347-2361.
- SCHUBERT, N., GARCÍA-MENDOZA, E. & PACHECO-RUIZ, I. 2006. Carotenoid composition of marine red algae. *Journal of Phycology*, 42, 1208-1216.
- SCHWARZ, A.-M., HAWES, I., ANDREW, N., STEVE MERCER, V. C. & THRUSH, S. 2005. Primary production potential of non-geniculate coralline algae at Cape Evans, Ross Sea, Antarctica. *Marine Ecology Progress Series*, 294, 131-140.
- SEMESI, I. S., KANGWE, J. & BJÖRK, M. 2009. Alterations in seawater pH and CO₂ affect calcification and photosynthesis in the tropical coralline alga, *Hydrolithon* sp. (Rhodophyta). *Estuarine, Coastal and Shelf Science*, 84, 337-341.
- SEYMOUR, J. R., SIMÓ, R., AHMED, T. & STOCKER, R. 2010. Chemoattraction to Dimethylsulfoniopropionate Throughout the Marine Microbial Food Web. *Science*, 329, 342-345.
- SEYMOUR, R. J., TEGNER, M. J., DAYTON, P. K. & PARNELL, P. E. 1989. Storm wave induced mortality of giant kelp, *Macrocystis pyrifera*, in Southern California. *Estuarine, Coastal and Shelf Science*, 28, 277-292.
- SHANAHAN, T. M., OVERPECK, J. T., ANCHUKAITIS, K. J., BECK, J. W., COLE, J. E., DETTMAN, D. L., PECK, J. A., SCHOLZ, C. A. & KING, J. W. 2009. Atlantic Forcing of Persistent Drought in West Africa. *Science*, 324, 377-380.
- SHAW, G. 1983. Bio-controlled thermostasis involving the sulfur cycle. *Climatic Change*, 5, 297-303.
- SHENOY, D. M. & PATIL, J. S. 2003. Temporal variations in dimethylsulphoniopropionate and dimethyl sulphide in the Zuari estuary, Goa (India). *Marine Environmental Research*, 56, 387-402.
- SHEPHERD, A., IVINS, E. R., A, G., BARLETTA, V. R., BENTLEY, M. J., BETTADPUR, S., BRIGGS, K. H., BROMWICH, D. H., FORSBERG, R., GALIN, N., HORWATH, M., JACOBS, S., JOUGHIN, I., KING, M. A., LENAERTS, J. T. M., LI, J., LIGTENBERG, S. R. M., LUCKMAN, A., LUTHCKE, S. B., MCMILLAN, M., MEISTER, R., MILNE, G., MOUGINOT, J., MUIR, A., NICOLAS, J. P., PADEN, J., PAYNE, A. J., PRITCHARD, H., RIGNOT, E., ROTT, H., SØRENSEN, L. S., SCAMBOS, T. A., SCHEUCHL, B., SCHRAMA, E. J. O., SMITH, B., SUNDAL, A. V., VAN ANGELEN, J. H., VAN DE BERG, W. J., VAN DEN BROEKE, M. R., VAUGHAN, D. G., VELICOGNA, I., WAHR, J., WHITEHOUSE, P. L., WINGHAM, D. J., YI, D., YOUNG, D. & ZWALLY, H. J. 2012. A Reconciled Estimate of Ice-Sheet Mass Balance. *Science*, 338, 1183-1189.
- SHORT, F., CARRUTHERS, T., DENNISON, W. & WAYCOTT, M. 2007. Global seagrass distribution and diversity: A bioregional model. *Journal of Experimental Marine Biology and Ecology*, 350, 3-20.
- SIEVERT, S. M., KIENE, R. P. & SCHULZ-VOGT, H. N. 2007. The sulphur cycle. *Oceanography*, 20, 117-123.
- SIMO, R., ARCHER, S. D., PEDROS-ALIO, C., GILPIN, L. & STELFOX-WIDDECOMBE, C. E. 2002. Coupled dynamics of dimethylsulfoniopropionate and dimethylsulfide cycling and the microbial food web in surface waters of the North Atlantic. *Limnology and Oceanography*, 47, 53-61.
- SIMO, R., GRIMALT, J. O. & ALBAIGÉS, J. 1997. Dissolved dimethylsulphide, dimethylsulphoniopropionate and dimethylsulphoxide in western Mediterranean waters. *Deep Sea Research Part II: Topical Studies in Oceanography*, 44, 929-950.

- SIMO, R., GRIMALT, J. O., PEDROS-ALIO, C. & ALBAIGÉS, J. 1995. Occurrence and transformation of dissolved dimethyl sulfur species in stratified seawater (western Mediterranean Sea). *Marine Ecology Progress Series*, 127, 291-299.
- SIMPSON, R. H. & RIEHL, H. 1981. *The hurricane and its impact*, Oxford: Basil Blackwell.
- SIMS, D. W. & QUAYLE, V. A. 1998. Selective foraging behaviour of basking sharks on zooplankton in a small-scale front. *Nature*, 393, 460-464.
- SJOBLAD, R. D. & MITCHELL, R. 1979. Chemotactic responses of *Vibrio alginolyticus* to algal extracellular products. *Canadian Journal of Microbiology/Revue Canadienne de Microbiologie*, 25, 964-967.
- SMITH, C. & HIGSON, A. 2012. Research needs in ecosystem services to support algal biofuels, bioenergy and commodity chemicals production in the UK. York: NNFCC.
- SMITH, J. E. & PRICE, N. 2011. Carbonate chemistry on remote coral reefs: natural variability and biological responses. *OCB News*, 4, 7-11.
- SNYDER, M. A., SLOAN, L. C., DIFFENBAUGH, N. S. & BELL, J. L. 2003. Future climate change and upwelling in the California Current. *Geophysical Research Letters*, 30, 1823.
- SOARES, A. G., SCHLACHER, T. A. & MCLACHLAN, A. 1997. Carbon and nitrogen exchange between sandy beach clams (*Donax serra*) and kelp beds in the Benguela coastal upwelling region. *Marine Biology*, 127, 657-664.
- SOLOMON, S., QIN, D., MANNING, M., CHEN, Z., MARQUIS, M., AVERYT, K. B., TIGNOR, M. & MILLER, H. L. (eds.) 2007. *Contribution of Working Group I to the Fourth Assessment Report of the Intergovernmental Panel on Climate Change, 2007* Cambridge, UK and New York, USA: Cambridge University Press.
- SPIELMEYER, A. & POHNERT, G. 2012. Influence of temperature and elevated carbon dioxide on the production of dimethylsulfoniopropionate and glycine betaine by marine phytoplankton. *Marine Environmental Research*, 73, 62-69.
- SPIESE, C. E., KIEBER, D. J., NOMURA, C. T. & KIENE, R. P. 2009. Reduction of dimethylsulfoxide to dimethylsulfide by marine phytoplankton. *Limnology and Oceanography*, 54, 560-570.
- STANLEY, S. M., RIES, J. B. & HARDIE, L. A. 2002. Low-magnesium calcite produced by coralline algae in seawater of Late Cretaceous composition. *Proceedings of the National Academy of Sciences*, 99, 15323-15326.
- STARK, H., BROWN, S. S., GOLDAN, P. D., ALDENER, M., KUSTER, W. C., JAKOUBEK, R., FEHSENFELD, F. C., MEAGHER, J., BATES, T. S. & RAVISHANKARA, A. R. 2007. Influence of nitrate radical on the oxidation of dimethyl sulfide in a polluted marine environment. *Journal of Geophysical Research*, 112, D10S10.
- STEFELS, J. 2000. Physiological aspects of the production and conversion of DMSP in marine algae and higher plants. *Journal of Sea Research*, 43, 183-197.
- STEFELS, J., CARNAT, G., DACEY, J. W. H., GOOSSENS, T., ELZENGA, J. T. M. & TISON, J.-L. 2012. The analysis of dimethylsulfide and dimethylsulfoniopropionate in sea ice: Dry-crushing and melting using stable isotope additions. *Marine Chemistry*, 128-129, 34-43.
- STEFELS, J., DACEY, J. W. H. & ELZENGA, J. T. M. 2009. In vivo DMSP-biosynthesis measurements using stable-isotope incorporation and proton-transfer-reaction mass spectrometry (PTR-MS). *Limnology and Oceanography: Methods*, 7, 595-611.
- STEINBERG, P. D. & DE NYS, R. 2002. Chemical Mediation of Colonization of Seaweed Surfaces. *Journal of Phycology*, 38, 621-629.
- STELLER, D. & CÁCERES-MARTINEZ, C. 2009. Coralline algal rhodoliths enhance larval settlement and early growth of the Pacific calico scallop *Argopecten ventricosus*. *Marine Ecology Progress Series*, 396, 49-60.
- STELLER, D. L., RIOSMENA-RODRIGUEZ, R., FOSTER, M. S. & ROBERTS, C. A. 2003. Rhodolith bed diversity in the Gulf of California: the importance of rhodolith structure and consequences of disturbance. *Aquatic Conservation: Marine and Freshwater Ecosystems*, 13, S5-S20.
- STENECK, R. S., GRAHAM, M. H., BOURQUE, B. J., CORBETT, D., ERLANDSON, J. M., ESTES, J. A. & TEGNER, M. J. 2002. Kelp forest ecosystems: biodiversity, stability, resilience and future. *Environmental Conservation*, 29, 436-459.
- STROM, S., WOLFE, G., HOLMES, J., STECHER, H., SHIMENECK, C., LAMBERT, S. & MORENO, E. 2003a. Chemical defense in the microplankton I: Feeding and growth rates of heterotrophic protists on the DMS-producing phytoplankton *Emiliania huxleyi*. *Limnology and Oceanography*, 48, 217-229.
- STROM, S., WOLFE, G., SLAJER, A., LAMBERT, S. & CLOUGH, J. 2003b. Chemical defense in the microplankton II: Inhibition of protist feeding by β -dimethylsulfoniopropionate (DMSP). *Limnology and Oceanography*, 48, 230-237.
- STUMPP, M., DUPONT, S., THORNDYKE, M. C. & MELZNER, F. 2011a. CO₂ induced seawater acidification impacts sea urchin larval development II: Gene expression patterns in pluteus

- larvae. *Comparative Biochemistry and Physiology - Part A: Molecular Integrative Physiology*, 160, 320-330.
- STUMPP, M., WREN, J., MELZNER, F., THORNDYKE, M. C. & DUPONT, S. T. 2011b. CO₂ induced seawater acidification impacts sea urchin larval development I: Elevated metabolic rates decrease scope for growth and induce developmental delay. *Comparative Biochemistry and Physiology - Part A: Molecular Integrative Physiology*, 160, 331-340.
- SU, C., LEI, L., DUAN, Y., ZHANG, K.-Q. & YANG, J. 2012. Culture-independent methods for studying environmental microorganisms: methods, application, and perspective. *Applied Microbiology and Biotechnology*, 93, 993-1003.
- SUGGETT, D. J., LE FLOC'H, E., HARRIS, G. N., LEONARDOS, N. & GEIDER, R. J. 2007. Different strategies of photoacclimation by two strains of *Emiliania huxleyi* (Haptophyta). *Journal of Phycology*, 43, 1209-1222.
- SUGGETT, D. J., OXBOROUGH, K., BAKER, N. R., MACINTYRE, H. L., KANA, T. M. & GEIDER, R. J. 2003. Fast repetition rate and pulse amplitude modulation chlorophyll a fluorescence measurements for assessment of photosynthetic electron transport in marine phytoplankton. *European Journal of Phycology*, 38, 371 - 384.
- SUMMERS, P. S., NOLTE, K. D., COOPER, A. J. L., BORGEAS, H., LEUSTEK, T., RHODES, D. & HANSON, A. D. 1998. Identification and Stereospecificity of the First Three Enzymes of 3-Dimethylsulfoniopropionate Biosynthesis in a Chlorophyte Alga. *Plant Physiology*, 116, 369-378.
- SUNDA, W., KIEBER, D. J., KIENE, R. P. & HUNTSMAN, S. 2002. An antioxidant function for DMSP and DMS in marine algae. *Nature*, 418, 317-320.
- SUNDA, W. G., LITAKER, R. W., HARDISON, D. R. & TESTER, P. A. 2005. Dimethylsulfoniopropionate (DMSP) and its relation to algal pigments in diverse waters of the Belize coastal lagoon and barrier reef system. *Marine Ecology-Progress Series*, 287, 11-22.
- SUSSMAN, M., WILLIS, B. L., VICTOR, S. & BOURNE, D. G. 2008. Coral Pathogens Identified for White Syndrome (WS) Epizootics in the Indo-Pacific. *PLoS ONE*, 3, e2393.
- SUZUKI, A. & KAWAHATA, H. 2003. Carbon budget of coral reef systems: an overview of observations in fringing reefs, barrier reefs and atolls in the Indo-Pacific regions. *Tellus B*, 55, 428-444.
- TEE, K. T., SMITH, P. C. & LEFAIVRE, D. 1993. Topographic upwelling off southwest Nova Scotia. *Journal of Physical Oceanography*, 23, 1703-1726.
- TEICHERT, S., WOELKERLING, W., RÜGGERBERG, A., WISSHAK, M., PIEPENBURG, D., MEYERHÖFER, M., FORM, A., BÜDENBENDER, J. & FREIWALD, A. 2012. Rhodolith beds (Corallinales, Rhodophyta) and their physical and biological environment at 80°31'N in Nordkappbukta (Nordaustlandet, Svalbard Archipelago, Norway). *Phycologia*, 51, 371-390.
- THOMAS, S., BURDETT, H., TEMPERTON, B., WICK, R., SNELLING, D., MCGRATH, J. W., QUINN, J. P., MUNN, C. & GILBERT, J. A. 2010. Evidence for phosphonate usage in the coral holobiont. *ISME J*, 4, 459-461.
- TIERNEY, P. W. & JOHNSON, M. E. 2012. Stabilization Role of Crustose Coralline Algae During Late Pleistocene Reef Development on Isla Cerralvo, Baja California Sur (Mexico). *Journal of Coastal Research*, 244-254.
- TODD, J. D., CURSON, A. R. J., DUPONT, C. L., NICHOLSON, P. & JOHNSTON, A. W. B. 2009. The *dddP* gene, encoding a novel enzyme that converts dimethylsulfoniopropionate into dimethyl sulfide, is widespread in ocean metagenomes and marine bacteria and also occurs in some Ascomycete fungi. *Environmental Microbiology*, 11, 1376-1385.
- TODGHAM, A. E. & HOFMANN, G. E. 2009. Transcriptomic response of sea urchin larvae *Strongylocentrotus purpuratus* to CO₂-driven seawater acidification. *Journal of Experimental Biology*, 212, 2579-2594.
- TOOLE, D. A. & SIEGEL, D. A. 2004. Light-driven cycling of dimethylsulfide (DMS) in the Sargasso Sea: Closing the loop. *Geophysical Research Letters*, 31, L09308.
- TOTH, G. 2007. Screening for induced herbivore resistance in Swedish intertidal seaweeds. *Marine Biology*, 151, 1597-1604.
- TOTH, G. B. & PAVIA, H. 2000. Water-borne cues induce chemical defense in a marine alga (*Ascomyllum nodosum*). *Proceedings of the National Academy of Sciences*, 97, 14418-14420.
- TOWNSEND, D. W. & KELLER, M. D. 1996. Dimethylsulfide (DMS) and dimethylsulphonioipropionate (DMSP) in relation to phytoplankton in the Gulf of Maine. *Marine Ecology Progress Series*, 137, 229-241.
- TRENBERTH, K. E., DAI, A., RASMUSSEN, R. M. & PARSONS, D. B. 2003. The changing character of precipitation. *Bulletin of the American Meteorological Society*, 84, 1205-1217.

- TRENBERTH, K. E., JONES, P. D., AMBENJE, P., BOJARIU, R., EASTERLING, D., TANK, A. K., PARKER, D., RAHIMZADEH, F., RENWICK, J. A., RUSTICUCCI, M., SODEN, B. & ZHAI, P. (eds.) 2007. *Observations: Surface and Atmospheric Climate Change*, Cambridge, UK and New York, USA: Cambridge University Press.
- TRIPATI, A. K., ROBERTS, C. D. & EAGLE, R. A. 2009. Coupling of CO₂ and Ice Sheet Stability Over Major Climate Transitions of the Last 20 Million Years. *Science*, 326, 1394-1397.
- TURNER, S. M., MALIN, G., BAGANDER, L. E. & LECK, C. 1990. Interlaboratory Calibration and Sample Analysis of Dimethyl Sulfide in Water. *Marine Chemistry*, 29, 47-62.
- TURNER, S. M., MALIN, G., LISS, P. S., HARBOUR, D. S. & HOLLIGAN, P. M. 1988. The Seasonal Variation of Dimethyl Sulfide and Dimethylsulfoniopropionate Concentrations in Nearshore Waters. *Limnology and Oceanography*, 33, 364-375.
- TURNER, S. M., MALIN, G., NIGHTINGALE, P. D. & LISS, P. S. 1996. Seasonal variation of dimethyl sulphide in the North Sea and an assessment of fluxes to the atmosphere. *Marine Chemistry*, 54, 245-262.
- URSI, S., PEDERSÉN, M., PLASTINO, E. & SNOEIJS, P. 2003. Intraspecific variation of photosynthesis, respiration and photoprotective carotenoids *Gracilaria birdiae* (Gracilariales: Rhodophyta). *Marine Biology*, 142, 997-1007.
- VAIRAVAMURTHY, A., ANDREAE, M. O. & IVERSON, R. L. 1985. Biosynthesis of dimethylsulfide and dimethylpropiothetin by *Hymenomonas carterae* in relation to sulfur source and salinity variations. *Limnology and Oceanography*, 30, 59-70.
- VALLADARES, F., SANCHEZ-HOYOS, A. & MANRIQUE, E. 1995. Diurnal Changes in Photosynthetic Efficiency and Carotenoid Composition of the Lichen *Anaptychia ciliaris*: Effects of Hydration and Light Intensity. *The Bryologist*, 98, 375-382.
- VAN ALSTYNE, K., KOELLERMEIER, L. & NELSON, T. 2007. Spatial variation in dimethylsulfoniopropionate (DMSP) production in *Ulva lactuca* (Chlorophyta) from the Northeast Pacific. *Marine Biology*, 150, 1127-1135.
- VAN ALSTYNE, K. & PUGLISI, M. 2007. DMSP in marine macroalgae and macroinvertebrates: Distribution, function, and ecological impacts. *Aquatic Sciences - Research Across Boundaries*, 69, 394-402.
- VAN ALSTYNE, K. L. 2008. The distribution of DMSP in green macroalgae from northern New Zealand, eastern Australia and southern Tasmania. *Journal of the Marine Biological Association of the UK*, 88, 799-805.
- VAN ALSTYNE, K. L. & HOUSER, L. T. 2003. Dimethylsulphide release during macroinvertebrate grazing and its role as an activated chemical defense. *Marine Ecology Progress Series*, 250, 175-181.
- VAN ALSTYNE, K. L., PELLETREAU, K. N. & KIRBY, A. 2009. Nutritional preferences override chemical defenses in determining food choice by a generalist herbivore, *Littorina sitkana*. *Journal of Experimental Marine Biology and Ecology*, 379, 85-91.
- VAN ALSTYNE, K. L., WOLFE, G. V., FREIDENBURG, T. L., NEILL, A. & HICKEN, C. 2001. Activated defense systems in marine macroalgae: evidence for an ecological role for DMSP cleavage. *Marine Ecology Progress Series*, 213, 53-65.
- VAN BOEKEL, W. H. M., HANSEN, F. C., RIEGMAN, R. & BAK, R. P. M. 1992. Lysis-induced decline of a *Phaeocystis* spring bloom and coupling with the microbial food web. *Marine Ecology Progress Series*, 81, 269-276.
- VAUGHAN, D., MARSHALL, G., CONNOLLEY, W., PARKINSON, C., MULVANEY, R., HODGSON, D., KING, J., PUDSEY, C. & TURNER, J. 2003. Recent Rapid Regional Climate Warming on the Antarctic Peninsula. *Climatic Change*, 60, 243-274.
- VEGA THURBER, R., WILLNER-HALL, D., RODRIGUEZ-MUELLER, B., DESNUES, C., EDWARDS, R. A., ANGLY, F., DINSDALE, E., KELLY, L. & ROHWER, F. 2009. Metagenomic analysis of stressed coral holobionts. *Environmental Microbiology*, 11, 2148-2163.
- VILA-COSTA, M., DEL VALLE, D. A., GONZÁLEZ, J. M., SLEZAK, D., KIENE, R. P., SÁNCHEZ, O. & SIMÓ, R. 2006. Phylogenetic identification and metabolism of marine dimethylsulfide-consuming bacteria. *Environmental Microbiology*, 8, 2189-2200.
- VILA-COSTA, M., KIENE, R. P. & SIMO, R. 2008. Seasonal variability of the dynamics of dimethylated sulfur compounds in a coastal northwest Mediterranean site. *Limnology and Oceanography*, 53, 198-211.
- VOGT, M., VALLINA, S. & VON GLASOW, R. 2008. New Directions: Correspondence on "Enhancing the natural cycle to slow global warming". *Atmospheric Environment*, 42, 4803-4805.
- VOGT, M., VALLINA, S. M., BUITENHUIS, E. T., BOPP, L. & LE QUÉRÉ, C. 2010. Simulating dimethylsulphide seasonality with the Dynamic Green Ocean Model PlankTOM5. *Journal of Geophysical Research*, 115, C06021.

- WALZ. 2012. Available: http://www.walz.com/products/chl_p700/diving-pam/red_blue_version.html [Accessed 29th May 2012].
- WALZ 2007. *Junior PAM chlorophyll fluorometer*, Effeltrich: Heinz Walz GmbH.
- WALZ 1999. *Photosynthesis yield analyzer Mini-PAM*, Effeltrich: Heinz Walz GmbH.
- WEBSTER, N. S., SOO, R., COBB, R. & NEGRI, A. P. 2011. Elevated seawater temperature causes a microbial shift on crustose coralline algae with implications for the recruitment of coral larvae. *ISME J*, 5, 759-770.
- WEBSTER, N. S., UTHICKE, S., BOTTÉ, E. S., FLORES, F. & NEGRI, A. P. 2013. Ocean acidification reduces induction of coral settlement by crustose coralline algae. *Global Change Biology*, 19, 303-315.
- WEBSTER, N. S., UTHICKE, S., BOTTÉ, E. S., FLORES, F. & NEGRI, A. P. 2012. Ocean acidification reduces induction of coral settlement by crustose coralline algae. *Global Change Biology*, n/a-n/a.
- WEIDNER, S., ARNOLD, W., STACKEBRANDT, E. & PÜHLER, A. 2000. Phylogenetic Analysis of Bacterial Communities Associated with Leaves of the Seagrass *Halophila stipulacea* by a Culture-Independent Small-Subunit rRNA Gene Approach. *Microbial Ecology*, 39, 22-31.
- WHITE, A. J. & CRITCHLEY, C. 1999. Rapid light curves: A new fluorescence method to assess the state of the photosynthetic apparatus. *Photosynthesis Research*, 59, 63-72.
- WIESEMEIER, T. & POHNERT, G. 2007. Direct quantification of dimethylsulfoniopropionate (DMS) in marine micro- and macroalgae using HPLC or UPLC/MS. *Journal of Chromatography B-Analytical Technologies in the Biomedical and Life Sciences*, 850, 493-498.
- WILKINSON, C. (ed.) 2008. *Status of coral reefs of the world: 2008*. Australian Institute for Marine Science.
- WILSON, A., AJLANI, G., VERBAVATZ, J.-M., VASS, I., KERFELD, C. A. & KIRILOVSKY, D. 2006. A Soluble Carotenoid Protein Involved in Phycobilisome-Related Energy Dissipation in Cyanobacteria. *The Plant Cell Online*, 18, 992-1007.
- WILSON, S., BLAKE, C., BERGES, J. A. & MAGGS, C. A. 2004. Environmental tolerances of free-living coralline algae (maerl): implications for European marine conservation. *Biological Conservation*, 120, 279-289.
- WINGENTER, O. W., ELLIOT, S. M. & BLAKE, D. R. 2007a. New Directions: Enhancing the natural sulfur cycle to slow global warming. *Atmospheric Environment*, 41, 7373-7375.
- WINGENTER, O. W., HAASE, K. B., ZEIGLER, M., BLAKE, D. R., SHERWOOD, R. F., SIVE, B. C., PAULINO, A., THYRHAUG, R., LARSEN, A., SCHULZ, K., MEYERHOFER, M. & REIBESSELL, U. 2007b. Unexpected consequences of increasing CO₂ and ocean acidity on marine production of DMS and CH₂ClI: Potential climate impacts. *Geophysical Research Letters*, 34, L05710.
- WINTERS, G., LOYA, Y., ROTTGERS, R. & BEER, S. 2003. Photoinhibition in Shallow-Water Colonies of the Coral *Stylophora pistillata* as Measured in Situ. *Limnology and Oceanography*, 48, 1388-1393.
- WIRTZ, M. & DROUX, M. 2005. Synthesis of the sulfur amino acids: cysteine and methionine. *Photosynthesis Research*, 86, 345-362.
- WOLFE, G. & STEINKE, M. 1996. Grazing-activated production of dimethyl sulfide (DMS) by two clones of *Emiliania huxleyi*. *Limnology and Oceanography*, 41, 1151-1160.
- WOLFE, G. V., SHERR, E. B. & SHERR, B. F. 1994. Release and consumption of DMS from *Emiliania huxleyi* during grazing by *Oxyrrhis marina*. *Marine Ecology Progress Series*, 111, 111-119.
- WOLFE, G. V., STEINKE, M. & KIRST, G. O. 1997. Grazing-activated chemical defence in a unicellular marine alga. *Nature*, 387, 894-897.
- WOLFE, G. V., STROM, S. L., HOLMES, J. L., RADZIO, T. & OLSON, M. B. 2002. Dimethylsulphoniopropionate cleavage by marine phytoplankton in response to mechanical, chemical or dark stress. *Journal of Phycology*, 38, 948-960.
- WOOD, S. N. 2006. *Generalised Additive Models. An Introduction with R*, Boca Raton: Taylor & Francis.
- WOOD, S. N. 2003. Thin plate regression splines. *Journal of the Royal Statistical Society: Series B (Statistical Methodology)*, 65, 95-114.
- WOODHOUSE, M. T., CARSLAW, K. S., MANN, G. W., VALLINA, S. M., VOGT, M., HALLORAN, P. R. & BOUCHER, O. 2010. Low sensitivity of cloud condensation nuclei to changes in the sea-air flux of dimethyl-sulphide. *Atmos. Chem. Phys.*, 10, 7545-7559.
- WOODRUFF, S. D., WORLEY, S. J., LUBKER, S. J., JI, Z., ERIC FREEMAN, J., BERRY, D. I., BROHAN, P., KENT, E. C., REYNOLDS, R. W., SMITH, S. R. & WILKINSON, C. 2011. ICOADS Release 2.5: extensions and enhancements to the surface marine meteorological archive. *International Journal of Climatology*, 31, 951-967.

- WORTMANN, U. G. & PAYTAN, A. 2012. Rapid Variability of Seawater Chemistry Over the Past 130 Million Years. *Science*, 337, 334-336.
- WRIGHT, K. L. B., PICHEGRU, L. & RYAN, P. G. 2011. Penguins are attracted to dimethyl sulphide at sea. *The Journal of Experimental Biology*, 214, 2509-2511.
- YATES, K. K. & HALLEY, R. B. 2006. CO_3^{2-} concentration and pCO_2 thresholds for calcification and dissolution on the Molokai reef flat, Hawaii. *Biogeosciences*, 3, 357-369.
- YOCH, D. C. 2002. Dimethylsulfoniopropionate: Its sources, role in the marine food web, and biological degradation to dimethylsulfide. *Applied and Environmental Microbiology*, 68, 5804-5815.
- YOSHIKAWA, T. & FURUYA, K. 2006. Effects of diurnal variations in phytoplankton photosynthesis obtained from natural fluorescence. *Marine Biology*, 150, 299-311.
- YVON, S. A., PLANE, J. M. C., NIEN, C. F., COOPER, D. J. & SALTZMAN, E. S. 1996. Interaction between nitrogen and sulfur cycles in the polluted marine boundary layer. *Journal of Geophysical Research*, 101, 1379-1386.
- ZHANG, J., NAGAHAMA, T., ABO, M., OKUBO, A. & YAMAZAKI, S. 2005. Capillary electrophoretic analysis of dimethylsulfoniopropionate in sugarcane and marine algal extracts. *Talanta*, 66, 244-248.
- ZHANG, W., PERRIE, W. & VAGLE, S. 2006. Impacts of winter storms on air-sea gas exchange. *Geophysical Research Letters*, 33, L14803.
- ZHANG, Z., FALTER, J., LOWE, R. & IVEY, G. 2012. The combined influence of hydrodynamic forcing and calcification on the spatial distribution of alkalinity in a coral reef system. *Journal of Geophysical Research*, 117, C04034.
- ZHOU, C.-X., XU, J.-L., YAN, X.-J., HOU, Y.-D. & JIANG, Y. 2009. Analysis of Dimethylsulfide and Dimethylsulfoniopropionate in Marine Microalgae Culture. *Chinese Journal of Analytical Chemistry*, 37, 1308-1312.
- ZUBKOV, M. V., FUCHS, B. M., ARCHER, S. D., KIENE, R. P., AMANN, R. & BURKILL, P. H. 2002. Rapid turnover of dissolved DMS and DMSP by defined bacterioplankton communities in the stratified euphotic zone of the North Sea. *Deep Sea Research Part II: Topical Studies in Oceanography*, 49, 3017-3038.

Appendix A

Example annotated R code for identifying the most parsimonious GAM model for time series data presented in Chapter 5. This example relates to DMSd concentrations at the maerl bed (MB) site.

```
# Two data files are required: datafile 1 - average DMSd concentrations
at each timepoint; datafile 2 - individual replicates at each time point.

# Import data file 1: decimal year (dec.yr.av), temperature (temp.av),
cloud cover (cc.av), daylength (dl.av), DMSd concentration (dmsd.av)
mb.av=read.table("C:\\Users\\0903304b\\Desktop\\mb.av.txt", header=T)
attach(mb.av)

# Show column headers
names(mb.av)

# Plot DMSd concentration against time
plot(dmsd.av~dec.yr.av)

# Cross-correlation of DMSd against temperature. Max lag of 11 because
there are 11 data points in the time series
dmsd.temp.ccf = ccf(dmsd.av, temp.av, lag.max=11)

# Plot DMSd-temperature cross-correlation function - identify if DMSd is
affected by previous temperature values (lags)
dmsd.temp.ccf

# Cross-correlation of DMSd against cloud cover. Max lag of 11 because
there are 11 data points in the time series
dmsd.cc.ccf = ccf(dmsd.av, cc.av, lag.max=11)

# Plot DMSd-cloud cover cross-correlation function - identify if DMSd is
affected by previous cloud cover values (lags)
dmsd.cc.ccf

# Cross-correlation of DMSd against daylength. Max lag of 11 because
there are 11 data points in the time series
dmsd.dl.ccf = ccf(dmsd.av, dl.av, lag.max=11)

# Plot DMSd-daylength cross-correlation function - identify if DMSd is
affected by previous daylength values (lags)
dmsd.dl.ccf

# Import data file 2: decimal year (dec.yr), temperature (temp), cloud
cover (cc), daylength (dl), DMSd concentrations (dmsd), log10(DMSd)
concentrations (dmsd.log)
mb=read.table("C:\\Users\\0903304b\\Desktop\\mb.dmsd.txt", header=T)
attach(mb)

# Show column headers
names(mb)

# Plot paired scatterplot of all data
pairs(cbind(mb$dmsd, mb$temp, mb$cc, mb$dl), panel=panel.smooth)
pairs(mb, panel=panel.smooth)
```

```
# Identify interactions between temperature and cloud cover
n.given = co.intervals(temp,4)
s.given = co.intervals(cc,4)
coplot(dmsd~cc|temp, data = mb, panel=panel.smooth, given=list(n.given))

# Using log10(DMSd)
coplot(dmsd.log~cc|temp, data = mb, panel=panel.smooth,
given=list(n.given))

# Identify interactions between temperature and daylength
n.given = co.intervals(temp,4)
s.given = co.intervals(dl,4)
coplot(dmsd~temp|dl, data = mb, panel=panel.smooth, given=list(n.given))

# Using log10(DMSd)
coplot(dmsd.log~temp|dl, data = mb, panel=panel.smooth,
given=list(n.given))

# Identify interactions between cloud cover and daylength
n.given = co.intervals(cc,4)
s.given = co.intervals(dl,4)
coplot(dmsd~dl|cc, data = mb, panel=panel.smooth, given=list(n.given))

# Using log10(DMSd)
coplot(dmsd.log~dl|cc, data = mb, panel=panel.smooth,
given=list(n.given))

# Open mgcv package in R
library(mgcv)

# GAM model 1: Temperature
modell = gam(mb$dmsd.log ~ s(temp))

# Plot smoothing function
modell

# Retrieve basic statistics
gam.check(modell)
summary(modell)

# GAM model 2: Cloud cover
model2 = gam(mb$dmsd.log ~ s(cc))

# Plot smoothing function
model2

# Retrieve model statistics
gam.check(model2)
summary(model2)

# GAM model 3: daylength
model3 = gam(mb$dmsd.log ~ s(dl))

# Plot smoothing function
model3

# Retrieve model statistics
gam.check(model3)
summary(model3)

# GAM model 4: temperature and cloud cover
model4 = gam(mb$dmsd.log ~ s(temp) + s(cc))

# Plot smoothing functions
model4
```

```
# Retrieve model statistics
gam.check(model4)
summary(model4)

# GAM model 5: temperature and daylength
model5 = gam(mb$dmsd.log ~ s(temp) + s(dl))

# Plot smoothing functions
model5

# Retrieve model statistics
gam.check(model5)
summary(model5)

# GAM model 6: cloud cover and daylength
model6 = gam(mb$dmsd.log ~ s(cc) + s(dl))

# Plot smoothing functions
model6

# Retrieve model statistics
gam.check(model6)
summary(model6)

# GAM model 7: temperature, cloud cover and daylength
model7 = gam(mb$dmsd.log ~ s(temp) + s(cc) + s(dl))

# Plot smoothing functions
model7

# Retrieve model statistics
gam.check(model7)
summary(model7)

# Where interactions have been identified in coplot, run more models
including interacting smooth functions in the form of s():s()

# Test for most significant model
anova.model = anova(model1, model2, model3, model4, model5, model6,
model7, test="Chi")

# Display anova results
anova.model

# Select the most parsimonious model and plot the model with the data
residuals and confidence intervals
plot(model2, resid=T, cex=1, pch=16)
```